

# **MODIFICATION OF SHORT FIBRE REINFORCED PP AND HDPE USING NANOSILICA**

*Thesis submitted to the*

**COCHIN UNIVERSITY OF SCIENCE AND TECHNOLOGY**

*in partial fulfilment of the requirements  
for the award of the degree of*

**DOCTOR OF PHILOSOPHY**

*under the*

**FACULTY OF TECHNOLOGY**

*by*

**SINTO JACOB**



**DEPARTMENT OF POLYMER SCIENCE AND RUBBER TECHNOLOGY  
COCHIN UNIVERSITY OF SCIENCE AND TECHNOLOGY  
KOCHI - 682 022, INDIA.**

**May 2009**



T34

## Modification of Short Fibre Reinforced PP and HDPE Using Nanosilica

Submitted by

**Sinto Jacob**

Dept. of Polymer Science and Rubber Technology

Cochin University of Science and technology

Kochi – 22, Kerala, India

sintojacob@rediffmail.com

Research Supervisor

**Dr. K.E.George**

Professor, Dept. of Polymer Science and Rubber Technology

Cochin University of Science and technology

Kochi – 22, Kerala, India

kegeorge@cusat.ac.in



**Department of Polymer Science and Rubber Technology**  
**Cochin University of Science and Technology**  
**Kochi - 682 022, India.**

---

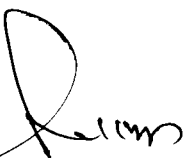
**Dr. K.E.George**  
Professor

Phone: 0484-2575723 (Off)  
0484-2577850 (Res)  
e mail : kegeorge@cusat.ac.in

### **CERTIFICATE**

This is to certify that the thesis entitled **“Modification of short fibre reinforced PP and HDPE using nanosilica”** which is being submitted by Mr. Sinto Jacob, in partial fulfilment of the requirements for the award of the degree of Doctor of Philosophy, to the Cochin University of Science and Technology, Kochi-22, is a record of the bonafide research work carried out by him under my guidance and supervision, in the Department of Polymer Science and Rubber Technology, Kochi-682022, and no part of the work reported in the thesis has been presented for the award of any degree from any other institution.

Kochi-22  
May, 2009

  
\_\_\_\_\_  
Dr.K.E.George  
(Supervising Teacher)

## DECLARATION

I hereby declare that the work presented in this thesis entitled **“Modification of short fibre reinforced PP and HDPE using nanosilica”** is based on the original research work carried out by me under the guidance and supervision of **Dr. K.E.George**, Professor, Department of Polymer Science and Rubber Technology, Cochin University of Science and Technology, Kochi-682 022 and no part of the work reported in this thesis has been presented for the award of any degree from any other institution.

Kochi - 22

May, 2009



Sinto Jacob

എന്റെ ഗുരുഭൂതൻ

# *Acknowledgement*

---

*I humbly bow before the Almighty God for showering His blessings on me, and for giving me the strength and wisdom to reach this mile stone in my life.*

*I believe that the completion of this thesis was possible only through the direct and indirect help extended by the people within and outside of POLYMER SCIENCE and RUBBER TECHNOLOGY family. It has been great, working at PS CRT and I enjoyed the last 4 years here. First of all, I would like to thank Prof. K.E.George for giving me an opportunity and complete freedom to do research work. His remarks and comments were quite inspiring. It would have been difficult to finish the thesis timely and successfully without his support and guidance. His contribution towards structuring the thesis is highly acknowledged. I express my gratitude for his interesting remarks and enthusiastic discussions (also about non-academic topics).*

*I am extremely grateful to Dr.Thomas Kurian, Head of the Department and Dr.Rani Joseph, former Head of the Department for providing all facilities during my research work. With pleasure, I thank all faculty members, especially Dr.Philip Kurian, Dr.Eby Thachil, Dr.Sunil K. Narayanankutty and Smt. Jayalatha of this Department for their wholehearted co-operation throughout the course of my work.*

*I enjoyed my first conference and lasting discussions on polymer chemistry with my friends Anoop, Sreeroop, Elizabeth, Pramitha, Zeena*

*chechi, and her husband Anees. I thank them for presenting such precious moments.*

*I would like to extend my gratitude to Sri. Jude Martin Mendez, Sln. Grd. Lecturer, St. Alberts College, Ernakulam, Thanks for your constructive reading which helped me in improving my thesis and looking at it in to a broader perspective.*

*Let me take this opportunity to thank my teacher colleagues Dr. Sreenivasan P. V, Dr. Raju P, Dr. Maya K, S, Dr. Joshy M. K, Dr. Unnikrishnan K, P., Dr. Prema, Dr. Sunil Jose, Bhuvaneshwary M.G, Parameswaran, Renjana Devi and Dr. Mary Alexander, who made my research tenure a pleasant and memorable experience.*

*I am especially thankful to Newson who always found time for discussion whenever I approached him. His ability to pick up the thread and find apt solutions for problems is very impressive. I am also thankful to Abilash. G who helped me to shape thesis in many ways. I used to enjoy the moments of interesting discussions with him and is as loud and talkative as always. I had many discussions with Leny teacher on the mechanical behavior studies and her view of approaching the things from different perspectives strengthened my concepts. I am very thankful to Mr. Bipinbal for his help in the complicated world of polymer modification. I highly appreciate Sona narayanan for her suggestions regarding crystallization studies. I am also grateful to Newly chechi for her critical comments and valuable suggestions. I express my heartfelt regards to Nisha Nandakumar as an observer in construction of my*

*thesis. I thank reaserch scholars Saisy, Renju, Nimmi, Vidya.G, Vidya Francis, Anna, Ajilesh, Ratheesh, Julie chechi, Jenish Paul, Jasmine, Denny teacher, Sabura teacher, Preetha teacher and Jolly sir, for the proper help in nice time during my thesis work.*

*I gratefully acknowledge the valuable help extended to me by my senior Dr.Thomas N. Abraham during the initial stages of my research work. I also sincerely acknowledge the help and advice from Dr. Sony Varghese and Dr. Litty Allen, NIT, Kozhikode.*

*I am also thankful to my friends Anesh, Lijo, Jinto, Murukesan, Jaya kumar, Jomon, Arun, Reshmi, Bolie Therattil, Kannan, Mahesh, Shibulal and Dhinuraj for helping me in difficult times. I am grateful to my co-research scholors Dr.Nisha, Dr.Aswathi, Dhanya, Dr.Saritha, Dr.Priya, Vijaylakshmi, Neena, and Dr.Anoop Anand of the Department of Polymer Science and Rubber Technology for their co-operation in my course of experience. The most beloved comes always last, especially when it comes to thanking and expressing gratitude. I am very much thankful to my beloved friends Mr. Rajesh Menon and Sreekanth Varma for the selfless help during the course of my research life.*

*I also extend my sincere thanks to the members of the non-teaching staff of the Department of Polymer Science and Rubber Technology, CVSAT, for their support at different stages of my research work.*

*I would like to express my heartfelt thanks to Dr. Lovely Mathew, Sln. Grd. Lecturer, Newman College, Thodupuzha. I will never forget her inspiring words, affection and love offered to me.*



*My thesis is just incomplete and meaningless if I am not leaving a note for the heartfelt love and boundless care Suma teacher have always showered on me. She was there with me in each and every footstep I made in my research and career. In spite of her hectic life she spared a lot of time for me for which, I am greatly thankful to Pichu and Kittu. She used to scold and correct me just like a mother and supported me as a friend at times when I failed in my duties. The materialization of this work is just because of her advice, love, support and above all her prayers. Thank you, dear teacher.*

*There are more people whom I should thank but it is too difficult to put all names here. My parents & family members, friends, colleagues and everyone who has helped me directly or indirectly. I extend my sincere thanks to all of them.*

## Preface

The reinforcement with nanofillers greatly improves the properties of thermoplastics. The ability to develop and process nanocomposite materials into various products will be of critical importance in the development of polymer products in the coming years. The need to promote organophilicity in place of the natural hydrophilic character in inorganic nano materials is a crucial prerequisite for the good performance of nanocomposites. Sufficiently small fillers can give good reinforcement, even when matrix/domain bonding is poor. Short fibre reinforced composites are finding ever-increasing applications in engineering and consumer products. Short fibres are used in order to improve or modify certain thermo-mechanical properties of polymeric materials so as to meet specific applications requirements or to reduce cost of the fabricated article. Short fibres can be directly incorporated into thermoplastics during processing along with other additives and the resulting composites are amenable to the standard processing steps and various type of moulding operations. But in most of the cases fibre reinforced composites require fairly high fibre loading to get the desired property. Higher fibre loading causes higher fibre misalignment and increases the chance for the voids during manufacturing processes. This causes reduction in properties of short fibre reinforced composites. Hence a composite with low filler loading is always the optimum choice. Addition of small volume of nanofillers into fibre composites can effectively improve the properties. This type of hybrid nanocomposites based thermoplastics are expected to possess attractive performance even at low filler loading.

The present study was undertaken to prepare nanosilica by a simple cost effective means and to use it as a potential nanomodifier in thermoplastic matrices and to develop useful composites. Nanosilica was prepared from sodium silicate and dilute hydrochloric acid by polymer induced crystallization technique under controlled conditions. The silica surface was modified by silane coupling agent to decrease the agglomeration and thus to increase the reinforcement with polymer. The pristine nanosilica and modified nanosilica were used to make nano-micro hybrid composites. Short glass fibres and nylon fibres were used as microfillers. The hybrid nanocomposites based on Polypropylene (PP) and High density poly ethylene (HDPE) are prepared. The mechanical, thermal, crystallization and dynamic mechanical properties of the composites are evaluated. The thesis is divided into seven chapters.

Chapter 1 is an introduction and a review of the earlier studies in this field. Scope and objectives of the present work are also discussed.

The details and specifications of the materials used and the experimental procedures for the preparation and characterization of nanocomposites and nano-micro hybrid composites adopted in the present study are given in Chapter 2

Synthesis, characterization and modification of nanosilica is described in chapter 3. Nanosilica was synthesized by polymer induced crystallization route using sodium silicate, and hydrochloric acid under controlled conditions. Chitosan, second abundant biopolymer in nature was used as the polymer medium. The modification of silica was done using vinyl triethoxysilane. The silica was characterized by using X-ray diffraction (XRD), Scanning Electron Microscopy (SEM), Transmission Electron Microscopy (TEM), BET Adsorption and Infrared Spectroscopy (IR). Nanosilica prepared by this method had a particle size lower than that of the commercially available silica. Presence of chitosan in the reaction reduced the particle size of the synthesized silica. The modification of silica reduced the agglomeration of silica. XRD results showed that the silica was in amorphous state.

The potential use of nanosilica as reinforcing filler in polypropylene and high density polyethylene described in Chapter 4. The mechanical properties of the polypropylene-silica nanocomposites and HDPE-silica nanocomposites are presented. The mechanical properties of both composites with modified silica and maleic anhydride grafting of the polymers are also presented in this chapter. Modified nanosilica is found to be potential reinforcing filler in polypropylene and HDPE. Mechanical properties such as tensile properties, flexural properties and impact strength of the composites are found to improve with filler loading. Filler-matrix interaction improves upon modification of nanosilica. The nucleating efficiency of both silica and modified nanosilica altering the crystallizing behaviour of PP and HDPE was evaluated using DSC. Isothermal and non-isothermal methods were used for the study. Dynamic mechanical analysis and thermogravimetry were also carried out to understand the dynamic and thermal properties of the composites. Maleic anhydride grafting improves the overall property of the composites.

The effect of synthesized nanosilica and modified silica on short fibre reinforced PP composites is described in Chapter 5. Fibre loading was varied from 0 to 30 weight percentage. This chapter is divided into two sections. The effect of nanosilica/modified silica in short glass

fibre/polypropylene composite is given in Section 5A. The effect of maleic anhydride treatment in this nano-micro hybrid composite is also presented. The mechanical properties of the hybrid composites are found to improve with maleic anhydride treatment. Dynamic mechanical properties and thermal stability of the hybrid composite are also found to improve by maleic anhydride treatment. The nucleation effect of nano-micro hybrid is found to be increased by the presence of modified silica and maleic anhydride treatment. The effect of nanosilica/modified nanosilica in short nylon fibre/PP composite is described in Section 5 B. Mechanical properties, thermal stability, crystallization behaviour and dynamic mechanical analysis of the nano-micro hybrid composites are investigated. Maleic anhydride treatment improves the properties of the composites in this case also.

The nano-micro hybrid modification of HDPE is presented in Chapter 6. Nanosilica and modified nanosilica were used as nano fillers. The fibre loading was varied from 0 to 30 wt.%. This chapter is divided into two sections. The effect of nanosilica/modified silica in short glass fibre/HDPE composites is described in Section 6A. The mechanical properties of the hybrid composites are found to be improves by modification of silica. Dynamic mechanical properties, thermal stability and crystallization effect of the nano-micro hybrid composites are also found to depend on modified silica and maleic anhydride treatment. The effect of nanosilica/modified nanosilica in short nylon fibre/HDPE composite is described in Section 6 B. Mechanical properties, thermal stability, crystallization studies and dynamic mechanical analysis of the nano-micro hybrid composites were evaluated. The properties vary with the presence of silica, modified silica, fibre loading and maleic anhydride treatment.

The summary and conclusions of the study are given in Chapter 7.

# Contents

## Chapter 1

### Introduction

1.1 Introduction	2
1.2 Thermoplastic matrix for composite preparation	3
1.2.1 Polypropylene	5
1.2.2 High density polyethylene	7
1.3 Classification of composites	8
1.4 Short fibre reinforced thermoplastic composites	12
1.4.1 Fibre reinforcements used in composites	15
1.4.2 Reinforcing mechanism of short fibres	17
1.5 Nanocomposites	20
1.6 Silica	21
1.6.1 Production of silica	22
1.6.2 Nanosilica	23
1.6.3 Synthesis of nanosilica	24
1.6.4 Chitosan	24
1.6.5 Uses of nanosilica	25
1.7 Coupling agent	26
1.8 Hybrid composites	28
1.9 Scope and objectives of the present work	29

## Chapter 2

### Materials and Methods

2.1 Materials	37
2.2 Composite preparation	38
2.2.1 Melt mixing	39
2.2.2 Preparation of test specimen	39
2.3 Mechanical properties	40

2.3.1 Tensile properties	40
2.3.2 Flexural properties	40
2.3.3 Impact strength	41
2.4 Dynamic mechanical analysis (DMA)	41
2.5 Differential scanning calorimetry (DSC)	42
2.6 Thermogravimetric analysis (TGA)	43
2.7 Scanning electron microscopy (SEM)	44

### **Chapter 3**

#### **Synthesis, modification and characterization of nanosilica**

3.1 Introduction	47
3.2 Experimental	54
3.2.1 Experimental setup	54
3.2.2 Synthesis of nanosilica	56
3.2.3 Modification of nanosilica	57
3.3 Results and Discussion	58
3.3.1 Bulk density	58
3.3.2 Surface area	59
3.3.3 Infra red spectroscopy	60
3.3.4 X-Ray diffraction (XRD)	60
3.3.5 Scanning electron microscopy (SEM)	62
3.3.6 Transmission electron microscopy (TEM)	63
3.3.7 Thermogravimetric analysis (TGA)	64
3.3 Conclusions	65

### **Chapter 4**

#### **Thermoplastic - silica nanocomposites**

##### **Part - a**

##### **Polypropylene-silica nanocomposite**

4a.1 Introduction	71
4a.2 Experimental	73
4a.3 Results and discussion	73

4a.3.1 Polypropylene silica nanocomposites	73
4a.3.2 Effect of matrix modification on PP-silica nanocomposites	78
4a.3.3 Dynamic mechanical analysis	82
4a.3.4 Crystallization characteristics	87
4a.3.5 Thermogravimetric analysis	93
4a.4 Conclusions	95
<b>Part – b</b>	
<b>High density polyethylene-silica nanocomposites</b>	
4b.1 Introduction	103
4b.2 Experimental	104
4b.3 Results and discussion	104
4b.3.1 HDPE - silica nanocomposites	104
4b.3.2 Effect of matrix modification on HDPE-Silica nanocomposites	109
4b.3.3 Dynamic mechanical analysis	112
4b.3.4 Crystallization characteristics	115
4b.3.5 Thermogravimetric analysis	119
4b.4 Conclusions	121
<b>Chapter 5</b>	
<b>Modification of polypropylene - short fibre composite with nanosilica/modified nanosilica</b>	
<b>Part - a</b>	
<b>Polypropylene-glass fibre-silica hybrid nanocomposite</b>	
5a.1 Introduction	125
5a.2 Experimental	126
5a.3 Results and discussion	127
5a.3.1 Polypropylene-glass fibre composite	127
5a.3.2 Modification of PP-glass fibre composite with silica/modified silica	132
5a.3.3 Effect of matrix modification on the mechanical properties nano-micro hybrid composite	135
5a.3.4 Dynamic mechanical analysis	139

5a.3.5 Crystallization characteristics	143
5a.3.6 Thermogravimetric analysis	148
5a.4 Conclusions	150
<b>Part - b</b>	
<b>Polypropylene-nylon fibre-silica hybrid nanocomposites</b>	
5b.1 Introduction	153
5b.2 Experimental	154
5b.3 Results and discussion	154
5b.3.1 Polypropylene-nylon fibre composite	154
5b.3.2 Modification of PP-nylon fibre composite with silica/modified silica	159
5b.3.3 Effect of matrix modification on nano-micro hybrid composites	162
5b.3.4 Dynamic mechanical analysis	165
5b.3.5 Crystallization characteristics	169
5a.3.6 Thermogravimetric analysis	173
5b.4 Conclusions	175
<b>Chapter 6</b>	
<b>Modification of HDPE-short fibre composite with nanosilica/modified nanosilica</b>	
<b>Part – a</b>	
<b>High density polyethylene-glass fibre-silica hybrid nanocomposite</b>	
6a.1 Introduction	179
6a.2 Experimental	180
6a.3 Results and discussion	180
6a.3.1 High density polyethylene-glass fibre composite	180
6a.3.2 Modification of HDPE-glass fibre composite with silica/modified silica	183
6a.3.3 Effect of matrix modification on hybrid composites of HDPE	186
6a.3.4 Dynamic mechanical analysis	189
6a.3.5 Crystallization characteristics	193



6a.3.6 Thermogravimetric analysis	196
6a.4 Conclusions	198
<b>Part – b</b>	
<b>High density polyethylene-nylon fibre-silica hybrid nanocomposites</b>	
6b.1 Introduction	201
6b.2 Experimental	201
6b.3 Results and discussion	202
6b.3.1 High density polyethylene-nylon fibre composites	202
6b.3.2 Modification of HDPE-nylon fibre composite with silica/modified silica	205
6b.3.3 Effect of matrix modification on nano-micro hybrid composites of HDPE	208
6b.3.4 Dynamic mechanical analysis	211
6b.3.5 Crystallization characteristics	215
6b.3.6 Thermogravimetric analysis	219
6b.4 Conclusions	221
<b>Chapter 7</b>	
<b>Summary and conclusions</b>	223

# Chapter 1

## Introduction

The properties of polymer products are determined by their chemical structures, as well as processing steps and can be well tuned with additives. A number of additives such as fibrous or particulate fillers, antioxidants, colorants, processing aids etc. are used in engineering novel structures. The use of glass fibres to reinforce polymers such as polypropylene and polyamides in engineering applications is a well known example. Usually, fibrous loading levels range from 20 to 50 weight percent in engineering products. However due to the addition of this much filler the advantages of polymers over metals such as: ease of processing and low density has to be compromised at least to some extent.

In the current era of "Nanotechnology", expectations are running high concerning the use of nanosized additives to obtain fantastic performance even at low loadings. Nanoclays and carbon nanotubes (CNT) are the most widely employed nano fillers. Groundbreaking work was done at Toyota<sup>1</sup> by dispersing nanoclay in nylon-6 via in-situ polymerization of caprolactam. After that scientists are trying to disperse nanoparticles in polymers. At the IUPAC meeting in Paris (July, 2004), it was concluded<sup>2</sup> that real benefits of "nano-effects" in the polymer domain are still to be expected, if any. Many attempts were reported to disperse nanoclays and CNTs directly in polymer melts; but with only very little success. In many cases for nanocomposites the melt-viscosity increases and hence processibility decreased due to agglomeration and even entangling (for CNTs) of the nanoparticles.<sup>3</sup> As stated above, the properties of polymers are not determined by the chemical structure alone but equally well by the processing step and the use of additives to tune or boost the performance further. The use of smart additives will be the prime topic in the forthcoming decades and the use of nano-sized silica particles along with micro sized fibres as described in the thesis is likely to be a potential modifier.

The present study aims to investigate the use of synthesized nanosilica for modifying polymer based and polymer short fibre based nanocomposites to widen the spectrum of application of the polymer. A brief introduction to the subject is presented in this chapter. An outline of the principal objectives of the work is given at the end of the chapter.

## 1.1 INTRODUCTION

Polymers have played an important role since the beginning of life. DNA, RNA, proteins and polysaccharides are the well-known natural polymers which play a vital role in plant and animal life. Natural polymers have been exploited as materials for providing clothing, weapons, shelter, writing materials and other requirements. In the nineteenth century, natural polymers were modified to meet technical requirements and classical examples are nitrocellulose, cellophane and natural rubber. The fact that natural rubber (cis-polyisoprene) could be cross-linked (vulcanized) with sulphur (Goodyear 1847) stimulated the development of the rubber industry with useful products such as tyres for cars. The lack of supply of natural rubber during World War II from Indonesia, Malaysia, etc. to USA and Europe, triggered in fact the start of the synthetic rubber industry, based on synthetic polymer molecules such as SBR (Styrene-Butadiene Rubber). After Staudinger introduced the concept of polymers as chain molecules in the 1920s, synthetic polymer molecules have been made in the first half of the 20<sup>th</sup> century, e.g. the polyamides (nylons) by Carothers at DuPont, but with limited commercial success. The synthetic polymer (plastic) industry took really off the ground in the 1950s when Ziegler and Natta invented catalyst systems to produce stereo regular polymers such as (isotactic) polypropylenes and (linear) polyethylenes. The impact of their invention has been major as evidenced by a production volume of approx. 35 million tonnes/annum of polypropylene, viz. 7 kg per capita per annum!

A composite material can be designed when it is often desirable to have some of the properties of one material coupled with some of the properties of another material. Composites are prevalent in both nature and among engineered materials. When one breaks a rod of metal the polycrystalline nature becomes evident in the roughness of the surface of the break. The rocks, such as sandstone are aggregates of grains; some other rocks, such as granite, are aggregates of crystals. The study of composites in a

geological context is important to the oil industry and for the study of earthquakes. Construction materials such as wood and concrete are composites. Bone is a porous composite. Fibreglass and lightweight carbon fibre composites have found applications ranging from the aerospace industry to sports equipment.

Colloidal suspensions, emulsions, foams, slurries, and clays are all examples of composites. Clouds, fog, mist, and rain are composites of air and water. High-altitude clouds are composites of air and ice crystals. Suspensions of volcanic dust in the upper atmosphere are known to significantly perturb temperatures around the earth. Air itself is an inhomogeneous medium with fluctuations in density that cause the twinkling of stars. Sea ice is a composite of ice and brine pockets, and modeling of its properties is important in global climate prediction. Solid rocket propellant is a composite of aluminum particles in an oxidizing matrix. Even chocolate chip ice cream is a composite. Basically, composites are materials that have inhomogeneities on length scales that are much larger than the atomic scale (which allows us to use the equations of classical physics at the length scales of the inhomogeneities) but which are essentially (statistically) homogeneous at macroscopic length scales or at least some intermediate length scales.

## **1.2 THERMOPLASTIC MATRIX FOR COMPOSITE PREPARATION**

The matrix in reinforced plastics may be either a thermosetting or thermoplastic resin. The major thermosetting resins used in conjunction with glass-fibre reinforcement are unsaturated polyester resins and, to a lesser extent, epoxy resins. These resins have the advantage that they can be cured (cross-linked) at room temperature, and non-volatiles are liberated during curing.

Thermoplastics (or simply plastics) account for 70 percent of all polymers produced. Depending on the intrinsic properties, applications, volume and use, thermoplastics are further classified into:

### **Commodity Plastics**

Comprising the four major large volume plastics: poly(ethylene) (PE), poly(propylene) (PP), the combination of the latter two are often referred to as polyolefins, poly(vinyl chloride) (PVC) and poly(styrene) (PS).

## Engineering Plastics

Comprising the polymers possessing usually a better high temperature performance compared with the commodity plastics such as polyamides (Nylons), polyesters such as poly(ethylene terephthalate) (PET) and poly(butylene terephthalate) (PBT), poly(carbonate) (PC), poly(methyl methacrylates) (PMMA), poly(phenylene ether) (PPE) etc.

## Specialty Polymers

High performance engineering (HPE) thermoplastics such as poly(ether sulfone) (PES) and poly(ether ether ketone) (PEEK), intrinsic conducting polymers, etc.

The division of current polymers in the three categories mentioned above is, however, subject to change. For example the strong growth of PET in the past decades, notably in bottle applications, gives this polymer a commodity status. The same applies to some extent to poly(carbonate). In general Engineering Plastics show a trend towards *commoditization*, both in terms of volume and market price.

Various thermoplastics have been used as matrices for reinforcements. Typically, the matrix has considerably lower density, stiffness and strength than those of the reinforcing material, but the combination of matrix and reinforcement imparts high strength and stiffness, while still possessing a relatively low density. In a composite the matrix is required to fulfill the following functions:

- To bind together the reinforcements by virtue of its cohesive and adhesive characteristics
- To protect them from environments and handling.
- To disperse and maintain the desired orientation and spacing of the filler.
- To transfer stresses to the filler by adhesion and/or friction across the interface when the composite is under load, and thus to avoid any catastrophic propagation of cracks and subsequent failure of the composites.
- To be chemically and thermally compatible with the reinforcing fillers.
- To be compatible with the manufacturing methods which are available to fabricate the desired composite.

Thermoplastic matrices were developed to provide cheaper alternative to thermosets and to improve the upper use temperature of polymer matrix composites. Thermoplastics readily flow under stress at elevated temperatures, so allowing them to be fabricated into the required component; solidifies and retains their shape when cooled to room temperature.<sup>4</sup> These polymers may be repeatedly heated, fabricated and cooled and consequently scrap may be recycled. Unlike thermosets, thermoplastics are not cross-linked, and can therefore melt. They derive their strength and stiffness from the inherent properties of the monomer units and the very high molecular weight. They are semi crystalline or amorphous in nature. Thermoplastics have superior toughness to thermosets. Among thermoplastic resins used as the matrix in reinforced plastics, the largest tonnage group is the polyolefins, followed by nylon, polystyrene, thermoplastic polyesters, acetal, polycarbonate, and polysulfone. The choice of any thermoplastic is dictated by the type of application, the service environment, and the cost.

### **1.2.1 Polypropylene**

Polypropylene was first introduced in 1957. It was the Italian company Montecatini that succeeded in this polymerization. It is the lightest of the common plastics (specific gravity of about 0.9) has a higher softening point, lower shrinkage and immunity to stress-cracking. PP is made by the polymerization (by Ziegler process) of propylene monomer obtained from the cracking of petroleum products.<sup>5</sup> Presence of a methyl group attached to alternate carbon atom on the chain backbone can alter the properties of the polymer. Based on that the polymer can be made in isotactic (crystallizable) PP (i-PP), syndiotactic or atactic (noncrystallizable), PP (a-PP) forms (Figure 1.1).

Semicrystalline PP is a thermoplastic material containing both crystalline and amorphous phases. The relative amount of each phase depends on structural and stereochemical characteristics of the polymer chains and the conditions under which the resin is converted to final products such as fibres, films, and various other geometric shapes during fabrication by extrusion, thermoforming, or moulding.

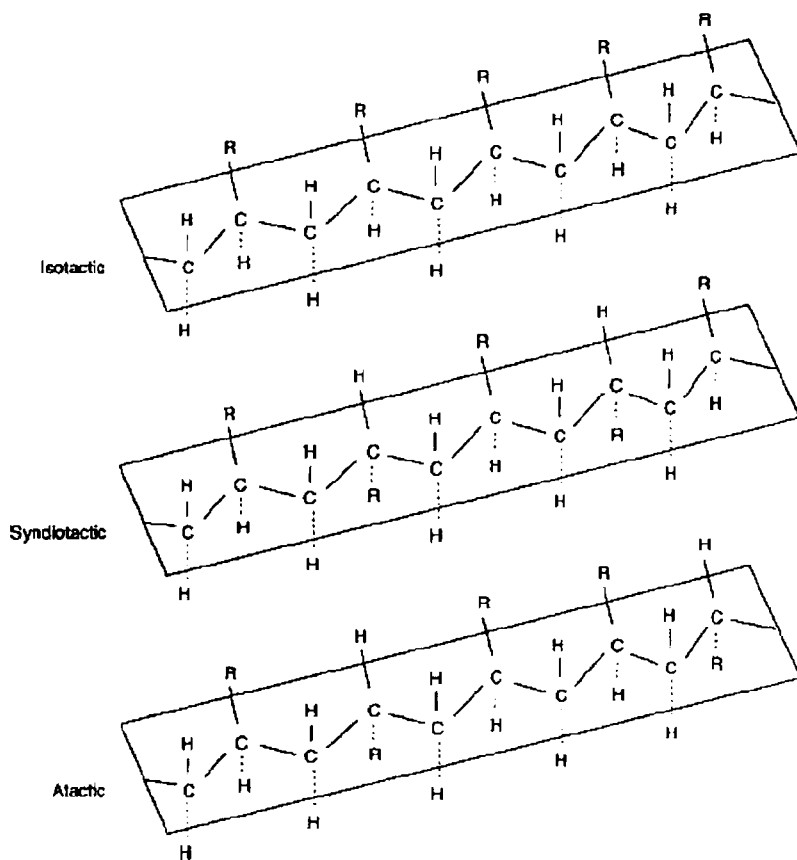


**Figure 1.1:** Stereochemical configurations of polypropylene

Polypropylene has excellent and desirable physical, mechanical, and thermal properties when used in room-temperature applications. It is relatively stiff and has a high melting point, low density, and relatively good resistance to impact. These properties can be varied in a relatively simple manner by altering the chain regularity (tacticity) content and distribution, the average chain lengths, the incorporation of a co-monomer such as ethylene into the polymer chains, and the incorporation of an impact modifier into the resin formulation. Isotactic PP has a melting point of about 165 °C and has excellent electrical properties, chemical inertness and moisture resistance.<sup>6</sup> PP is moulded into films, hollow ware, toys, bottles, automotive components, disposable syringes, battery cases, rope, carpeting etc.<sup>7</sup>

## 1.2.2 High density polyethylene

Polyethylene is a wax like thermoplastic softening at about 80-130° C with a density less than that of water. It is tough but has moderate tensile strength, is an excellent electrical insulator and has very good chemical resistance. The mechanical properties are very dependent on the molecular weight and on the degree of branching of the polymer.

High density polyethylene (Linear) (Figure 1.2) can be produced in several ways, including radical polymerization of ethylene at extremely high pressures, coordination polymerization of ethylene and polymerization of ethylene with supported metal-oxide catalysts. Typical linear polyethylene's are highly (over 90%) crystalline polymers, containing less than one side chain per 200 carbon atoms in the main chain. Melting point is near 127°C and density is in the range of 0.95- 0.97g/cm<sup>3</sup>.

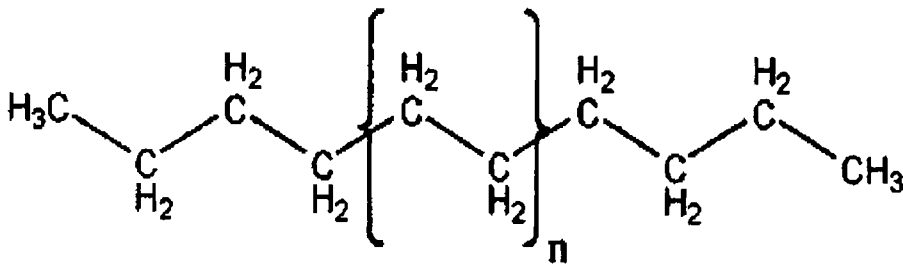


Figure 1.2: Molecular structure of HDPE

It is a colorless odorless tough waxy solid. Water absorption is less than 0.005% and it is insoluble in any solvent at room temperature but dissolves in many of the solvents above 100 °C. Its molecular weight ranges between 100,000 and 200,000. Most of the differences in properties between branched and linear polyethylene can be attributed to the higher crystallinity of the latter polymers, linear polyethylene's are decidedly stiffer than the branched material and have a higher crystalline melting point and greater tensile strength and hardness. The good chemical resistance of branched polyethylene is retained or enhanced, and such properties as low-temperature brittleness and low permeability to gases and vapors are improved in the linear material.

About 40% of the HDPE is used for the production of bottles and other containers by blow moulding. About 25% is used in the injection moulding of crates, pails, tubs, caps and closures and house wares. Other major uses are described below.



- The high molecular weight HDPE with frictional melt indices are used in the manufacture of carrier bags, garbage bag, drum and pipe.
- Medium molecular weight varieties ( $M_w=2.5 \times 10^5$ ) find applications as wrapping paper, grease proof paper for meat and flowering package.
- HDPE is used for the manufacture of pipes from 25 mm to 800 mm diameter for transport of water and chemicals.
- Used for making sheets for lining of chemical vessels and tank ducting for air conditioning, extraction of dust, fumes, humidification, for fabricating chimneys and large diameter pipes, vacuum forming of a variety of products.
- For making of monofilaments for fishing nets, tugs, ropes, twines, chemical fillers, woven or knotted sacks, sport netting, mosquito nets and curtain fly screens, fabrics for furniture cane for furniture etc.
- HDPE is preferred, when higher mechanical abuse, higher tear, temperature resistance, tensile and shear strength are required. It is used as coating on paper.
- HDPE is used for making cups and saucers, plates, dishes, safety helmets, housing for electric plugs, battery casing, toys and display boxes.

Similar end-uses with advantage of better rigidity, better resistance to breaking, better surface appearance and stability at boiling water temperatures. It could therefore supply both the specialty and the commodity. The expected annual growth rate of HDPE is 4% and about 40-50% of the annual global market size for the Philips catalyst is used for the production of HDPE.

### 1.3 CLASSIFICATION OF COMPOSITES

Composites can be classified in different ways according to

- a. The occurrence of the composites - **natural**, **synthetic**
- b. The matrix material - metal (**MMC**), ceramics (**CMC**), polymer (**PMC**)
- c. The form of their structural components - **fibrous** (fibres in a matrix), **laminar** (layers of materials) and **particulate** (particles in a matrix)

- d. The size of the constituents - **macro** ( $>10^{-6}\text{m}$ ), **micro** ( $10^{-6}\text{-}10^{-8}\text{m}$ ) and **nano** ( $10^{-9}\text{m}$ ).

Fibre reinforced composites contain reinforcements having lengths higher than cross sectional dimension. Fibrous reinforcement represents physical rather than a chemical means of changing a material to suit various engineering applications.<sup>8</sup> These can be broadly classified as shown in figure 1.3.

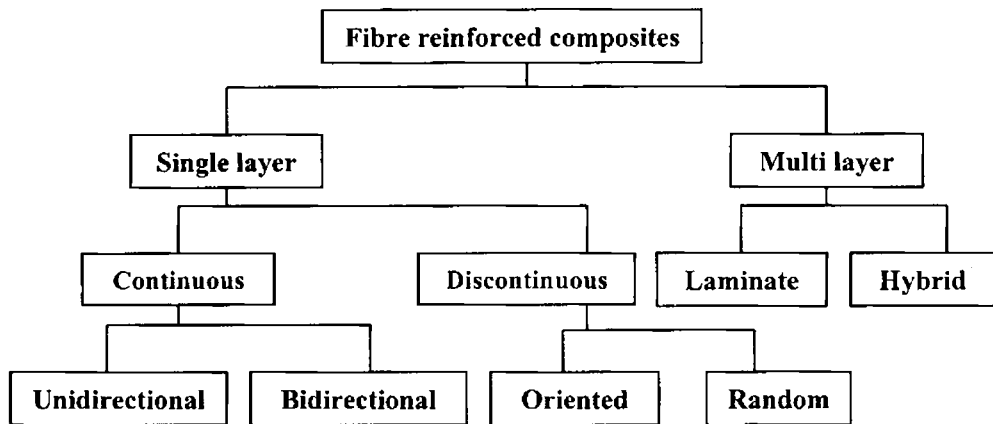


*Figure 1.3: Classification of fibrous composites*

Composites in which the reinforcements are discontinuous fibres or whiskers can be produced so that the reinforcements have either random or biased orientation. Material systems composed of discontinuous reinforcements are considered single layer composites. The discontinuities can produce a material response that is anisotropic, but in many instances the random reinforcements produce nearly isotropic composites. Continuous fibre composites can be either single layer or multilayered. The single layer continuous fibre composites can be either unidirectional or woven, and multilayered composites are generally referred to as laminates. The material response of a continuous fibre composite is generally orthotropic. Schematics of both types of fibrous composites are shown in figure 1.4.

Reinforcing fibre in a single layer composite may be short or long based on its over all dimensions. Composites with long fibres are called continuous fibre reinforcement and composite in which short or staple fibres are embedded in the matrix are termed as discontinuous fibre reinforcement (short fibre composites). In continuous fibre composites fibres are oriented in one direction to produce enhanced strength. In short fibre composites, the length of short fibre is not too high to allow individual fibres to entangle with each other nor too small for the fibres to lose their fibrous nature. The reinforcement is uniform in the case of composites containing well dispersed short fibres. There is a clear distinction between the behavior of short and long fibre composites.

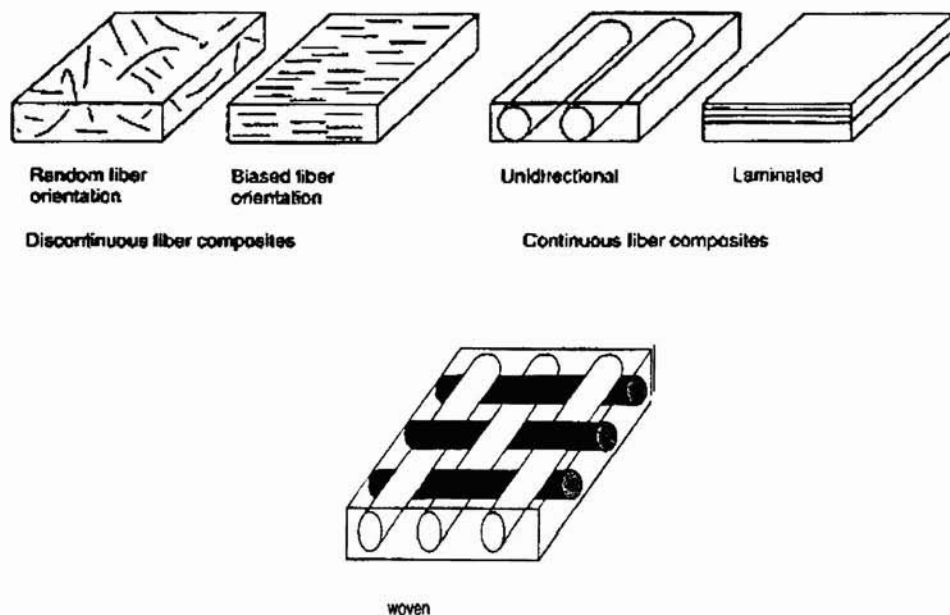


*Figure 1.4. Schematic representation of fibrous composite*

A laminate is fabricated by stacking a number of laminae in the thickness direction. Generally three layers are arranged alternatively for better bonding between reinforcement and the polymer matrix, for example plywood and paper. These laminates can have unidirectional or bi-directional orientation of the fibre reinforcement according to the end use of the composite. A hybrid laminate can also be fabricated by the use of different constituent materials or of the same material with different reinforcing pattern. In most of the applications of laminate composite, man made fibres are used due to their good combination of physical, mechanical and thermal behavior.

Composite materials incorporated with two or more different types of fillers especially fibres in a single matrix are commonly known as hybrid composites. Hybridisation is commonly used for improving the properties and for lowering the cost of conventional composites. There are different types of hybrid composites classified according to the way in which the component materials are incorporated. Hybrids are designated as i) sandwich type ii) interply iii) intraply and iv) intimately mixed.<sup>9</sup> In sandwich hybrids, one material is sandwiched between layers of another, whereas in interply, alternate layers of two or more materials are stacked in regular manner. Rows of two or more constituents are arranged in a regular or random manner in intraply hybrids while in intimately mixed type, these constituents are mixed as much as possible so that no concentration of either type is present in the composite material

The particulate class can be further sub divided into flake (flat flakes in a matrix) or skeletal (composed of a continuous skeletal matrix filled by a second material)

A composite whose reinforcement is a particle with all the dimensions are roughly equal are called particulate reinforced composites. Particulate fillers are employed to improve high temperature performance, reduce friction, increase wear resistance and to reduce shrinkage.<sup>10</sup> The particles will also share the load with the matrix, but to a lesser extent than a fibre. A particulate reinforcement will therefore improve stiffness but will not generally strengthen.

A particulate composite is characterized as being composed of particles suspended in a matrix. Particles can have virtually any shape, size or configuration. There are two subclasses of particulates: flake and filled skeletal: A flake composite is generally composed of flakes with large ratios of platform area to thickness, suspended in a matrix material. A filled/skeletal composite is composed of a continuous skeletal matrix filled by a second material (Figure 1.5).

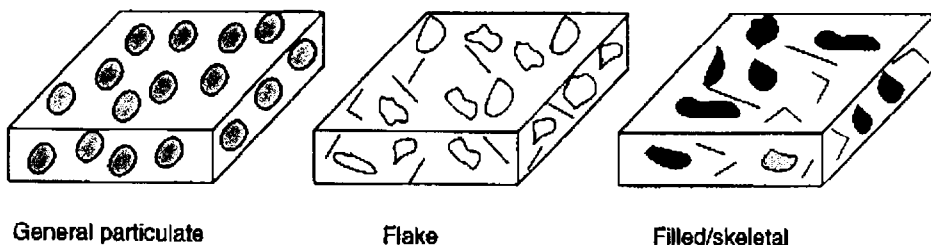


Figure 1.5: Schematic representation of particulate composite

## **1.4 SHORT FIBRE REINFORCED THERMOPLASTIC COMPOSITES**

Fibre reinforced composites consist of fibres of high strength and modulus embedded in a matrix with distinct interfaces between them. Fibre reinforcement improves the stiffness and the strength of the matrix. In the case of polymers that are not tough in the non-reinforced form, the toughness may also increase.<sup>11</sup> The fibre reinforced composites exhibit anisotropy in properties. The maximum improvement in properties is obtained with continuous fibre reinforcement. However, short fibre reinforced composites offer many advantages like ease of fabrication, low production cost and possibility of making complex shaped articles, over continuous fibre reinforcement. The performance of the composite is controlled by the fibres and depends on factors like aspect ratio, orientation of fibres and fibre-matrix adhesion. Discontinuous fibre reinforced composite form an important category of materials used in engineering applications. The use of fibre reinforced plastics (FRP) composites for the production of rebars and pre stressing tendons in civil engineering and transportation applications are becoming increasingly important in recent years.<sup>12</sup>

Major constituents in a fibre reinforced composite material are the reinforcing fibres and a matrix, which act as a binder for the fibres. Coupling agents and coatings used to improve the wettability of the fibre with the matrix and fillers used to reduce the cost and improve the dimensional stability are the other commonly found constituents in a composite.

Fibre-reinforced polymer composites are used in variety of applications such as aircraft, space, automotive, sporting goods, marine, infrastructure, electronics (printed circuit boards), building construction (floor beams), furniture (chair springs), power industry (transformer housing), oil industry (offshore oil platforms), medical industry (bone plates), oxygen tanks etc. Thermoplastic polymer composites are attractive because the addition of short fibres to the thermoplastic results in some very cost effective property improvements whilst retaining the processability of the thermoplastic. The potential to be easily repaired and/or re-shaped makes them easier to recycle and reuse compared with thermosetting matrix composites. The short fibre thermoplastic composite is manufactured by mixing prechopped fibre with thermoplastic in a twin-screw compounding extruder or internal mixer. In this case, some fibre breakage occurs

during processing and moulding so the lengths will be further reduced. The most effective technology is to introduce the continuous roving at a venting port directly into the molten thermoplastic. The high shear in the extruder ensures the fibre and plastic are intimately mixed; in this type of materials the fibres are dispersed as individual filaments instead of bundles or strands. The compound is then extruded through a 'spaghetti' die then either chilled & chopped into pellets or chopped directly with a hot face cutter. The resultant pellets are dried and injection moulded to get the product. They are typically about 4 mm in diameter and length and contain up to 30% by volume of fibre (up to 50% by weight according to the density of the polymer).

Passing continuous roving through liquid polymer using a fluidized bed of polymer powder or a crosshead die on an extruder makes the long fibre composite. This is then passed through a die to force the polymer to infiltrate the roving. Finally it is chopped into pellets, typically 10 mm long and 4 mm in diameter. When moulded, some fibre breakage occurs but the overall fibre length distribution will be much higher than for the short fibre material. This allows greater reinforcement efficiency to be attained, together with greater relative toughness.

In amorphous materials, heating leads to polymer chain disentanglement and a gradual change from a rigid to a viscous liquid. In crystalline materials, heating results in the sharp melting of the crystalline phase to give an amorphous liquid. Both amorphous and crystalline polymers may have anisotropic properties resulting from molecular orientation induced during processing and solidification. In composite systems, however, the properties are largely depending on the character of the filler reinforcement.

The attraction of short fibre composites are the enhanced mechanical properties and good processability. Stiffness is enhancement is depend on the stiffness of the fibre used, the fibre fraction, the length distribution and the orientation achieved in the moulding. Strength is also enhanced but not as much as the stiffness; this is due to a reduction in the fracture strain. This low fracture strain, often only 1-2%, is some times an embarrassment but the impact energy

is often enhanced by fibre reinforcement. There are two further important effects: the heat distortion temperature is raised and the coefficient of thermal expansion is reduced. This allows the fibre reinforced grade to be utilized at higher service temperatures, reduces in-mould shrinkage and generally improves dimensional stability. Dimensional stability is very important for intricate components, which need to be manufactured to close tolerances. Some typical properties are given in table 1.1.

**Table 1.1: Typical properties of selected short fibre reinforced thermoplastics**

Polymer	Fibre	$V_f$	E (GPa)	$X_T$ (MPa)	Charpy impact (KJm <sup>-2</sup> )	HDT (°C)
Polypropylene	None	0	1.9	39	2.7	60
Polypropylene	Glass	0.20	7.5	110	8.0	155
Polyamide 6,6	None	0	3.2	105	>25	100
Polyamide 6,6	Glass	0.20	10	230	40	250
Polyamide 6,6	Carbon	0.20	20	250	10	255
Polycarbonate	Glass	0.20	9.0	135	40	160
Polyoxymethylene	Glass	0.20	9.0	140	9.0	165
Polyphenylenesulphide	Glass	0.20	11	155	20	263
Polyphenylenesulphide	Carbon	0.20	17	185	20	263
Poly ether ether ketone	Carbon	0.20	16	215	-	310

E= Young's modulus,  $X_T$  = Tensile strength, HDT= Heat distortion temperature

These polymer composite systems are often termed 'engineering compounds' because their mechanical properties extend beyond the commodity levels expected from bulk polymers and they are used in multicomponent compounds for specific applications. Compounds may include colorants, viscosity modifiers, stabilizers, matrix modifiers, interfacial bond enhancers or secondary fillers.

The commodity polymers are typically used in combination with short fibre reinforcement. Mineral fillers are also commonly used in lower performance applications. E-glass fibres are used in the vast majority of reinforced injection moulding compounds on cost grounds, but carbon fibres (usually high strength type) and Kevlar type fibres may be compounded for specialist applications. Conductive fibres such as steel are used to impart dielectric preproperties.

At the turn of the century several promising projects in industry concerning the development of novel plastics, e.g. the polyketones at Shell, were terminated. It becomes increasingly difficult to introduce new polymers in the market in view of the general trend of *commoditization* with a strong focus on cost reduction by increasing the scale of operations, e.g. polyolefin plants with a capacity up to 500 kilotonnes per annum. The world of plastics has seemingly become mature and no new polymers with market potential for engineering applications are expected in the coming decades.<sup>2</sup> Consequently, the focus is on exploring the ultimate performance of existing polymers.

### **1.4.1 Fibre Reinforcements used in composites**

Fibres are the principal constituents in a fibre-reinforced composite material. They occupy the largest volume fraction in a composite laminate and share the major portion of the load acting on a composite structure. Proper selection of the fibre type, fibre volume fraction, fibre length, and fibre orientation is very important, since it influences the density, tensile strength and modulus, compressive strength and modulus, fatigue strength as well as fatigue failure mechanisms, electrical and thermal conductivities and cost of a composite. Reinforcements are of two types—synthetic and natural.

#### **1.4.1.1. Synthetic fibres**

##### **a. Glass fibres**

The attempt to use glass fibre as an apparel material was highlighted at the Columbian Exposition in Chicago in 1893. It was the second man-made fibre, next to rayon, to be of commercial importance. Glass fibre is the best known reinforcement in high performance composite applications due to its appealing combination of good properties and low cost. The major ingredient of glass fibre is silica which is mixed with varying amounts of other oxides. The different types of glass fibres commercially available are E and S glass. The letter 'E' stands for 'electrical' as the composition has a high electrical resistance and 'S' stands for strength.<sup>13,14,15</sup> Chopped strands ranging in length from 3.2 to 12.7 mm (0.125–0.5 in.) are used for making short glass fibre composite in injection-moulding operations.

##### **b. Carbon fibres**

Carbon fibres are commercially manufactured from three different precursors - rayon, polyacrylonitrile (PAN) and petroleum pitch. They have high tensile strength—



weight ratios, very low coefficient of linear thermal expansion (which provides dimensional stability in such applications as space antennas), high fatigue strengths, and high thermal conductivity. Their high cost has so far excluded them from widespread commercial applications. They are mainly used in aerospace industry due to its outstanding mechanical properties combined with low weight.

#### c. Aramid fibres

Aramid fibres are highly crystalline aromatic polyamide fibres that have the lowest density and the highest tensile strength-to-weight ratio among the current reinforcing fibres. Kevlar is the trade name of aramid fibres available in market. They are used in many marine and aerospace applications where lightweight, high tensile strength, and resistance to impact damage. The major disadvantages of aramid fibre-reinforced composites are their low compressive strengths and difficulty in cutting or machining

#### d. Polyolefin's

The most common example of high strength polyolefin fibre is ultra high molecular weight polyethylene (UHMWPE). The potential applications of polyolefin fibres include ballistic protection and sporting goods.

**Table 1.2:** Mechanical properties of some mineral and synthetic fibres

[Ref: Bledzki A. K. and Gassan J., *Prog. Polym. Sci.* (1999) **24**: 221]

Fibre	Sp. Gravity	Tensile strength(GPa)	Young's Modulus(GPa)	Strain to Failure (%)
Nylon 66	1.14	1.10	5.52	18
Kevlar 49	1.45	3.62	131	2.8
E-Glass	2.54	3.45	72.4	4.8
Carbon	1.76	3.20	86.9	1.4
Aramid	1.40	3-3.15	6.3-6.7	3.3-3.7

#### 1.4.1.2. Natural fibres

One of the major renewable resource materials throughout the world is natural fibres. There are about 2000 species of useful fibre plants in various parts of the world and these are used for many applications. Jute, sisal, hemp, remi, sisal, coconut and coir, the major source

of natural fibres, are the examples of natural fibres. Some of them have aspect ratios  $>1000$  and can be woven easily. Recently polymer composites are prepared by replacing the more expensive and non-renewable synthetic fibres.

Natural fibres are classified into three major types as animal fibres, vegetable fibres and mineral fibres. All animal fibres such as silk, wool and mohair are complex proteins. They are resistant to most organic acids and to certain powerful mineral acids. They constitute the fur or hair that serves as the protective epidermal covering of animals. Silk is an exception to this, which is extruded by the larvae of moths and insects and is used to spin their cocoons. It is the only filament that commonly reaches a length of more than 1000 m. Several silk filaments can be gathered to produce textile yarn and staple form is used to manufacture spin yarns. Naturally crimped wool fibres produce air trapping yarns that are used for insulating materials. An important class of naturally occurring mineral fibre is asbestos.

Natural fibre composites have following advantages

1. They are environment-friendly, that is they are biodegradable, energy consumption to produce them is very small.

2. The density of natural fibres is in the range of  $1.25-1.5 \text{ g/cm}^3$  compared with  $2.54 \text{ g/cm}^3$  for E-glass fibres and  $1.8-2.1 \text{ g/cm}^3$  for carbon fibres.

3. The modulus-weight ratio of some natural fibres is greater than that of E-glass fibres, which means that they can be very competitive with E-glass fibres in stiffness-critical designs.

4. Natural fibre composites provide higher acoustic damping than glass or carbon fibre composites, and therefore are more suitable for noise attenuation, an increasingly important requirement in interior automotive applications.

5. Natural fibres are much less expensive than glass and carbon fibres.

### **1.4.2 Reinforcing Mechanism of Short Fibres**

The reinforcing mechanism of fibre in a unidirectional composite can be explained as follows. The composite satisfies the equation 1.1 when a tensile or compressive load is applied parallel to the fibre direction. This equation is applicable under perfect conditions of adhesion between fibre and matrix.<sup>16</sup>

$$\varepsilon_c = \varepsilon_f = \varepsilon_m \quad 1.1$$

where  $\varepsilon_c$ ,  $\varepsilon_f$  and  $\varepsilon_m$  are the strain in composite, fibre and matrix respectively. If it is assumed that both fibres and matrix behave elastically, then the following equations can be applied.

$$\sigma_f = E_f \varepsilon_f \quad 1.2$$

$$\sigma_m = E_m \varepsilon_m \quad 1.3$$

Hence

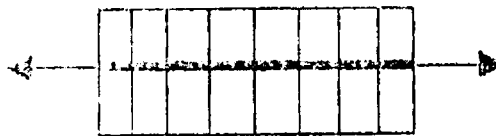
$$\sigma_c / E_c = \sigma_m / E_m = \sigma_f / E_f \quad 1.4$$

where  $\sigma_c$ ,  $\sigma_f$  and  $\sigma_m$  are stress developed in composites, fibre and matrix respectively. Similarly,  $E_c$ ,  $E_f$  and  $E_m$  are the modulus of composites, fibre and matrix respectively. Generally  $E_f$  is greater than  $E_m$  and so the stress in the fibre is greater than that in the matrix. Thus the fibre can bear a major part of the applied load. In the analysis of long fibre-reinforced composites, any effect associated with fibre ends are neglected. But in the case of short fibre reinforced composites, the end effects become progressively significant due to the decrease in aspect ratio of the fibre. This result in the reduction of fibre efficiency in reinforcing the matrix and also causes an early fracture of the composite.

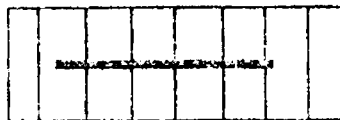
Consider an oriented fibre composite in which fibres are aligned parallel to the direction of application of force. A single fibre is embedded in a matrix of lower modulus. Imagine perpendicular lines running through the fibre-matrix interface in a continuous manner in the unstressed state as shown in the figure 1.6b. The matrix and the fibre will experience different tensile strains because of their different moduli. When the composite is loaded axially, the longitudinal strain in the matrix will be higher than that in the adjacent fibre due to lower modulus of the former. When force is applied, the imaginary vertical lines in the continuous fibre composite will not be distorted (Fig.1.6a). But these lines in short fibre composite will be distorted as in figure 1.6c because at the region of fibre ends, the matrix will be deformed more than that in the region along the fibre. This difference in the longitudinal strains creates a shear stress distribution around the fibres

in the direction of the fibre axis and so the fibre is stressed in tension. The applied load is transferred from matrix to fibre across the interface because of this shear stress distribution.

When mechanical force is applied to the polymeric matrix, it spreads smoothly through the matrix until it reaches the matrix- fibre interface. If the interface is well bonded, the stress is transferred across it into the fibre and then spread throughout the fibre. This process occurs at all the fibre-matrix interfaces in the composite. Thus it is obvious that load will be transferred to the fibre only if the interface is strong and a perfect bond exists between the two constituents. Hence strong interface is a must for high reinforcing efficiency.



1.6a Continuous fibre composite deformed



1.6b. Short fibre composite un-deformed



1.6c Short fibre composite deformed

**Figure 1.6:** Effect of stretching force on the strain around long and short fibre in a low modulus matrix

## 1.5 NANOCOMPOSITES

The materials made of two or more phases one of which has at least one dimension in a nanometric size range are called nanocomposites.<sup>17</sup> Particles in nanometer region are about 100-1000 times the size of a typical atom. The phases may be inorganic-inorganic, inorganic-organic or organic-organic and the resulting material may be amorphous, crystalline or semi-crystalline.<sup>18</sup> The concept of enhancing properties and improving characteristics of materials through the creation of multiple-phase nanocomposites is not recent. The idea has been practiced ever since civilization started and humanity began producing more efficient materials for functional purposes. In addition to the large variety of nanocomposites found in nature and in living beings (such as bone), an excellent example of the use of synthetic nanocomposites in antiquity is the constitution of Mayan paintings developed in the Mesoamericas. Characterization of these painting samples reveals that the structure of the paints consisted of a matrix of clay mixed with organic colorant (indigo) molecules. They also contained inclusions of metal nanoparticles encapsulated in an amorphous silicate substrate, with oxide nanoparticles on the substrate.<sup>19</sup> Bone is an excellent example of a self-healing biological nanocomposite in which an organic host phase is formed, followed by highly regulated mineralization processes. The basic structure of bone is a mineralized collagen fibril (matrix) consisting of on average 65% mineral (hydroxyapatite crystals), the remainder being organic material and water. Nanocomposites display new and some times improved mechanical, electronic, catalytic, optical and magnetic properties not exhibited by the individual phases or by their macrocomposite and microcomposite counterparts. The basic reason for this improvement is not completely understood. However, scientists believe it is related to confinement. "Quantum size" effects, and some times coulombic charging effects originating from the ultrafine sizes, morphology, and interfacial interactions of the phases involved.<sup>20,21,22</sup> The outstanding reinforcement of nanocomposite is primarily attributed to the large interfacial area per unit volume or weight of the dispersed phase. The nanolayers have much higher aspects ratio than typical microscopic aggregates.<sup>23,24</sup>

The major advantages of nanocomposites over conventional composites are:

1. Lighter weight due to low filler loading
2. Low cost due to fewer amount of filler use

3. Improved properties such as mechanical, thermal, optical, electrical, barrier etc., compared with conventional composites at very low loading of filler.

Three types of nanocomposites can be distinguished depending upon the number of dimensions of the dispersed particles in the nanometer range.<sup>25</sup> as follows,

1. Nanocomposites that can be reinforced by isodimensional nanofillers which have three dimensions in the nanometer range. Eg:-Spherical silica nanoparticles obtained by in-situ sol-gel methods or by polymerization promoted directly from their surface.<sup>26,27,28</sup>
2. Nanocomposites which can be reinforced by fillers which have only two dimensions in the nanometer scale. Eg:- Carbon nanotube or cellulose whiskers.<sup>29</sup>
3. The reinforcing phase, in the shape of platelets, has only one dimension on a nano level. Eg:- Clays and layered silicates.

Polymer based organic/inorganic nanocomposites have gained increasing attention in the field of materials science.<sup>30,31,32</sup> Effect of acrylic polymer and nanocomposite with nano-SiO<sub>2</sub> on thermal degradation and fire resistance of ammonium polyphosphate–dipentaerythritol–melamine (APP–DPER–MEL) coating was studied by Zhenyu and co workers.<sup>33</sup> Effect of microstructure of acrylic copolymer/terpolymer on the properties of silica based nanocomposites prepared by sol–gel technique was studied by Patel et al.<sup>34</sup> Bandyopadhyay et al<sup>35</sup> studied the reaction parameters on the structure and properties of acrylic rubber/silica hybrid nanocomposites prepared by sol-gel technique.

## 1.6 SILICA

Silicon dioxide or Silica (SiO<sub>2</sub>) is one of the most abundant oxide materials in earth's crust. It exist both in the pure state and in silicates, (e.g., in quartz, agate, amethyst, chalcedony, flint, jasper, onyx and rock crystal), opal, sand, sandstone, clay, granite and many other rocks. Usually it is insoluble in water, slightly soluble in alkalies and soluble in dilute hydrofluoric acid. It's pure form is colorless to white. It exists in two forms, amorphous and crystalline (quartz, tridymite, cristobalite). In crystalline form, the structures are characterized by tetrahedral configuration of atoms within the crystals, whereas in the amorphous form, the SiO<sub>4</sub> (silicate) subunits show no regular lattice

pattern. In silicon dioxide, silicon atom uses d orbitals for bonding and hence  $\text{SiO}_2$  exists as infinite three-dimensional structures and it is a high melting solid.<sup>36</sup> The amorphous silica absorbs about 4% moisture and can be represented as  $\text{SiO}_2 \cdot n\text{H}_2\text{O}$ . It consists of silicon and oxygen arranged in a tetrahedral structure. Surface silanol concentration (silanol groups  $-\text{Si}-\text{O}-\text{H}$ ) influence the degree of hydration. A general silica structure is depicted in figure I. 7.

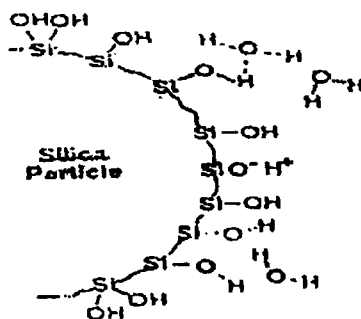
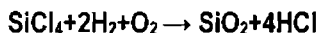
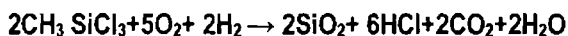


Figure I. 7: Surface of silica

### 1.6.1 Production of silica

Two methods have been used in preparing nanoscale silica: the gas phases (or the drying method) and the deposition preparation method (or the wet method).

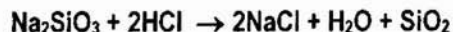
The principle of the gas-phase method is burning the silica precursor under an atmosphere of pure hydrogen gas and purified air (oxygen). This burning process is shown below: colloidal pyrogenic silica is produced by reaction of silicon tetrachloride at high temperatures with water



The reaction products are quenched immediately after coming out of the burner. Pyrogenic silica is too active and expensive.<sup>37</sup> Fumed or pyrogenic silica is silicon dioxide containing less than 2% combined water.

The second method (wet method) is to aggregate the nanoparticles with a depositing reagent such as ammonia or amine. First, a precursor of either  $\text{Na}_2\text{SiO}_3$  or  $\text{CaSiO}_3$  is used to prepare nanoparticles of silica by reaction with hydrochloric acid.

Acidification of alkali silicate solutions under controlled conditions produces precipitated silica.<sup>38</sup>



Precipitated silica is silicon dioxide containing about 10-14% water. They are reinforcing fillers giving composites of high tensile strength, tear resistance, abrasion resistance and hardness.

The smallest physically observable primary particle for precipitated silica is about 15-20  $\mu\text{m}$  and for fumed silica it is about 15  $\mu\text{m}$  in size. The surface forces of the small primary particles are so high that many particles agglomerate to form the so called secondary particles. At present, silica is mainly used in fields such as coatings, engineering plastics, automobile tyres etc.

### 1.6.2 Nanosilica

Nanosilica consists of spherical particles having a diameter less than 100 nm. Chemically speaking, they are made of silicon and oxygen atoms (Figure 1.8).



*Figure 1.8: Chemical structure of nanosilica*

Although silica was up to now widely used in polymer formulation as additives to master the system rheology and enhance mechanical properties of the polymers, nanosilica throws the door wide open for new applications. Silica synthesis evolved during last decades from thermal hydrolysis of silane resulting in not easily dispersible aggregated, nanoparticles to sol-gel process resulting in well-defined nanoparticles highly compatible with the targeted matrix. Processes enabling chemically tuned and well integrated particles together with the nanoscale effect are a highway to high performance nanocomposite materials having enhanced mechanical properties and excellent surface properties.



### 1.6.3 Synthesis of Nanosilica

Several methods are used to produce nanosilica from various sources.<sup>39</sup> A cheap and environment friendly route towards the synthesis of Polyvinyl alcohol/nanosilica hybrid composites has been presented by Tapasi et al.<sup>40</sup> This is a sol-gel method in which the acid plays a catalytic role in enhancing sol-gel condensation of silicon alkoxides within polyvinyl alcohol. First colloiddally stable silica was prepared by the acid neutralization with an objective to increase the gelation time and decrease rate of self-condensation of silica. At lower PVA concentration the silica has a tendency to undergo self-condensation and at higher PVA concentration, co-condensation occurs.

Nanosilica can be synthesized by precipitation method using sodium silicate and hydrochloric acid in presence of a polymeric dispersing agent. Polyvinyl alcohol, starch and carboxyl methyl cellulose were found to be good dispersing agent because they are macromolecules and contain a large number of hydroxyl groups per molecule.

### 1.6.4 Chitosan

Chitosan (*N*-glucosamine) is usually obtained by the chemical or enzymatic deacetylation of chitin (*N*-acetylglucosamine)<sup>41</sup> obtained from the shell of commercially harvested *Arthropoda*, such as shrimp, crab etc. Chitin is a homopolymer of 1-4 linked 2-acetamido-2-deoxy- $\beta$ -D-glucopyranose with some of the deacetylated glucopyranose residues (2-amino-2-deoxy- $\beta$ -D-glucopyranose). Chitin is considered the second most plentiful biomaterial, following cellulose. Chitin is insoluble in most common solvents, whereas chitosan dissolves in many common aqueous acidic solutions. Chitosan has found applications in many areas such as agriculture, paper, textiles, wastewater treatment, medical & pharmaceutical uses and nutritional dietary additive.<sup>42</sup>

Chitosan is a unique basic polysaccharide and most commercial and laboratory products tend to be a copolymer of *N*-acetylglucosamine (NAG) and *N*-glucosamine repeat units. The ratio of two repeating units depends on the source and preparation of chitosan, but the glucosamine units predominate. The structure of chitosan is similar to that of cellulose, except at carbon-2, where the hydroxy group of cellulose is replaced by an amino group.

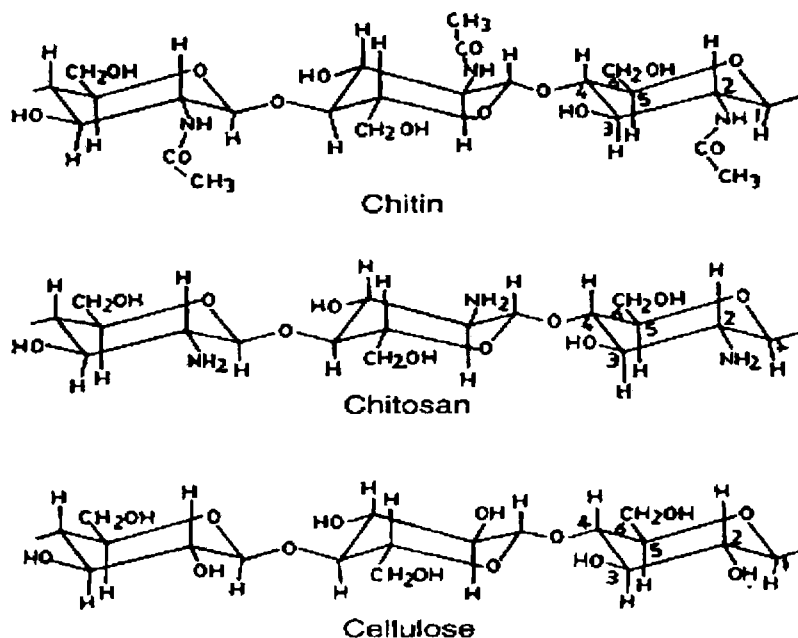


Figure 1.9: Structural unit of Chitin, Chitosan and Cellulose

The easy availability and the presence of plenty of hydroxyl groups are the main criteria for the selection of chitosan as dispersing medium for the preparation of nanosilica.

### 1.6.5 Use of nanosilica

1. Nanosilica reinforced with elastomers improves modulus, elongation, tear strength, and abrasion resistance of the product. They are used in shoes, tires, pipes etc.
2. The properties of polymers like flame retardancy, barrier properties, transparency and scratch resistance enhanced by nanosilica.
3. It is used in drug encapsulation, as catalytical vehicles and supports, preparations, particular calibration stands, chromatography, other separations and catalysis
4. Due to their optimal property, nanosilica is used in battery separators.
5. In opto-electronics nanosilica is used in protective coatings and encapsulation of electro-optically active materials.

6. It has been found that silica aero-gels coated on surface of granular activated carbon has four times more ability to remove uranium, chromium and arsenic from water supplies.
7. Nano- sized silica abrasives are being researched for use in chemical-mechanical polishing of copper, to minimized mechanical stress during polishing and reduce defects such as surface scratches, copper peeling, dishing and erosion.
8. Nanosilica filled room temperature vulcanized silicone rubber has higher erosion resistance, lower hydrophilicity and lesser surface roughness and which is used as insulators in coastal areas
9. The film of nanosilica known as Xerocoat, when applied to glass/mirror, cuts unwanted reflections from glass, letting more light through, hence reducing fogging and improves vision.
10. Adsorption as a carrier for liquid active ingredients (Vitamines A and E and choline chloride for animals, dispersants and surfactants)

## 1.7 COUPLING AGENT

The properties of a polymer cannot enhance unless there is a good adhesion between filler and matrix polymer. The functionality of the filler is controlled by surface treatments which is used to bond an organic molecule either chemically (covalent bond) or physically (coating of waxes, starches etc.) to the filler surface. A coupling agent is a substance that couples or bonds the filler to the polymer matrix.<sup>43</sup> To do this effectively, the coupling agent must have a unique structure. On one hand, it must be able to interact with the filler, which is polar in nature, while on the other hand, it must be compatible with the nonpolar molecular chains of the polymer.

The use of coupling agents started in early 1940, marketed as Volan A for use in polyester-glass fibre reinforced plastic. They are now used with particulate fillers like silica, silicates and clays for use in rubbers.<sup>44,45</sup> Titanium coupling agents have the general formula  $(RO)_m-Ti-(OX-R-Y)_n$  [eg: isopropyl tri(dioctyl pyrophosphide)titanate].

Silane coupling agents belong to a class of organosilane compounds having at least two different types of reactive groups bonded to the silicon atom in a molecule. One type of the reactive groups (eg: methoxy, ethoxy, silanolic hydroxyl groups etc.) are reactive with various inorganic materials such as glass, silica, metals, to form a chemical bond with surface of inorganic filler while the other type of the reactive groups (eg: vinyl, epoxy, methacryl amino, mercapto etc.) are reactive with various kinds of organic materials or matrix to form chemical bond.<sup>46</sup> Some of silane coupling agents is given in table 1.3. The type of functional group needed depends on the chemical structure of the polymer. For polymers that have functional groups present in their backbone, it is easy to select a silane with a specific organofunctional group with which it will react. For example, in polyamides, silanes that have amino groups are commonly used. The abundance of carboxylic acid end groups, present along the polyamide molecular chain, provides reaction sites for the silane amine groups.

**Table 1.3: Silane coupling agents**

Classification	Chemical nature	Molecular Weight	Specific gravity 25°C
Vinylsilane	Vinyltrichlorosilane	161.5	1.26
	Vinyltris( $\beta$ -methoxyethoxy)silane	208.4	1.04
	Vinyltriethoxysilane	190.3	0.90
	Vinyltrimethoxysilane	148.2	0.97
Acryloxy	3-metacryloxypropyl-trimethoxysilane	248.4	1.04
	$\beta$ -(3,4epoxycyclohexyl)-ethyltrimethoxysilane	246.4	1.06
Epoxy silane	<i>r</i> -glycidoxypropyl-trimethoxysilane	236.3	1.07
	<i>r</i> -glycidoxypropyl-methyldiethoxysilane	248.4	0.98
Aminosilane	N- $\beta$ (aminoethyl)- <i>r</i> -Aminopropyl-Trimethoxysilane	222.4	1.02
	N- $\beta$ (aminoethyl)- <i>r</i> -Aminopropyl-Methyldiethoxysilane	206.4	0.97
	3-aminopropyl-Triethoxysilane	221.4	0.94
Others	N-phenyl- <i>r</i> -Aminopropyl-trimethoxysilane	255.4	1.07
	<i>r</i> -mercaptopropyl-trimethoxysilane	196.4	1.06
	<i>r</i> -chloropropyl-trimethoxysilane	198.7	1.08

The silane coupling agents are used to improve the performance of fibre reinforced plastics, paints & surface coatings, adhesives, modification of surface properties of inorganic fillers etc.<sup>47</sup> The modification of nanosilica with silane coupling agent decreases the agglomeration tendency of nanoparticles.

## 1.8 HYBRID COMPOSITES

The strength and stiffness of the composite is mainly determined by the reinforcement. Composite reinforcement may be in the form of fibres, particles or whiskers. Particles have no preferred directions and are mainly a means to improve properties or lower the cost of material. The composite development based on reinforcement of two or more different types of fillers in a single matrix leads to multi-component composites (Hybrid composites) with a great diversity of material properties. The reinforcement may be different types of fibres, particulate fillers or both. Research has revealed that the behavior of hybrid composites appears to be the weigh sum of the individual components in which there is a more favorable balance between the advantages and disadvantages inherent in any composite material.<sup>48</sup> The properties of hybrid composites are controlled by factors such as nature of matrix, nature, length and relative composition of the reinforcements, fibre matrix interface and hybrid design.<sup>49</sup> Sisal and glass fibres are good examples of hybrid composites possessing very good combined properties.<sup>50</sup> Due to the superior properties of glass fibres, the mechanical properties of the hybrid composites increase with increase in the volume fraction of glass fibres. Thomas et al. have studied the properties of sisal/sawdust hybrid fibre composites with phenol formaldehyde resin as a function of sisal fibre loading.<sup>51</sup> It was found that mechanical properties like tensile and flexural strength increased with sisal fibre content. This is due to the fact that the sisal fibre possesses moderately higher strength and modulus than saw dust. Mishra et al<sup>52</sup> studied the mechanical properties of sisal and pineapple /glass fibre reinforced polyester composites. They found that the addition of small amount of glass fibres to the pineapple leaf fibre and sisal fibre reinforced polyester matrix enhanced the mechanical properties of the resulting hybrid composites. Rozman et al<sup>53</sup> studied the tensile and flexural properties of polypropylene/oil palm/glass fibre hybrid composites and found that incorporation of both fibres into the polypropylene matrix improved the tensile and flexural strength by the increasing level of overall fibre loading. Junior et al<sup>54</sup> used plain weaved hybrid ramie-cotton fibres as reinforcement for polyester matrix. The tensile behavior was

dominated by the volume fraction of the ramie fibres aligned in the test direction. Cotton fibre had a minor reinforcement effect. This was due to the weak cotton polyester interface as well as poor cotton alignment. Hybrid composites containing glass fibre mat and coir fibre mat in polyester matrix were prepared by Rout et al.<sup>55</sup> Hybrid composites containing surface modified coir fibres showed significant improvement in flexural strength and reduced water absorption. Sreekala et al.<sup>56</sup> prepared high performance phenol formaldehyde composite reinforced with oil palm and glass fibres. It has been found that there exists a positive hybrid effect for the flexural modulus and unnotched impact strength. Natural rubber composite reinforced with sisal/oil palm, sisal/coir hybrid fibres were prepared by Maya et al.<sup>57</sup> and Haseena et al.<sup>58</sup> found that the hybridization had a significant effect in improving the mechanical properties of the natural rubber composite when compared with the composite containing individual fibres.

The hybrid composites based on particulate fillers and fibres has also been studied.<sup>59,60,61</sup> Synthesis, fabrication, mechanical, electrical, and moisture absorption study of epoxy polyurethane-jute and epoxy polyurethane-jute-rice/wheat husk hybrid composites was reported by Mavan et al.<sup>62</sup> Jamal and co workers studied the tensile properties of wood flour/kenaf fibre polypropylene hybrid composites.<sup>63</sup> Study on morphological, rheological, and mechanical properties of PP/SEBS-MA/SGF hybrid composites was done by Mohseni et al.<sup>64</sup> Property optimization in nitrile rubber composites via hybrid filler systems was reported by Nugay.<sup>65</sup> Rheological behavior of hybrid rubber nanocomposite was studied by Bandyopadhyay and co workers.<sup>66</sup>

## **1.9 SCOPE AND OBJECTIVES OF THE PRESENT WORK**

At present, the area of additives in polymers is ill-defined and often lacks a proper scientific understanding. In the late 1980s, Wu<sup>67</sup> proposed, for nylon/rubber composites, that the matrix ligament thickness<sup>68</sup> is the single parameter in determining the improvement in mechanical properties of plastics, especially in semi-crystalline plastics. However, later it was proven that the cavitations and oriented crystalline layer around particles are also important parameters. In the mid-1990s, Argon and co-workers proposed a mechanism based on stress delocalization and debonding which facilitate plastic stretching for improving both the toughness as well as modulus for inorganic hard-particle (CaCO<sub>3</sub>) filled PP and PE,<sup>69,70</sup> considered for some time to be the holy grail.

However, the effect of flow was neglected in these studies. The presence of filler particles affects the structure development during flow (injection moulding). Recently, Schrauwen<sup>71</sup> showed that the improvement in CaCO<sub>3</sub>-filled PE and PP as observed by Argon and co-workers is mainly dependent on the flow history and the explanation put forth by Argon and co-workers does not hold.

During the last one decade nanoscience and nanotechnology has grown rapidly. The domain of nanocomposite materials is attracting both academic and industrial researchers due to the strong reinforcement effects at low volume fraction of nanofillers. Recent attention has been focused on the suitability of such composites in high performance application. The concept of short fibre hybrid nanocomposites for load bearing applications is fairly new. Property enhancements are expected due to higher Young's modulus of the short fibre reinforcement and finely distributed reinforcing nanofillers such as nanosilica, carbon nanotube etc. The studies so far reported proved that utilization of short fibres as reinforcement in polymer composites offer economical, environmental and qualitative advantages. By incorporating particulate nanofillers along with short fibres, high performance hybrid composites can be prepared. They may find application in automotive, construction and household appliances. However, thermoplastic hybrid composites based on short fibre and nanofiller has not been subjected to a systematic evaluation.

Hybridization is commonly used for improving the properties and for lowering the cost of conventional composites. It is generally accepted that properties of hybrid composites are controlled by factors such as nature of matrix, nature, length and relative composition of the reinforcements, fibre matrix interface and hybrid design. The hybrid composites based on nanofillers and fibres need to be studied in detail. PP is cheap, can be reprocessed several times without significant loss of properties and can be easily modified to achieve specific requirements. The service requirements of this thermoplastic in different areas of application are so wide. In order to compete with standard engineering plastics such as polyamides, in terms of the high demands on stiffness and strength, PP has to be reinforced and glass fibres are the major reinforcing elements used for this purpose. Hence it is proposed to reinforce PP with nano and micro fillers to generate a new class of hybrid composite. The study is proposed to be extended to HDPE also. The performances of the hybrid composites can be evaluated by studying their physical and mechanical properties.

The salient objectives of the current investigation are to:

- 1) synthesize nanosilica by a cost effective method
- 2) modify nanosilica surface by a silane coupling agent
- 3) develop PP/silica and HDPE/silica nanocomposites
- 4) prepare PP/glass fibre/nanosilica and HDPE/glass fibre/nanosilica hybrid nanocomposites
- 5) prepare PP/nylon fibre/nanosilica and HDPE/nylon fibre/nanosilica hybrid nanocomposites
- 6) develop chemically modified PP and HDPE hybrid nanocomposites
- 7) investigate the effect of the hybrid fillers on the mechanical (both static and dynamic), crystallization and thermal characteristics of PP and HDPE



## REFERENCES

1. Y.Kojima, A.Usuki, M.Kawasumi, A.Okada, Y.Fukushima; *J. Mater. Res.* **1993** , 8, 1185.
2. Forum Discussion at 40th IUPAC International Symposium on Macromolecules, *Macro 2004*, Paris, France, 4th-9th July **2004**.
3. S.B.Kharchenko, J.F.Douglas, J.Obrzut, E.A. Grulke, K.B.Migler, *Nat.. Mater.* **2004**, 3, 564.
4. F.L. Mathews, R.D.Rawlings; *Engineering Composites*, 1st ed. Chapman and Hall, **1994**.
5. J.A.Brydson; *Plastics Materials*, NEWNES – BUTTEERWORTHS, London, **1975**.
6. J.W.Gilman, C.L.Jackson, A.B.Morgan, R.H.Harris, E.Monias, E.P.Gianellis, M.Wuthenow, D.Hilton, S.H.Philips; *Chem.Mater.* **2000**, 12, 1866.
7. P.Sharma, W.Miao, A.Giri, S.Raghunathan, Nanomaterials; *Manufacturing, processing and applications*, Dekker Encyclopedia of Nano Science, **2004**.
8. S.B.Warner; *Fibre Science*, Prentice Hall, Engle wood Cliffs, New Jersey, **1995**
9. P.K.Mallick; *Fibre reinforced composite materials, manufacturing and design*, Marcel Dekker,Inc., New York, **1988**.
10. T.Richardson; *Composites-a design guide*, Industrial Press Inc.,200 Madison Avenue,Newyork, **1987**.
11. S.K.De, J.R.White; *Short fibre polymer composites*, Woodhead Publishing Ltd., Cambridge, England, **1996**.
12. A.L.Kalamkrov, H.Q.Liu, D.O.MacDonald; *Composites Part B* **1998**, 29B: 21.
13. K.L.Loewenstein; *The Manufacturing Technology of Continuous Glass Fibres*, 3rd ed. Amsterdam: Elsevier, **1993**.

14. J.R.Gonterman, W.W.Wolf, N.Y.Alfred; *The Technology of Glass Fibres*,: Proceedings of 1st International Conference on Advances in the Fusion of Glass by American Ceramic Society, **1988**, pp. 7.1–7.15
15. P.Gupta; *Fibre Reinforcement for Composite Materials*. Composite Materials Series Vol. 2. New York: Elsevier, **1988**.
16. D.A.Bhagwan, J.B.Lawrence; *Analysis and performance of fiber composites*, John Wiley & sons, New York, **1980**.
17. (a) P.M.Ajayan,L.S.Schadler, P.V.Braun; *Nanocomposite Science and Technology*, Wiley-VCH, **2003**.  
(b) A.Michael, D.Philippe; *Mater. Sci. Eng.* **2000**, 28,1.  
(c) S.J.Komarneni; *J. Mater. Chem.* **1992**, 2, 1219.  
(d) E.P.Giannelis; *Adv. Mater.* **1996**, 8, 29.
18. C.Oriakhi; *Journal of chemical education*, **2000**, 77, 9.
19. M. Jose-Yacaman, L. Rendon, J. Arenas, M. C. Serra Puche; *Science* **1996**, 273, 223.
20. G.A.Ozin; *Adv.Mater.* **1992**, 4, 612.
21. M.Learner, C.Oriakhi, A.Goldstein; *Handbook of nanophase materials*, Dekker, New York, **1997**.
22. S.Komarneni; *J.Mater.Chem.* **1992**, 2, 1219.
23. S.Yariv, H.Cross; *Organo-Clay Complexes and Interactions*, Marcel Dekker, New York, **2002**.
24. H.Van Olphen; *An introduction to Clay Colloid Chemistry*, 2<sup>nd</sup> ed., Wiley, New York, **1973**.
25. A.Michael, D.Philippe; *Mater. Sci. Eng.* **2000**, 28,1.

26. J.E.Mark ; *Polym.Eng. Sci.* **1996**, 36, 2905.
27. J.Wen, G.L.Wilkes; *Chem. Mater.* **1996**, 8, 1667.
28. T.Von Werne, T.E.Patten; *J. Am.Chem. Soc.*, **1999**, 121, 7409.
29. P.Calvert; *Carbon Nanotubes*, Editor, T.W.Ebbesen; CRC Press, Boca Raton, **1992**.
  - (a) M.S.Dresselhaus, P.A.Dresselhaus; *Carbon Nanotubes : Synthesis, Structure, Properties and Applications*, Vol.80, Eds., Springer-Verlag, Heidelberg, **2001**.
  - (b) V.Favier, G.R.Canova, S.C.Shrivastava, J.Y.Cavaille; *Polym. Eng. Sci.* **1997**, 37, 1732.
  - (c) L.Chazeau, G.R.Canova, J.Y.Cavaille, R.Dendievel, B.Boutherin; *J. Appl. Poym. Sci.* **1999**, 71, 1797.
30. F.Nastase, Stamatina, N.Claudia, D. Mihaiescu, A.Moldovan; *Prog. Solid State Chem.*, **2006**, 34, 191.
31. Q.Dong-ming, B.Yong-zhong, W.Zhi-xue, H.Zhi-ming; *Polymer*, **2006**, 47, 4622.
32. Y.Xiaoming, D.Tingyang,L.Yun; *Polymer*, **2006**, 47, 441.
33. W.Zhenyu, H.Enhou, K.Weiz; *Polym. Degrad. Stab.* **2006**, 91, 1937.
34. S.Patel, A.Bandyopadhyay, V.Vijayabaskar, A.K.Bhowmick; *Polymer*, **2005**, 46, 8079.
35. A.Bandyopadhyay, M.D.Sarkar, A.K.Bhowmick; **2005**, 95, 1418.
36. S.Wolff, U.Goer, M.J.Wang; *Eur.Rubber.J.* **1994**, 16, 1619.
37. H.Werner; *Rubber Technology Handbook*, Anser Publishers, Munich, **1989**.
38. J.D.Lee; *Concise inorganic chemistry*, Fourth edn., Chapman and Hall ltd., London, **1991**.
39. A.Krysztafkiewicz; *Chemia Stosowana*, **1984**, 28, 477.

- (a) A.Krysztafkiewicz; *Chemia Stosowana*, **1987**, 31, 127.
  - (b) Marciniec, A.Krysztafkiewicz, L.Domka; *Colloid Polym. Sci.*, **1983**, 261, 306.
  - (c) W.Stober, A.Fink, E.Bohn; *J. Colloid Interface Sci.*, **1968**, 26, 62.
  - (d) S.Ulrich, H.Nichola; *Synthesis of Inorganic Materials*, Wiley, New York.
  - (e) J.K.Kenneth; *Nanoscale Materials in Chemistry*, Wiley interscience.
40. T.Kotoky, S.K.Dolui; *J. Sol. Gel. Sci. Technol.*, **2004**, 20, 107.
  41. C.Jeuniaux ; *Adv. Chitin Sci.* **1996**, 1, 1.
  42. S.Koide; *Nutr. Res.* **1998**, 18(6), 1091.
  43. E.D.Plueddeman; *Silane Coupling Agents*, New York: Plenum Press, **1982**.
  44. Rigbi; *Adv.Polym.Sci.*, **1980**, 36, 21.
  45. B.Boonstra; *Polymer* **1979**, 20, 691.
  46. G.Kraus; J.E.Mason; *J.Polym.Sci.*, **1951**, 6, 625.
  47. F.R.Eirich; *Mech.Behav.Mater.Proc.* 1<sup>st</sup> Int.conf., **1972**, 3, 405.
  48. J.Hartikainen, P.Hine, K.Friedrich; *Comp.Sci.Technol.*, **2005**, 65, 257.
  49. M.Idicula, N.R.Neelakandan, S.Thomas, S.Oommen, K.Joseph; *J. Appl. Polym. Sci.* **2005**, 96, 1699.
  50. G.Kalaprasad, K.Joseph, S.Thomas; *J.Comp.Mater.* **1997**, 31, 509.
  51. M.Idicula, S.K.Malhotra, S.Thomas; *Comp.Sci.Technol.*, **2005**, 65, 106.
  52. S.Mishra ; *Comp. Sci. Technol.* **2003**, 63, 1377.
  53. H.D.Rozman, H.Ismail; *Euro. Polym. J.* **2001**, 37, 1283.
  54. C.Z.P.Junior, V.M.Fonseca, S.N.Monteiro; *Polymer Testing* **2004**, 23, 131.
  55. J.Rout, M.Misra, S.S.Tripathy, A.K.Mohanty; *Comp. Sci. Technol.* **2001**, 61,1303.

56. M.S.Sreekala, N.R.Neelakandan, S.Thomas; *J. Polym. Eng.* **1997**, 16, 265.
57. J.Maya, K.T.Varghese; *Comp. Sci. Technol.* **2004**, 64, 955.
58. A.P.Haseena, G.Unnikrishnan; S.Thomas; *Comp. Interf.* **2004**, 11, 489.
59. R.Ahmed, A.Ahmed, A.Tarek, B.Mohamed; *J.Appl.Poym.Sci.* **2007**, 106, 3502.
60. I.L.Vladimir, I.V.Bakeeva, P.P.Elena, G.D.Lilija, P.Z.Vitaly; *J.Appl.Poym.Sci.* **2007**, 105, 2689.
61. A.Khairul, H.B.Khairiah; *J.Appl.Poym.Sci.* **2007**, 105, 2488.
62. S.IMavani, N.M.Mehta, P.H.Parsania; *J.Appl.Poym.Sci.* **2007**, 106, 1228.
63. M.Jamal, T.Mehdi, C.H.John, G.Ismaeil; *J.Appl.Poym.Sci.* **2007**, 105, 3054.
64. M.G.Mohseni, A.Arefazar, N.Nazockdast; *J.Appl.Poym.Sci.* **2007**, 104, 2704.
65. N.Nugay, B.Erman; *J.Appl.Poym.Sci.* **2001**, 79, 366.
66. A.Bandyopadhyay, M.Sanker, A.K.Bhowmick; *Rubber.Chem.Technol.* **2005**, 78, 806.
67. S.Wu, C.P.Bosnyak, K.Sehanobish; *J.Appl.Poym.Sci.* **1997** 65, 2209.
68. Y.Ou, F.Yang, Z.Yu ; *J.Poym.Sci.Part B :Polym.Phys.* **1998**, 36, 789.
69. (a) O.K.Muratoglu, A.S.Argon, R.E.Cohen, M.Weinberg; *Polymer* **1995**, 36, 921.  
(b) Z.Bartczak, A.S.Argon, R.E.Cohen, M.Weinberg; *Polymer* **1999**, 30, 2331.
70. M.W.L.Wilbrink, A.S.Argon, R.E.Cohen, M.Weinberg ; *Polymer* **2001** 42, 10155.
71. (a) B.A.G.Schrauwen, *Ph.D. Thesis*, **2003**, Technische Universiteit Eindhoven, Eindhoven, The Netherlands. (b) B.A.G.Schrauwen, L.E.Govaert, G.W.M.Peters, H.E.H.Meijer; *Macromol. Symp.* **2002**, 185, 89.

# Chapter 2

## Materials and Methods

### 2.1 MATERIALS

#### 2.1.1 Polypropylene (PP)

Polypropylene homopolymer (REPOL H200MA) with a melt flow index of 20g/10 min, was supplied by Reliance Industries Limited, Mumbai.

#### 2.1.2 High Density Polyethylene (HDPE)

High Density Polyethylene (HDPE) (HD50MA 180), with a melt flow index of 18g/10 min was supplied by Haldia Petrochemicals, Mumbai.

#### 2.1.3 Glass fibre

E-glass fibre with a diameter of about 13 $\mu$ m was obtained from Sharon industries Ltd. Kochi.

#### 2.1.4 Nylon fibre

Nylon 6 fibre of diameter 0.3mm (style S392-374 and cord denier 3656-3886) was obtained from M/S SRF Ltd., Chennai, India and was chopped to approximately 10mm. Specifications of Nylon-6 fibre are given in the table 2.1

#### 2.1.5 Sodium silicate

Sodium silicate solution (60%) was obtained from M/s Minnar Chemicals, Kochi.

#### 2.1.6 Hydrochloric acid (HCl)

HCl (AR grade) used was procured by M/s Loba chemicals with an acidimetric assay of 35-38%.

### **2.1.7 Chitosan**

It was supplied by India Sea Foods Ltd., Kannamaly, Kochi, Kerala.

### **2.1.8 Vinyl triethoxy silane (VTES)**

Vinyl triethoxy silane (98%) was supplied by Lancaster synthesis, East gate, England.

### **2.1.9 Other chemicals**

Acetic acid for dissolving chitosan was manufactured by Merk, India Ltd. Dicumyl peroxide (DCP - 40% active) was used as the initiator. Maleic anhydride for grafting was supplied by Aldrich.

## **2.2 COMPOSITE PREPARATION**

Three types of composites (nanocomposites, short fibre composites and nano-micro hybrid composites) were prepared. Different composites were prepared by melt mixing<sup>1</sup> method using Thermo Haake Rheometer (Rheocord 600p) (Figure 2.1). The mixing chamber has a volumetric capacity of 69cm<sup>3</sup> and was fitted with roller type rotors. The rotors rotate in opposite directions in order to effect a shearing force on the material mostly by shearing the material against the walls of the mixing chamber. The granules in the desired proportion are fed to the mixing chamber through a vertical chute with a ram. There is a small clearance between the rotors which rotate at different speeds at the chamber wall. In these clearances dispersive mixing takes place. The shape and motion of rotors ensure that all particles undergo high intensive shearing flow in the clearances.

The mixer consists of three sections and each section is heated and controlled by its own heater and temperature controller. Since mechanical dissipation heat is developed in the small gap between rotors and chamber, the heat conducts to the centre bowl and rises the set temperature. In this case, the heater and centre bowl is automatically shut off and circulation of cooling air is activated.

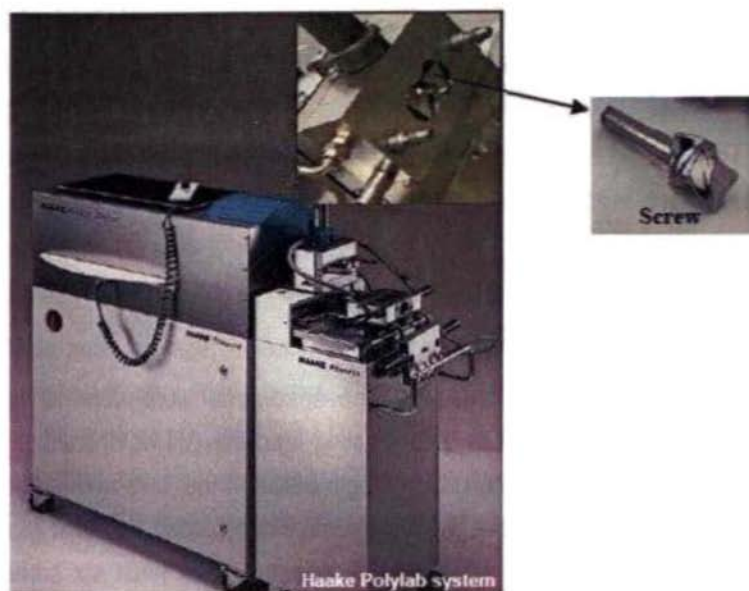


**Figure 2.1:** Thermo Haake Polylab system (inset picture-mixing chamber & rotor)

### 2.2.1 Melt mixing

All materials (PP, HDPE, glass fibre, nylon fibre and nanosilica [prepared by precipitation method]) were dried by keeping them in an oven at a temperature of 100 °C for 4 hrs before mixing.

To prepare nanocomposite the pure material and nanosilica were together fed into the chamber and mixed well. To make fibre composite the pure material was fed into the chamber first and waited for 3 minutes to melt the material. Then the fibres were added into the chamber and mixing continued to obtain short fibre composite. To make hybrid composite the pure material and nanosilica were together fed into the chamber and waited for 3 minutes to melt and mix the materials. Then the fibres were added into the chamber and mixing continued to get hybrid composite. The maleic anhydride (MA) grafted composites were prepared by adding DCP and MA at 6<sup>th</sup> minute of mixing according to US patent 4,753,997. The temperature selected depends on the nature of material. A mixing time of 8 minutes was given at rotor speed of 50 rpm.

### 2.2.2 Preparation of test specimen

The hot mix from the mixing chamber was immediately pressed using a hydraulic press at a pressure of 100 kN/cm<sup>2</sup> and the resulting sheets were cut into small



pieces. The test specimens were prepared using a semi-automatic plunger type injection moulding machine with a barrel temperature of 190 °C, injecting the molten samples at a pressure of 1000 kg/cm<sup>3</sup>. The specimens were moulded at identical conditions and the properties were taken as the average property of six samples.

## 2.3 MECHANICAL PROPERTIES

### 2.3.1 Tensile properties

The tensile properties of the specimens were determined using dumb-bell shaped samples with a Universal Testing Machine (UTM, Shimadzu AG-1) with a load cell of 50kN capacity. The gauge length between the jaws at the start of each test was adjusted to 40mm and the measurements were carried out at a cross head speed of 50mm/min according to ASTM-D-638. Average of at least six sample measurements were taken to represent each data point

### 2.3.2 Flexural properties

Flexural properties of the composites were measured by a three-point loading system using universal testing machine (UTM, Shimadzu AG-1) with a load cell of 50kN capacity according to ASTM-D-790. Rectangular shaped specimens were used for the flexural test and the testing was done at a crosshead speed of 5mm/min.

The flexural strength is given by

$$S = 3PL / 2bd^2$$

where  $S$ = flexural strength,  $P$ = maximum load at the moment of break,  $b$ = width of the specimen,  $L$ = length of the span and  $d$ = the thickness of the specimen.

The maximum strain ( $r$ ) in the outer fibres is given by

$$r = 6Dd / L^2$$

where,  $D$  is the deflection.

The flexural modulus is calculated from the slope of initial portion of the flexural stress-strain curve.<sup>2</sup>

### **2.3.3 Impact strength**

Impact resistance is the ability of the material to resist breaking under a shock loading or the ability to resist fracture under stress applied at high speed. The impact properties of polymeric materials are directly related to the overall toughness of the material. Toughness is defined as the ability of the polymer to absorb applied energy. The area under the stress-strain curve is directly proportional to the toughness of the material. Higher the impact strength of the material, higher will be the toughness and vice versa.

The methods such as Izod, Charpy, Gardner, tensile impact etc. are usually used to measure the impact resistance of plastics. The Izod impact strength of the injection moulded samples is determined as per ASTM-D-256. Rectangular strips of dimensions 12x10x3 mm are used as the test specimens. The tests are carried out using REIL IMPACTOR JUNIOR (CEAST) machine with a pendulum of 4kJ and striking velocity of 3.46m/s.

A pendulum swings on its track and strikes the sample. The energy lost as the pendulum continues on its path is measured from the distance of follow through. The impact energy is directly read from the machine.

$$\text{Impact strength} = \text{Impact energy(J)}/\text{Thickness(m)}$$

## **2.4 DYNAMIC MECHANICAL ANALYSIS (DMA)**

Dynamic mechanical analysis is used to determine the dynamic properties such as storage modulus ( $E'$ ), Loss modulus ( $E''$ ) and the damping or internal friction  $\tan \delta$  ( $E''/E'$ ) by measuring the response of the material to periodic forces.<sup>3</sup> Generally the dynamic measurements are carried out over a frequency range at a constant temperature or over a temperature at a constant frequency.

Dynamic mechanical analysis is suitable to measure the dynamic response of polymers under a given set of conditions. The principle of Dynamic mechanical test method is to impart a sinusoidal mechanical strain on to a solid or viscoelastic liquid and to resolve the stress into real and imaginary components corresponding to elastic and viscous states. In viscoelastic studies, the applied force and resulting deformation both vary sinusoidal with time. The strain will also be sinusoidal but will be out of phase with stress. This phase lag results from the time necessary for molecular rearrangements and

is associated with the relaxation phenomena. This phase lag is expressed as an angle ' $\delta$ '. The modulus is a ratio between stress and strain. For visco elastic materials, the modulus is a complex quantity.

$$E^* = E' + i E''$$

$E'$  = storage modulus corresponding to the elastic response to the deformation and it is a measure of stiffness.

$E''$  = loss modulus corresponding to the plastic response to the deformation and it is associated with the dissipation of energy as heat when material is deformed.

$E''/E' = \tan \delta$ , useful for determining the occurrence of molecular transition such as glass transition temperature.

Storage modulus, loss modulus,  $\tan \delta$  are used to generate the information about crystalline as well as amorphous nature in polymers. The variation of these components as a function of temperature is used to study the molecular motion in the polymers

The dynamic mechanical thermal analysis was conducted using rectangular test specimens having a dimension of 60mm x 4mm x 2mm with dual cantilever clamp using a Dynamic Mechanical Analyser (model Q800, TA instruments). The tests were carried out by temperature sweep (temperature ramp from 30 °C to 150 °C at 3 °C/min ) method at a constant frequency of 1Hz to get the dynamic storage modulus ( $E'$ ) and loss modulus ( $E''$ ) of the samples. The samples were subjected to dynamic strain amplitude of 0.1146%.

## 2.5 DIFFERENTIAL SCANNING CALORIMETRY (DSC)

Differential scanning calorimeter (DSC) is a technique for studying the thermal behavior of a material as a function of temperature as they go through physical or chemical changes with absorption or evolution of heat. It used to investigate thermal transitions, including phase changes, crystallization, melting, glass transitions of a material as a function of temperature.<sup>4,5,6</sup> Heat flow, i.e heat absorption (endothermic) or heat emission (exothermic), is measured as a function of time or temperature of the sample and the result is compared with that of a thermally inert reference. The materials, as they undergo changes in chemical and physical properties, which are detected by transducers, which changes into electrical signals that are collected and analyzed to give

thermograms. DSC directly gives a recording of heat of flow rate ( $C_p$ ) against temperature. The kinetics of phase transformation can also be studied by DSC. The degree of crystallinity ( $x$ ) can be measured as a function of time,

$$X = \Delta H (\text{observed}) / \Delta H_f (100\% \text{ crystalline})$$

The melting and crystallization parameter, such as melting point ( $T_m$ ), Heat of fusion ( $\Delta H_f$ ) temperature of crystallization ( $T_c$ ), and Heat of crystallization were used for the comparison of composites. Two different types of DSC instruments are generally used, heat flux and power compensation. In heat flux type of DSC, the sample and reference are heated in a common block and measure the differential temperature ( $\Delta T$ ) between the cells. In power compensation type of DSC, the sample and reference has individual heaters.  $\Delta W$ , the difference between the power output of the sample and reference cells in order to maintain the same programmed temperature in each cell is measured.

DSC Q 100 (TA Instruments) equipped with a RCS cooling system was used to study thermal transitions of the samples. The samples (7-10mg) were heated from 30 °C to 180 °C at 20 °C/min and cooled to 50°C at 10 °C/min under nitrogen atmosphere (60ml/min flow) to get the non-isothermal crystallization characteristics of the samples.

## 2.6 THERMOGRAVIMETRIC ANALYSIS (TGA)

Thermogravimetric analysis(TGA) is a technique by which the mass of the sample is monitored as a function of temperature or time, while the substance is subjected to a controlled temperature programme.<sup>7</sup> Thermogravimetric analysis is used to investigate thermal degradation. TGA Q50 (TA Instruments) was used at a heating rate of 20 °C/min from room temperature to 600 °C with 8-12 mg of sample. The chamber (furnace) was continuously swept with nitrogen at a rate of 90ml/min. The corresponding weight changes were noted with the help of an ultra sensitive microbalance. The data of weight loss versus temperature and time was recorded online in the TA Instrument's Q series Explorer software. The analysis of the thermogravimetric (TG) and derivative thermogravimetric (DTG) curves were done using TA Instrument's Universal Analysis 2000 software version 3.3B.

## **2.7 SCANNING ELECTRON MICROSCOPY (SEM)**

SEM was used to investigate the morphology of fractured surfaces.<sup>8</sup> In SEM, the electron beam incident on the specimen surface causes various phenomena of which the emission of secondary electrons is used for the surface analysis. Emitted electron strikes the collector and the resulting current is amplified and used to modulate the brightness of the cathode ray tube. There is a one- to- one correspondence between the number of secondary electrons collected from any particular point on the specimen surface and the brightness of the analogous point on the screen and thus an image of the surface is progressively built up on the screen.

The tensile fracture surfaces was sputter coated with gold and examined under Scanning Electron Microscope (JEOL JSM 840 A).

## REFERENCES

1. S.Weil, G.Shiji, F.Changshui, X.dong, R.Quan; *J.Mater.Sci.* **1999**, 34, 5995.
2. W.E.Gottfried; *Polymeric materials: structure properties applications*, Hanser publishers, Munich.
3. M.Takayuki; *Dynamic Mechanical Analysis of Polymeric Materials*, Elseviour, Amsterdam, **1978**.
4. C.Busigin, R.Lahtinern, G.Thomas, R.T.Woodharms; *Polym.Eng. Sci.* **1984**, 24, 169.
5. W.P.Zhu, G.P.Zhang, J.Y.Yu, G.Dai; *J.Appl.Polym.Sci.* **2004**, 91, 431.
6. T.Labour, G.Vigier, R.segeula, C.Gauthier, G.Orange, Y.Bomal; *J.Polym.Sci.PartB: Polym.Phys.* **2002**, 40, 31.
7. C.M.Neil, G.allen; editor, *Comprehensive polymer science*, Vol.5, Pergamon press, New York, **1989**.
8. W.E.Arthur; *Atlas of polymer morphology*, Hanser, New York, **1989**.

# Chapter 3

## Synthesis, modification and characterization of nanosilica

### 3. 1 INTRODUCTION

The potential applications of nanomaterials in various fields have caught the attention of academic and industrial research world in the last decade. Nanotechnology is emerging to revolutionize the world we live in with radical break through in areas such as materials and manufacturing, electronics, medicine and healthcare, environment and energy, chemical and pharmaceutical, biotechnology and agriculture, computation and information technology etc. The uniqueness of nanoparticles is that their properties can be selectively controlled by controlling the size, morphology and composition of constituents. The new material thus obtained will have enhanced or entirely different properties from their parent materials. Despite the current interest nanoparticles are not a new phenomenon, with scientists being aware of colloids and sols, for more than 100 years. The scientific investigation of colloids and their properties was reported by Faraday (1857) in his experiments with gold. He used the term "divided metals" to describe the material which he produced. Zsigmondy (1905) describes the formation of a red gold sol which is now understood to comprise particles in the 10 nm size range. Many well known industrial processes also produce materials which have dimensions in the nanometre size range. An example is the synthesis of carbon black by flame pyrolysis (approximately 6 million tonnes per year) which produces a powdered form of carbon, usually highly agglomerated but has a primary particle size in the order of 100 nm. Other common materials such as fumed silica ( $\text{SiO}_2$ ), ultrafine titanium dioxide ( $\text{TiO}_2$ ) and ultrafine metals produced by similar thermal processes thermal spraying and coating, welding, working of diesel engines etc. also gives particles in nanometer size range. Nanometre sized particles are also found in the atmosphere where they originate from combustion sources

(traffic, forest fires), volcanic activity, and from atmospheric gas to particle conversion processes such as photochemically driven nucleation. In fact, nanoparticles are the end product of a wide variety of physical, chemical and biological processes, some of which are novel and radically different, others of which are quite commonplace.

Recently, the technological innovation of low-cost and large-scale synthesis process of nanoparticles with less than 100 nm in diameter is developing, and various kinds of nanoparticles are applied as the raw materials in the different fields, for example, cosmetic, medical supplies, catalysts, pigments, toner and ink. From the scientific and engineering points of view studies on the effect of solid nanofillers on polymers are of great important because their unique properties and numerous potential applications such as enhancement of conductivity, optical activity, toughness etc. Nanofillers based on clay,<sup>1</sup> silica,<sup>2,3</sup> ZnO, carbon nanotubes<sup>4,5,6</sup> etc. also impart enhanced physical and chemical properties to polymers even at low concentration. Understanding the interaction between nanofiller and a polymer matrix is a key to explore the source of reinforcement by these fillers.

Silica has been used as reinforcing material in different polymers such as polymethacrylates, polyimides, polyamides, polyacrylics, polyoleifns, elastomers etc.<sup>7</sup> The specific function of the filler is based on the specific resin system, particle size, surface area, loading and surface modification. Because of the high bond energy in Si-O bond, silica has high thermal stability and posses a very low thermal expansion coefficient. The silica containing nanocomposites show very good resistance to staining and remarkable barrier properties to gases and moisture.<sup>8,9,10</sup>

The synthesis and characterization of nano scale silica is currently of great interest as silica has higher thermal tolerance and lower thermal conductivity, refractive index, dielectric constant and Young's modulus. Such materials have tremendous potential application in the field of optoelectronics, nanocomposites, ceramics, rubber technology and biomedical materials, in addition to displaying great promise in applications involving catalysis and chemical separations.

Verónica Morote-Martínez and co-workers used nanosilica for improving the mechanical and structural integrity of natural stone by applying unsaturated polyester



resin-nanosilica hybrid thin coating.<sup>11</sup> Different amounts (0.5–3 wt.%) of nanosilica was added to improve several properties, particularly the mechanical properties. Addition of nanosilica imparted pseudoplasticity and thixotropy to the UPR resin and an increase in viscosity was also produced. In the cured composites, improved thermal properties in UPR were reached by adding nanosilica due to the creation of a network between the filler and the polymer matrix. The improved properties in UPR obtained by adding nanosilica produced enhanced impact resistance to coated marble pieces, as both stiffness and toughness were also improved.

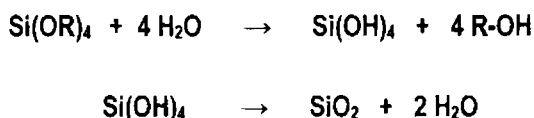
Achilias *et.al* studied the effect of silica nanoparticles on solid state polymerization of poly(ethyleneterephthalate).<sup>12</sup> From the experimental measurements and the theoretical simulation results, it was proved that nanosilica in small amounts (less than 1 wt %) enhances both the esterification and transesterification reactions at all studied temperatures acting as a co-catalyst. However, as the amount of nanosilica increases a number of inactive hydroxyl groups were estimated corresponding to participation of these groups in side reactions with the nanosilica particles. These side reactions lead initially to branched PET chains and eventually (5 wt% n-SiO<sub>2</sub> concentration) to crosslinked structures.

Epoxy–nanocomposite resins filled with 12-nm spherical silica particles improved their thermal and mechanical properties as a function of silica loading.<sup>13</sup> The addition of small amounts of silica nanoparticles to the cement paste can reduce the calcium leaching rate of the cement paste.<sup>14</sup> Xiaowei Gao and co workers has found that the antioxidant efficiency of the nanosilica-immobilized antioxidant was superior to the corresponding low molecular counterpart (AO), based on the measurement of the oxidation induction time (OIT) of PP/nanosilica-immobilized antioxidant and PP/AO compounds containing an equivalent antioxidant component.<sup>15</sup> Nangeng Wen and co workers used nanosilica for the preparation of raspberry-like organic–inorganic composite spheres with poly(vinyl acetate) (PVAc) as core and nanosilica particles as shell.<sup>16</sup> The hydrogen bonds between nanosilica particles and PVAc were strong enough for the formation of long-stable composite spheres with raspberry-like morphology.

The introduction of nanosilica particle with a spherical diameter of about 20 nm into the Portland cement paste improved the performance of Portland cement-based

composites. Portland cement composite with nanosilica had a more solid, dense and stable bonding framework.<sup>17</sup> The gas barrier properties of nanosilica filled latex membranes were very high.<sup>18</sup> Nanosilica has been used in different polymers as a reinforcing material and also as a special purpose additive to improve their properties for specific applications.<sup>19</sup>

Sol-gel technology<sup>20,21</sup> has been used extensively in the synthesis of nanosilica. Sol-gel synthesis of silica<sup>22,23</sup> is based on the hydrolysis of alkoxy-silanes like tetra-ethoxy-silane or tetra-methoxy-silane, according to the reaction.<sup>24,25,26</sup>



Acidic or basic catalyst could be used. The proportion of Si-OH, Si(OH)<sub>2</sub> and Si(OH)<sub>3</sub> change during process, which first gives a swollen gel. It is then dried, heated and densified into final monolithic piece of silica. The gelation may correspond to a cross-linking process taking place between macromolecular species of polysiloxanes containing free Si-OH molecules. In the presence of acids, probability of formation of Si(OH)<sub>4</sub> is small and condensation reaction start before complete hydrolysis of Si(OR)<sub>4</sub> to Si(OH)<sub>4</sub> can occur. Under basic condition Si(OH)<sub>4</sub> is easily formed by the preferential hydrolysis of the rest of the OR groups belonging to a partially hydrolyzed Si(OR)<sub>4</sub> and some silicon alkoxide molecules tend to remain non-hydrolyzed. Hydrolysis of tetra-ethoxy-silane is initiated with alcohol solvent in the presence of acid/basic catalyst and the gelation requires several days. Another method is exposing TEOS and water to ultrasound in the presence of acid catalyst and the gelling time for this 'Sonogel' was about 115-200 min. This gel is then heated at high temperatures to obtain fine powder of silica.

Nanosilica can also be produced in a form of a dry powder via pyrolysis of tetraalkoxysilanes or tetrachlorosilane in the presence of water as well as by direct hydrolysis of sodium methasilicate or tetraalkoxysilanes.<sup>27,28</sup> Several methods are used to produce nanosilica from different sources.<sup>29,30,31</sup> Saito *et al.* have synthesized nano silica from Per-Hydro-Poly-Silazane (PHPS) with mild conditions using steam as catalyst.<sup>32</sup> Density and refractive index of silica prepared from PHPS were close to silica glass. This

work was carried out to study the effects of hydroxyl group and architecture of organic polymers on polystyrene/silica nano composites. Chrusoid and Slusarski have prepared nano silica from a stable emulsion of alkoxysilanes by the addition of a surfactant and heating the emulsion to remove the residual materials.<sup>33</sup> The addition of surfactant is necessary to lower the interfacial energy and minimize the surface energy between two liquids. Emulsion was formed with solution containing 60% mineral oil and 40% heptane and then they were heated to 450 °C to burn off residual mineral oil and un-reacted alkoxide group. Fujiwara *et al.* has modified the sol-gel method using acid anhydride instead of water for reacting with the organosilanes and condensation of alkoxy silane proceeded at a lower temperature of 150 °C.<sup>34</sup> In this method, Diglycidyl ethers of bisphenol-A (DGEBA) was added as the precursor of epoxy resin into the alkoxy silane mixture to produce epoxy resin / silica nano composite. Kim, Liu and Zachariah have suggested the aerosol-assisted sol-gel method to produce nanosilica.<sup>35</sup> In this method, Tetraethoxysilane (TEOS), water and ethanol were allowed to react according sol-gel chemistry. Sufficient hydrolysis time was given and then the solution was aerosolized with sodium chloride. Sodium chloride was employed both as an agent to accelerate the kinetics of silica gelation and as a templating medium to support the formation and stability of pore structures.

Kotoky and Dolui used sodium silicate with dilute hydrochloric acid as catalyst in poly(vinyl alcohol) to produce poly(vinyl alcohol)/silica nano composites.<sup>36</sup> This is a sol-gel method in which the acid plays a catalytic role in enhancing sol-gel condensation of silicon alkoxides within the poly(vinyl alcohol). The reaction mixture was stirred for 30 minutes at 60 °C, pH maintained between 1 and 2. The sol-gel mixture was passed through cation exchange resin amberlite for the removal of Na<sup>+</sup> ions. After 24 hrs at ambient temperature the sample gelled and this was then dried for another 48 hrs at 47°C.

Cocoon shaped nanosilica particles have been synthesised by Arai and co workers.<sup>37</sup> The particles were prepared from TMOS, water, ammonia and methanol by a sol-gel method. The method is to add the methanol solution of TMOS at a constant supply rate to a mixture of water, ammonia and methanol. Effects of various reaction conditions such as temperatures, supply rates of TMOS, and amounts of TMOS determined the diameter and shape of the particles. High temperature makes particles

with high aspect ratio and small diameter. And the mechanism of forming the cocoon shaped particle was also discussed. It was concluded that the primary particles were generated at the beginning stage of reaction and two of them became the cocoon shaped particle. These cocoon shaped nanosilica particles is used for polishing applications. For high polishing efficiency, particles with the diameter between 40 nm and 210 nm are to be used. As a result, best diameter of particles for abrasive is 40–100 nm with respect to polishing efficiency and surface finish.

Nittaya *et al.* have synthesized nanosilica from rice husk ash (RHA). Rice husk ash was washed with water and then burned at 700 °C for 6 hrs.<sup>38</sup> RHA samples were stirred with 3N sodium hydroxide solutions and was heated in a covered Erlenmeyer flask for 3 hours. Pure silica was extracted by refluxing with 6N HCl for 4 hours and then washed repeatedly using de-ionised water to make it acid free. It was then dissolved in 2N NaOH by continuous stirring for 10 hrs on a magnetic stirrer and then concentrated H<sub>2</sub>SO<sub>4</sub> was added to adjust pH in the range of 7.5 - 8.5. The precipitated silica was washed repeatedly with warm de-ionised water till the filtrate was completely alkali-free. After the washing process silica powder was dried at 50 °C for 48 h in the oven. Jal and co-workers synthesised nanosilica by precipitation method characterized it by various analytical tools.<sup>39</sup> From transmission electron micrograph the silica particles were found to have almost spherical shape with a dimension of ~50 nm. The surface area was found to be of 560 m<sup>2</sup> g<sup>-1</sup> and density 2.2 g cm<sup>-3</sup>. From thermogravimetric analysis the total silanol density in the silica was found to be 7.68 nm<sup>-2</sup>. The number of reactive silanols that formed hydrogen bond with water molecules was found to be 2.48. The infrared spectral data supported the presence of hydrogen bonded silanol group and the siloxane groups in silica.

The reinforcing action of fillers in polymers depends on several factors such as chemical character of polymer and filler, type of filler, polymer filler phase relation, the adhesion of polymer to filler, the polymer formation conditions in the presence of filler and so on. If the filler is inorganic in nature the surface modification is necessary to improve the interaction of filler with organic polymer. To improve the chemical affinity of silica with polymer, several modifying agents and various ways are used for the surface modification.<sup>40</sup>

The chemical character of nanosilica surface should be modified to decrease the activity of silica fillers. Otherwise the nucleating tendency of individual nanoparticles will cause growth of the particles by aggregation and thus to proceed to agglomerated bigger particles (Figure 3.1). This will decrease the interaction and dispersion of filler in polymer.

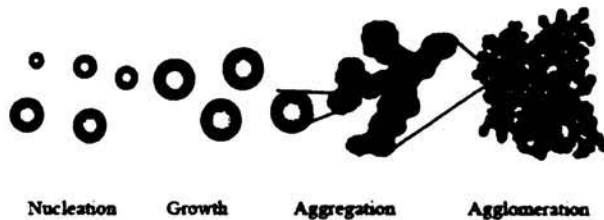


**Figure 3.1:** Growth of silica particles

The chemical character of silica can be altered by various reactions which leads to chemical bonds between modifying substance and silica surface. For that purpose coupling agents of borate, silane or titanate are used. Silane coupling agents are very attractive group of compounds capable of promoting interaction of silica to polymer. The application of silane coupling agents is principally aimed to decrease the hydrophilic character of silica and to introduce new organic functional groups capable of reacting with different polymers. Figure 3.2 shows how surface modification of silica the open doors to a variety of polymer systems.

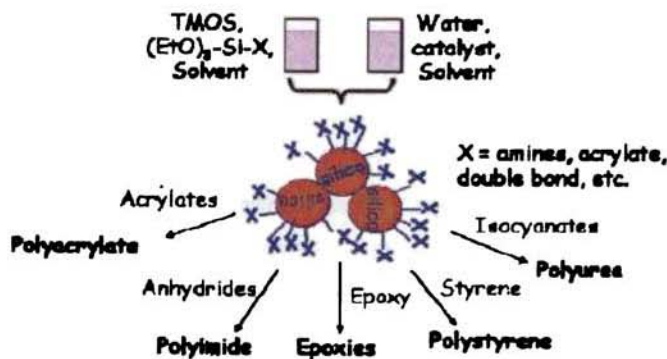


**Figure 3.2:** Schematic representation of interaction of modified silica with variety of polymers

This chapter describes the synthesis of nanosilica from sodium silicate and hydrochloric acid by precipitation method under controlled conditions using chitosan as dispersing agent. Compared to the more commonly used tetraethoxysilane (TEOS) or tetramethoxysilane (TMOS) sodium silicate is a cost effective silica source. Moreover, by using a purely aqueous medium, the expensive and very often toxic, solvent could be avoided. The precipitation method was selected because of the following reasons:-

- It involves the use of commonly available sodium silicate and mineral acid.
- It is possible to produce nanosized silica particles under controlled conditions
- It does not require very long gelation and drying times as required for sol-gel process.
- The catalyst used in the sol-gel process may remain as impurities.
- Silica synthesized by the sol-gel process was observed to contain many lattice defects.
- The byproducts can be easily removed by washing with distilled water.

Chitosan is used as the dispersing agent because it contains macromolecules with a large number of hydroxyl groups per molecule. It would produce a matrix into which synthesized silica would be incorporated, thus producing silica in the nanoscale. The interaction between the hydroxyl groups of chitosan and the hydroxyl groups of silica would result in co-condensation.

## **3.2 EXPERIMENTAL**

### **3.2.1 Experimental setup**

#### **i. Reactor**

The experiments were carried out using a reactor of 500ml capacity. After optimizing the concentration, laboratory scale synthesis was done using a 3000ml Borosil beaker as the reactor.



**Figure 3.3:** Reactor setup

#### **ii. Stirring and heating**

A mechanical stirrer provided with three leaf blade was used for stirring the slurry. The speed of the stirrer was varied from 30 rpm to 150 rpm depending on the concentration of the slurry and the optimum was found to be 50-60 rpm. Heating was done using a hot plate which was set constant at 70 °C.

#### **iii. Filtration**

Vacuum filtration was done using a Buchner funnel, suction flask, tubing and a vacuum pump.

#### **iv. Drying**

Hot air oven with a temperature setting adjustable to 300 °C was used. The cake obtained after filtration was scrapped out and spread out evenly on a glass plate using a glass rod. Glass plate was then placed in the oven and dried for the required time at 100 °C.

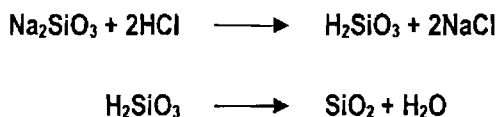
## v. Calcination

A muffle furnace with a temperature range of 50 °C to 1200 °C was used for calcinations. The dried sample was ground into fine powder and then kept in the muffle furnace at 600 °C for 3 hrs. During this time the organic part will go and we get fine silica powder.

### 3.2.2 Synthesis of nanosilica

Silica was prepared from sodium silicate and HCl using chitosan as the matrix. A 2% solution of chitosan in 2% acetic acid solution was prepared. This was then intimately mixed with stoichiometric amount of 1N HCl required for the preparation of silica in the reacting vessel. 10% sodium silicate solution prepared in distilled water was then added dropwise to the above stirring mixture at a temperature of 60 °C. The pH of the mixture was maintained between 1 and 2 to get nanosize silica. If HCl is added into the sodium silicate solution it is difficult to maintain the pH in the range 1-2 and there is a chance of gelation causing an increase in size of the particles and stirring also became difficult. After the addition of sodium silicate the reaction mixture was stirred continuously for a period of 2 hours and the temperature was maintained at 70 °C. This enables the uniform distribution of the chitosan medium in the reaction mixture, so that it could act as a matrix to collect the formed particles. It also enabled the conversion of silicic acid, formed by the reaction between HCl and sodium silicate, into silica.

The reaction between sodium silicate and dil.HCl is given below:



The acid plays a catalytic role in enhancing the co-condensation of silicon oxides within the dispersing agent's matrix. It is expected that the addition of the above dispersing agent would produce a matrix into which synthesized silica would be incorporated, thus producing silica in the nanoscale. The interaction between the hydroxyl groups of dispersing medium and the hydroxyl groups of silica would result in co-



condensation. Hydrogen bonding between the polymer and the developing polysilicate network leads to system homogeneity.

After completion of reaction, the resultant slurry was kept at room temperature for 24 hours and then makes it neutral to regenerate chitosan. It was then filtered by vacuum filtration. The solution containing regenerated chitosan was slowly poured into the Buchner funnel, always maintaining a slurry level of not more than 70% of the funnel height. After completely emptying out the solution into the funnel, the washing was started with distilled water. The washings continued until all the sodium chloride was removed. The cake obtained after washing was scraped out using a scrapper and spread evenly on a glass plate of dimension 20 cm x 20 cm. This was then placed in a hot air oven at a temperature of 70 °C for 24 hrs. The cake thus obtained was then ground to obtain fine powder. After complete drying it was calcined in a muffle furnace at 600 °C for 3 hrs to get fine silica powder.

### **3.2.3 Modification of nanosilica**

The surface of silica was modified by hydrolysis followed by condensation reaction of vinyl triethoxysilane. These reactions were done by the addition of HNO<sub>3</sub> and NH<sub>4</sub>OH as catalysts. The nanosilica particles (0.1g/ml) were sonicated for 1 hour to get a homogeneous aqueous dispersion of silica. The dispersion was acidified by adding dilute HNO<sub>3</sub> solution. Vinyl triethoxysilane (0.2M) was added to the acidified silica dispersion and the mixture was stirred for 3 minutes at 60 °C to undergo the hydrolysis reaction. Ammonium hydroxide solution was then added to the mixture to make it alkaline and the mixture was further stirred for 1 hour at 60 °C for the completion of condensation reaction. This was then filtered, washed with distilled water and dried to get fine particles of modified silica. The reaction scheme is shown in figure 3.4. The modified particles were then characterized by various techniques such as TEM, FTIR, TGA etc.

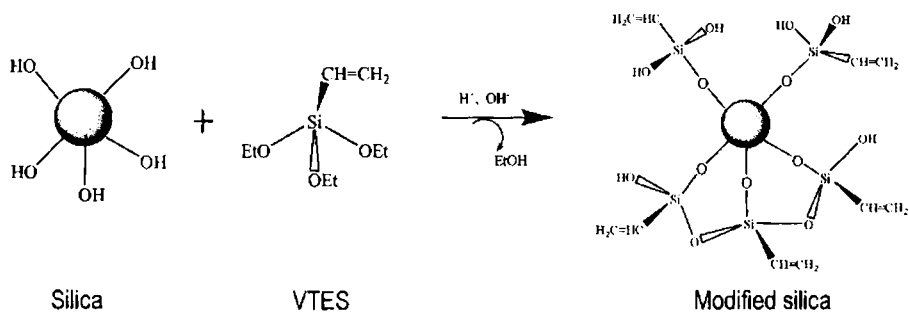


**Figure 3.4:** Modified silica formation

### 3.3 RESULTS AND DISCUSSION

#### 3.3.1 Bulk density

The bulk density values of synthesized silica samples were compared with commercially available silica (Table 3.1). It is found that the bulk density of prepared nanosilica is higher than the commercial silica and modified nanosilica. This may be due to the smaller particle size of synthesized silica compared to that of other samples.

**Table 3.1:** Bulk densities of silica

Sample	Bulk Density (g/cm <sup>3</sup> )
Commercial silica	0.98
Silica prepared without dispersing medium	1.103
Silica prepared in Chitosan medium	1.2924
Modified silica	1.1863

Bulk density of synthesized silica using chitosan medium is higher than that prepared without chitosan. This shows that chitosan helps to reduce the particle size and is a good medium for nanoparticle formation. It is expected that the addition of chitosan would act as a matrix into which silica would be incorporated and thus producing silica of lower particle size with higher bulk density.

Bulk density is found to decrease with modification. This indicates that the particle size increases with modification. This is as expected that the presence of modifying group on the surface of the nanoparticles would increase the particle size.

### **3.3.2 Surface area**

The surface area obtained for different samples by BET adsorption method are given in table 3.2. From the table it is clear that synthesized silica has higher surface area than that of commercial silica and modified silica.

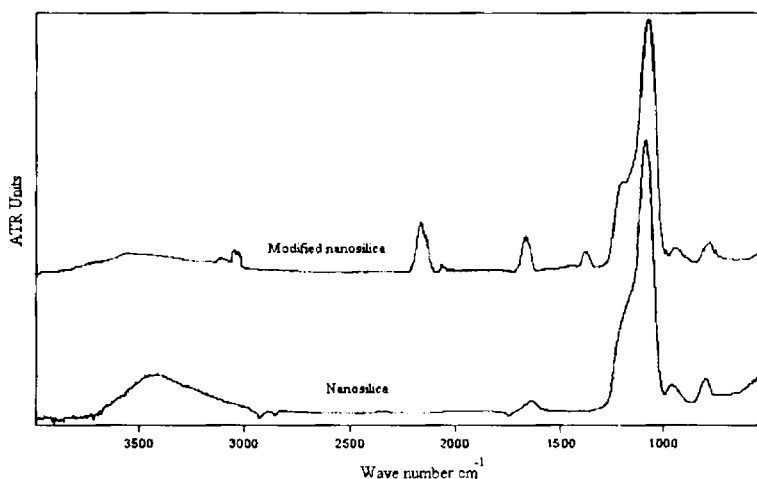
**Table 3. 2:** Surface area of the silica samples.

<b>Samples</b>	<b>Surface area (m<sup>2</sup>/g)</b>
Commercial silica	178
Silica prepared without dispersing medium	195
Synthesized silica	295
Modified silica	198

The surface areas of the particles are found to be higher as the particle size decreases. The above table shows that the prepared nanosilica has lower particle size. The surface area of the synthesized silica without chitosan is found to be much lower than the nanosilica.

The modified silica is found to have lower surface area compared to all samples. This is in confirmation with the observation that the presence of modifying group on the surface which decreases the adsorption of nitrogen on the surface of the particles. This indicates that modification of the silica surface is effective.

### 3.3.3 Infra Red Spectroscopy



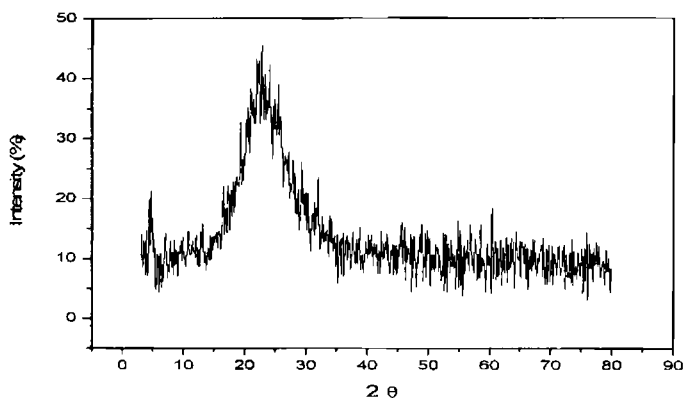
**Figure 3.5:** IR spectra of the silica samples

Figure 3.5 shows the IR spectra of the silica and modified silica. The broad band between 2800 and 3750  $\text{cm}^{-1}$  for silica is due to silanol -OH groups and adsorbed water. The predominant peak at 1080  $\text{cm}^{-1}$  is due to siloxane bonds (Si-O-Si). The peaks between 1000 and 700  $\text{cm}^{-1}$  are attributed to vibration modes of the gel net work.<sup>41</sup> Silica samples show similar IR spectrum. It can be concluded that all samples consist predominantly of silicon oxide. The two additional peaks at 1690  $\text{cm}^{-1}$  and 2140  $\text{cm}^{-1}$  of modified silica show the presence of modifying organic group. In comparing the spectra of the nanosilica and modified nanosilica it is found that there is a reduction in intensity of broad peak between 3000  $\text{cm}^{-1}$  and 3437  $\text{cm}^{-1}$  (of -OH stretching) in the case of the modified silica. Lesser number of hydroxyl groups in modified silica results in lower particle agglomeration.

### 3.3.4 X-Ray Diffraction (XRD)

X-Ray is an important tool to identify the crystalline nature, purity and size of materials. The X-Ray diffraction patterns of the silica and modified silica samples are

shown in figures 3.6 and 3.7. Strong broad peak observed around  $22-23^\circ$  is the characteristic of amorphous  $\text{SiO}_2$ .<sup>42</sup> This shows that the synthesized silica, commercial silica and modified silica are in an amorphous state. The full width at half maximum ( $\beta$ ) is used to determine the particle size using the Debye-Sherrer formula. The average particle size ( $C_s$ ) of the silica samples is given in the table 3.3.



**Figure 3.6:** XRD pattern of prepared nanosilica

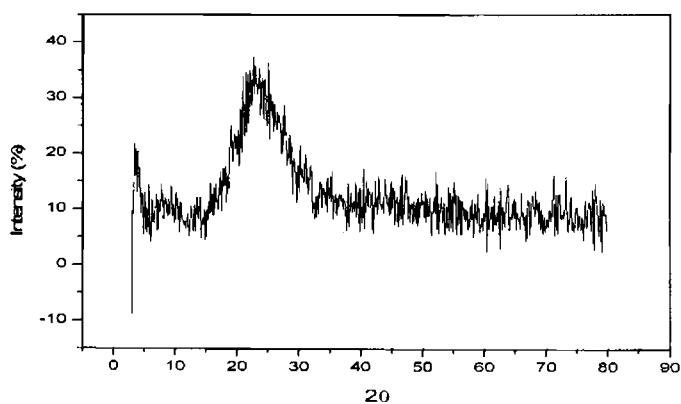


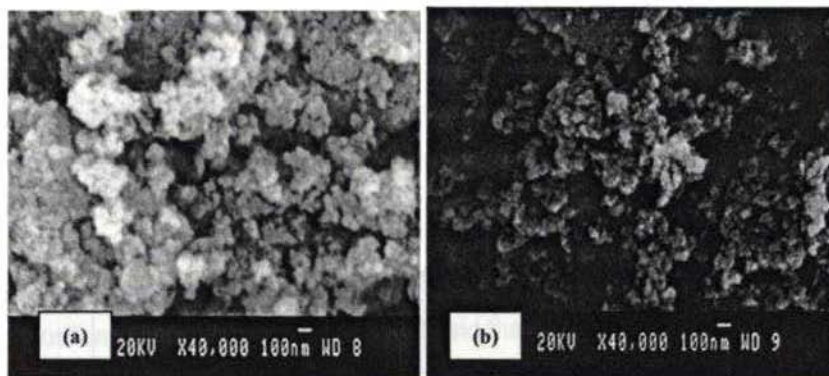
**Figure 3.7:** XRD pattern of modified nanosilica

**Table 3.3:** Average Particle size of the silica samples

Sample	Average Particle size ( nm)
Commercial silica	34
Silica prepared without dispersing medium	22
Synthesized silica	16
Modified silica	20

### 3.3.5 Scanning Electron Microscopy (SEM)

Figures 3.8 a & b show the SEM micrographs of the silica synthesized without chitosan and with chitosan medium respectively at 40,000X magnification. These micrographs show that the silica prepared in chitosan medium has lower particle size than that prepared without chitosan. It is seen that the size of both type of silica are in nanometer range. The silica prepared without chitosan are highly agglomerated and have larger particle size compared to the other.

**Figure.3.8:** SEM micrograph of nanosilica prepared

a) without chitosan b) with chitosan medium

From the SEM analysis it is evident that the introduction of dispersing medium in the reaction system gives lower particle size and less agglomerated silica.

### 3.3.6 Transmission Electron Microscopy (TEM)

The TEM image of synthesized nanosilica in chitosan medium and its diffraction pattern are given in figure 3.9. It shows that even though the average particle size is low (~16nm) the particles are agglomerated. The corresponding diffraction pattern indicates that the nano particles are amorphous in nature.<sup>43</sup>

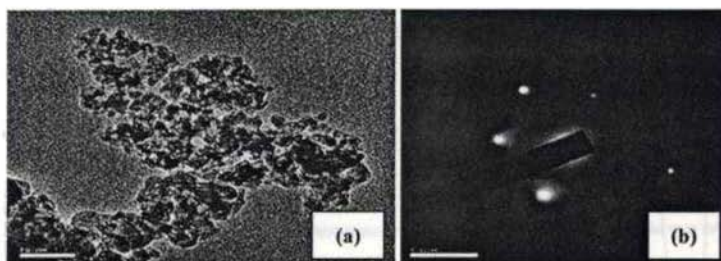


**Figure 3.9:** TEM image of the nanosilica a) synthesized in chitosan medium b) diffraction pattern

The TEM image obtained for the modified nanoparticle is shown in figure 3.10. It shows that the agglomeration tendency of the particles decreased by the modification. The average particle size is about 22nm which is higher than than the nanosilica. This is an evidence for the modification. From TEM image we can observe that the modification by organic group is effective to reduce the agglomeration.

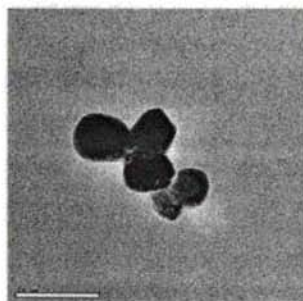


**Figure 3.10:** TEM image of modified nanosilica

### 3.3.7 Thermogravimetric analysis (TGA)

The thermogravimetric curve obtained for synthesized silica in chitosan medium is given in figure 3.11. It shows about 8% weight losses within 150 °C and after that it does not show further reduction in weight. The loss of weight is due to the adsorbed moisture in the sample.

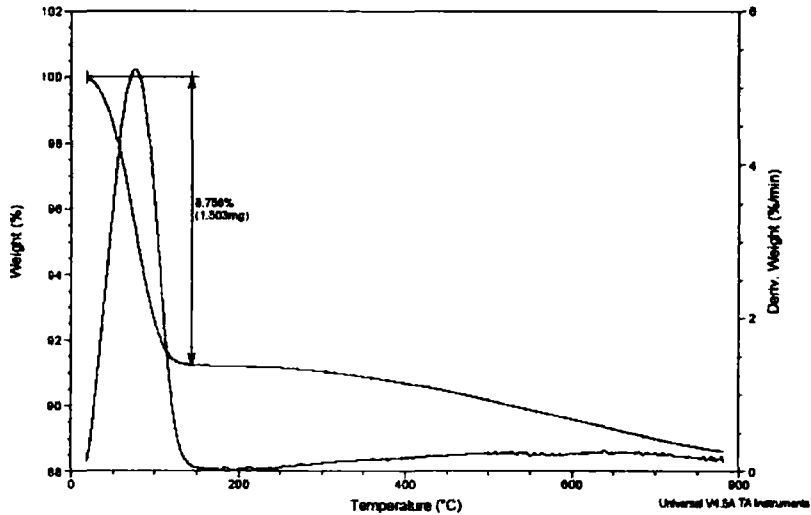


**Figure.3.11:** TG trace of the synthesized silica

The TG curve obtained for modified silica (Figure 3.12) shows that there is no appreciable degradation within 150 °C. This shows that moisture adsorption is very much reduced by the modification. The sample shows gradual reduction in weight from 200 °C to 800 °C. This is due to the presence of organic group around the surface of the particles.



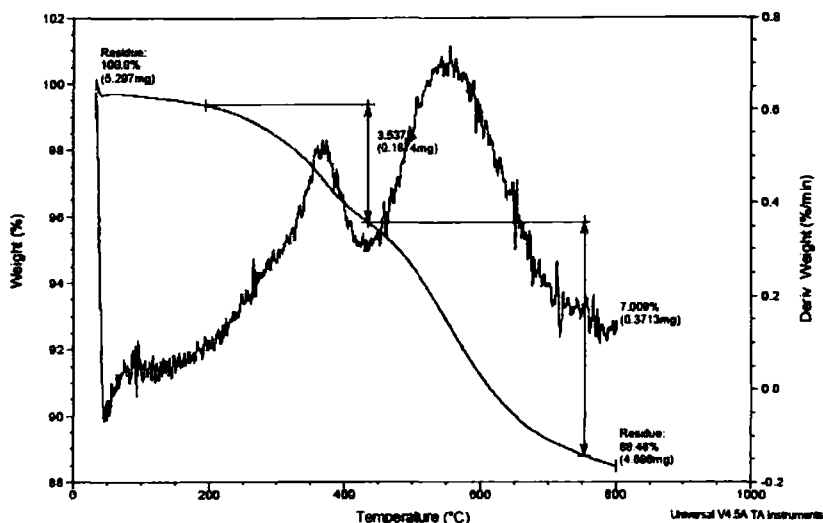


**Figure 3.12: TG trace of the modified silica**

### 3.3 CONCLUSIONS

Under controlled conditions nanosilica can be successfully prepared by a precipitation route. Chitosan medium can be used for the preparation of inorganic particles. The particle size of the silica can be controlled by using the precipitation medium and its concentration. Nanosilica prepared by this method has a particle size less than 18 nm which is lower than that of the commercially available silica. The particle size of silica was found to be 14 nm from the XRD results and the surface area was found to be 395 m<sup>2</sup>/g by BET method. IR spectroscopy shows the absence of side products on silica particles. XRD and TEM results show that the synthesized silica is predominantly amorphous in nature. TEM images show that the agglomeration tendency of the nanoparticles can be reduced by the modification without much increment in size. Thermogravimetric analysis shows that moisture absorption can be reduced by the modification of silica.

## REFERENCES

1. Y.Kojima, A.Usuk, M.Kawasumi, A.Okada, T.Kurauchi, O.Kamigaito; *J.Polym.Sci. Part A: Polym. Chem.* **1993**, 31, 1755.
  - (a) S.Hambir, N.Bulakh, P.Kodgire, R.Kalgaonkar, J.P.Jog; *J.Polym.Sci.Part B: Polym. Phys.* **2001**, 39, 446.
  - (b) S.Sadhu, A.K.Bhowmick; *J.Polym.Sci.Part B:Polym.Phys.* **2004**, 42, 1573.
  - (c) Y.Ke, C.Long, Z.Qi; *J. Appl. Polym. Sci.* **1999**, 71, 1139.
2. K.A.Mauritz, R.Ju; *Chem. Mater.* **1994**, 6, 2269.
3. Z.H.Huang, K.Y.Qiu; *Polymer* **1997**, 38, 521.
4. S.Iijima, C.Brabec, A.Maiti, J.Bernholc; *J. Chem. Phys.* **1996**, 104, 2089.
5. E.W.Wong, P.E.Sheehan, C.M.Lieber; *Science* **1997**, 277, 1971.
6. N.G.Chopra, L.Benedict, V.Crespi, M.Cohen, S.Louie, A.Zettl, *Nature* **1995**, 377, 135.
7. F.Yang, Y.Ou, Z.Yu; *J.Appl.Polym.Sci.* **1998**, 69, 355.
  - (a) J.Kolarik, O.Dukh, L.Matejka; *Polymer* **2000**, 41, 1449.
  - (b) K.Qui, Z.Huang; *Polymer* **1997**, 38, 521.
  - (c) M.Smaih, C.Joly, R.Noble; *Chem.Mater.* **1999**, 11, 2331.
  - (d) Y.Yang, J.Yin, Z.Qi, Z.Zhu; *J.Appl.Polym.Sci.* **1999**, 73, 2977.
  - (e) T.Mallouk, J.Ollivier, S.Johnson; *Science* **1999**, 283.
  - (f) C.H.Landry, B.Coltrain; *Polymer* **1992**, 33, 7.
8. B.Borup, R.Edelmann, R.Mehnert; *Eur.Coat.J.* **2003**, 6, 21.
9. B.Atsumi, T.Toshihiko, E.Yuichi, U.Takashi; *Proc.Rad.Tech.Sia.*, Yokohama, Japan, **1997**, 522.

10. S.Zhou, L.Wu, J.Sun; *Prog.Org.Coat.* **2002**, 45, 33.
11. V.Morote-Martínez, V.Pascual-Sánchez, J.M.Martín-Martínez; *Eur. Polym. J.* **2008**, 44, 3146.
12. D.S.Achilias, D.N.Bikiaris, V.Karavelidis, G.P.Karayannidis; *Eur. Polym. J.* **2008**, 44, 3096.
13. C.Chenggang, S.J.Ryan, W.S.Dale, W.B.Jeffery; *Polymer* **2008**, 49(17), 3805.
14. J.J.Gaitero, I.Campillo, A.Guerrero; *Cem. Concr. Res.* **2008**, 38, 1112.
15. G.Xiaowei, M.Xiangfu, W.Haitao, W.Bin, D.Yanfen, Z.Shimin, Y.Mingshu; *Polym. Degrad. Stab.* **2008**, 93( 8), 1467.
16. W.Nangeng, T.Qinqiong, C.Min, W.Limin; *J. Colloid Interface Sci.* **2008**, 320, 152.
17. S.Jeng-Ywan, C.Ta-Peng, H.Tien-Chin; *Mater. Sci. Eng.A* **2006** 424, 266.
18. S.Ranimol, C.Ranganathaiah, V.Siby, K.Joseph; *Polymer* **2006**, 47, 858.
19. (a) V.M.Gun'ko, V.I.Zarko, E.F.Voronin, E.V.Goncharuk, L.S.Andriyko, N.V.Guzenko, L.V.Nosach, W.Janusz; *J. Colloid Interface Sci.* **2006**, 300, 20.  
(b) Y.Wang-zhang, M.Peng, Y.U.Qiu-ming, T.Ben-Zhong, Q.Zheng; *Chemical Research in Chinese Universities*, **2006**, 22, 797.  
(c) N.García, T.Corrales, J.Guzmán, P.Tiemblo; *Polym. Degrad. Stab.* **2007**, 92, 635.  
(d) J.Vega-Baudrit, M.Sibaja-Ballesteros, V.Patricia, R.Torregrosa-Maciá, J.M.Martín-Martínez; *Int. J. Adhes. Adhes.* **2007**, 27, 469.  
(e) A.L.Daniel-da-Silva, F.Pinto, J.A.Lopes-da-Silva, T.Trindade, B.J.Goodfellow, A.M.Gil; *J. Colloid Interface Sci.* **2008**, 320, 575.  
(f) J.Berriot, F.Lequeux, H.Montes, H.Pernot; *Polymer* **2002**, 43, 6131.  
(g) A.Zhu, A.Gai, W.Zhou, Z.Shi; *Appl. Surf. Sci.* **2008**, 254, 3745.

- (h) X.J.Xiang, J.W.Qian, W.Y.Yang, M.H.Fang, X.Q.Qian; *J. Appl. Polym. Sci.* **2006**, 100, 4333.
  - (i) L.Matejka, O.Dukh, H.Kamizova, D.Hlavata, M.Spirkova; *Polymer* **2004**, 45, 3267.
  - (j) K.Chatterjee, K.Naskar; *Polym. Eng. Sci.* **2008**, 48,1077.
  - (k) R.N.Mahalling, S.Kumar, T.Rath, C.K.Das; *J. Elastomers Plast.* **2007**, 39, 253.
  - (l) C.S.Reddy, C.K.Das; *Polym. Polym. Compos.* **2008**, 14, 281.
  - (m) V.B.Jose, V.P.Virtudes, M.M.Jose; *Int. J. Adhes. Adhes.* **2006**, 26, 378.
20. J.E.Mark, Y.C.Lee, P.A.Bianconi; *ACS Symposium Series*, California **1995**, 585.
  21. S.Patel, B.Abhijit, V.Vijayabaskar, A.K.Bhowmick; *Polymer*, **2005**, 46, 8079.
  22. S.Rajatendu, B.Abhijit, S.Sunil, T.K.Chaki, A.K.Bhowmick; *Polymer* **2005**, 46, 3343.
  23. M.W.Ellsworth, G.Douglas; *Polymer News* **1999**, 24 531.
  24. B.Abhijit, D.S.Mousumi, A.K.Bhowmick; *J Polym.Sci.Part B:Polym.Phy.* **2005**, 43, 2399.
  25. B.Abhijit, A.K.Bhowmick, D.S.Mousumi; *J Appl.Polym.Sci.*, **2004**, 93, 2579.
  26. B.Abhijit, D.S.Mousumi, A.K.Bhowmick; *J Appl.Polym.Sci.*, **2005**, 95, 1418.
  27. D.S.Gian, Z.Yujun, F.Maurizio, Z.Luca, G.Rocha; *J. European Ceramic Society* **2005**, 25, 277.
  28. C.Jerzy, S.Ludomiri; *Mater.Sci.* **2003**, 21, 4, 461.
  29. G.Thomas, H.Sebastian, B.Michael, K.Guido; *Angew Chem* **2004**, 43 (42). 5697.
  30. J.Jinting, K.Ken-ichi, P.Lihua, T.Masataka; *Colloids and Surfaces* **2004**, 38,3,121
  31. M.Atanu, B.Asim, I.Toyoko; *J.Nanosci.Nanotechnol.* **2004**, 4, 1052.
  32. S.Reiko, K.Shin-ichiro, H.Takayoshi; DOI 10.1002/ app.21959, Wiley Interscience.

33. C.Jerzy, S.Ludomir; *Mater.Sci.*, **2003**, 21,4, 461.
34. F.Masahiro, K.Katsunori, T.Yuko, N.Ryoki; *J.Mater.Chem.* **2004**, 14, 1195.
35. S.H.Kim, B.Y.H.Liu, Zachariah; *Langmuir* **2004**, 20, 2523.
36. T.Kotoky, S.K.Dolui; *J.Sol Gel.Sci.Technol.*, **2004**, 20, 107.
37. Y.Arai, H.Segawa, K.Yoshida; *J.Sol.Gel.Sci.Technol.*, **2004**, 34, 79.
38. T.Nittaya, N.Apinon; *J.Nat.Sci. Special Issue on Nanotechnology* **2008**, 7(1) 59.
39. K.Jal, M.Sudarshan, A.Saha, P.Sabita, B.K.Mishra; *Colloids and surfaces A* **2004**, 240, 173.
40. (a) E.P.Pleuddemann; *Silane coupling agents*, Plenum press, New York, London, **1978**.  
(b) S.J.Monte, G.sugerman; *Current application of titanate coupling agents in filled thermoplastic and thermosets*, 36th Annual conf., Reinforced Hastics/composites Institute, **1981**.  
(c) H.Chiang, N.I.Liu, J.L.Koenig; *J.Colloid Interface Sci.*, **1982**, 86, 26.  
(d) C.H.Chiang, H.Ishida, J.L.Koenig; *J.Colloid Interface Sci.*, **1980**, 74, 396.  
(e) M.Kranz, L.Domka, A.Kryszstafkiewicz, M.Maik; *Polimery*, **1979**, 24, 86.
41. K.Jal, M.Sudarshan, A.Saha, P.Sabita, B.K.Mishra; *Colloids and surfaces A* **2004**, 240, 173.
42. W.J.Byung, C.H.Kim, G.H.Tae, J.B.Park; *Const. Build. Mater.* **2007**, 21, 1351.
43. T.Nittaya, N.Apinon; *J.Nat.Sci. Special Issue on Nanotechnology* **2008**, 7(1) 59.

# Chapter 4

## Thermoplastic - silica nanocomposites

### Part - a

#### Polypropylene-silica nanocomposites

##### 4a.1 INTRODUCTION

There is an increasing need for polymer-based nanocomposite materials due to the developments in traditional industry and advanced materials. These needs pave the way for a unique and new market for improving traditional products.<sup>1,2,3</sup> At present, the diverse organic polymers with high yield find their applications in fibres, resins, rubbers and their composites including polymer-polymer and inorganic reinforcing polymer composites. Due to difficult dispersion behaviour, the composites of nanoparticle filling polymer develop relatively slowly, while the polymer-inorganic nanocomposite materials by insitu polymerization technology increase rapidly. There is a great potential in the modification of traditional materials. So far, the insitu intercalation polymerization technique is thought to be one of the best choices for dispersing nanoparticles in the polymer melt. It may provide a very large number of new products for daily life and industrial applications.

A large number of inorganic materials, such as glass fibre, talc, calcium carbonate, and clay minerals have been successfully used as additives to improve various properties of polymers.<sup>4</sup> Inorganic particle filled polymer nanocomposites, notably nano-clays,<sup>5,6</sup> have attracted great interest over last decade.<sup>7,8</sup> Nanoparticle filled polymers are attracting considerable attention since they can produce property enhancement that are sometimes even higher than the conventional filled polymers at volume fractions in the range of 1-5%. Rong *et.al.* and Wu *et.al.* have reported the improvement of tensile

performance of low nanoparticle filled polypropylene composite.<sup>9,10</sup> The inorganic fillers are used for improving stiffness, toughness, hardness, chemical resistance, dimensional stability and gas barrier properties of PP. The mechanical and physical properties of PP composites strongly depend on the filler size, shape, aspect ratio, interfacial adhesion, surface characteristics and degree of dispersion.<sup>11</sup>

Polypropylene (PP) is a semi-crystalline polymer which is very versatile in nature and is one of the fastest growing classes of thermoplastics.<sup>12</sup> This growth is attributed to its attractive combination of low cost, low density, high heat distortion temperature, and mouldability. The extraordinary versatility of unfilled virgin PP and reinforced polypropylene suits a wide spectrum of end-use applications for fibres, films, and molded parts. However, the shortcomings in physical and chemical properties limit the universal use of polypropylene. For example in packaging, polypropylene resins have poor oxygen barriers. Most designs to improve polypropylene gas barrier properties involve either addition of higher barrier plastics via a multilayer structure or surface coatings. Even if effective, the increased cost of these approaches negates the big attraction of 'low cost' for using polypropylene. The incorporation of inorganic particulate fillers has been proved to be an effective way of improving the mechanical properties and in particular the toughness of polypropylene. Stamhuis has shown that talc filler can significantly increase the impact resistance of polypropylene, if it is physically blended with either an SBS or an EPDM elastomer.<sup>13</sup> Hadal and Misra have reported that modulus of polypropylene has been improved by talc and wollastonite.<sup>14</sup> Radhakrishnan and Saujanya have reported that the needle shaped  $\text{CaSO}_4$  can improve the properties of PP with its high aspect ratio.<sup>15</sup> Silica filled composites gaining importance in consumer goods, automotive applications and electrical & electronic engineering appliances.<sup>16,17,18</sup> Fillers cannot modify the properties of composites unless there is good adhesion with polymer matrix. The hydrophobic polymer and the hydrophilic filler cause a significant problem in enhancing the adhesion between the filler and the matrix. This problem can overcome by increasing the affinity between the two phases either by in-situ polymerization or by use of coupling agents.<sup>19,20,21</sup>

In this part of study the PP/silica nanocomposites preparation using silica and VTES modified silica are discussed with focus on the mechanical, thermal and dynamic mechanical performance. The influence of maleic anhydride grafting of PP/silica nanocomposites also investigated.

## **4a.2 EXPERIMENTAL**

Nanosilica reinforced PP composites were prepared by a simple melt-compounding method.<sup>22</sup> The melt mixing of PP with unmodified and modified nanosilica was performed in a Torque Rheometer (Thermo Haake Rheocord 600) at 180 °C and at a rotor speed of 50 rpm for 8 min. The concentration of nanosilica was varied from 0-3 wt%. The variation of torque with time of mixing was monitored. The torque stabilized to a constant value in this mixing time. The resulting compound was hot pressed into thin sheets and cut into pieces. The matrix was modified with maleic anhydride according to US patent, 4,753,997. Dumb-bell and rectangular shaped specimens were prepared by injection moulding in a semiautomatic laboratory injection moulding machine.

The tensile properties of the samples were determined using a Universal Testing Machine (Shimadzu AG 1) at a crosshead speed of 50 mm/min as per ASTM-D-638. Flexural properties of the composites were measured by three point loading system as per ASTM-D-790 at a crosshead speed of 5 mm/min. Impact strength of the samples were determined using Resil impactor junior (Ceast) (ASTM-D256). Thermogravimetric analysis (TGA) was done using TGA Q50 (TA instruments). The crystallization behaviour was analyzed using DSC Q100 (TA instruments). The storage modulus and mechanical damping ( $\tan \delta$ ) was measured using dynamic mechanical analyzer model Q800 (TA instruments). The morphology of the tensile fractured surface was also investigated using scanning electron microscope (SEM).

## **4a.3 RESULTS AND DISCUSSION**

### **4a.3.1 Polypropylene silica nanocomposites**

#### **4a.3.1.1 Torque studies**

The variation of mixing torque with time at different filler loading is given in figure 4a.1. A mixing time of 8 minutes was adequate, since the torque stabilized to a constant value during this time in all cases. The stabilization of the torque may be an indication of attainment of a stable structure after a good level of mixing. The torque values slightly changes with the concentration of silica particles. This shows that the particulate filler undergo good mixing under the given conditions.



Initially torque increases with the charging of PP, but decreases with melting and levels off in about 2 minutes. The composite preparation was done by adding nanosilica/modified nanosilica at the start along with PP. Here also the torque stabilized at a constant value in about 2 min. It is clear from the figure that there is no appreciable change in torque on continued mixing up to 8 min. This indicates that there is no appreciable degradation during the mixing stage.

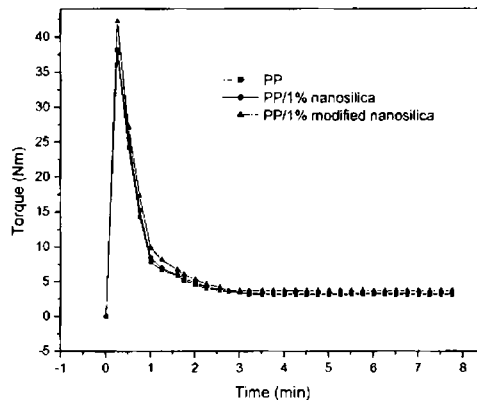


**Figure 4a.1:** Variation of mixing torque with time of PP/silica nanocomposites

The variation of mixing torque with time of mixing of modified silica in PP also showed the same behaviour as above. But the end torque was found to be little higher than the former. In this case also the mixing time was fixed as 8 minutes.

#### 4a.3.1.2 Tensile properties

The inclusion of fillers in the PP matrix leads to a significant increase in mechanical properties. Zhao *et al.*<sup>23</sup> observed the increase of tensile performance by the incorporation of nano filler. Svehlova *et al.*<sup>24</sup> mentioned that a better filler dispersion leads to a higher modulus. Hence a higher mechanical performance of nanocomposites is an indication of better filler dispersion. Reddy *et al.*<sup>25</sup> observed that the modification of silica surface leads to better filler dispersion and wetting in PP matrix. The effect of nanosilica and modified nanosilica concentration on the tensile properties of the composites are shown in figure 4a.2. For this study the concentration of silica particles in the matrix was varied from 0 to 3 weight percent of PP.

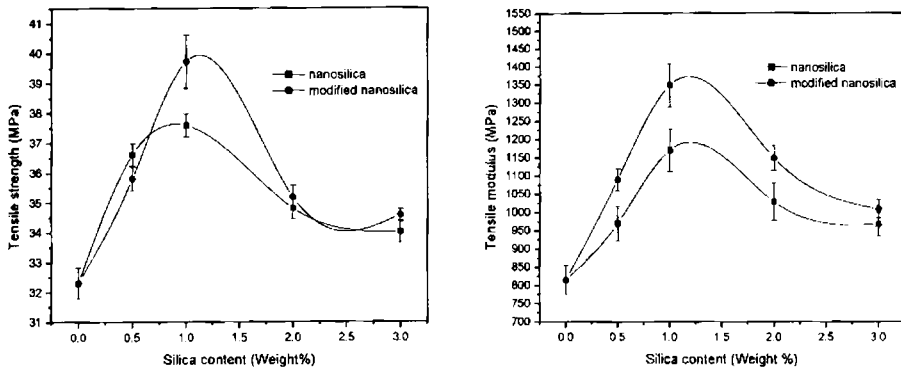


**Figure 4a.2:** Variation of tensile strength and modulus of PP-silica/modified silica nanocomposites with silica content

The figures show an increase in tensile properties and a maximum value is obtained at 1wt.% of silica loading. This may be due to good filler dispersion and effective interaction of the nanoparticles with PP at this composition.<sup>26</sup> There is a gradual reduction in strength and modulus values after this composition. At higher particulate loading, there is a tendency for the silica nanoparticles to aggregate heavily. The tensile strength and tensile modulus improved by approximately 16% and 43% respectively with unmodified silica particles. The corresponding values for modified nanosilica/PP composites are 23% and 73% respectively.

In a composite, the interfacial stress transfer efficiency and extent of induced deformation determines the mechanical performance. Generally particulate composites do not exhibit high tensile strength and elongation to break due to weak interfacial adhesion. There will be considerable improvement in these properties if the bonding between filler and matrix is strong. Figure 4a.2 shows that the adhesion between the filler and matrix is improved by the use of modified nanosilica. The use of modified nanosilica gives about 30% improvement of modulus when compared with the use of unmodified silica. The modification of silica surface by vinyl group enhances the hydrophobic character of the inorganic particles that lead to good interaction (wetting) with the organic matrix. The decrease in strength and modulus after a particular composition may be due to the poor dispersion of silica particles by the agglomeration within the polymer matrix.

The hardness and % of elongation of nanosilica and modified nanosilica/PP composites are listed in table 4a.1. The results indicate that 1wt.% silica gives effective reinforcement by melt mixing. The elongation to break was found to be increasing with modified silica content and is slightly higher than the same amount of unmodified nanosilica addition. This may be due to the better wetting of modified nanosilica by the polymer. This also implies that the better adhesion between the nanosilica and PP is the key factor for the improvement of properties.

**Table 4a.1:** Effect of silica/modified silica content on hardness and elongation

S* Content (Wt.%)	Hardness (Shore D)	Elongation (%)	MS** Content (Wt.%)	Hardness (Shore D)	Elongation (%)
0.0	56	8.13	0.0	56	8.13
0.5	58	7.45	0.5	60	7.87
1	61	6.81	1	64	7.52
2	62	6.24	2	66	7.21
3	64	5.98	3	69	6.87

\*S → nanosilica, \*\*MS → modified nanosilica

#### 4a.3.1.3 Flexural properties

The comparison of flexural strength and modulus of PP nanocomposites prepared with nanosilica and modified nanosilica is shown in figure 4a.3.

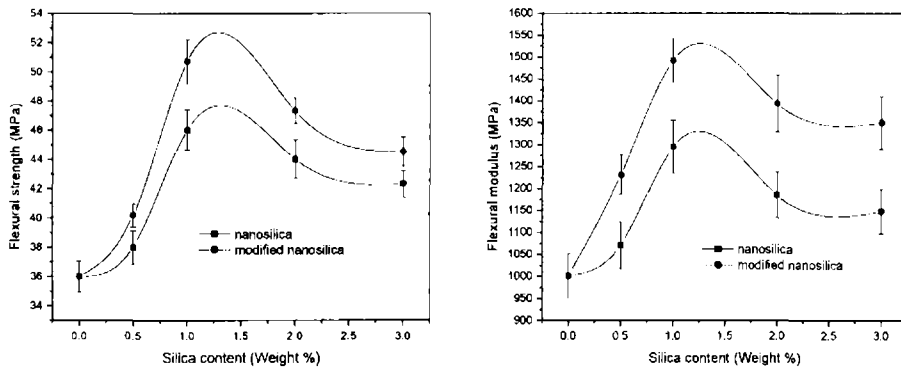


**Figure 4a.3:** Variation of flexural strength and modulus of PP-silica/modified silica nanocomposites

With modified silica, the flexural modulus as well as strength of PP increases considerably. The figures also show that the concentration of silica that can be added to PP to obtain maximum values in flexural loads in both cases is again 1%. The incorporation of modified silica at this composition increases the modulus around 48% and strength around 40%. The effective reinforcement may be due to uniform dispersion and good interfacial interaction of modified nanosilica with PP matrix. The modification of silica has resulted to enhance the adhesion between the hydrophobic PP and the hydrophilic silica particles.

#### 4a.3.1.4 Impact strength

The impact strength of plastics can be improved by several techniques. The incorporation of rubbery particles is a good method but this results in reduction of other properties like elastic modulus, tensile strengths etc. of the material.<sup>27,28</sup> In general, for a material to be very tough and to have high impact resistance there must be some mechanism for spreading the stored energy to be absorbed. The use of rigid fillers to toughen polymers has also been received considerable attention.<sup>29</sup>

The use of nanoparticles to improve the toughness of the polymers has been increased recently. Chen *et al.*<sup>30</sup> reported that the fracture toughness of PP increased five fold by incorporating nanometer-scale CaCO<sub>3</sub> and the CaCO<sub>3</sub> particles acted as stress concentrators to promote toughening mechanism. Nanoclay also used to improve the impact strength.<sup>31</sup> The effect of nanosilica and modified nanosilica on the toughness of PP is shown in figure 4a.4

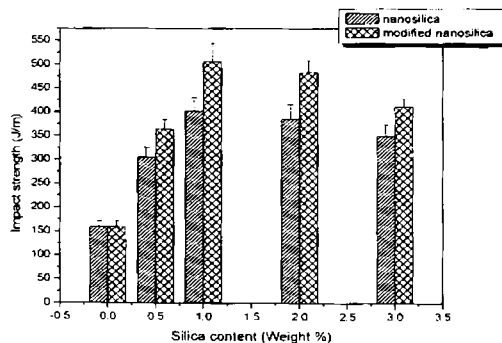


**Figure 4a.4:** Effect of nanosilica/modified nanosilica concentration on impact strength of PP

Here also the higher impact strength of PP composite is found at 1wt.% silica loading. The increase in impact strength is about 125% with nanosilica, and is about 200% with modified nanosilica. This may be due to the presence of organic group on silica surface which improved the compatibility between filler and the matrix.<sup>32</sup> In case of poor adhesion between phases, the moment at which the matrix actually separates from the particles depend on the particle size due to subsequent debonding sequence (void forming) that would lead to specimen failure. Hence, large sized particles are undesirable when the adhesion between matrix and filler is poor. Because of the high surface energy of the nanosilica, at higher filler concentration the particles agglomerate to form bigger sized particles. Hence above 1wt.% silica addition impact strength is found to be decreasing.

### 4a.3.2 Effect of matrix modification on PP-silica nanocomposites

#### 4a.3.2.1 Torque studies

The variation of mixing torque with time at different filler loading is shown in figure 4a.5. The mixing time of 8 minutes was fixed, since after grafting also the torque value is found to be steady by this time in all cases.

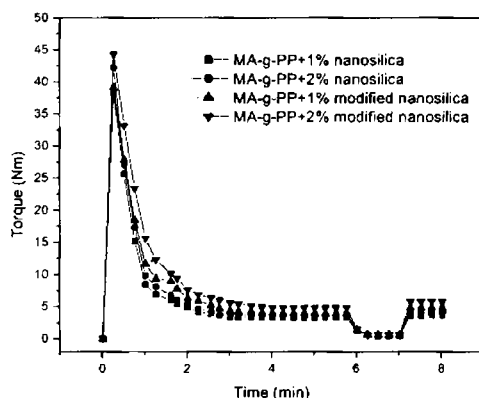


**Figure 4a.5:** Variation of mixing torque with time of MA-g-PP-silica/modified silica nanocomposites

### 4a.3.2.2 Tensile properties

The effect of chemical treatment on the tensile properties of nanosilica/modified nanosilica-PP composites are shown in figure 4a.6. From the figures, it is clear that the matrix modification improves the tensile strength of the composites. The improvement in the tensile modulus even at 1% silica loading is particularly significant which shows that the matrix has become stronger by the modification even though it is not pronounced at higher particulate loading.

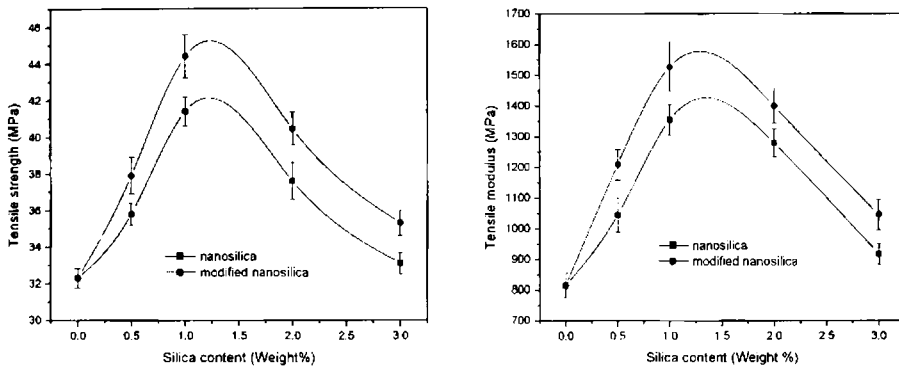


**Figure 4a.6:** Variation of tensile and modulus strength of MA-g-PP-silica/modified silica nanocomposites with silica content

Both figures show similar behaviour (increasing till 1wt.% silica addition and then decreasing) for the variation of tensile properties. The tensile properties are found to be better for MA grafted PP composites for all compositions when compared to PP composites.

At 1wt.% silica concentration, tensile strength improved about 16% for nanosilica and about 43% for modified nanosilica in MA-g-PP matrix as compared to pure PP. The modulus which is an important property of the nanocomposite shows 73% improvement for MA-g-PP composite with 1wt.% vinyl group modified nanosilica.

The improvement in the tensile properties may be due to the better dispersion of nanoparticles in PP matrix as suggested by Svehlova *et al.*<sup>33</sup> The -OH group on silica

surface and maleic anhydride group present in the backbone of PP experience electrostatic interaction which gives better adhesion between filler and matrix in MA-g-PP/silica composite. But in MA-g-PP/modified nanosilica composite there may be two types of interactions.

1. Interaction due to the attraction between –OH groups present on the surface of silica and maleic anhydride groups present in the backbone of PP
2. Interaction between vinyl group in VTES-g-SiO<sub>2</sub> and polymer backbone

This will decrease the crowding of the nanoparticles and increase the bonding between filler and matrix. Hence interfacial stress transfer efficiency will be higher for these nanocomposites.

In general, particulate composites exhibit a reduced tensile strength and elongation at break due to weak interfacial adhesion. However, when bonding between fillers and matrix is strong enough then we can expect considerable improvement in tensile strength compared to unfilled matrix.

The hardness and % of elongation of nanosilica or modified nanosilica/MA-g-PP composites are listed in table 4a.2.

**Table 4a.2:** Effect of silica content on hardness and elongation

S Content (Wt.%)	Hardness (Shore D)	Elongation (%)	MS Content (Wt.%)	Hardness (Shore D)	Elongation (%)
0.0	56	8.13	0.0	56	8.13
0.5	62	7.63	0.5	63	7.94
1	65	7.45	1	67	7.68
2	68	7.01	2	71	7.32
3	70	6.92	3	73	7.19

#### 4a.3.2.3 Flexural properties

The flexural properties of the nanocomposites of MA-g-PP are shown in figure 4a.7. There is a significant improvement in the flexural properties at all filler loading. The maximum improvement occurs at 1wt.% silica content. This is probably due to the decrease in particulate-matrix interaction by the agglomeration at higher filler loadings

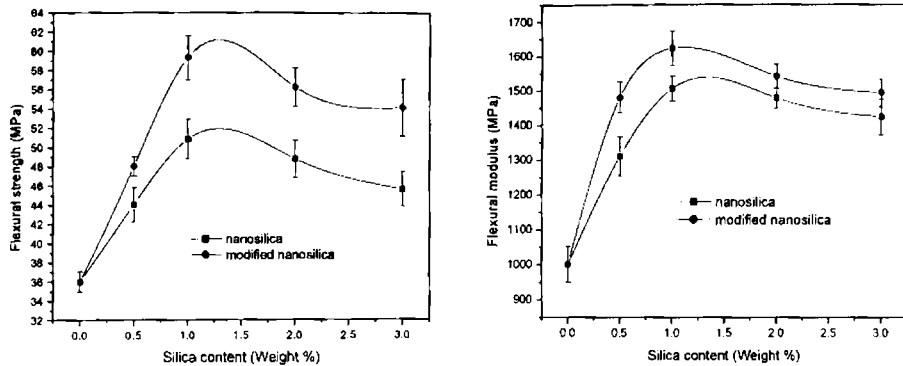


**Figure 4a.7:** Variation of flexural strength and modulus of MA-g-PP-silica/modified silica nanocomposites

With modified silica, the flexural modulus and strength of PP increase considerably and the maximum value is obtained at 1% silica content. At this composition the modulus increases by 61% and strength 58% for modified silica composite. The efficient reinforcement may be due to uniform dispersion and good interfacial interaction of modified nanosilica with MA-g-PP matrix.

After 1% nanosilica addition, the tensile and flexural properties are found to decrease. This can be ascribed to the poor dispersion of nanoparticles at higher filler concentration. This suggests that the melt mixing route or melt mixing at 50 rpm is not enough to increase the effective interaction between nanofiller and matrix at higher concentration of nanofiller.

#### 4a.3.2.4 Impact strength

The impact strength of the nanocomposites prepared using MA-g-PP matrix is shown in figure 4a.8.



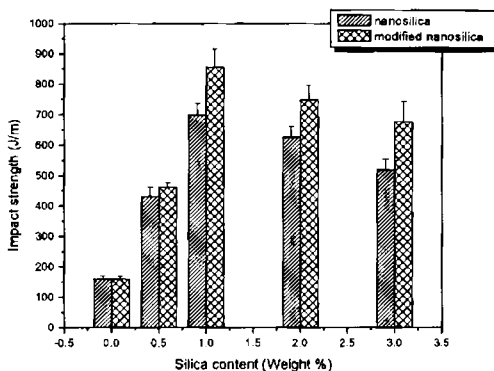


**Figure 4a.8:** Effect of nanosilica/modified nanosilica concentration on impact strength of MA-g-PP

At 1wt.% addition, the impact strength increases around 200% for the nanosilica composite but for modified nanosilica the enhancement is around 325%. The higher the interaction between the two phases, the higher is the stress that can be applied before it breaks. Naturally, it is believed that the nature of the filler/matrix interfacial layer is responsible for the impact property of the composites. When untreated nanosilica is added to MA-g-PP, an increase in impact strength is observed. Increasing the filler loading beyond 1wt.% decreases the impact strength due to uneven dispersion of the nanoparticles in the matrix. The addition of modified nanosilica into MA-g-PP performs much better than the other, demonstrating that the interfacial interaction in the composite is enhanced due to the chemical bonding between the vinyl group of the silica and MA-g-PP. The stronger interfacial adhesion would somewhat hinder molecular movement, leading to higher resistance to the crack development in the matrix polymer.

### 4a.3.3 Dynamic mechanical analysis

Dynamic storage modulus ( $E'$ ) is the most important property to assess the load-bearing capability of a nanocomposite material, which is very close to the flexural modulus<sup>34</sup> and is usually used to study the relaxations in polymers. The ratio of the loss modulus ( $E''$ ) to the storage modulus ( $E'$ ) is known as mechanical loss factor ( $\tan \delta$ ). DMA was performed on composites to determine the effect of fillers, on mechanical

properties of the polymer. An analysis of storage modulus and  $\tan \delta$  curves is very useful in ascertaining the dynamic performance of a sample under stress and temperature. This is related to the impact properties of a material. It represents the ratio of the dissipated energy to the stored energy and is related to the glass transition temperature of the polymer.

The storage modulus of the PP-silica nanocomposite as a function of temperature at 1Hz is shown in figure 4a.9. It shows a steady decrease of the modulus with temperature. The storage modulus of the nanocomposites is found to be higher than pure polymer at all temperatures. This may be due to the stiffening effect of silica, and efficient stress transfer between the PP matrix and nanosilica.

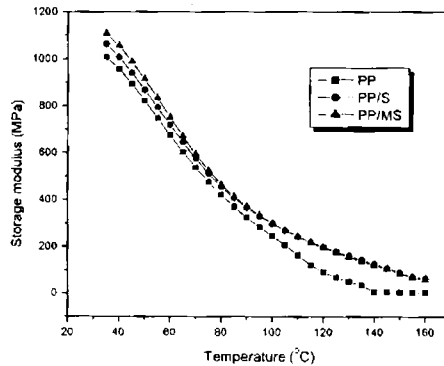


**Figure 4a.9:** Variation of storage modulus of PP-silica/modified silica nanocomposites with temperature

It has been suggested that the enhancement of the storage modulus and glass transition temperature results from the strong interfacial interaction between the polymer and filler and the restricted segmental motion of polymer chains at the organic-inorganic interface.<sup>35,36</sup> An increase in storage modulus of PP matrix was observed by adding ZnO particle by Zhao *et.al.*<sup>37</sup> This is expected owing to the stiffness improvement of inorganic particles.

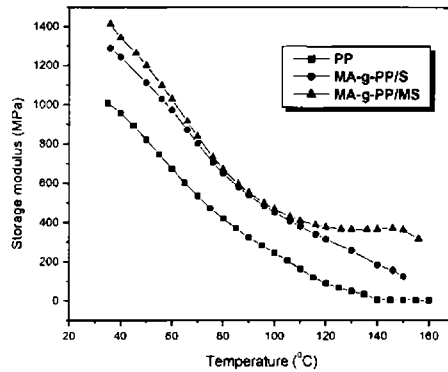


**Figure 4a.10:** Variation of storage modulus of MA-g-PP-silica/modified silica nanocomposites with temperature

The variation of storage modulus with temperature for pure PP and MA-g-PP/silica composites are shown in figure 4a.10. Here also the  $E'$  values show a steady decrease of the moduli with temperature. The storage modulus of the nanocomposites is found to be higher than the pristine polymer at all temperatures but the maleic anhydride (MA) grafting makes a pronounced effect on it. This shows that the MA groups present in the polymer backbone increase the interaction between filler and matrix causing an efficient stress transfer between the PP matrix and silica.

Table 4a.3. shows the storage modulus and relative (normalized) storage modulus ( $E'_c/E'_m$  where  $E'_c$  and  $E'_m$  are the storage moduli of composite and matrix respectively) values of nano-micro hybrid composites at temperatures 50, 100 and 150 °C.

**Table 4a.3:** Variation of storage modulus and normalized storage modulus of PP-silica/modified silica nanocomposites at 50, 100 and 150 °C

Sample	Storage modulus (MPa)			Normalized storage modulus		
	50 °C	100 °C	150 °C	50 °C	100 °C	150 °C
PP	821.4	245.4	4.93	1	1	1
PP/S	866.6	297.6	89.89	1.06	1.216	18.236
PP/MS	913.1	299.9	86.22	1.116	1.226	17.49
*MA-g-PP/S	1029	407.4	124.9	1.25	1.66	25.33
MA-g-PP/MS	1200	468.3	362	1.46	1.91	73.43

\*MA-g-PP → Maleic anhydride grafted PP

When compared to pristine PP the storage modulus and the normalized storage modulus of the composite is increased at all temperatures. The normalized modulus values at 50 °C and 100 °C do not show considerable variation, but at 150 °C high normalized modulus values are obtained by maleic anhydride grafting.

Figure 4a.11 and Figure 4a.12 show the variation of loss factor ( $\tan \delta$ ) of PP-silica nanocomposites. The MA grafting and incorporation of nanofiller reduces the  $\tan \delta$  values of the composite by restricting the movement of polymer molecules, and also due to the reduction in the viscoelastic lag between the stress and the strain.<sup>38,39</sup> The  $\tan \delta$  values were lowered in the composites compared to the pristine polymer may also because of the less matrix by volume to dissipate the vibrational energy. The  $\tan \delta$  values of the composites are significantly lowered with maleic anhydride grafting. The lowering of  $\tan \delta$  value is a measure of enhanced interfacial bond strength and the adhesion between the filler and matrix.

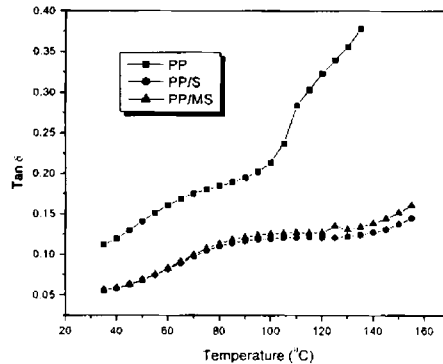


**Figure 4a.11:** Variation of loss factor of PP-silica/modified silica nanocomposites with temperature

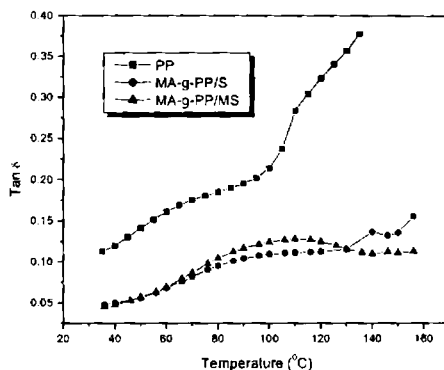


**Figure 4a.12:** Variation of loss factor of MA-g-PP-silica/ modified silica nanocomposites with temperature

The exact role of nanofiller-polymer interface in controlling the modulus is becoming clearer. The modulus of Nylon 6/clay composites as a function of the ionic strength of the clay was examined by Shelly *et al.*<sup>40</sup> The types of matrix-nano filler interaction (Figure 4a.13) responsible for modulus changes in polymer/clay composites are also studied.<sup>41</sup> It is not clear that whether the modulus increase caused by different type of interactions and/or the ionic strength is due to an increase in the interfacial shear stress (the load-bearing efficiency of the nano filler), the ability of the nano filler to constrain the polymer, or increases in degree of crystallinity. These effects are all related, and the exact mechanism is still an open question.

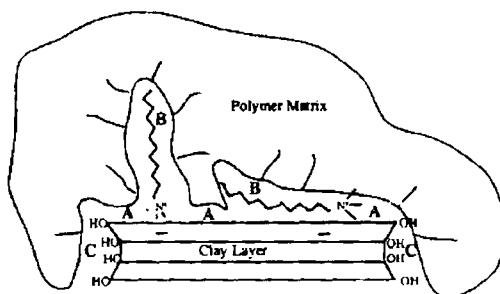


**Figure 4a.13:** Types of interfacial interactions occurring in polymer-organoclay nanocomposites including direct binding (adsorption) of the polymer to the basal siloxane oxygens (type A), "dissolving" of the onium ion chains in the polymer matrix (type B), and polymer binding to hydroxylated edge sites (type C).\*

\* Reproduced from Shi *et al.* Chem.Mater. 1996;8:1584

It is found that the improvement in dynamic mechanical properties of polymer nanocomposites above the glass transition temperature ( $T_g$ ) is more significant than below  $T_g$ .<sup>42</sup> Figure 4a.14 shows this clearly for PP/montmorillonite composites. The modulus increases by a factor of 2 below  $T_g$ , and it increases by a factor of 2.5 above  $T_g$ . This shows that strong matrix-filler interaction takes place above  $T_g$ . That is why the present study focused on the dynamic mechanical study above room temperature (above  $T_g$ ). As the surface area of the filler increases the interaction also increases, hence the modulus also increases. The addition of higher volume fraction of nano fillers decreases the modulus of the composite due to aggregation of filler (decreases the surface area).<sup>43</sup>

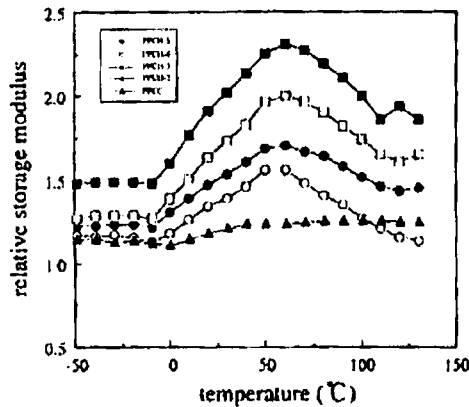


Figure 4a.14: Relative dynamic storage modulus of polypropylene-clay nanocomposites as a function of temperature at filler loadings of 2– 5 wt. percent†

#### 4a.3.4 Crystallization characteristics

Differential scanning calorimetry (DSC) is one of the most widely accepted techniques of thermal analysis for studying the crystallization characteristics of polymers and their composites. The materials, as they undergo temperature changes, will undergo changes in chemical and physical properties, which are detected by transducers, which convert the changes into electrical signals that are collected and analyzed to give thermograms. In DSC, the crystallization characteristics are studied from the heat flows associated with the corresponding transitions as a function of time and temperature,

† Reproduced from Agag *et al.* Polymer 2001;42:3399

which help us to obtain qualitative information regarding the melting and phase transitions of the composites.

Polypropylene is a semi-crystalline commodity thermoplastic. The presence of inorganic filler affects the crystallization behaviour of the polymer. The crystallization may have a major influence on the structure of composites and thereby on the mechanical properties. Hence it is important to study the crystallization kinetics of a semi crystalline polymer which determines the final properties of a polymeric product.<sup>44</sup>

#### 4a.3.4.1 Non-isothermal Crystallization

The effect of nanosilica on the crystallization characteristics of melt compounded PP-silica nanocomposite samples was analyzed first with non-isothermal DSC experiments. The crystallization temperatures ( $T_c$ ), the apparent melting temperatures ( $T_m$ ) and the corresponding enthalpies ( $\Delta H_c$  and  $\Delta H_m$ ) for all the samples are reported in table 4a.4.

**Table 4a.4:** Thermal characteristics of PP & PP-silica/modified silica nanocomposites

Sample	$T_c$ (°C)	$\Delta H_c$ (J/g)	$T_m$ (°C)	$\Delta H_m$ (J/g)
PP	110.7	104.6	165.73	102.7
PP/S	114.55	102	164.61	86.03
PP/MS	116.72	94.88	161.26	89.46
MA-g-PP/S	122.71	100.9	164.9	94.63
MA-g-PP/MS	126.75	97.16	166.75	97.92

Figure 4a.15 shows the DSC cooling scans of PP-silica nanocomposite samples. During cooling from the melt, the silica containing samples show crystallization exotherms earlier than pristine PP, as also seen from the corresponding  $T_c$  values indicated in table 4a.4. It is found that the nanocomposite sample containing 1wt% silica crystallizes about 4 °C earlier than pristine PP. This indicates that silica can act as nucleating agent for PP crystallization.

The  $T_c$  values increase with modified silica and matrix modification, even though the silica concentration is constant. This shows that the nucleation effect will increase with surface area, good dispersion and effective interaction of the filler with the matrix. The agglomerating tendency of the nanosilica decreases by the presence of vinyl group on the surface and may provide higher surface area and good dispersability in the matrix. The matrix modification further increases the interaction between the filler and matrix so as to increase the crystallization. That is why the presence of modified silica in MA grafted matrix causes a rise of 16 °C in the crystallization temperature.

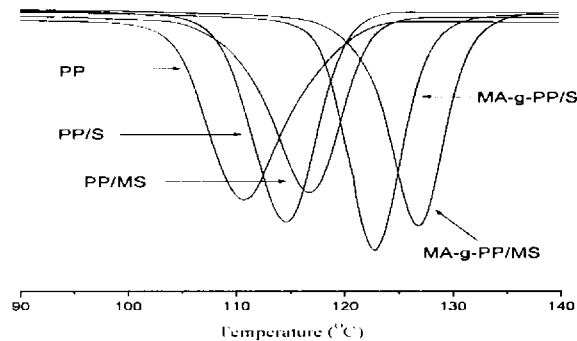


**Figure 4a.15:** DSC cooling scans (10 °C/min from 180 °C melt) of PP-silica/modified silica nanocomposite samples

The non-linear dependence of the SWNT as a nucleating agent in the polymer matrix has also been reported by Valentini *et al.* and Probst *et al.*<sup>45,46</sup> Figure 4a.16 indicates the non-isothermal crystallization curves of PP and PP-SWNT nanocomposites showing this behaviour. The authors describe the observed reduction in the  $\Delta H_c$  values as a result of the proportional reduction of PP concentration in the composites.



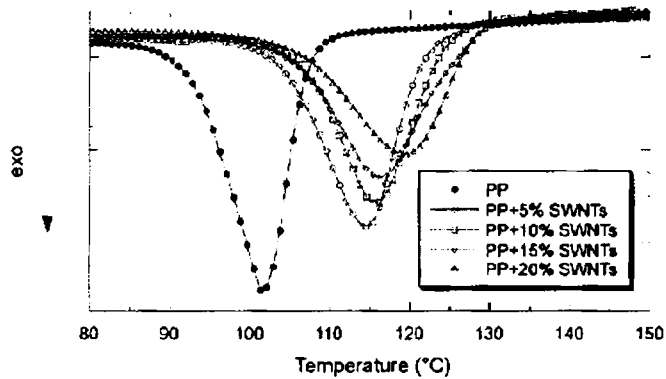


**Figure 4a.16:** DSC cooling scans of PP and PP-SWNT nanocomposites<sup>‡</sup>

The crystallization temperature and the degree of supercooling ( $\Delta T = T_m - T_c$ ) may be a measure of crystallizability; i.e. smaller the  $\Delta T$ , higher the crystallizability. The  $\Delta T$  values of the PP-silica nanocomposites given in table 4a.5 are smaller by  $\sim 5$  to  $15$  °C than that of pristine PP. This reveals that the crystallizability of the nanocomposites is higher than that of PP.

**Table 4a.5:**  $\Delta T$  values of PP & PP-silica/modified silica nanocomposite samples

Sample	$\Delta T$ (°C)	% of crystallization
PP	55.03	39.63
PP/S	50.06	41.56
PP/MS	44.54	43.22
MA-g-PP/S	42.19	45.71
MA-g-PP/MS	40	47.31

#### 4a.3.4.2 Isothermal crystallization

Figure 4a.17 shows the typical isothermal crystallization curves of PP-silica nanocomposite samples at five temperatures (110, 115, 120, 125 and 130 °C). The time

corresponding to the maximum in the heat flow rate (exotherm) is taken as the peak time of crystallization ( $t_{\text{peak}}$ ). Such peaks are seen at each of the five isothermal crystallization temperatures for 1wt% silica nanocomposites, with the earlier or faster crystallization (smaller  $t_{\text{peak}}$ ) corresponding to lower temperature of isothermal crystallization as compared to pristine PP. In the case of pure PP, no peak is seen at the highest temperature of 130 °C because crystallization is very slow and would require longer time than the 4 minutes employed in the DSC program. On the other hand, for the nanocomposite samples with 1wt% silica, the rate of crystallization is so fast near the lowest temperatures that most of the crystallization occurs during the cooling scan (60°C/min) employed to reach the temperatures (110 or 115 °C). This results in absence of exothermic peaks in the heat flow curves at those temperatures.

The peak crystallization time of PP-silica nanocomposite samples are plotted against the crystallization temperatures (figure 4a.18). It is noticeable that the  $t_{\text{peak}}$  values of the nanocomposite samples reduced to less than 50% as compared to pristine PP due to the presence of silica. With the modified silica and matrix grafting there is further increase in the crystallization rate (as indicated by the decrease in  $t_{\text{peak}}$ ), demonstrating the role of modification on the surface of silica and polymer backbone for enhancing the rate of crystallization by better matrix-filler interaction.

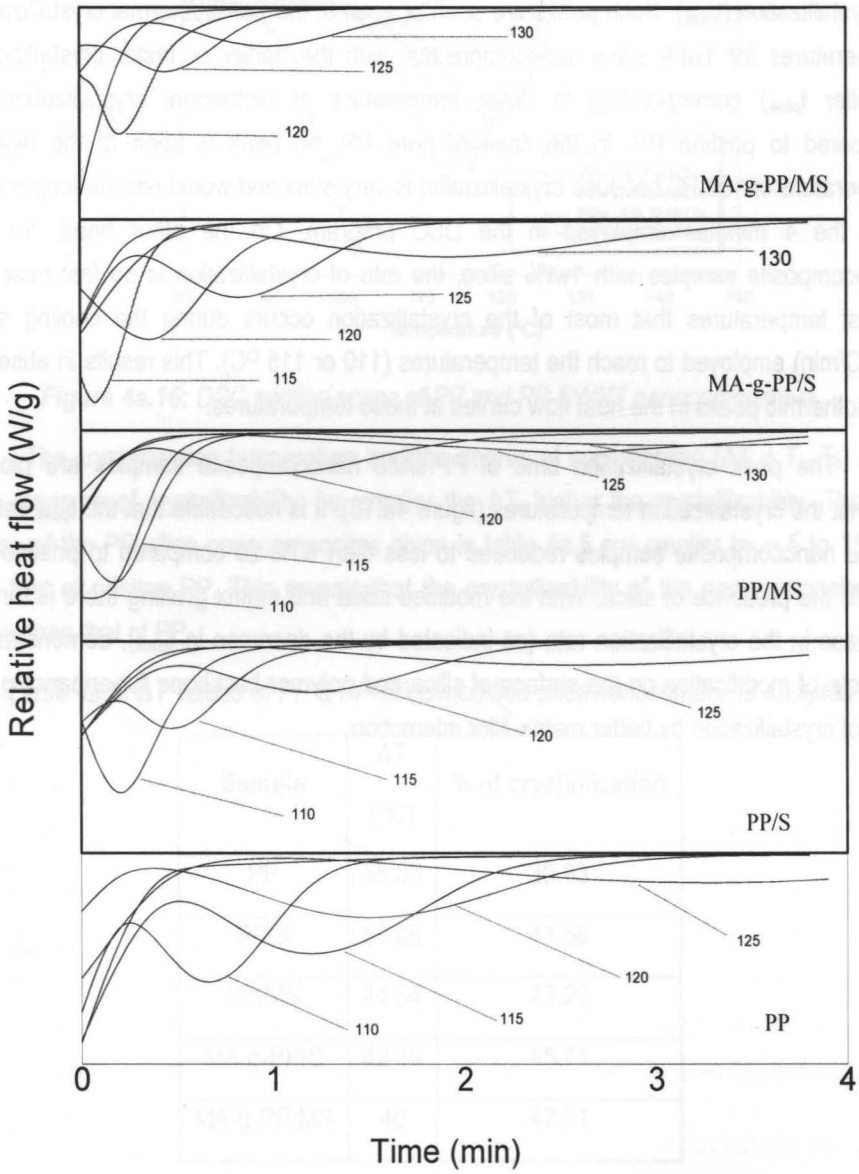


**Figure 4a.17:** Heat flow during isothermal crystallization of PP-silica/modified silica nanocomposites

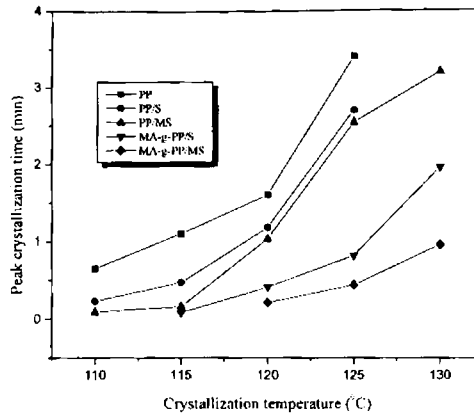


**Figure 4a.18:** Effect of silica/modified silica content on the peak crystallization time of the nanocomposites at different isothermal crystallization temperature

### 4a.3.5 Thermogravimetric analysis

The understanding of thermal stability and degradation characteristics of polymers and polymeric compounds are essential for the processing and application purposes. Thermal analysis is considered as an important analytical method to understand the structure–property relationship and mastering the technology for the industrial production of different polymeric materials.

It is well known that thermal stability of a polymeric material can be improved by inorganic nanofillers.<sup>47</sup> Strong interaction between the polymer and filler is essential for achieving good mechanical properties and thermal stability.<sup>48</sup> The inorganic nanofillers have poor dispersibility in the polymer matrix because of their hydrophilic nature of surface. The use of a coupling agent usually improves the interfacial adhesion between the inorganic nanofillers and the polymer matrix. Chan *et al.* reported that  $\text{CaCO}_3$  particles in polypropylene (PP) improved the thermal stability of PP. Li *et al.* observed that the flame retardant properties of PP improved by using starch as a filler.

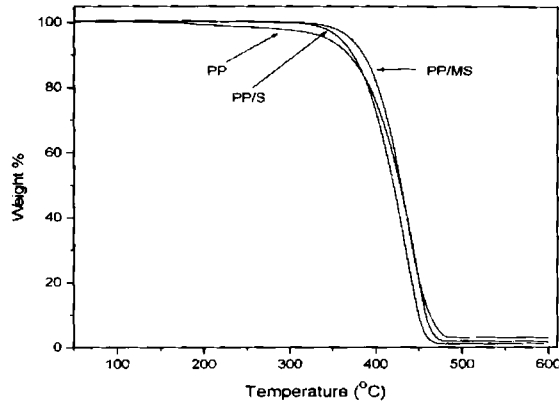


**Figure 4a.19:** Thermogravimetric traces of PP and PP-Silica/modified silica nanocomposites

The thermal stability of the composites usually assessed by thermogravimetry (TGA) in which the mass loss of the sample is monitored as a function of temperature or time.<sup>49</sup> The TG curves of PP/silica composites and MA-g-PP/silica composites are given in figures 4a.19 and 4a.20 respectively. The temperature of onset of degradation ( $T_i$ ), the temperature at which the rate of decomposition is maximum ( $T_{max}$ ) and the residue at 600°C are given in table 4a.6.

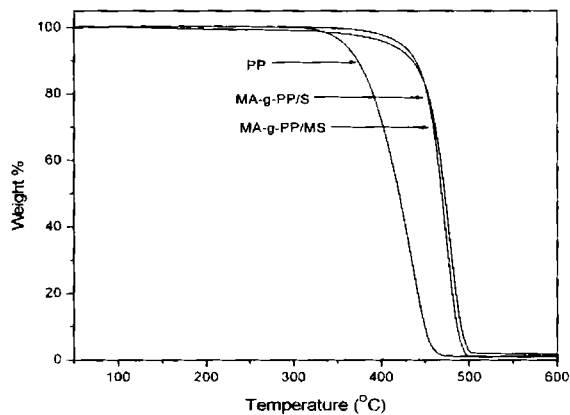


**Figure 4a.20:** Thermogravimetric traces of PP and MA-g-PP-Silica/modified silica nanocomposites

All samples show similar degradation pattern (single step degradation). PP/silica composites start the degradation around 390 °C. The  $T_{max}$  values show slight improvement in thermal stability because of the presence of silica and modified silica. The degradation of maleic anhydride grafted PP/silica composites start around 450 °C. This shows that the thermal stability of maleic anhydride grafted composites improves notably. This shows that the polar nature of polymer increases the interaction of filler with matrix and hence increases the cross linking between the chains.

**Table 4a.6:** Degradation characteristics of PP and its composites

Sample	Onset temp ( $T_i$ ) (°C)	Peak max ( $T_{max}$ ) (°C)	Residue at 600 °C
PP	387	436	0.6
PP/S	396	438	1.3
PP/MS	399	446	1.9
MA-g-PP/S	450	470	1.97
MA-g-PP/MS	453	477	1.77

#### 4a.4 CONCLUSIONS

The study shows that PP-silica nanocomposites can be successfully prepared by melt-mixing method and that

- The incorporation of modified nanosilica improves the properties of PP nanocomposites.
- Effective reinforcement occurs by modified nanosilica.
- Chemical modification of the matrix significantly improves the properties of nanosilica composites.

- The presence of modified nanosilica with MA-g-PP showed all round performance.
- The crystallization temperature of PP enhances with the presence of modified nanosilica and maleic anhydride grafting.
- The presence of nanosilica and modified nanosilica enhances the thermal stability of composites.
- The dynamic properties are also improved with the addition of silica. The properties show further improvement with silica modification and maleic anhydride grafting.

## REFERENCES

1. Y.C.Ke; *Chin. Pat.Appl.* 02157993.8, 2002.
2. Z.Qi, Y.C.Ke; *Chin. Pat.* ZL97 104055.9.
3. Y.C.Ke; *Brier materials for packages*, Meetings of plastics and its processing, Asia and Pacific regions, Shangai, 2003, 11.
4. (a) J.Z.Liang, R.K.Y.Li; *Polymer* 1999, 40, 3191.  
(b) Q.Yuan, W.Jiang, L.J.An, R.K.Y.Li; *Polym.Adv.Technol.* 2004, 15, 409.  
(c) W.C.Zuiderduin, C.Westzaan, J.Huetink, R.J.Gaymans; *Polymer* 2003, 44, 261.  
(d) M.Alexander, P.Dubois; *Mater.Sci.Eng.* 2000, 28, 1.  
(e) M.Kato, A.Usuki, A.Okhada; *J.Appl.polym.Sci.* 1997, 66, 1781.  
(f) A.Oya, Y.Kurokawa; *J.Mater.Sci.* 2000, 35, 1045.  
(g) G.Galgali, C.Ramesh, A.Leela; *Macromolecules* 2001, 34, 852.  
(h) M.Kawasumi, N.Hasegawa, M.Kato, A.Usuki, A.Okada; *Macromolecules* 1997, 30, 6333.  
(i) C.M.Chan, J.Wu, J.X.Li, Y.K.Cheung; *Polymer* 2002, 43, 2981.  
(j) Q.Fu, G.H.Wang, J.S.Shen; *J.Appl.Polym.Sci.* 1993, 49, 673.  
(k) Q.Yuan, W.Jiang, H.X.Zhang, J.H.Yin, L.J.An, R.K.Li; *J.Polym.sci.Part B: Polym.Phys.* 2001, 38, 1855.
5. J.W.Gilman, C.L.Jackson, A.B.Morgan, R.Harris; *Jr.Chem.Mater* 2000, 12, 1866.
6. Y.Kojima, A.Usuki, M.Kawasumi, A.Okada, Y.Fukushima, T.Kurauchi, O.Kamigaito; *J.Mater.Res.* 1993, 8, 1185.
7. P.B.Messersmith, E.P.Giannelis; *J.Polym.Sci.Pol.Chem.* 1995, 33, 1047.
8. R.A.Vaia, G.Price, P.N.Ruth, H.T.Nguyen, Lichtenhan; *J.Appl.Clay.sci.* 1999, 15, 67.



9. M.Z.Rong, M.Q.Zhang, Y.X.Zheng, H.M.Zheng, K.Friedrich; *Polymer* **2001**, 42, 3001.
10. C.L.Wu, M.Q.Zhang, M.Z.Rong, K.Friedrich; *Compos.Sci.Technol.* **2002**, 62, 1327.
11. (a) A.Tabitiang, R.Venables; *Eur.Polym.J.* **2000**, 36, 137.  
(b) K.Premphet, P.Horanot; *Polymer* **2000**, 41, 9283.  
(c) A.Bartczakz, S.Argon, R.E.cohen, M.Weinberg; *Polymer* **1999**, 40, 2347.  
(d) J.Z.Liang, R.K.Y.Li; *J.Appl.Polym.Sci* **2000**, 77, 409.  
(e) K.Mituisi, S.Kodama, H.Kawasaki; *Polym.Eng.Sci.* **1985**, 25, 1069.  
(f) G.X.Weij, H.J.Sue; *J.Mat.Sci.* **2000**, 35, 555.  
(g) J.Jangaar, A.T.Dibenedetto; *Polym.Eng.Sci.* **1993**, 33, 559.  
(h) Z.Demjen, B.Pukanszky, N.Jozsef; *Composites Part A* **1998**, 29, 323.  
(i) R.Rothon; *Particulate Filled Polymer Composites*, Wiley, New York, **1995**.  
(j) S.Lapshin, A.I.Isayev; *J.Vinyl and additive Technology* **2006**, 12(2), 78.  
(j) M.Fujiyama, T.Wakinino; *J.Appl.Polym.Sci.* **1991**, 42, 2749.
12. E.Moore; *Polypropylene Handbook: Polymerization, Characterization, Properties, Processing and applications*, Hanser-Gardner, Clicinnati, **1996**.
13. J.E.Stamhuis; *Polym.Compos.* **1984**, 5, 202.
14. R.S.Hadal, R.D.K.Misra; *Mater.Sci.Eng.A* **2004**, 374.
15. S.Radhakrishnan, C.Saujanya; *J.Mater.Sci.* **1998**, 33, 1069.
16. R.N.Rothon; editor, *Particulate filled polymer composites*, Harlow, Longman: Essex, UK, **1995**.
17. Y.Mizutani, S.Nago; *J.Appl.Polym.Sci.* **1999**, 72, 1489.
18. M.Hideo, S.Yutaka, T.Sumio; *Polypropylene resin composition for automobile*

19. J.Jeffrey , K.I.Jacob, T.Rina, M.A.Sharaf, J.Iwona; *Mater.Sci.Eng.* **2005**, 393, 1.
20. K.W.Allen; *J.Adhesion Sci.Technol.* **1992**, 6, 23.
21. S.Zhang, B.Schindler, G.Nicholson, Bayer; *J.High.Resolut.Chromotogr.* **1995**, 18, 579.
22. G.Z.Li, L.Wang, H.Toghinani, T.L.Daulton, Pittman; *Polymer* **2002**, 43, 4167.
23. H.Zhao, K.Robert,Y. Li; *Polymer* **2006**, 47, 3207.
24. V.Svehlova, E.Polouek; *Angew. Makromol. Chem.* **1994**, 214, 91.
25. C.S.Reddy, C.K.Das; *J.Appl.Polym.Sci.* **2006**, 102, 2117.
26. Y.Li, J.Yu, Z.X.Guo; *J.Appl.Polym.Sci.* **2002**, 84, 827.
27. A.Lazzari, C.B.Bucknall; *J.Mater.Sci.* **1993**, 28, 6709.
28. A.Lazzari, C.B.Bucknall; *Polymer* **1995**, 36, 2895.
29. (a) R.N.Rothon; *Particulate filled polymer composites*, Harlow, Longman Scientific and Technical, **1995**.  
(b) R.N.Rothon; *Jancar J.*, **1999**, 139, 67.  
(c) A.S.Argon, Z.Bartezak, R.E.Cohen, O.K.Muratoglu; *Novel mechanism of toughening of plastics, advances in modeling and experiments*, Symposium series, 759, Washington D.C., ACS, **2000**, 42, 2347.  
(d) Z.Bartezk, A.S.Argon, R.E.Cohen, M.Weinberg; *Polymer* **1999**, 40, 2347.  
(e) M.W.L.Wilbrink, A.S.Argon, R.E.Cohen, M.Weinberg; *Polymer* **2001**, 42, 10155.  
(f) Y.S.Thio, R.E.Cohen, M.Weinberg; *Polymer* **2002**, 43, 3661.  
(g) Q.Fu, G.Wang; *Polym.Eng.Sci.* **1992**, 32, 94.  
(h) G.Levita, A.Marchetti, A.Lazzeri; *Polym.Compos.* **1989**, 10, 39.



30. T.Yong, H.Yuan, A.Rui, W.Zhengzhou, G.Zhou, C.Zuyao, F.Weicheng; *Macromol.Mater.Eng.* **2004**, 289,191.
31. K.Pravin, K.Rajendra, H.Sangeeta, B.Neelima; J.P.Jog, *J.Appl.Polym.Sci.* **2001**, 81,1786.
32. K.L.Mittal; *Silanes and other coupling agents*, VSP, The Netherlands, **1992**.
33. V.Svehlova, E.Polouek; *Angew. Makromol. Chem.* **1994**, 214, 91.
34. A.K.Saha, S.Das, D.Bhatta, B.C.Mitra; *J.Appl.Polym.Sci.* **1999**, 71, 1505.
35. M.Okamoto, S.Morita, H.Taguchi, Y.Kim, T.Kotaka, H.Tateyama; *Polymer*, **2000**, 41, 3887.
36. T.McNally, W.R.Murphy, C.Lew, R.Turner, G.Brennan; *Polymer*, **2003**, 44, 2761.
37. H.Zhao, K.Robert, Y. Li; *Polymer* **2006**, 47, 3207 .
38. A.K.Saha, S.Das, D.Bhatta, B.C.Mitra; *J. Appl. Polym. Sci.* **1999**, 71,1505.
39. D.Ray, B.K.Sarkar, S.Das, A.K.Rana; *Comp. Sci. Technol.* **2002**, 62, 911.
40. J.S.Shelly, P.T.Mather, K.L.DeVries; *Polymer* **2001**, 42, 5849.
41. H.Shi, T.Lan, T.J.Pinnavaia; *Chem. Mater.* **1996**, 8, 1584.
42. N. Hasegawa, M. Kawasumi, M. Kato, A.Usuki, A. Okada; *J.Appl. Polym. Sci.* **1998** 67, 87.
43. T. Agag, T. Koga, T. Takeichi; *Polymer*, **2001**, 42, 3399.
44. (a) Q.H.Zeng, A.B.Yu, G.Q.Lu; *Technology convergence in composite application*, Proc ACUN-3, UNSW, Sydney, Australia, **2001**.  
(b) T.Jianguo, W.Yao, L.Haiyan, A.Laurence; *Polymer* **2004**, 45, 2081.  
(c) P.Maiti, P.H.Nam, M.Okamoto, T.Kotaka, N.Hasegawa, A.Usuki; *Polym.Eng.Sci.* **2002**, 42, 1864.

- (d) W.Leelapornpisit, M.N.Ton-That, F.Perrin-Sarazin, K.C.Cole, J.Denault, B.Simard; *J.Polym.Sci.PartB:Polym.Phys.* **2005**, 43, 2445.
- (e) W.B.Xu, M.L.Ge, P.S.He; *J.Polym.Sci.PartB:Polym.Phys.* **2002**, 40, 408.
- (f) M.Avella, S.Cosco, M.L.Lorenzo, E.D.Pace, M.E.Errico; *J.Therm.Anal.Calorim.* **2005**, 80, 131.
45. O.Probst, E.M.Moore, D.E.Resasco, B.P.Grady; *Polymer* **2004**, 45, 4437.
46. L.Valentini, J.Biagiotti, J.M.Kenny, S.Santucci; *J. Appl. Polym. Sci.* **2003**, 87, 708.
47. (a) H.Wei-Gwo, W.Kung-Hwa, Chang-Mou; *Polymer* **2004**, 45, 5729.
- (b) Huei-Kuan, H.Chin-Feng, Jieh-Ming; *Polymer* **2008**, 49, 1305.
- (c) K.Chatterjee, K.Nasar; *Polym. Eng. Sci.* **2008**, 48, 1077.
- (d) Z.Ahamad, M.Ansel, D.Smedley; *Mech.Compos.Mater.* **2006**, 42, 419.
- (e) C.S.Reddy, C.K.Das; *Polym.Polym.Compos.* **2006**, 14(3), 281.
48. (a) X.J.Xiang, J.W.Qian, W.G.Yang, M.H.Fang, X.Q.Qian; *J.Appl Polym.Sci.* **2006**, 100, 4333.
- (b) R.N.Mahaling, S.Kumar, T.Rath, C.K.Das; *J. Elastomers Plast.* **2007**, 39, 253.
- (c) C.S.Reddy, C.K.Das; *Compos. Interfaces* **2005**, 11, 667.
- (d) R.N.Mahaling, C.K.Das; *Compos. Interfaces* **2005**, 11, 701.
- (e) R.Qianping, H.Hongyan, Y.Tian, W.Shishan, S.Jian; *Polym. Polym. Compos.*, **2008**, 14, 301.
49. S.Wang, Y.Hu, L.Song, Z.Wang, Z.Chen, W.Fan; *Polym.Degrad stab.* **2002**, 77, 423.

### High density polyethylene-silica nanocomposites

#### 4b.1 INTRODUCTION

From a theoretical point of view, the nanoeffects from the nanoparticles in the nanocomposites provide an important window to modify traditional polymers and related materials, and thus play an important role in reforming traditional industry. In other words, polymer nanocomposites can be applied to those fields where pure polymer materials have been used because of their advantages and unique properties derived from nanoscale structures. Nanocomposites exhibit low thermal expansion coefficient, improved mechanical properties, flame retardancy, higher barrier properties and swelling resistance.<sup>1</sup> Loading small amounts of inorganic nanoparticles usually produces superior properties in nanocomposites. For example, in nylon 6-MMT nanocomposites with a load as less as 5% (by wt), the heat distortion temperature (HDT) increases to 150 °C compared to the 65 °C of pure nylon 6, while its density remains nearly unchanged. The loading of inorganic nanoparticles with polymers have received great interest in recent years because it improves the strength and toughness of the polymer, which are not achievable with conventional filled polymers.<sup>2</sup> The properties of the composites are the result of a complex interplay between the individual constituent phases namely the matrix, the filler and the interfacial region.

High density polyethylene (HDPE), the world's largest volume using thermoplastic finds wide use in packaging, consumer goods, pipes, cable insulation etc. The availability and recyclability of HDPE make it a primary material in the material substitution chain. To encourage the application area of HDPE, it requires superior modulus, yield strength and high impact strength. Considerable enhancements in these mechanical properties of thermoplastic materials are realized by reinforcement with inorganic minerals such as mica, wallastonite, glass bead, talc and calcium carbonate.<sup>3</sup>

The present study aimed to produce HDPE and maleic anhydride grafted HDPE nanocomposites with silica and modified silica. Mechanical, thermal, crystallization and dynamic mechanical performance of the composites are analyzed.

## 4b.2 EXPERIMENTAL

HDPE/silica nanocomposites were prepared by melt-mixing method. This was performed in a Torque Rheometer (Thermo Haake Rheocord 600) at 150 °C and at a rotor speed 50 rpm for 8 min. The concentration of nanosilica and modified nanosilica was varied from 0 - 3wt%. The torque stabilized to a constant value within 8 minutes. The resulting compound was hot pressed into thin sheets and cut into pieces. The matrix was modified with maleic anhydride according to US patent, 4,753,997.

The tensile properties of the samples were determined using dumb-bell shaped samples on a Universal Testing Machine (Shimadzu AG-1) at a crosshead speed of 50 mm/min according to ASTM-D-638. Flexural properties of the composites were measured by three point loading system using Universal Testing Machine (Shimadzu AG-1) as per ASTM-D-790 at a crosshead speed of 5 mm/min. Impact strength of the samples was determined using Resil impactor junior (Ceast) (ASTM-D256). The dynamic mechanical performance, crystallization behaviour, thermal stability and morphology of the nanocomposites were analyzed using Dynamic Mechanical Analyser (DMA, Q800 TA instruments), Differential Scanning Calorimeter (DSC, Q100-TA instruments), Thermogravimetric analyzer (Q50 – TA instruments) and Scannig Electron Microscope (SEM, JEOL JSM 840 A) respectively.

## 4b.3 RESULTS AND DISCUSSION

### 4b.3.1 HDPE - silica nanocomposites

#### 4b.3.1.1 Torque studies

It has been widely established that the mechanical properties of crystalline polymeric materials strongly depend on processing conditions and techniques used to process the materials. The same polymeric material can be processed into a soft and flexible product or a strong and stiff product under different conditions. The variation of torque with different nanosilica loading is shown in figure 4b.1. The torque stabilized to a constant value within 8 min. Initially torque rises to a maximum value due to the charging of HDPE & silica and after that it declines to a constant value, showing the proper mixing and homogenization of the composites. The temperature of the mixing chamber was kept at 150 °C. From the figure, it is clear that there is no degradation during the mixing stage.

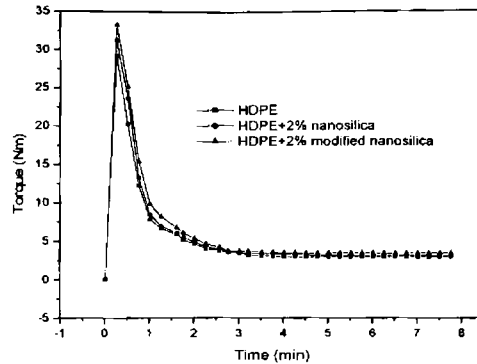


**Figure 4b.1:** Variation of mixing torque with time of HDPE/silica nanocomposites

The variation of mixing torque with time of mixing of modified nanosilica in HDPE is found to be same as that of the above case. In this case also, the mixing time was fixed as 8 minutes since the torque got stabilized by this time.

#### **4b.3.1.2 Tensile properties**

The response of a polymer to an external force is mainly through the motion of the chain segments of the coils, which dominates the yielding behaviour of the polymer.<sup>4,5</sup> When a semi-crystalline polymer is subjected to an external load, the chain segments in the crystalline regions slip causing the lamellae to disintegrate locally and the polymer to yield and neck.<sup>6,7</sup>

The effect of nanosilica and modified nanosilica on tensile performance of HDPE is shown in figure 4b.2.

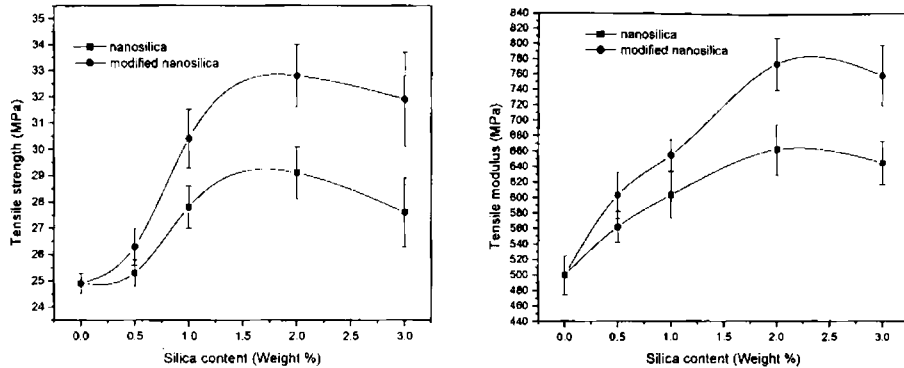


**Figure 4b.2:** Variation of tensile strength and modulus of HDPE-silica/modified silica nanocomposites with silica content

The results shows that there is an increase in the tensile strength and modulus from 0 to 2 wt.% nanosilica addition and then slightly decreases with increase in concentration of nanosilica. The tensile strength shows an increment of about 22% and modulus about 30% with 2wt.% modified nanosilica addition. So it is clear that modified nanosilica loading increases the strength and modulus of the matrix. This may be due to the uniform dispersion and good wetting of the modified nanosilica in the matrix by the help of the vinyl group on the surface. Uniform dispersion of nanoparticles is very important because, if the stress field gets concentrated around any aggregates in the matrix, the cracks will propagate rapidly and cause premature failure of the product. The modification of silica decreases the aggregation tendency by decreasing the surface energy of the nanosilica. The hardness and percentage elongation of nanosilica and modified nanosilica/HDPE composites are listed in table 4b.1. The shore D hardness also supports the above reinforcement. The elongation at break is found to decrease with increasing nanosilica loading, indicating that the nanocomposites become somewhat brittle.



**Table 4b.1:** Effect of nanosilica/modified nanosilica content on hardness and elongation

S Content (Wt.%)	Hardness (Shore D)	Elongation (%)	MS Content (Wt.%)	Hardness (Shore D)	Elongation (%)
0.0	60	14.8	0.0	60	14.8
0.5	61	12.9	0.5	62	13.3
1	63	11.5	1	65	12.6
2	66	9.7	2	68	10.9
3	68	5.4	3	70	6.7

### 4b.3.1.3 Flexural properties

A comparison of flexural strength and modulus of nanocomposites prepared using nanosilica and modified nanosilica in HDPE matrix are shown in figure 4b.3. With the addition of 2wt.% nanosilica in HDPE, the flexural strength and modulus increases about 30% & 28% respectively, and the modified nanosilica makes an improvement of about 45% and 40% respectively. The properties increases steadily at the level of 2% and then shows a slight decline in values. This means that a satisfactory reinforcement can be obtained with the incorporation of nanosilica in HDPE matrix. The surface modified nanoparticles undergo uniform dispersion and good interfacial interaction with HDPE matrix. This accounts for the better reinforcement of modified nanosilica with HDPE.

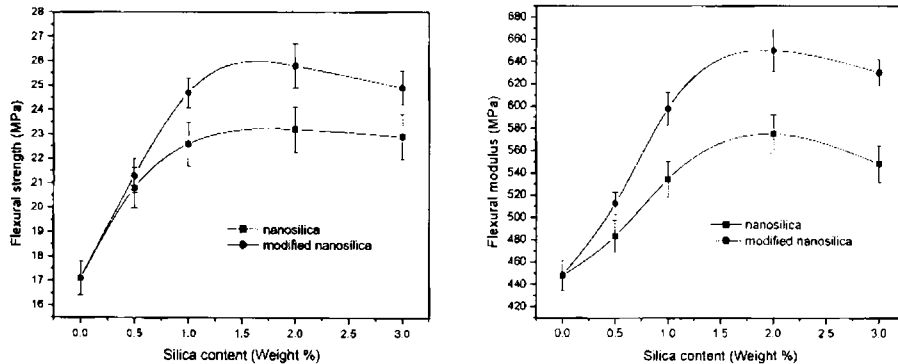


**Figure 4b.3:** Variation of flexural strength and modulus of HDPE-silica/modified silica nanocomposites

#### 4b.3.1.4 Impact strength

The energy dissipating actions that occur in the vicinity of a sharp crack is related to the toughness of a material. The interfacial interaction between fillers and polymer matrix significantly influence the mechanical properties of a particulate filled composite. Friedrich<sup>8</sup> highlighted that semi-crystalline polymers consisting of small spherulites are generally tougher than those containing coarse spherulites because larger spherulites have weak boundaries. He also provided the evidence for the effect of this morphology. Ouderni and Philips<sup>9</sup> studied on the effect of crystallinity and found that an increase in crystallinity or spherulite size decreases the toughness and thus confirmed Friedrich's conclusion. The behaviour of the composite depends on crystallinity, crystal structure (morphology), lamellar thickness and interfacial interactions. Increase in lamellar thickness with percentage of filler is an indication of reinforcement. Hence yield stress in neat semicrystalline polymers is proportional to lamellar thickness. In HDPE-nanosilica composites, there is no appreciable change in crystallinity and the reinforcement indicate an increase in lamellar thickness.

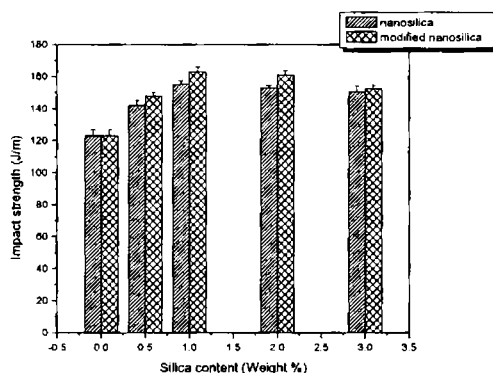


**Figure 4b.4:** Effect of nanosilica/modified nanosilica concentration on impact strength of HDPE

Unnotched Izod impact strength of HDPE-silica/modified silica nanocomposites is depicted in figure 4b.4. With 2wt.% of modified nanosilica, the impact strength of HDPE increases by about 30%; but with 2wt.% nanosilica, enhances the impact strength of

about 25%. This shows that the toughness of the composites increased by both nanosilica and modified nanosilica content.

### 4b.3.2 Effect of matrix modification on HDPE-Silica nanocomposite

#### 4b.3.2.1 Torque studies

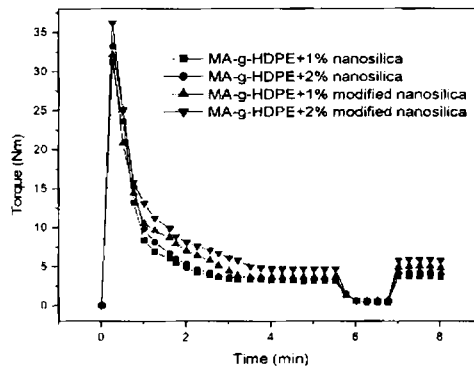
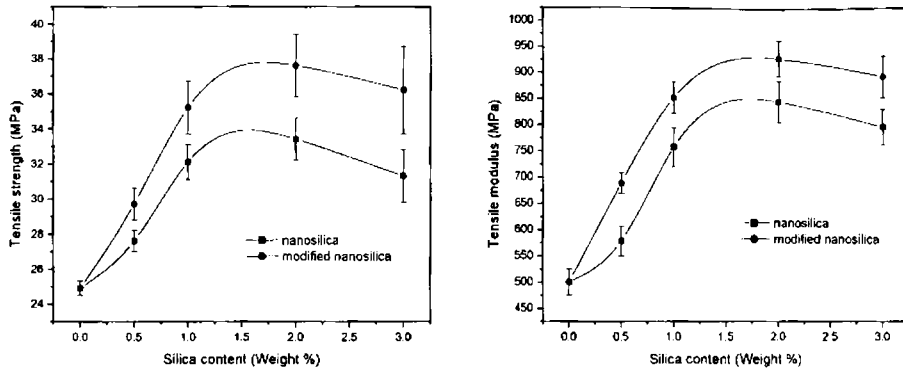


Figure 4b.5: Variation of mixing torque with time of HDPE-silica/modified silica nanocomposites

The variation of mixing torque with time at different filler loading is shown in figure 4b.5. The torque values are found to be steady within the mixing time.

#### 4b.3.2.2 Tensile properties

The enhancement in properties of nanocomposites even at low filler loading may depend on the nature of the interactions between the filler and the matrix. Wang *et al.* prepared maleated polyethylene/clay nanocomposite by melt mixing and studied their properties.<sup>10</sup> The effect of nanosilica and modified nanosilica on tensile performance of MA-g-HDPE is shown in figure 4b.6.



**Figure 4b.6:** Variation of tensile strength and modulus of MA-g-HDPE-silica/modified silica nanocomposites with silica content

The results shows that there is an increase in tensile strength and modulus till 2wt.% silica addition and then a slight decreases with increase in concentration of silica. The tensile strength showed an increment of about 50% and modulus about 80% at this concentration with modified nanosilica addition.

The shore D hardness also supports this observation. The elongation at break is found to decrease with increase nanosilica loading, indicating that the nanocomposites become somewhat brittle.

**Table 4b.2:** Effect of nanosilica/modified nanosilica content on hardness and elongation

S Content (Wt.%)	Hardness (Shore D)	Elongation (%)	MS Content (Wt.%)	Hardness (Shore D)	Elongation (%)
0.0	60	14.8	0.0	60	14.8
0.5	63	13.2	0.5	64	14.1
1	65	12.8	1	67	13.5
2	67	10.6	2	71	11.7
3	70	7.3	3	73	9.1

### 4b.3.2.3 Flexural properties

A comparison of flexural strength and modulus of nanocomposites prepared using nanosilica and modified nanosilica in MA-g-HDPE matrix are shown in figure 4b.7 respectively.

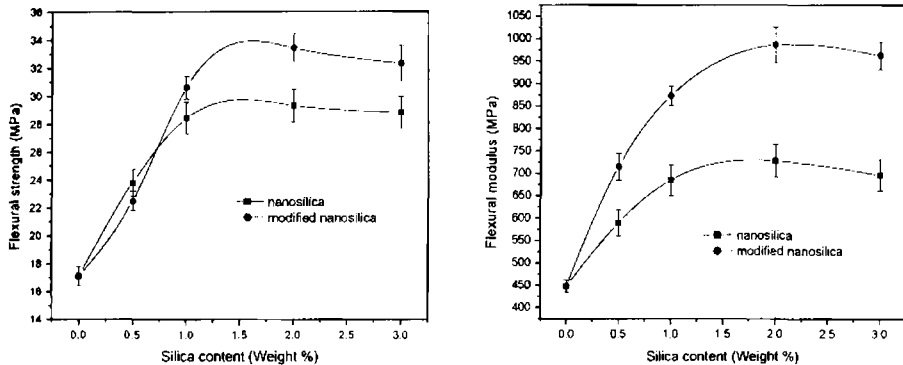


**Figure 4b.7:** Variation of flexural strength and modulus of MA-g-HDPE-silica/modified silica nanocomposites

With the addition of 2wt.% silica in MA-g-HDPE, the flexural strength and modulus increases by 70% and 60% respectively for nanosilica and 90% and 120% for modified nanosilica compared to pure HDPE. The properties increases steadily at the level of 2% and remain almost constant at higher compositions for silica. This means that a satisfactory reinforcement can be obtained with the incorporation of nanosilica in MA-g-HDPE matrix.

### 4b.3.2.4 Impact strength

The effect of nanosilica and modified nanosilica on MA-g-HDPE is shown in figure 4b.8. The increase in impact strength is prominent at 1wt.% silica addition.

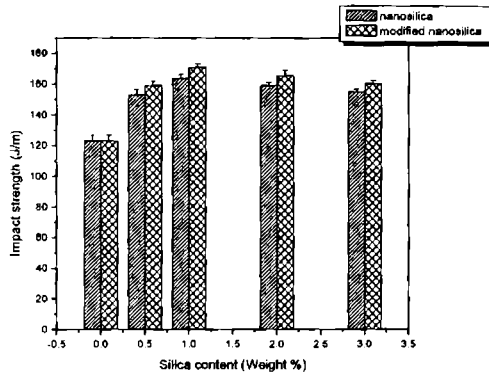


**Figure 4b.8:** Effect of nanosilica/modified nanosilica concentration on impact strength of MA-g-HDPE

The mechanical properties study showed that the modified nanosilica loading increases the strength and modulus of the matrix. This may be due to the uniform dispersion and good wetting of the modified nanosilica in the matrix by the help of the vinyl group on the surface. Uniform dispersion is very important because, in the case of a matrix with aggregates of particles, the stress field will be concentrated around any aggregates, such that the cracks will propagate rapidly, causing premature failure.

### 4b.3.3 Dynamic mechanical analysis

The dynamic storage modulus of the HDPE-silica nanocomposite as a function of temperature at 1Hz is shown in figure 4b.9. It shows a steady decrease of the moduli with temperature. The storage modulus of the nanocomposites showed an increase at all temperatures compared to pure polymer. The composite with modified nanosilica showed significant increase in storage modulus. This indicates the efficient stress transfer between matrix and modified nanosilica.

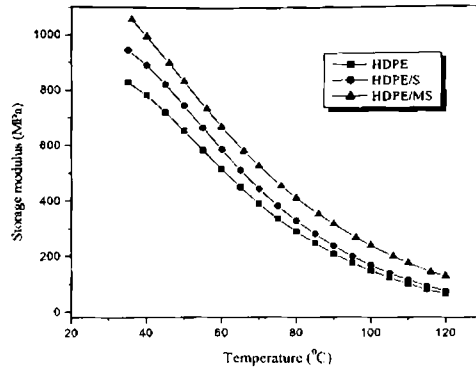


**Figure 4b.9:** Variation of storage modulus of HDPE-silica/modified silica nanocomposites with temperature

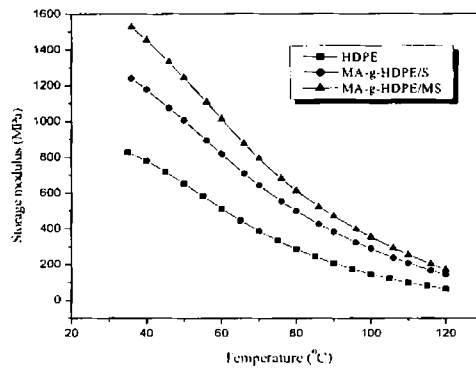


**Figure 4b.10:** Variation of storage modulus of MA-g-HDPE-silica/modified silica nanocomposites with temperature

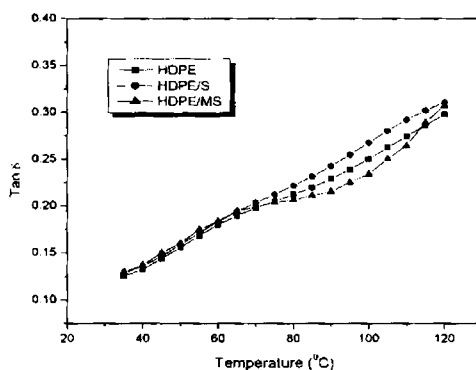
The variation of storage modulus with temperature for pure HDPE and MA-g-HDPE/silica composites are shown in figure 4b.10. The maleic anhydride (MA) grafting makes a noticeable increase in storage modulus at all temperatures. This shows that the MA groups present in the polymer backbone increase the interaction between filler and matrix, causing an efficient stress transfer between the HDPE matrix and silica.

Table 4b.3 shows the storage modulus and relative (normalized) storage modulus values of nano-micro hybrid composites at temperatures 40, 80 and 120 °C.

**Table 4b.3.** Variation of storage modulus and normalized storage modulus of HDPE-silica/modified silica composites at 40, 80 and 120 °C

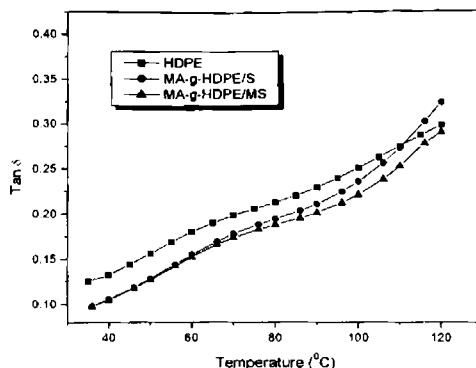
Sample	Storage modulus (MPa)			Normalized storage modulus		
	40 °C	80 °C	120 °C	40 °C	80 °C	120 °C
HDPE	781.2	286.3	63.49	1	1	1
HDPE/S	891	325.3	73.63	1.14	1.14	1.16
HDPE/MS	995.1	407.6	126.9	1.27	1.42	1.99
MA-g-HDPE/S	1178	499.5	143.6	1.51	1.74	2.26
MA-g-HDPE/MS	1454	613.2	169.9	1.86	2.14	2.68

The storage modulus and the normalized storage modulus of the composites increase with silica/modified nanosilica and MA-grafting at all temperatures. The normalized modulus values show a steady increase at 40 °C, 80 °C and 120 °C.



**Figure 4b.11:** Variation of loss factor of HDPE-silica/modified silica nanocomposites with temperature





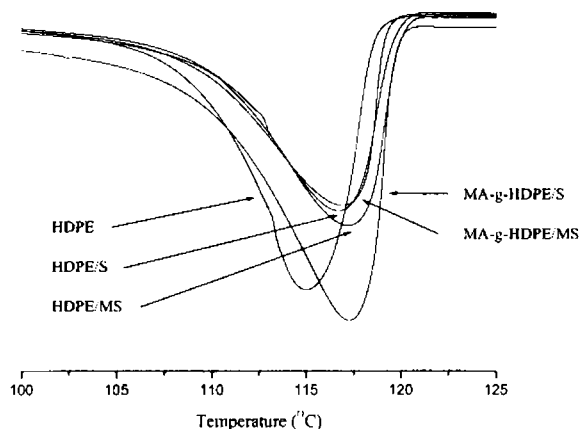
**Figure 4b.12:** Variation of loss factor of MA-g-HDPE-silica/modified silica nanocomposites with temperature

Figure 4b.11 and figure 4b.12 show  $\tan \delta$  versus temperature plots of HDPE-silica nanocomposites. The incorporation of nanosilica/modified silica has no effect on the  $\tan \delta$  values. But MA grafting reduces the  $\tan \delta$  values of the composite by restricting the movement of polymer molecules, and also due to the reduction in the viscoelastic lag between the stress and strain. The  $\tan \delta$  values were lowered in the composites compared to the pure polymer may also because of the fewer matrixes by volume to dissipate the vibrational energy. The  $\tan \delta$  values of the composite are significantly lowered with maleic anhydride grafting. The lowering of the  $\tan \delta$  value is a measure of enhanced interfacial bond strength and the adhesion between matrix and filler.

### 4b.3.4 Crystallization characteristics

#### 4b.3.4.1 Non-isothermal Crystallization

The non-isothermal crystallization characteristics of melt compounded HDPE-silica nanocomposite obtained from DSC experiments is shown in figure.4b.13 The crystallization temperatures ( $T_c$ ), the apparent melting temperatures ( $T_m$ ) and the corresponding enthalpies ( $\Delta H_c$  and  $\Delta H_m$ ) for all the samples are reported in table 4b.4.



**Figure.4b.13:** DSC cooling scans (10 °C/min from 160 °C melt) of HDPE-silica/modified silica nanocomposite samples

Figure.4b.13 indicates that for a given cooling rate, peak crystallization temperature ( $T_c$ ) is slightly higher than HDPE, as seen from the corresponding  $T_c$  values indicated in table 4b.4. This means that the addition of silica particles in HDPE increases the crystallization rate of HDPE. About 3 °C rise of  $T_c$  is observed for the composites prepared by 1% modified nanosilica addition and MA-grafting.

**Table 4b.4:** Thermal characteristics of HDPE-silica nanocomposite samples

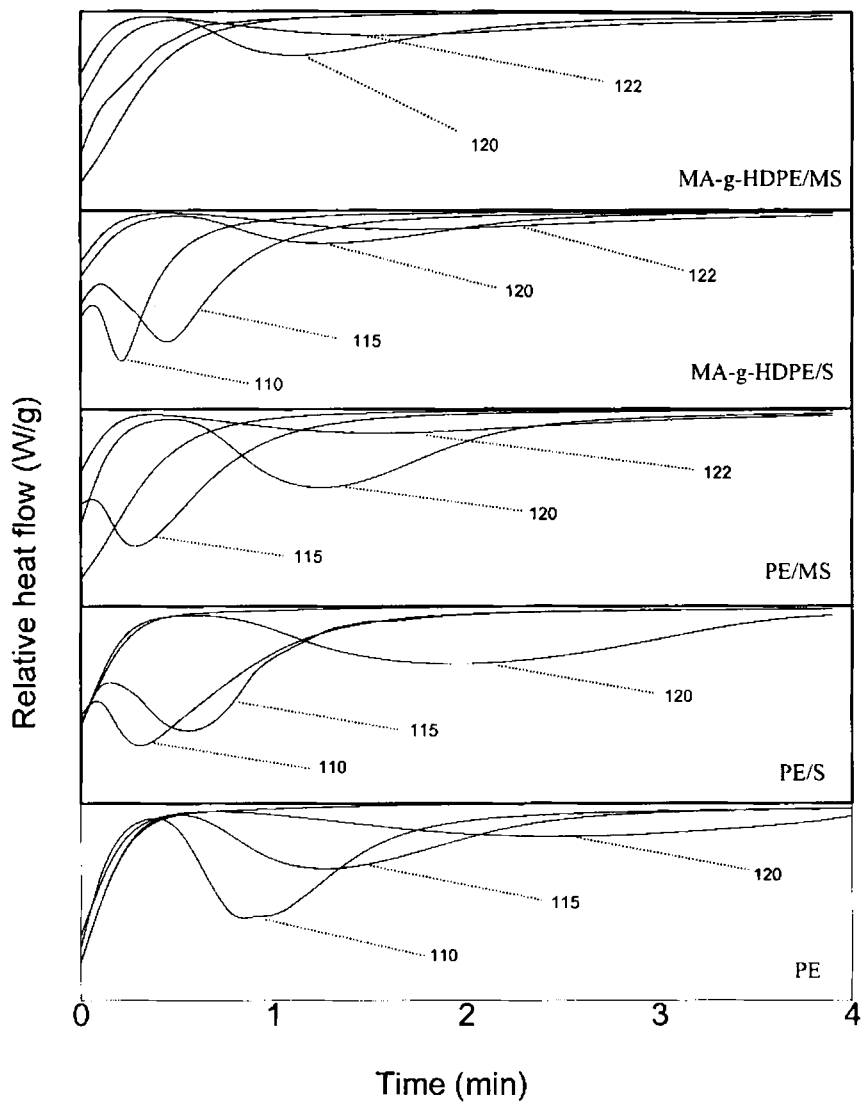
Sample	$T_c$ (°C)	$\Delta H_c$ (J/g)	$T_m$ (°C)	$\Delta H_m$ (°C)
HDPE	114.63	193.3	131.98	172.7
HDPE/S	116.74	156.2	130.64	135.6
HDPE/MS	117.18	163.6	132.15	154.3
MA-g-HDPE/S	116.9	155.6	131.02	141.2
MA-g-HDPE/MS	117.29	229.7	130.97	202.4

The  $T_c$  values increases with modified silica addition and matrix modification even though the silica concentration is constant. This tendency shows that the nucleation effect will increase with surface area, good dispersion and effective interaction of the filler and matrix. The agglomerating tendency of nanosilica decreases by the presence of vinyl group on the surface and may provide higher surface area and good dispersability in the matrix. The matrix modification further increases the interaction between filler and matrix so as to increase the crystallization.

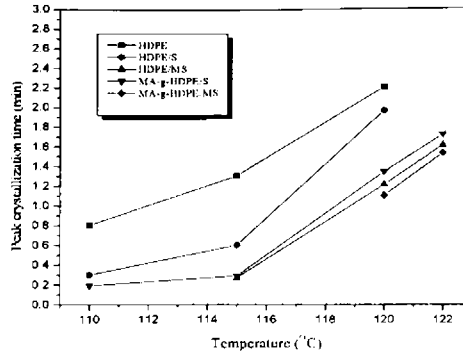
#### **4b.3.4.2 Isothermal crystallization**

Figure 4b.14 shows the typical isothermal crystallization curves of HDPE-silica nanocomposite samples at five temperatures (110, 115, 120, and 122 °C). The peak time of crystallization ( $t_{peak}$ ) can be seen at each of the four isothermal crystallization temperatures for HDPE-silica nanocomposite with 1wt% silica. No peak is seen at the highest temperature of 122 °C for pristine HDPE. This shows that the 4 minutes employed in the DSC program is not enough for crystallization. On the other hand the rate of crystallization of maleic anhydride grafted HDPE nanocomposite samples with 1wt% silica/modified silica, is so fast near the lowest temperatures that most of the crystallization occurs during the cooling scan (60 °C/min) employed to reach the temperature (110 or 115 °C).

The peak time of crystallization at different temperatures for all the HDPE-silica nanocomposite samples is plotted against the isothermal crystallization temperature (figure 4b.15). It is noticeable that the  $t_{peak}$  values of the nanocomposite samples is reduced to less than 50% as compared to pristine HDPE due to the presence of silica. Maleic anhydride grafting on the polymer backbone further increases the crystallization rate (as indicated by the decrease in  $t_{peak}$ ), which indicates a stronger interaction between the matrix and filler.



*Figure 4b.14: Heat flow during isothermal crystallization of HDPE-silica/modified silica nanocomposites*



**Figure 4b.15:** Effect of silica/modified silica content on the peak crystallization time of the nanocomposites at different isothermal crystallization temperature

### 4b.3.5 Thermogravimetric analysis

The addition of inorganic filler into polymer matrix increases the activation energy of thermal oxidation and thus it has some stabilization effect. The addition of talc, wollastonite and  $\text{CaCO}_3$  give more stability to HDPE.<sup>11</sup>

The thermogravimetric traces of HDPE, HDPE/silica composites and MA-g-HDPE/silica composites are given in figures 4b.16 and 4b.17 respectively. The temperature of onset of degradation ( $T_i$ ), the temperature at which the rate of decomposition is maximum ( $T_{\text{max}}$ ) and the residue at 600 °C are given in table 4b.5.

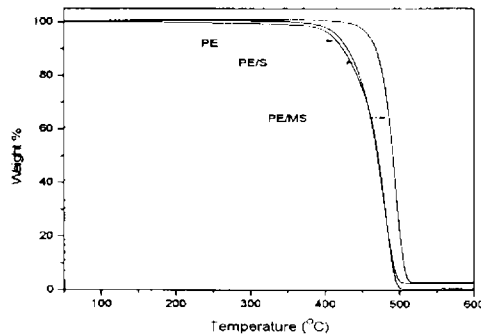


**Figure 4b.16:** Thermogravimetric traces of HDPE and HDPE-silica/modified silica nanocomposites

All samples show similar degradation pattern (single step degradation). Thermal degradation profiles of HDPE and its composites exhibit that most of the degradation events occur between 365 and 525 °C. The onset of degradation and  $T_{max}$  improved  $>60^{\circ}\text{C}$  and  $>15^{\circ}\text{C}$  for HDPE-modified silica composite compared to HDPE. This shows that the addition of nanosilica and modified silica effectively improve the thermal stability of the HDPE.

**Table 4b.5:** Degradation characteristics of HDPE and its composites

Sample	Onset temp. ( $T_i$ ) (°C)	Peak max ( $T_{max}$ ) (°C)	Residue at 600 °C (%)
HDPE	362.6	476	0.51
HDPE /S	446.7	480.2	2.7
HDPE /MS	477	494.21	2.3
MA-g-HDPE /S	473.3	495.1	3.4
MA-g-HDPE /MS	470.8	492.6	2.2

The thermal degradation of maleic anhydride grafted HDPE nanocomposites start at 460 °C. This shows that the thermal stability of nanocomposite is improved notably with maleic anhydride grafting.

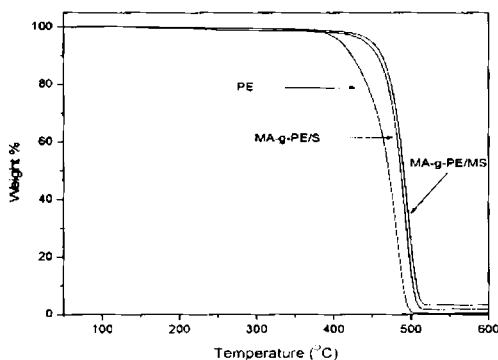


**Figure 4b.17:** Thermogravimetric traces of HDPE and MA-g-HDPE-silica/modified silica

## **4b.4 CONCLUSIONS**

The study shows HDPE-silica nanocomposites can be successfully prepared by melt-mixing method and that

- The incorporation of silica/modified nanosilica improved the properties of HDPE nanocomposites.
- Effective reinforcement occurs by modified nanosilica
- Chemical modification of the matrix also improves the properties of nanosilica composites.
- Maleicanhydride grafted HDPE show good performance upon modification with nanosilica.
- The crystallization temperature of HDPE slightly enhances with the presence of modified nanosilica and maleic anhydride grafting.
- The presence of nanosilica and modified nanosilica improves the thermal stability of composites.
- The dynamic properties are also improved with the addition of silica. The properties show further improvement with silica modification and maleic anhydride grafting.

## REFERENCES

- (a) Z.Bartczak, A.S.Argon, R.E.Cohen, M.Weinberg; *Polymer* **1999**, *40*, 2347.
  - (b) Y.Ke, C.Long, Z.Qi; *J.Appl.Polym.Sci.* **1999**, *71*, 1139.
  - (c) K.Yano, A.Usuki, A.Okada, *J.Polym.Sci. PartA:Polym.Chem.* **1997**, *35*, 2289.
  - (d) A.Pawlak, P.Zinck, A.Tgaleski, J.F.Gerald; *Macromol.Symp.* **2001**, *169*, 197.
  - (e) J.F.Rong, Z.H.Jing, H.Qli, M.Sheng; *Macromol.Rapid.Commun.* **2001**, *22*, 329.
- (a) H.Cai, F.Y.Yan, Q.J.Xue, W.M.Liu; *Polymer Testing* **2003**, *22*, 875.
  - (b) A.Uksuki, A.Tukigase, M.Kato; *Polymer* **2002**, *43*, 2185.
  - (c) P.B.Messersmith, E.P.Giannelis; *Chemistry of Materials*, **1994**, *6*, 1719.
  - (d) R.A.Vaia, K.D.Jandt, E.J.Karmer, E.P.Giannelis; *Macromolecules* **1995**, *28*, 8080.
  - (e) A.B.Morgan, W.G.Jeffrey; *J.Appl.Polym.Sci.* **2003**, *87*, 1329.
  - (f) G.Jimenez, N.Ogata, H.Kawai, T.Ogihara; *J.Appl.Polym.Sci.* **1997**, *64*, 2211.
- (a) J.P.Trotignon, J.Verdu, R.DeBoissard, A.DeVallois, B.Sedlaucek; *Polymer composites, Proceedings of Prague IUPAC microsposium on macromolecules*, Berlin:DeGrugter, **1985**, 191.
  - (b) A.Dasari; R.D.K.Misra, *Acta Mater.* **2004**, *52*, 1683.
  - (c) A.Dasari, S.Sarang, R.D.K.Misra; *Mater.Sci.Eng.A* **2004**, *368*, 191.
  - (d) Q.Yuan, W.Jiang, H.Z.Zhang, J.H.Yin, L.J.An, R.K.Y.Li; *J.Polym.Sci.Part B: polym.Phys.* **2001**, *39*, 1855.
  - (e) R.Yang, Y.liu, J.Yu, K.Wang; *Polymer Degradation and Stability* **2006**, *91*(8), 1651.



- (f) Y.S.Thio, A.S.Argon, R.E.Cohen, M.Weinberg; *Polymer* **2002**, 43, 3661.
  - (g) B.Haworth, C.L.Raymond, I.Sutherland; *Polym.Eng.Sci.* **2001**, 41, 1345.
  - (h) C.Albano, J.Gonzalez, M.Ichazo, C.Rosales, N.C.DeUrbina, C.Parra; *Compos.Stru.* **2000**, 49, 48.
  - (i) G.J.Price, D.M.Ansari; *Polym.Int.* **2004**, 53, 430.
  - (j) R.D.K.Misra, P.Nerlikar, K.Bertrand, D.Murphy; *Mater.Sci.Eng.A* **2005**, 384, 284.
  - (k) S.Sahebian, S.M.Zebarjaci, S.A.Saijadi, Z.Sherafat, A.Lazzeri; *J.Appl.Polym.Sci.* **2007**, 104(6), 3688.
4. K.Tashiro; *Prog.polym.Sci.* **1993**, 18, 377.
  5. P.J.Flory, D.Y.Yoon; *Nature* **1978**, 272, 226.
  6. J.X.Li, W.L.Cheung; *Polymer* **1998**, 39, 6935.
  7. J.X.Li, W.L.Cheung, C.M.Chan, *Polymer* **1999**.
  8. K.Friedrich; *Adv.Polym.Sci.* **1983**, 52/53, 225.
  9. M.Ouderni, P.J.Philips; *J.Eng.Appl.Sci.Phys.Ed.* **1977**, 15, 683.
  10. K.H.Wang, M.H.Chai, C.M.Koo, Y.S.Choi, I.J.Chung; *Polymer* **2001**, 42, 9819.
  11. Y.Rui, L.Ying, Y.Jian, W.Kunhua; *Polym.Deg.Stab.* **2005**, 46, 8202.

# Chapter 5

## Modification of polypropylene - short fibre composite with nanosilica/modified nanosilica

**Part - a**

### **Polypropylene-glass fibre-silica hybrid nanocomposites**

#### **5a.1 INTRODUCTION**

Fibre reinforced thermoplastic composites have incredibly attracted the polymer composite industry in the recent years. Thermoplastic composites have been replacements for thermoset composites in some applications, and have generated entirely new fields of application. Major attractions of thermoplastic composites include greater impact damage tolerance, i.e. improved toughness, postformability, and weldability. Their waste can be reduced and/or recycled more simply and valuably than thermoset materials. The use of short fibres as reinforcing agents in polymers opens up a new avenue for the utilization of waste fibres, available in plenty from fibre and textile industries. Recently short fibres have found a variety of applications in plastics due to the ease of mixing and consequent processing advantages in fabricating products of complicated design coupled with greater reinforcement. The properties of short-fibre-containing composites depend critically on fibre content, orientation and fibre-matrix interface.

Continuous improvement on the performance of glass fibre-reinforced polypropylene has been gaining ground to replace metal and other more expensive composite materials. Examples can be found in the weed trimmer from Black and Decker, the housing and adapter plate for pumps of Hayward pool products, air-cleaner housings

and trays for light trucks, hockey skate components, automotive fender liners, and ammunition boxes.<sup>1</sup> Glass fibre-reinforced polypropylene has certain advantages over other engineering plastics, the main ones being low cost and low specific gravity. While low dimension and thermal stability limits the scope of polypropylene composites, most schemes to improve polypropylene gas barrier properties involve either addition of higher barrier plastics via a multilayer structure or surface coatings. Although effective, the increased cost of these approaches negates one big attraction for using polypropylene in the first place-economy. Currently, the engineering applications employ glass or mineral-filled systems with loading levels ranging from 15 to 50wt%. This approach improves most mechanical properties, but polypropylene's ease of processing is somewhat compromised. At such high particle volume fractions, the processing of the material often becomes difficult and since the inorganic filler has a higher density than the base polymer, the density of the filled polymer is also increased and leads to greater moulded part weight. As a result the advantages of polymers, i.e., their ease of processing and light weight, is lost, which limits various applications of polypropylene composite. To overcome this drawback, a composite with improved properties and lower particle concentration is highly desired. With regard to this, the newly developed nano-micro composites would be competitive candidates.

In this part the effect of nano-micro hybrid (nanosilica and micro glass fibre) at different loadings on PP is discussed. The effect of modification of nanosilica and PP is also presented.

## 5a.2 EXPERIMENTAL

Short glass fibre reinforced polypropylene composites were prepared in a Torque Rheometer (Thermo Haake Rheocord 600). The variation of torque with time of mixing was monitored. The matrix was modified with maleic anhydride according to US patent, 4,753,997.

The modification of PP-glass fibre composites with nanosilica/modified nanosilica was also done in Torque Rheometer. 1 and 2wt.% of silica/modified silica loaded hybrid nanocomposites were prepared. The mixing time of 8 minutes was used at a rotor speed of 50 rpm. The temperature of the mixing was fixed as 180 °C. In all cases the torque stabilized to a constant value in this time.

Dumb-bell and rectangular shaped samples were prepared by injection moulding in a semiautomatic laboratory injection moulding machine. The tensile properties of the samples were determined using universal testing machine (Shimadzu) at a crosshead speed of 50 mm/min according to ASTM-D-638. Flexural properties of the composites were measured by three-point loading system using the universal testing machine according to ASTM-D-790. Impact strength of the samples was determined using Resil impactor junior (Ceast) (ASTM-D256). The crystallization behaviour was analyzed using DSC Q100 (TA instruments). The storage modulus and mechanical damping ( $\tan \delta$ ) was measured using a dynamic mechanical analyzer model Q800 (TA instruments).

## **5a.3 RESULTS AND DISCUSSION**

### **5a.3.1 Polypropylene-glass fibre composite**

#### **5a.3.1.1 Torque studies**

The variation of mixing torque with time of mixing at different fibre loading is shown in figure 5a.1. A mixing time of 8 minutes was fixed since the torque stabilized to a constant value during this time in all cases. The temperature of the mixing chamber was fixed as 180 °C. The stabilization of the torque may be related to the attainment of a stable structure after a good level of mixing. The torque values are increased with increase in fibre loading. This shows that there is not much degradation in length of the glass fibre and behaves as fibrous filler under the given conditions.

Initially torque increases with the charging of PP, but decreases with melting. After homogenization of PP, glass fibres were added. Then the torque rise again and levels off in about 5 min. Also, it is clear from the figure that there is no degradation during the mixing stage.

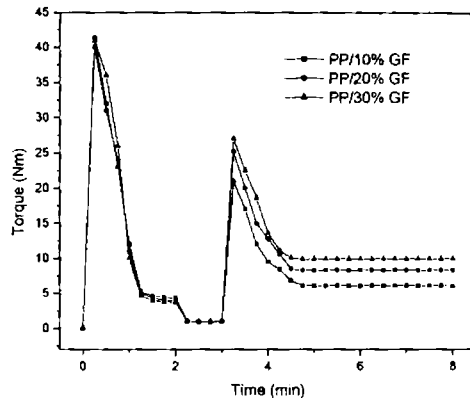


**Figure 5a.1:** Variation of mixing torque with time of PP/Glass fibre composites

### 5a.3.1.2 Effect of fibre length

#### a) Tensile properties

The effect of initial chopped length of the fibre has studied by Schweizer and Turkovich.<sup>2,3</sup> Schweizer used, a homopolypropylene Profax 6523 as the resin matrix with reinforcement as K-fibre in different lengths and found the average length of the glass fibre decreases by 0.005–0.0026 in. in the injection moulding process. The degradation in fibre length as a function of mixing time from 0 to 40 min in the polypropylene melt was carried out on the plasticorder torque rheometer by Fisa.<sup>4</sup> The transformation of input strand length into short broken fragments in the final compound occurred via two processes overlapping in time. First, the strand bundles are filamentized into individual fibres. The study showed significant fibre degradation at this stage. The higher the glass concentration, the shorter time it happens. The individual fibres are further broken down into small fragments as a result of shear stress in the melt. This fibre–melt interaction was confirmed by the continuing decrease of fibre length with mixing time at very low glass concentration. Increasing PP resin viscosity shows a strong decline of fibre length at 40% glass content. The effect of mixer rotor speed from 15 to 90 rpm on the final fibre length is negligible for 40wt% glass content. At 2wt% glass content, the fibre length decreases with the increase of rotor speed.

When the glass fibre-reinforced polypropylene compound is melted and injection moulded into the final part, the glass fibres are subject to degradation in the process and will cause lower tensile and flexural strengths of the composite.<sup>5</sup> The above observations showed that the processing conditions and methods have a direct effect on fibre breakage which in turn will affect the final mechanical properties. 10wt.% glass fibre filled polypropylene composite were prepared with different average fibre length of 2, 4, 6, 8 and 10 mm to study the effect of fibre length on the tensile strength. Figure 5a.2 shows the variation of tensile strength with fibre length.

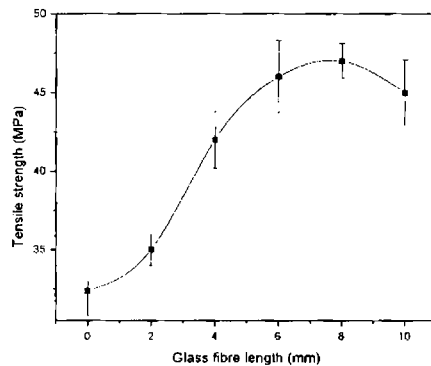


*Figure 5a.2: Variation of tensile strength with fibre length*

Figure 5a.2 shows that a steep increase in tensile strength is noticed up to 6mm fibre length and slight increase thereafter till 8mm fibre length and then decreases.

### **b) Flexural properties**

The effect of fibre length on the flexural strength is given in figure 5a.3. Flexural strength increases with increase in fibre length up to 6 mm and after 8 mm it decreases as in the case of the tensile strength.

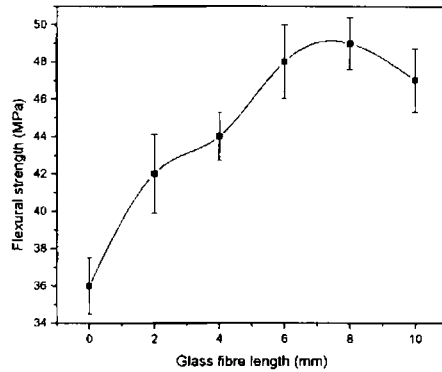


Figure 5a.3: Variation of flexural strength with fibre length

Tensile and flexural tests showed that the good reinforcements obtained between 6- 8 mm length of the glass fibre. Hence 8 mm length was taken as optimum fibre length for further studies.

### 5a.3.1.3 Effect of fibre loading

PP composites with 10, 20, 30, 40 and 50 weight percentages of glass fibre were prepared using glass fibres of 8mm length to study the effect of fibre loading.

#### a) Tensile properties

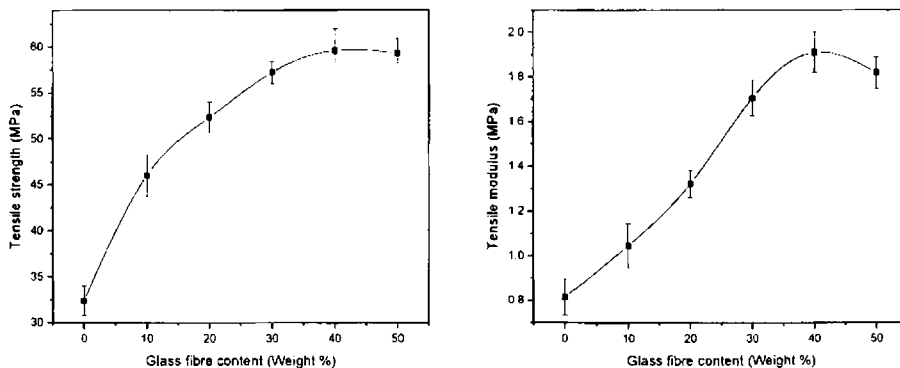
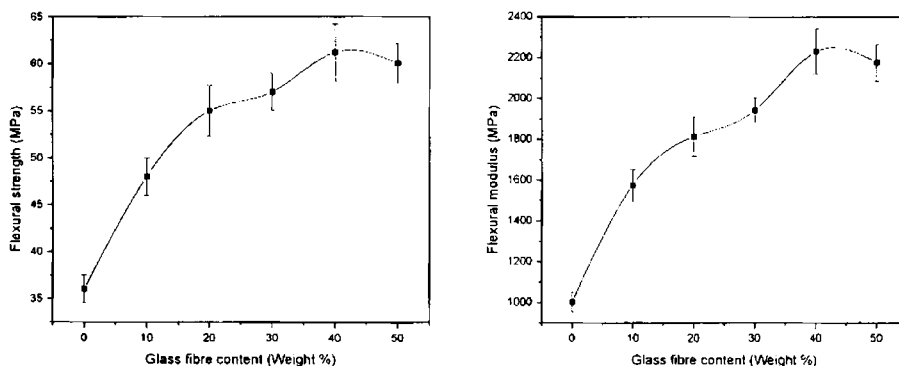


Figure 5a.4: Variation of tensile strength and modulus with fibre loading

Figure 5a.4 show the variation of tensile strength and tensile modulus of glass fibre/PP composites with fibre loading. The tensile strength increases with fibre loading up to 40% and then shows slight decrease. The decrease in strength at higher loading may be due to crowding of fibres, which prevents efficient matrix-fibre stress transfer. Generally tensile strength, tensile modulus flexural strength and flexural modulus of GFRP increase with glass content. But the melt flow decreases at higher glass fibre loading.<sup>6,7,8</sup>

### **b) Flexural properties**

The effect of fibre loading on the flexural strength and flexural modulus of glass fibre/PP composites is shown in figure 5a.5. From the figures it is clear that both flexural strength and modulus increases with fibre content. The maximum modulus is observed at 40% fibre loading. We already found that the tensile properties also increase with glass content.



**Figure 5a.5:** Variation of flexural strength and modulus with fibre loading

### **c) Impact strength**

Figure 5a.6 shows the effect of fibre loading on unnotched izod impact strength of glass fibre/PP composites. This shows that the impact strength increases till 20wt.% of glass fibre content and then decreases.



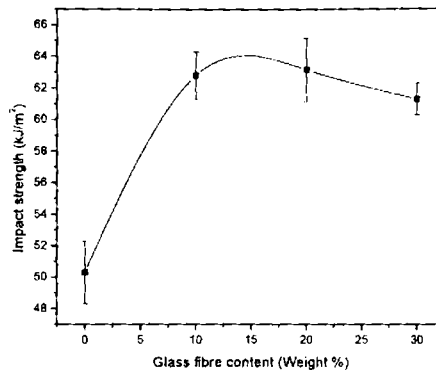


**Figure 5a.6:** Variation of impact strength with fibre loading

Notched Izod impact strength of GFRP increases with the glass content and peaks at either 20 or 30wt.% depending on the diameter of the fibre. But unnotched Izod impact strength decreases with more glass fibres in the composites.<sup>9,10,11</sup> The higher impact strength versus glass content is also reported by Karger Kocsis in both T and L notched specimens.<sup>12</sup> This contributes to the fact that the fibre avoids cracking path, mostly due to fibre debonding and pull-out process, increases with increasing glass content.

The observations of mechanical properties show that the tensile and flexural strength increase linearly with the glass content up to 30% by weight. The addition of glass fibres reduces the strain to failure. Higher fibre content results in a higher concentration of failure initiation sites and thus a lower tensile strain. The cause of lowering the mechanical properties at higher fibre content may be because of high void content and crowding of fibres.

### 5a.3.2 Modification of PP-glass fibre composite with silica/modified silica

#### 5a.3.2.1 Torque studies

The variation of mixing torque with time of mixing at different filler loading is shown in figure 5a.7. A mixing time of 8 minutes was fixed since the torque stabilized to a

constant value during this time. The temperature of the mixing chamber was also fixed as 180 °C. The initial and final torque values are not affected by nanofiller additions.

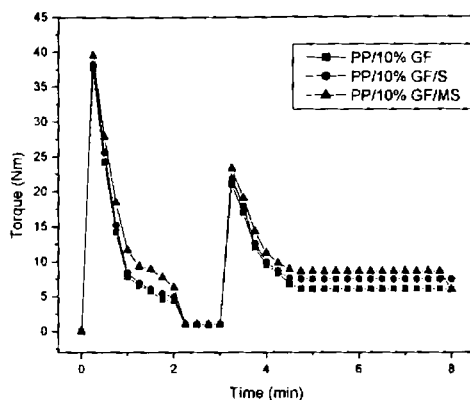


**Figure 5a.7:** Torque - Time curve of PP hybrid composites

The reinforcement of PP-glass fibre composites with 1wt.% nanosilica and modified nanosilica show better performance. Hence the properties of the 1wt.% nanosilica/modified nanosilica reinforced hybrid nanocomposites are discussed in detail.

### 5a.3.2.2 Tensile properties

When the nano filler disperse well with the aid of fibres the stress will be transferred effectively from the matrix to the nano filler by a shear transfer mechanism. Figure 5a.8 show the variation of tensile strength and tensile modulus of PP/glass fibre composites with fibre and silica/modified silica loading. The tensile strength increases with the nanosilica and modified silica addition into the PP/glass fibre composites. The increase with 10% glass fibre is more pronounced. There will be crowding of of fibres at higher loading and this prevents good interaction between fibre and nano filler with matrix and thus there will not be efficient stress transfer form the matrix.

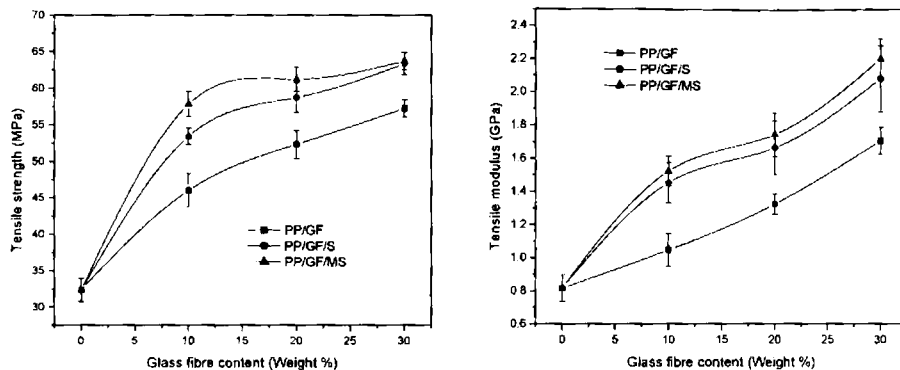


Figure 5a.8: Variation of tensile strength and modulus with fibre loading and silica content

### 5a.3.2.3 Flexural properties

Figure 5a.9 shows the effect of nanofiller loading on the flexural strength and flexural modulus of glass fibre/PP composites. From the figures it is clear that both flexural strength and modulus increase with fibre as well as nanosilica content. Here also modulus and strength increases with particulate filler addition to the short fibre composite.

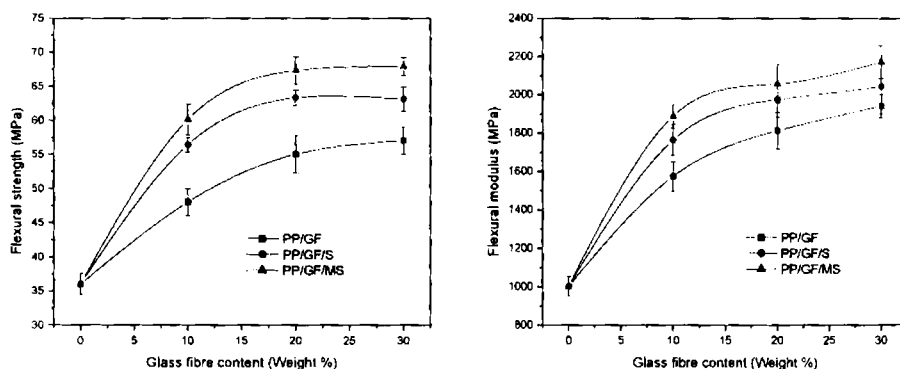
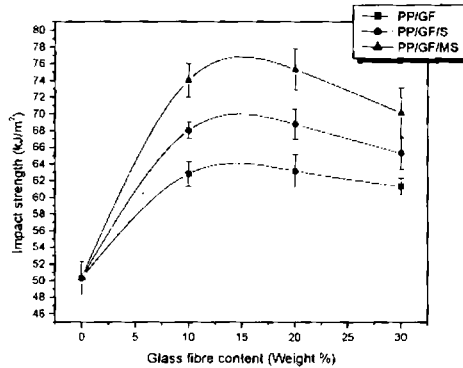


Figure 5a.9: Variation of flexural strength and modulus with fibre loading and silica content

### 5a.3.2.4 Impact strength

Figure 5a.10 shows the effect of nanofiller loading on impact strength of the composites. The figure shows increasing impact strength till 20% glass fibre loading and then decreases.

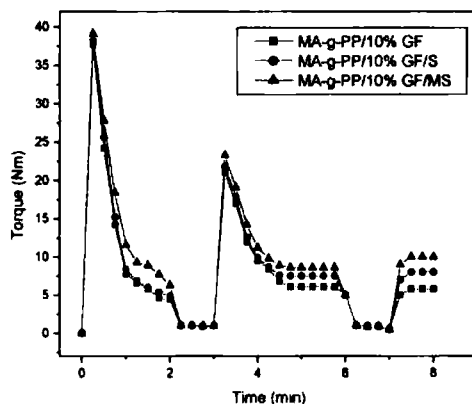


*Figure 5a.10: Variation of impact strength with fibre loading and silica content*

### 5a.3.3 Effect of matrix modification on the mechanical properties nano-micro hybrid composite

#### 5a.3.3.1 Torque studies

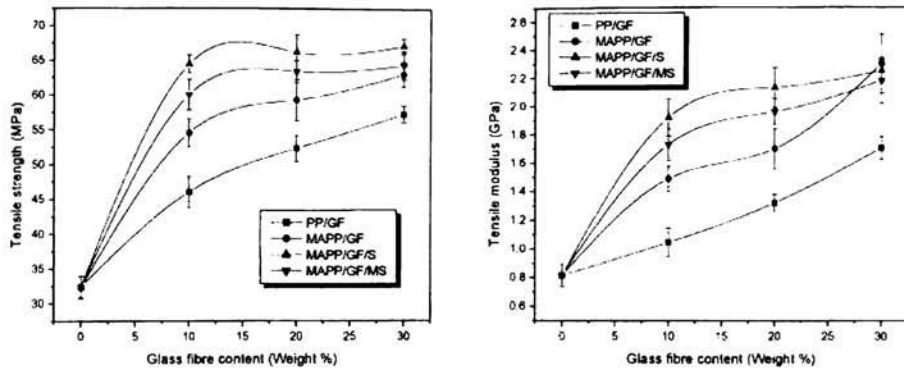
The variation of mixing torque with time of mixing at different filler loadings is shown in figure 5a.11. A mixing time of 8 minutes was fixed since the torque stabilized to a constant value during this time. The temperature of the mixing chamber was also fixed as 180 °C. The matrix grafting affects the final torque value of the composites. This shows that matrix grafting increases the interaction of filler with matrix.



*Figure 5a.11: Torque – Time curves of MA grafted PP composites*

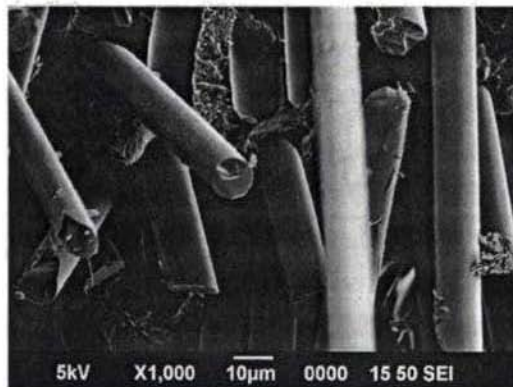
### 5a.3.3.2 Tensile properties

Figure 5a.12 shows the effect of chemical treatment on the tensile properties of glass fibre/PP composites and PP nano-micro hybrid composites. From the figures, it is clear that the matrix modification improves the tensile strength of the composites due to the strong interaction between the polar group in grafted PP and hydroxyl or silanol groups on the surface of the glass fibre. The improvement in the tensile modulus even at 10% fibre content is about 39%. This is particularly significant because it shows that the matrix has become stronger by the modification even though this is not very pronounced at higher fibre loading due to fibre crowding.



**Figure 5a.12:** Variation of tensile strength and modulus with fibre loading and silica content

The improvement of adhesion between the filler and MA treated matrix can be seen from the scanning electron micrographs (SEM) of the fractured surface of PP/glass fibre/silica hybrid nanocomposite and that of MA-g-PP/glass fibre/modified silica hybrid nanocomposites (Figures 5a.13 and 5a.14). The fractured surface of unmodified matrix shows holes and the fibre surface retain low amount of matrix indicating poor adhesion between the fibre and matrix while in the case of modified matrix, the fractured surface shows evidence for fibre breakage rather than pullout, and the fibre surface is fully covered with matrix indicating better interfacial adhesion.



**Figure 5a.13:** SEM picture of the fracture surface of PP hybrid nanocomposite

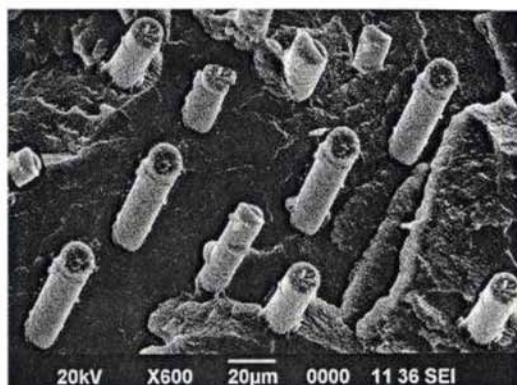


Figure 5a.14: SEM picture of the fracture surface of MA-g-PP hybrid nanocomposite

### 5a.3.3.3 Flexural properties

The flexural properties of the glass fibre/PP composites are compared with MA-g-PP hybrid composites in figure 5a.15. There is improvement in the flexural strength and modulus with modification at all investigated compositions. The maximum improvement occurs at lower fibre content. This is probably due to decrease in fibre/matrix interaction at higher fibre loadings by the crowding of fibres as discussed earlier.

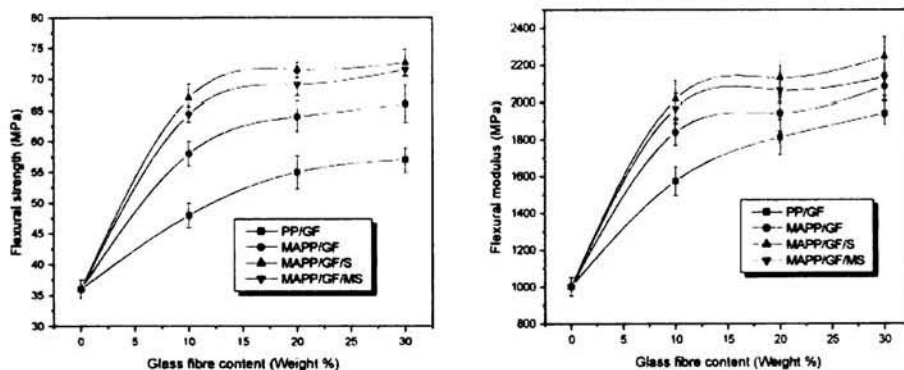
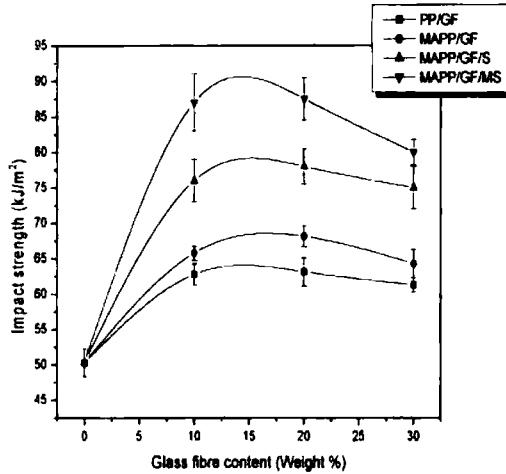


Figure 5a.15: Variation of flexural strength and modulus with fibre loading and silica content

### 5a.3.3.4 Impact strength

The impact strength of the glass fibre/PP composites are compared with MA-g-PP hybrid composites in figure 5a.16.



*Figure 5a.16: Variation of impact strength with fibre loading and silica content*

### 5a.3.4 Dynamic mechanical analysis

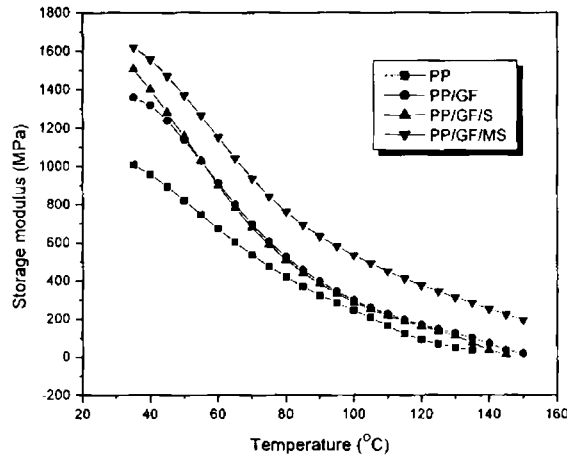
The damping mechanism in composite is mainly results from the viscoelastic nature of matrix and filler, the thermo elastic damping, the coulomb friction damping due to slip between the unbonded, debonded and bonded regions of filler-matrix interface and the energy dissipation occurring at cracks or delaminations.<sup>13</sup>

Figure 5a.17 illustrates the variation of storage modulus ( $E'$ ) with 1wt.% silica and modified silica on PP/10wt.% glass fibre as a function of temperature. It is found that the storage modulus of the PP fibre composite is increased with nanosilica and modified nanosilica and it is more pronounced at low temperatures. This increase in  $E'$  of the composites at different filler loading may be due to higher interfacial adhesion and bond strength between matrix resin and filler as reported by several authors.<sup>14,15</sup> The  $E'$  values are higher at modified silica loading at all temperatures. This may be caused by the better



bonding of nanofiller with fibre and matrix by the help of hydroxyl groups and organic groups present on the surface of nanofiller.

The decrease in modulus at high temperatures is associated with the chain mobility of the matrix and the thermal expansion occurring in the matrix resulting in reduced intermolecular forces.<sup>16,17</sup>



*Figure 5a.17: Variation of storage modulus of PP-glass fibre-silica hybrid composites with temperature*

Figure 5a.18 illustrates the variation of  $E'$  with 1wt.% silica and modified silica on MA-g-PP/10wt.% glass fibre as a function of temperature. Here also it is found that the storage modulus of the composites increased with of nanosilica/modified nanosilica. When compared to nanosilica composite, the composite containing modified nanosilica showed less  $E'$  values at lower temperatures and high  $E'$  values at higher temperatures.

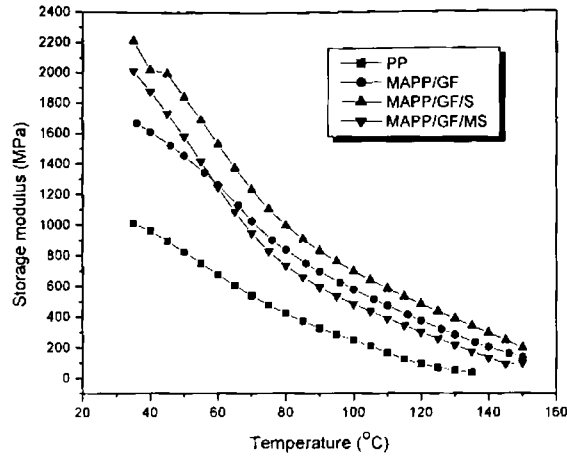


Figure 5a.18: Variation of storage modulus of MA-g-PP-glass fibre-silica hybrid composites with temperature

Table 5a.1 shows the storage modulus and relative (normalized) storage modulus ( $E'_c/E'_m$  where  $E'_c$  and  $E'_m$  are the storage moduli of composite and matrix respectively) values of nano-micro hybrid composites at temperatures 40, 75 and 120 °C.

Table 5a.1: Variation of storage modulus and normalized storage modulus of PP-glass short fibre composites with nanosilica/modified nanosilica at 40, 80 and 120 °C

Sample	Storage modulus (MPa)			Normalized storage modulus		
	40 °C	80°C	120 °C	40 °C	80 °C	120 °C
PP	957.5	474	90.25	1	1	1
PP/GF	1319	604.9	169.2	1.38	1.28	1.87
PP/GF/S	1399	588.3	160.7	1.46	1.24	1.78
PP/GF/MS	1558	841.1	376.1	1.63	1.77	4.17
MA-g-PP/GF	1609	895.7	371.8	1.68	1.89	4.12
MA-g-PP/GF/S	2021	1098	481.2	2.11	2.32	5.33
MA-g-PP/GF/MS	1877	823.5	298.3	1.96	1.74	3.31

The storage modulus and normalized storage modulus of the composites increased with the presence of silica/modified nanosilica at all temperatures, but MA-g-PP hybrid composites containing modified silica showed higher modulus only at higher temperature. The normalized modulus values at 40 °C and 80 °C do not show considerable variation, but at 120 °C high normalized modulus values are obtained by maleic anhydride grafting, compared to the pristine polymer.

The variation of  $\tan \delta$  values of PP-Glass fibre and MA-g-PP-Glass fibre composites with nanofiller as a function of temperature is shown in figure 5a.19 and 5a.20 respectively. Incorporation of stiff fibres and nanofiller reduces the  $\tan \delta$  values of the composite by restricting the movement of polymer molecules and also due to the reduction in the viscoelastic lag between the stress and strain.<sup>18,19</sup> The  $\tan \delta$  values were lowered in the composites compared to pure polymer may also because of the less matrix by volume to dissipate the vibrational energy. The figures indicate that the relatively high viscoelastic damping character ( $\tan \delta$  value) of the pure polymer becomes lowered on reinforcement with nano-micro hybrid. The height of  $\tan \delta$  curves of the composites is significantly lowered with maleic anhydride grafting. The lowering of the  $\tan \delta$  peak height is a measure of enhanced interfacial bond strength and adhesion between matrix and filler.

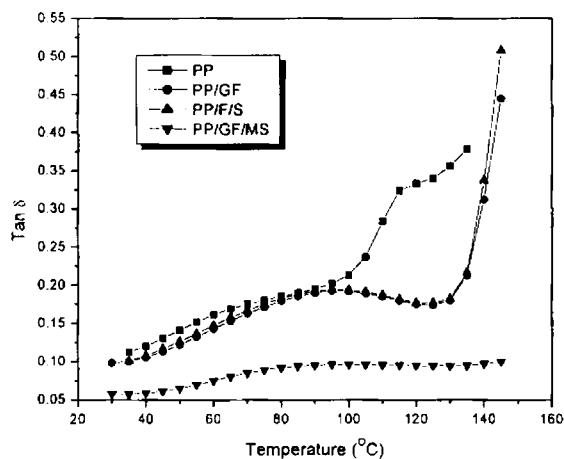
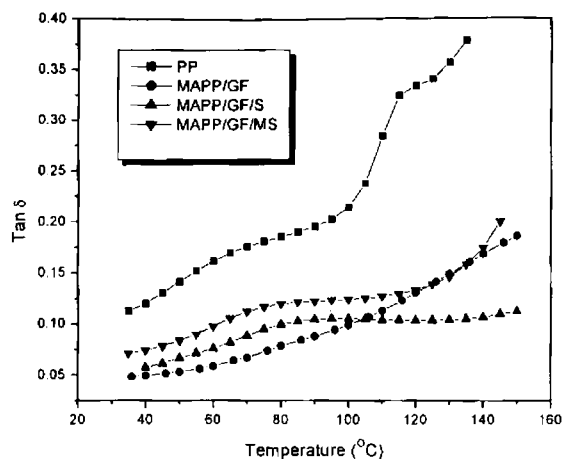


Figure 5a.19: Temperature dependence of  $\tan \delta$  values of PP hybrid nanocomposites



*Figure 5a.20: Temperature dependence of  $\tan \delta$  values of MA-g-PP hybrid nanocomposites*

### 5a.3.5 Crystallization characteristics

The changes in the crystallinity of the PP and PP hybrid composite samples were studied by differential scanning calorimetry. The DSC provides the information about the crystallinity aspects that has occurred in the polymer as a result of thermo mechanical processing. These curves provide the various parameters in crystallization such as peak crystallization temperature ( $T_c$ ), degree of crystallinity ( $X_c$ ), crystallization enthalpy ( $\Delta H$ ) etc.

#### 5a.3.5.1 Non-isothermal Crystallization

Non-isothermal crystallization experiments were done to study the effect of hybrid fillers on crystallization characteristics of melt compounded PP. The crystallization temperatures ( $T_c$ ), the apparent melting temperatures ( $T_m$ ) and the corresponding enthalpies ( $\Delta H_c$  and  $\Delta H_m$ ) for all the samples are reported in table 5a.2.

**Table 5a.2:** DSC-determined thermal characteristics of PP composites

Sample	T <sub>c</sub> (°C)	ΔH <sub>c</sub> (J/g)	T <sub>m</sub> (°C)	ΔH <sub>m</sub> (°C)
PP	110.7	104.6	165.73	102.7
PP/GF	113.48	71.03	162.02	70.85
MAPP/GF	124.09	85.83	162.2	83.19
PP/GF/S	124.15	85.33	166.3	80
PP/GF/MS	124.49	87.69	163.43	79.1
MAPP/GF/S	124.28	80.65	163.28	77.14
MAPP/GF/MS	126.11	89.56	161.45	86.92

Figure 5a.21 shows the DSC cooling scans of PP and its nano-micro hybrid composite samples. During cooling from the melt the hybrid composites showed crystallization exotherms earlier than pristine PP or PP/Glass fibre composite as also seen from the corresponding T<sub>c</sub> values indicated in table 5a.2. It is found that the hybrid composite with 1wt% silica crystallizes about 14 °C earlier than pristine PP where as PP/Glass fibre composite crystallizes only about 4 °C earlier than pure PP. This indicates that filler (nanosilica) together with micro filler (Glass fibre) can act as effective nucleating agent for PP crystallization.

The T<sub>c</sub> values continue to increase with modified silica and matrix modification even though the silica concentration is constant. This tendency shows that the nucleation effect will increase with surface area, good dispersion and effective interaction of the filler in the matrix. The agglomerating tendency of the nanosilica decreased by the presence of vinyl group on the surface and may provide higher surface area and good dispersability in the matrix. The matrix modification further increases the interaction between filler and matrix so as to increase the crystallization. That is why the presence of modified silica in modified matrix causes a rise of 16 °C in the crystallization temperature than pristine PP.

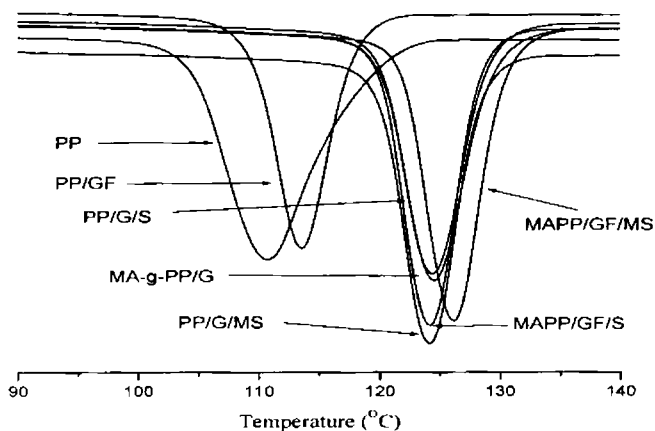


Figure 5a.21: DSC cooling scans (10 °C/min from 180 °C melt) PP composites

The crystallization temperature and the degree of supercooling ( $\Delta T = T_m - T_c$ ) is a measure of the crystallizability; i.e. smaller the  $\Delta T$ , higher the crystallizability. The  $\Delta T$  values of the PP and PP hybrid composites are given in table 5a.3 are smaller by ~ 7 to 20 °C than that of pure PP. This reveals that the crystallizability of the hybrid composites is higher than that of pure PP.

Table 5a.3:  $\Delta T$  values of PP and hybrid nanocomposites

Sample	$\Delta T$ (°C)	% of crystallization
PP	55.03	39.63
PP/GF	48.54	38.23
MAPP/GF	38.11	40.19
PP/GF/S	41.81	40.65
PP/GF/MS	38.94	41.21
MAPP/GF/S	39	41.27
MAPP/GF/MS	35.34	42.99

### 5a.3.5.2 Isothermal crystallization

Figure 5a.23 shows the typical isothermal crystallization curves of PP, PP/glass fibre and PP hybrid composite samples at five temperatures (110, 115, 120, 125 and 130 °C). The time corresponding to the maximum in the heat flow rate (exotherm) is taken as peak time of crystallization ( $t_{\text{peak}}$ ). Such peaks are seen at each of the five isothermal crystallization temperatures for hybrid composites with earlier or faster crystallization (smaller  $t_{\text{peak}}$ ) leads to lower temperature of isothermal crystallization as compared to pure PP. In the case of pure PP no peak is seen at highest temperature of 130 °C because crystallization is very slow and would require longer time than 4 minutes employed in DSC program. On the other hand for the hybrid composites the rate of crystallization is so fast near the lowest temperatures that most of the crystallization occurs during the cooling scan (60 °C/min) employed to reach the temperatures (110 or 115 °C). This results in absence of exothermic peak in the heat flow curves at those temperatures.

The peak time of crystallization at different temperatures for all PP hybrid nanocomposite samples is plotted against the isothermal crystallization temperature (Figure 5a.22). It is noticeable that the  $t_{\text{peak}}$  values for the hybrid composite samples is reduced to less than 50% as compared to pure PP due to the presence of nano and micro fillers. With modified silica and matrix grafting there is further increase in the crystallization rate (as indicated by the decrease in  $t_{\text{peak}}$ ).

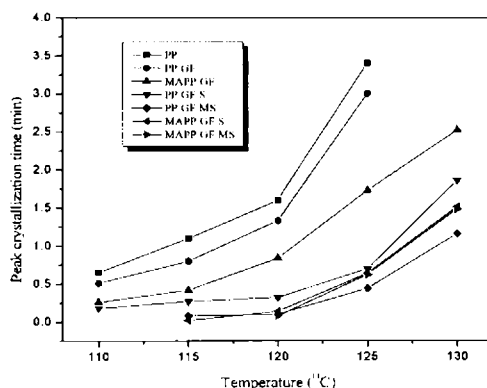
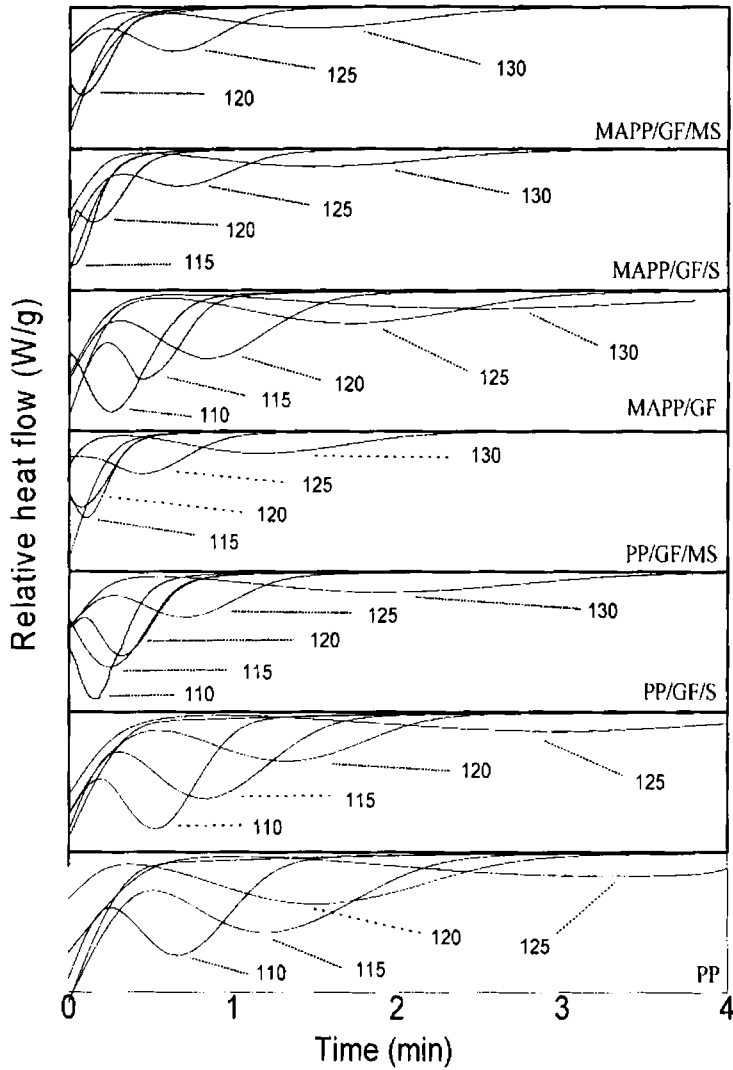


Figure 5a.22: Effect of silica concentration on the peak crystallization time of the



**Figure 5a.23:** Heat flow during isothermal crystallization of PP and its hybrid nanocomposites



### 5a.3.6 Thermogravimetric analysis

Thermal stability of the materials can be improved by inorganic nanofillers.<sup>20</sup> Morphology also affect the thermal stability of the composites.<sup>21</sup> The inorganic fillers industrially used to improve the mechanical properties of polymer materials have different effects on the thermal stability of PP. The decomposition temperature of PP was found to be increased with nanosilica, clay, CaCO<sub>3</sub> etc.<sup>22,23,24</sup>

The TG curves of PP and its composites are shown in figures 5a.24 and 5a.25. The temperature of onset of degradation ( $T_{\text{onset}}$ ), temperature at which maximum degradation occurs ( $T_{\text{max}}$ ) and the residue obtained at 600 °C are given in table 5a.4. In the case of PP degradation is observed in a single step. Up to 387 °C the sample is stable and thereafter sharp weight loss occurs. Degradation is completed at 464 °C and during this stage the weight loss observed is 98.74%. The hybrid composite samples also show single stage of degradation. The presence of hybrid filler increased the thermal stability of the PP and the degradation temperature rises >50 °C. This improvement in thermal stability of the hybrid composites may result from the better interaction or good dispersion of fillers in the matrix.

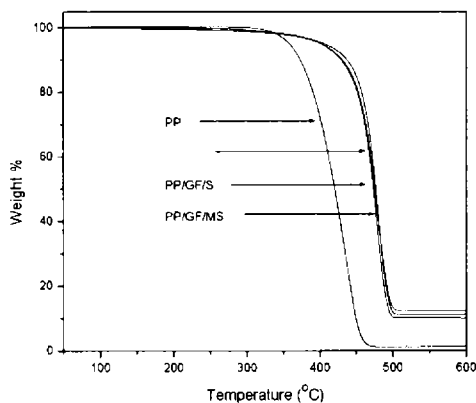
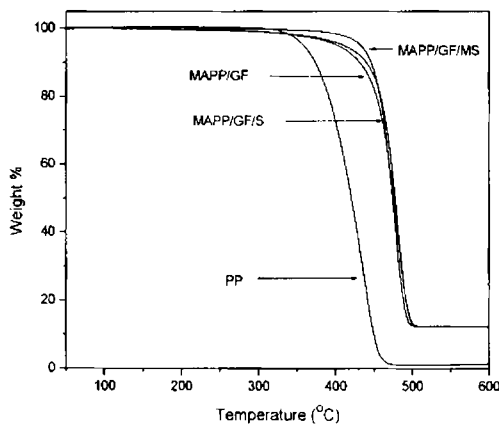


Figure 5a.24: Thermogravimetric traces of PP and PP hybrid composites

**Table 5a.4:** Degradation characteristics of PP and hybrid composites

Sample	Onset temp (°C)	Peak max	Residue at 600 °C
PP	387	436	0.6
PP/GF/S	453	476	12.2
PP/GF/MS	457	480	11.2
MAPP/GF	453	477	10
MAPP/GF/S	453	479	12.3
MAPP/GF/MS	458	480	12

The maleic anhydride grafted composite samples show the improved stability (Figure 5a.25).



**Figure 5a.25:** Thermogravimetric traces of PP and MA-g-PP hybrid composites

## 5a.4 CONCLUSIONS

The study shows that PP-glass fibre-silica hybrid nanocomposites can be fruitfully prepared by melt-mixing method and that

- Addition of 1wt.% modified nanosilica with PP-10wt.% glass composite shows all round performance.
- Storage modulus ( $E'$ ) is high for PP/G/MS composites at all temperatures. But maleic anhydride grafted hybrid composite shows good modulus with unmodified nanosilica.
- $\tan \delta$  decreases with the addition of nanofiller.
- The crystallization temperature of PP enhances with the presence of modified nanosilica.
- Thermogravimetric studies show that the thermal stability of composites is slightly enhanced by the addition of nanosilica/modified nanosilica with glass fibre.
- The modification of PP with nanosilica and micro glass fibre hybrid fillers is effective.

## REFERENCES

1. (a) T.Stevens; *Mechanical Eng*, 1990, 112, 30.  
(b) W.Ast; *Kunststoffe German Plastics* 1990, 80, 3.  
(c) D.Chundry, S.Edge, B.Maclver, J.Vaughn; *Plastics Formulating & Compounding* 1996, 2, 18.  
(d) C.Ausias, M.Vincent, I.Jarrin; *J.Thermoplastics Composite Materials* 1995, 8, 435.
2. R.A.Schweizer; *Polym.Plast.Tech. Eng.* 1982, 18, 81.
3. R.T.Von, L.Erwin; *Polym.Eng.Sci.* 1983, 23:743.
4. B.Fisa; *Polym.Compos.* 1985, 6, 232.
5. R.E.Richards, D.Sims; *Composites* 1971, 3, 214.
6. E.C.Hsu, C.S.Temple; *Fibre Glass Reinforced Thermoplastics: Effect of Reinforcement Parameters on Composite Properties*, 36th Annual Conference, Reinforced Plastics/Composite Institute, SPI, Washington, DC, 1981, 9-F,1.
7. X.Leguet, M.Ericson, D.Chundry, G.Baumer; *Filled and Reinforced Polypropylene Compounds as Alternatives to Engineering Resins*, ANTEC, SPE, Toronto, 1997, 2117.
8. S.E.Barbosa, J.M.Kenny; *J.Vinyl.Additive.Tech.* 1995, 1, 269.
9. E.C.Hsu, C.S.Temple; *Fibre Glass Reinforced Thermoplastics: Effect of Reinforcement Parameters on Composite Properties*, 36th Annual Conference, Reinforced Plastics/Composite Institute, SPI, Washington, DC, 1981, 9-F,1.
10. X.Leguet, M.Ericson, D.Chundry, G.Baumer; *Filled and Reinforced Polypropylene Compounds as Alternatives to Engineering Resins*, ANTEC, SPE, Toronto, 1997, 2117.

11. S.E.Barbosa, J.M.Kenny; *J.Vinyl.Additive.Tech.* **1995**, 1, 269.
12. J.K.Karger; *J.Polym.Eng.* **1991**, 10, 97.
13. H.Rozman, G.S.Tay, R.N.Kumar, A.Abusamah, H.Ismail, Z.A.M.Ishak, *Euro. Polym. J.*, **2001**, 37, 12831
14. D.Ray, B.K.Sarkar, S.Das, A.K.Rana, *Comp.Sci.Technol.*, **2002**, 62, 911.
15. S.H.Aziz, M.P.Ansell, *Comp.Sci.Technol.* **2004**, 64, 1219.
16. J.George, S.S.Bhagavan, S.Thomas; *J. Thermoplastic Comp. Mat.* **1999**, 12, 443.
17. P.V.Joseph, G.Mathew, K.Joseph, G.Groeninckx, S.Thomas; *Comp. Part A* **2003**, 34, 275.
18. D.Ray, B.K.Sarkar, S.Das, A.K.Rana; *Comp.Sci.Technol.* **2002**, 62, 911.
19. A.K.Saha, S.Das, D.Bhatta, B.C.Mitra; *J.Appl.Polym.Sci.* **1999**, 71, 1505.
20. (a) R.Reynaud, T.Jouen, C.Gauthier, G.Vigier; *Polymer* **2001**, 42, 7465.  
(b) N.Salahuddin, M.Shehata; *Polymer* **2001**, 42.  
(c) Y.H.Yua, C.Y.Lin, J.M.Yeh, W.H.Lin; *Polymer* **2003**, 44.  
(d) F.Yang, G.L.Nelson, *J.Appl.Polym.Sci.* **2004**, 91, 3553.  
(e) S.Yang, J.R.Castilleja, E.V.Barrera, K.Lozanova; *Polym.Degrad.Stab.* **2004**, 83, 383.  
(f) C.I.L.Park, W.W.Choi, M.H.O.Kim, O.K.Park; *J.Polym.Sci.B:Polym.Phy.* **2004**, 42, 1685.
21. S.Wang, Y.Hu, L.Song, Z.Wang, Z.Chen, W.Fan; *Polym.Degrad.Stab.* **2002**, 77, 423.
22. C.S.Reddy, C.K.Das, *J.Appl.Polym.Sci.*, **2006**, 102, 2117.
23. H.Sangeetha, B.Neelima, J.P.Jog; *Polym.Eng.Sci.* **2002**, 42(9), 1800.
24. N.Hasegawa, H.Okamoto, M.Kato, A.Usuki, *J.Appl.Polym.Sci.* **2000**, 78, 1918.

# Polypropylene-nylon fibre-silica hybrid nanocomposites

## 5b.1 INTRODUCTION

The need for attaining the right material for the innumerable engineering applications, cost-effective materials being continually developing and expanding. As the technology becomes more and more sophisticated the materials used also have to be much more efficient and reliable. Materials should be light in weight and should possess good strength and modulus. The use of composites has been growing steadily due to their attractive properties like durability, easy mouldability, light weight, noncorrosiveness, adequate strength, stiffness and load bearing qualities.

Polypropylene is a very versatile polymer. The properties of polypropylene can be modified by many ways to suit a wide variety of end-use applications.<sup>1</sup> Various fillers and reinforcements, such as glass fibre, mica, talc and calcium carbonate are typical ingredients that are added to polypropylene resin to attain cost-effective composite mechanical properties.<sup>2</sup> Thomas *et al.* studied about PP/short nylon fibre composites and found that the mechanical property and viscosity improved with fibre loading.<sup>3,4</sup> Elevated viscosity and loss of matrix elasticity are characteristic of highly filled composites.<sup>5,6,7</sup> Inhomogeneous filler distribution within the matrix<sup>8,9,10</sup> and anisotropy in properties have been reported for composites filled with elongated fillers.<sup>11</sup> Inhomogeneous structures, e.g., skincore morphology, are commonly imposed by melt flow patterns developing during processing.<sup>12,13</sup> In most cases these effects are undesirable, representing difficulties and limitations for industrial manufacturing.

Composites containing single filler are commonly used and investigated. However, the behavior of filler particles in systems containing two distinct fillers is rarely reported. The properties of hybrid composites of PP with carbon fibre & carbon black are studied by Drubetski *et al.*<sup>14</sup> In the few reported works, filler depletion in moulding's skin layers and detection of uncommon fibre orientation are described.<sup>15,16,17</sup> Nylon is one of the most important industrial fibres due to its high performance, low cost and recyclability. Presently, the research on nanosilica based products is mainly focused on improving the

mechanical and optical properties of polyolefins. But the agglomeration of nanoparticles during composite formation is a big problem. If we prepare composite with fibrous filler along with nano filler there is a chance of good dispersion of nanoparticles with the aid of fibrous micro filler and thus to improve the properties.

The present study addresses the mechanical and thermal properties of polypropylene based composites containing both nanosilica(S)/modified silica(MS) particles and nylon fibres (NF).

## **5b.2 EXPERIMENTAL**

Short nylon fibre reinforced polypropylene composites were prepared in a Torque Rheometer (Thermo Haake Rheocord 600). The matrix was modified with maleic anhydride according to US patent, 4,753,997. Dumbbell and rectangular shaped samples were prepared by injection moulding in a semiautomatic laboratory injection moulding machine. The tensile properties of the samples were determined using dumbbell shaped samples on a universal testing machine (Shimadzu) at a crosshead speed of 50 mm/min according to ASTM-D-638. Flexural properties of the composites were measured by three-point loading system using the universal testing machine according to ASTM standards.

The modification of PP-nylon fibre composite with nanosilica/modified nanosilica was also done in the Torque Rheometer. 1 and 2wt.% of silica/modified silica were added to PP-nylon fibre composite to get the nano-micro hybrid composite. A mixing time of 8 minutes was used at a rotor speed of 50 rpm. In all cases the torque stabilized to a constant torque in this time.

## **5b.3 RESULTS AND DISCUSSION**

### **5b.3.1 Polypropylene-nylon fibre composite**

#### **5b.3.1.1 Torque studies**

The variation of mixing torque with time of mixing at different fibre loading is shown in figure 5b.1. A mixing time of 8 minutes was fixed since the torque stabilized to a constant value during this time in all cases. The initial and final torque values are found to

increase with increase in fibre loading. This shows that nylon fibre remains in fibre form and behaves as fibrous filler under the given conditions.

Initially torque increases with the PP loading, but decreases with melting. After homogenization of PP, nylon fibres were added. Then the torque rises again and levels off in about 5 min. It is clear from the figure that there is no degradation in the mixing stage.

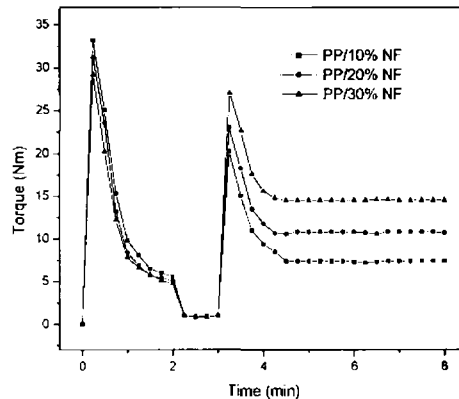


**Figure 5b.1:** Torque – Time curves of PP composites

### 5b.3.1.2 Tensile properties

#### a) Effect of fibre length

To study the effect of fibre length on tensile strength of the present system, 10% nylon fibre filled polypropylene composites were prepared with different average fibre length of 5, 10, 15 and 20 mm. When the fibres are of finite length, stress is assumed to be transferred from the matrix to the fibre by a shear transfer mechanism. For a given fibre, there is minimum fibre length required to build up the shear stress between fibre and resin to the value of tensile fracture stress of the fibre. More than or equal to this length, the maximum value of the load transfer from the matrix to the fibre can occur. If the fibre length is less than this length, the matrix cannot effectively grip the fibre to take the strain and the fibres will slip and be pulled out, instead of being broken under tension. The composite will then exhibit lower mechanical performance. This shortest fibre length



(pull-out length) is called the critical fibre length. This fibre length is an important property and affects ultimately the strength and elastic modulus of composites.

The maximum tensile strength of the composites (Figure 5b.2) is at 10 mm length of the fibre. Hence 10 mm length was taken as optimum fibre length for further studies.

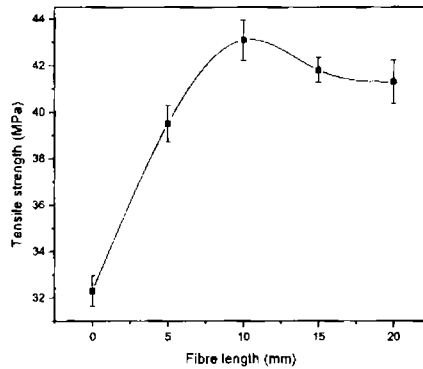


**Figure 5b.2:** Variation of tensile strength with fibre length

**b) Effect of fibre loading**

Figure 5b.3 shows the effect of the variation of tensile strength and tensile modulus of PP/ nylon fibre composite with fibre loading. The tensile strength increases with fibre loading up to 30% but decreases thereafter. The decrease in strength at higher fibre loading is probably due to crowding of fibres, which prevents efficient matrix-fibre stress transfer.

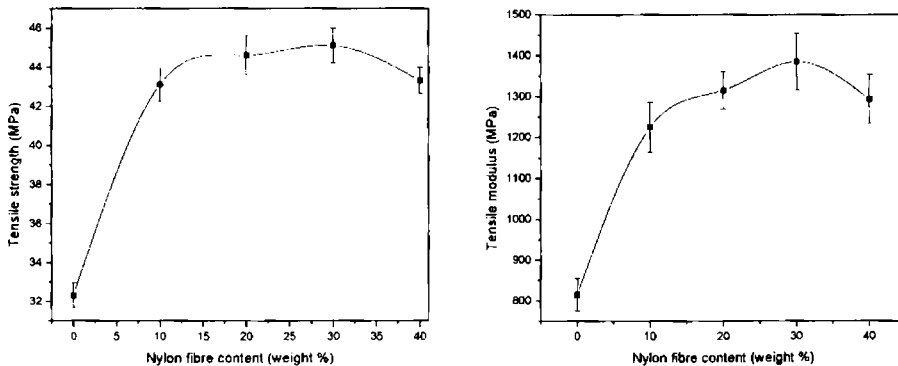


**Figure 5b.3:** Variation of tensile strength and modulus with fibre loading

### 5b.3.1.3 Flexural properties

#### a) Effect of fibre length

The effect of fibre length on the flexural strength is given in figure 5b.4. Flexural strength increases with increase in fibre length up to 10 mm and thereafter decreases as in the case of the tensile strength. These observations point to a optimum fibre length of about 10 mm both in the case of tensile and flexural loads.

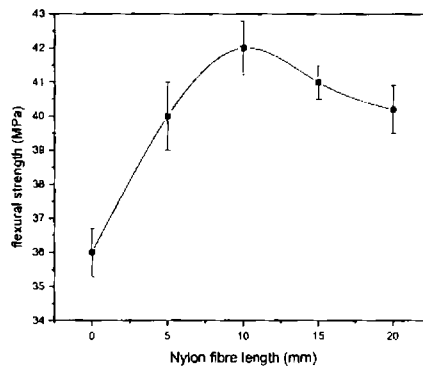


*Figure 5b.4: Variation of flexural strength with fibre length*

#### b) Effect of fibre loading

Figure 5b.5 shows the effect of fibre loading on the flexural strength and flexural modulus of PP/nylon fibre composites. From the figures it is clear that both flexural strength and modulus increases with fibre content. The maximum modulus is observed at 30% fibre loading.

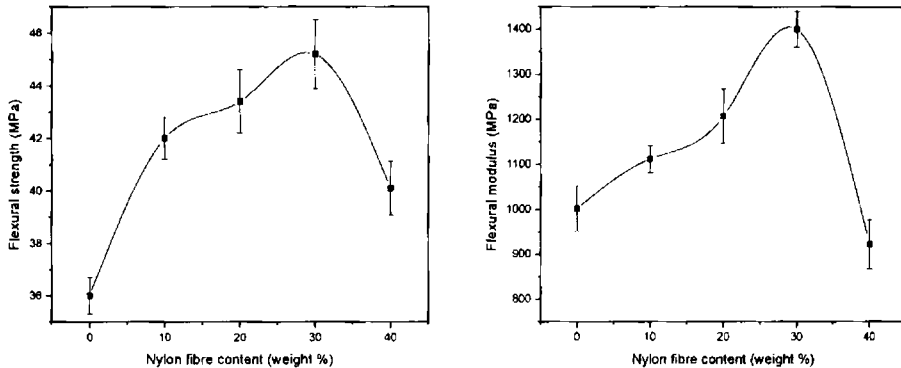


**Figure 5b.5:** Variation of flexural strength and modulus with fibre loading

The loading in flexure is an ideal case which causes normal stress in the direction of fibres and shear stress in the plane perpendicular to the loading nose. The mode of failure of unidirectional composites in flexure is very complex. Unidirectional composites, when stressed in flexure can fail in tension either longitudinally or transversely, or in shear at the matrix, matrix/fibre interface or fibre. The most common modes of failure are transverse splitting, brittle tensile failure fibre pullout, interfacial shear failure, compressive failure due to micro buckling or localized kinking of fibres and intra-laminar shear failure. When the span/thickness  $l/d$  ratio is less than 25, the failure occurs by fibre buckling localized in very narrow bands (kink bands). When loaded, either in flexure or in compression, some relief of local stresses accompanies the micro processes as the crack propagates from compressive side to the neutral plane. Further deflection of the beam causes a tensile failure of fibres on the tensile side of the beam, which leads to catastrophic failure of the specimen. In some cases, some amounts of inter laminar shear failure initiated from the kink bands, are observed on the compressive side. Constraints imposed on the beam by contact with load pin may also inhibit the initiation of buckling in flexural testing.

### 5b.3.2 Modification of PP-nylon fibre composite with nanosilica/modified nanosilica

To study the effect of nanosilica/modified nanosilica on the tensile strength of the nylon fibre-PP composite, PP-nylon fibre with 1 and 2wt.% of nano fillers were prepared. When the nano filler disperse well with the aid of fibres, the stress will be transferred effectively from the matrix to the nano filler and fibre by a shear transfer mechanism. From figure 5b.3 it is observed that good mechanical properties of the composites are associated with 10 mm length of the fibre. Hence 10 mm length was taken as optimum fibre length for further studies. The reinforcement of PP/nylon fibre composites with 1wt.% nanosilica and modified nanosilica show better performance. Hence the properties of 1wt.% nanosilica/modified nanosilica reinforced composites are discussed in detail.

#### 5b.3.2.1 Torque studies

The variation of mixing torque with time of mixing at different filler loading is shown in figure 5b.6. A mixing time of 8 minutes was fixed since the torque stabilized to a constant value during this time.

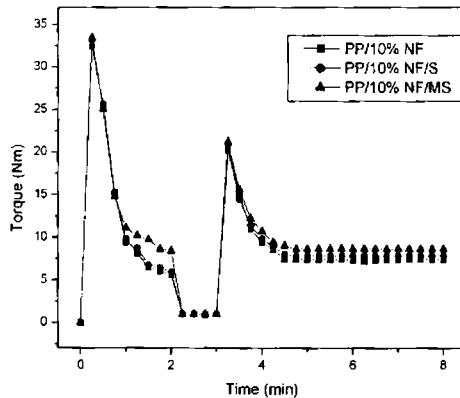


*Figure 5b.6: Torque – Time curves of PP composites*

### 5b.3.2.2 Tensile properties

Figure 5b.7 shows the effect of variation of tensile strength and tensile modulus of PP/nylon fibre composites with fibre and nanosilica/modified nanosilica loading. The tensile strength increases with fibre loading up to 20% and thereafter levels off. The decrease in strength at higher loading is probably due to crowding of nanofiller and also due to the crowding of fibres, which prevents efficient stress transfer from the matrix.

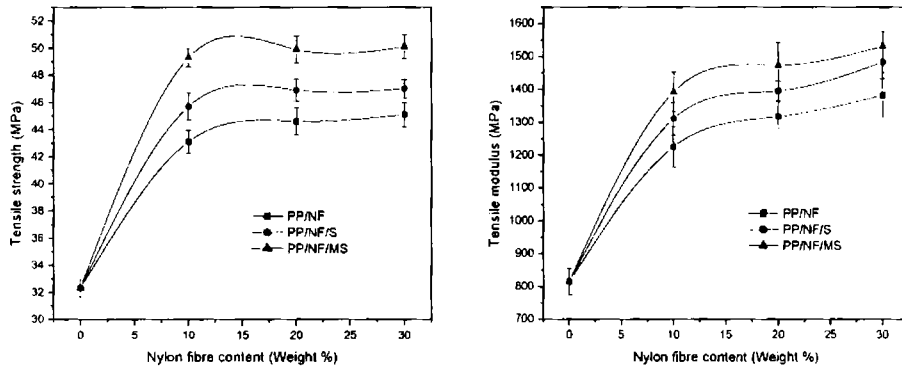


**Figure 5b.7:** Variation of tensile strength and modulus with fibre loading and silica content

### 5b.3.2.3 Flexural properties

Figure 5b.8 shows the effect of nanofiller loading on the flexural strength and flexural modulus of PP/nylon fibre composites. From the figures it is clear that both flexural strength and modulus increases with fibre as well as nanosilica content. The modulus change at 10% fibre loading with nano filler is more significant.

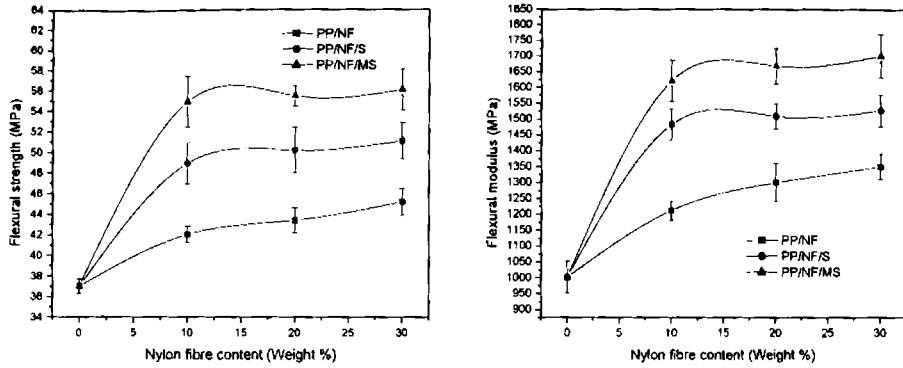


Figure 5b.8: Variation of flexural strength and modulus fibre loading and silica content

### 5b.3.2.4 Impact strength

Figure 5b.9 shows the effect of nanofiller loading on the impact strength of PP hybrid composites. From the figure it is found that the impact strength increases with nanosilica content only at 10% fibre loading.

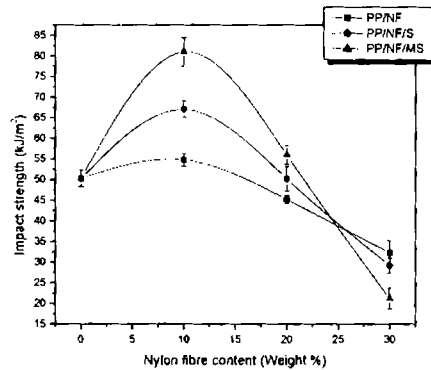


Figure 5b.9: Variation of impact strength with fibre loading and silica content

### 5b.3.3 Effect of matrix modification on nano-micro hybrid composites

#### 5b.3.3.1 Torque studies

The variation of mixing torque with time of mixing at different filler loading is shown in figure 5b.10. A mixing time of 8 minutes was fixed since the torque stabilized to a constant value during this time. The temperature of the mixing chamber was also fixed as 180 °C. The nano filler additions and MA grafting affect the initial and final torque values. This shows MA grafting has some effect during the formation of the composite.

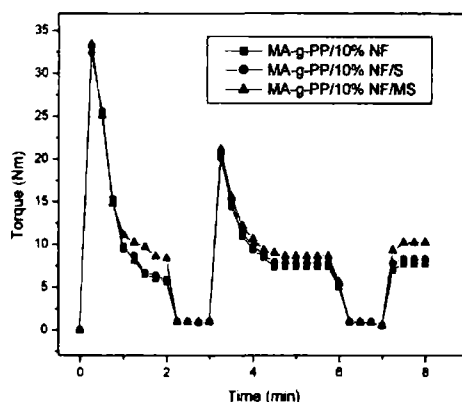
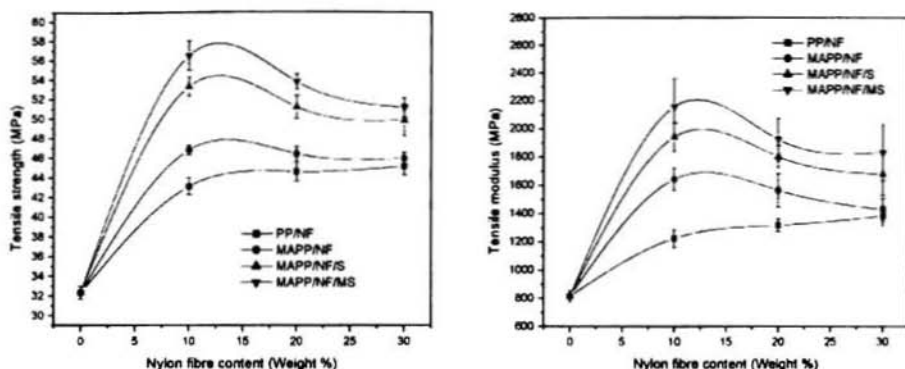


Figure 5b.10: Torque – Time curves of MA-g-PP composites

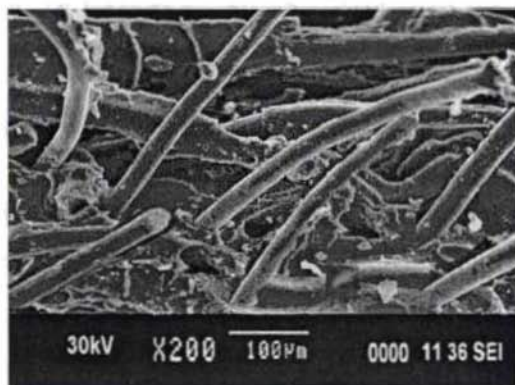
#### 5b.3.3.2 Tensile properties

Figure 5b.11 shows the effect of chemical treatment on the tensile properties of hybrid composite.<sup>18</sup> From the figures it is clear that the matrix modification improves the tensile strength of the composites due to the strong interaction between the polar group in nylon fibre/nanosilica and the grafted functional group in the polymer backbone. The improvement in the tensile modulus at 10% fibre content and 1% nanofiller is particularly significant which shows that the matrix has become stronger by the modification, even though this is not pronounced at higher fibre loading due to fibre crowding.



**Figure 5b.11:** Variation of tensile strength and modulus with fibre loading and silica content

The improvement of adhesion between the filler and MA treated matrix can be seen from the scanning electron micrographs (SEM) of the fractured surface of PP/nylon fibre/silica hybrid nanocomposite and that of MA-g-PP/nylon fibre/modified silica hybrid nanocomposites (Figures 5a.12 and 5a.13). The fractured surface of unmodified matrix shows holes and the fibre surface retain low amount of matrix indicating poor adhesion between the fibre and matrix while in the case of modified matrix, the fractured surface shows evidence for fibre breakage rather than pullout, and the fibre surface fully covered with matrix indicating better interfacial adhesion.



**Figure 5b.12:** SEM picture of the fracture surface of PP hybrid nanocomposite



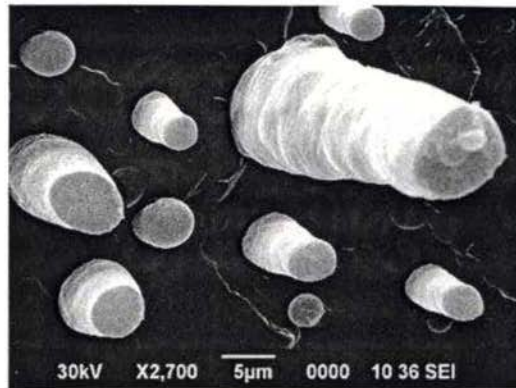


**Figure 5b.13:** SEM picture of the fracture surface of MA-g-PP hybrid nanocomposite

### 5b.3.3.3 Flexural properties

The flexural properties of the PP/nylon fibre composites are compared with MA-g-PP hybrid composites in figure 5b.14. The hybrid composites show a significant improvement in flexural strength and modulus by the modification.

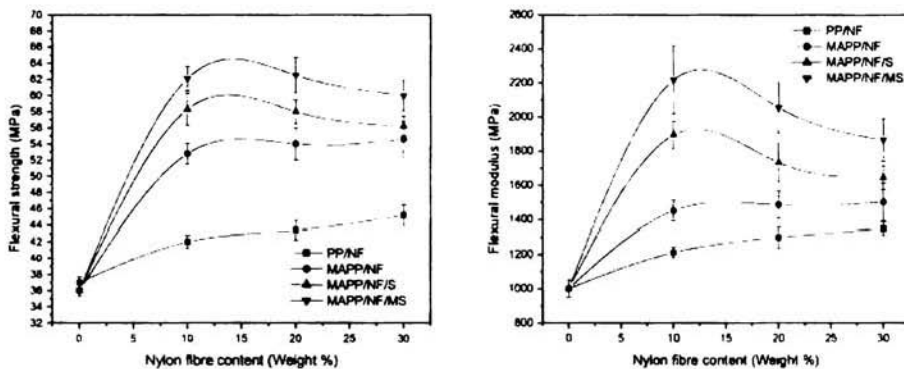


**Figure 5b.14:** Variation of flexural strength and modulus with fibre loading and silica content

### 5b.3.3.4 Impact strength

The impact strength of the PP/nylon fibre composite is compared with MA-g-PP hybrid composites in figure 5b.15. There is a significant improvement in flexural strength and modulus by modification of all the fibre compositions investigated. The maximum

improvement occurs at lower fibre content. This is probably due to decrease in fibre/matrix interaction at higher fibre loadings by the crowding of fibres as discussed earlier.

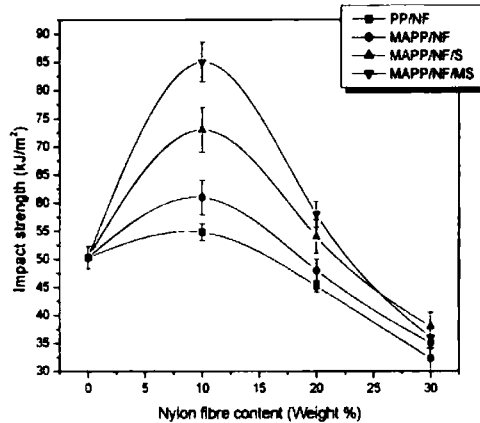
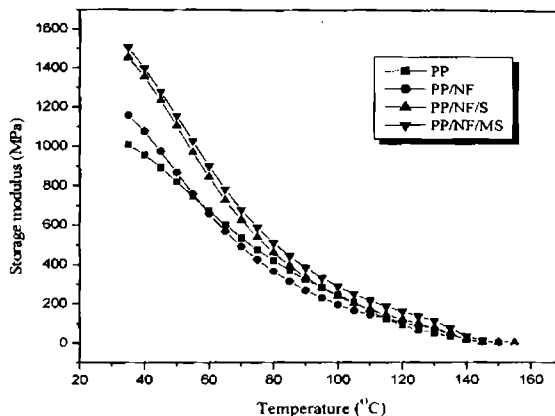


Figure 5b.15: Variation of impact strength with fibre loading and silica content

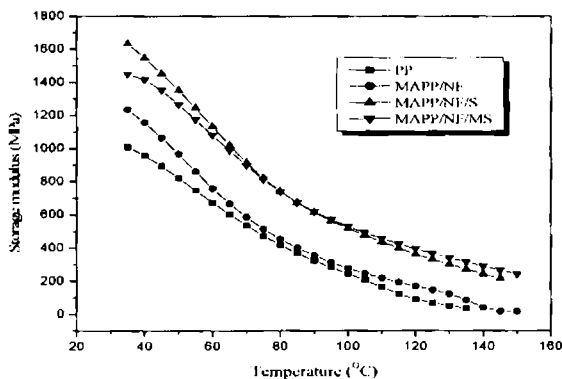
### 5b.3.4 Dynamic mechanical analysis

Figure 5b.16 illustrates the variation of storage modulus ( $E'$ ) with the addition of 1wt.% silica and modified silica on PP/10wt.% nylon fibre as a function of temperature. It is found that the storage modulus of the composites increased with the presence of nanosilica and modified nanosilica and it is more pronounced at low temperatures. This increase in  $E'$  of the composites at higher fibre loading is due to greater interfacial adhesion and bond strength between matrix resin and filler as reported by several authors.<sup>19,20</sup> The  $E'$  values are higher at modified silica loading at all temperatures. This may be caused by the better bonding of nano filler with fibre and matrix by the help of organic group present on the surface of nanofiller.



**Figure 5b.16:** Variation of storage modulus of PP/nylon fibre-silica hybrid composites with temperature

Figure 5b.17 illustrates the variation  $E'$  with 1wt.% silica and modified silica on MA-g-PP/10wt.% nylon fibre as a function of temperature. Here also it is found that the storage modulus of the composites increased with the presence of nanosilica/modified. When compared with nanosilica filled composite, the composite containing modified nanosilica showed low  $E'$  values at lower temperatures but high  $E'$  values at higher temperatures. The decrease in modulus at higher temperature is associated with the chain mobility of the matrix<sup>21</sup> and the thermal expansion occurring in the matrix resulting in reduced intermolecular forces.<sup>22</sup>



**Figure 5b.17:** Variation of storage modulus of MA-g-PP-nylon fibre-silica hybrid composites with temperature

Table 5b.1 shows the storage modulus and relative (normalized) storage modulus ( $E'_c/E'_m$  where  $E'_c$  and  $E'_m$  are the storage moduli of composite and matrix respectively) values of nano-micro hybrid composites at temperatures 40, 80 and 120 °C.

**Table 5b.1.** Variation of storage modulus and normalized storage modulus of PP/nylon short fibre composites with nanosilica/modified nanosilica at 40, 80 and 120 °C

Sample	Storage modulus (MPa)			Normalized storage modulus		
	40 °C	80 °C	120 °C	40 °C	80 °C	120 °C
PP	957.5	474	90.25	1	1	1
PP/NF	1077	423.8	103.9	1.12	0.89	1.15
PP/NF/S	1355	536.6	119.4	1.42	1.13	1.32
PP/NF/MS	1399	588.3	160.7	1.46	1.24	1.78
MAPP/NF	1157	515.5	169.2	1.21	1.09	1.87
MAPP/NF/S	1547	821.7	363.4	1.62	1.73	4.03
MAPP/NF/MS	1414	813.3	394.9	1.48	1.72	4.38

The storage modulus and the normalized storage modulus of the composites increased with the presence of silica/modified nanosilica at all temperatures, but MA-g-PP composite containing modified silica showed higher modulus only at higher temperature. The normalized modulus values at 40 °C and 80 °C do not show considerable variation, but at 120 °C high normalized modulus values are obtained by maleic anhydride grafting, compared to the pure polymer.

The variation of  $\tan \delta$  of PP/nylon fibre and MA-g-PP/nylon fibre composites with nano filler loading, as a function of temperatures is shown in figure 5b.18 and 5b.19 respectively. Incorporation of stiff fibres and nanofiller reduces the  $\tan \delta$  peak of the composite by restricting the movement of polymer molecules, and also due to the reduction in the viscoelastic lag between the stress and the strain.<sup>23,24</sup> The  $\tan \delta$  values were lowered in the composites compared to the pure polymer may also because of the less matrix by volume to dissipate the vibrational energy. The figures indicate that the relatively high viscoelastic damping character ( $\tan \delta$  value) for the pure polymer becomes

lowered on reinforcement with nano-micro hybrid. The height of  $\tan \delta$  peaks of the composites is significantly lowered with maleic anhydride grafting as expected. The lowering of the  $\tan \delta$  peak height is a measure of enhanced interfacial bond strength and adhesion between the fillers and the matrix.

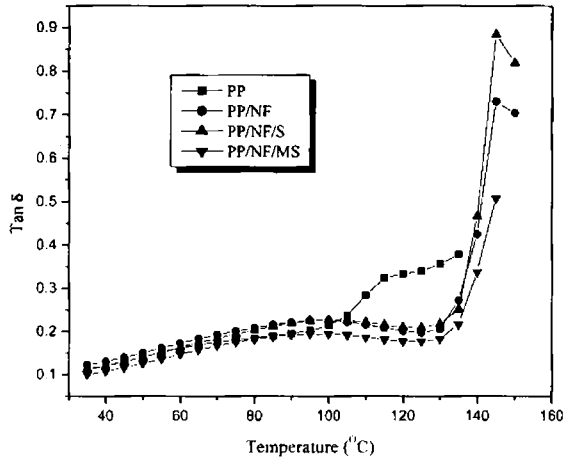


Figure 5b.18: Temperature dependence of  $\tan \delta$  values of PP hybrid nanocomposites

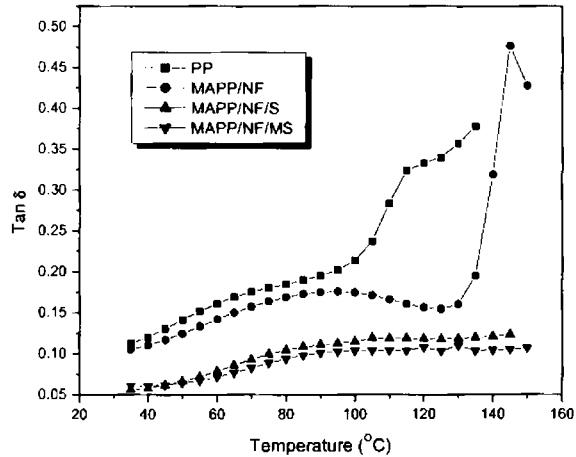


Figure 5b.19: Temperature dependence of  $\tan \delta$  values of MA-g-PP hybrid nanocomposites

### 5b.3.5 Crystallization characteristics

The presence of fillers usually affects the crystallization behaviour of a polymer. The crystallization may have a major influence on the structure of composites and thereby on the mechanical properties. Hence it is very important to study the crystallization kinetics of composites which determines the final properties of a polymeric product. Differential Scanning Calorimetry (DSC) is the widely accepted technique to study the crystallization and thermal behaviour of polymer.

#### 5b.3.5.1 Non-isothermal Crystallization

The effect of nano-micro hybrid on the crystallization characteristics of melt compounded PP nanocomposite samples was analyzed first with non-isothermal DSC experiments. The crystallization temperatures ( $T_c$ ), the apparent melting temperatures ( $T_m$ ) and the corresponding enthalpies ( $\Delta H_c$  and  $\Delta H_m$ ) for all the samples are reported in table 5b.2.

**Table 5b.2:** Thermal characteristics of PP, PP/short fibre composite and nano-micro hybrid composites

Sample	$T_c$ (°C)	$\Delta H_c$ (J/g)	$T_m$ (°C)	$\Delta H_m$ (J/g)
PP	110.7	104.6	165.73	102.7
PP/NF	111.2	82.26	162.13	83.98
MAPP/NF	121.3	86.71	163.25	83.28
PP/NF/S	111.7	82.48	163.92	86.6
PP/NF/MS	112.66	83.33	162.72	80.03
MAPP/NF/S	125	89.88	163.34	84.05
MAPP/NF/MS	126.49	88.2	160.94	83.56

Figure 5b.20 shows the DSC cooling scans of PP and Nylon fibre/silica/modified silica composite samples with PP and MA-g-PP. During cooling from the melt, the hybrid

composite samples show crystallization exotherms earlier than pure PP, as also seen from the corresponding  $T_c$  values indicated in table 5b.2.

The  $T_c$  values show small increment with silica and modified silica addition in PP/nylon fibre composites. But the MA grafting show a noticeable increment for the  $T_c$  value. It is found that the hybrid sample prepared with MA grafted PP crystallizes about 15 °C earlier than pure PP. This indicates that grafting increases the interaction of matrix with filler and thus the hybrid filler can act as nucleating agent for PP crystallization.

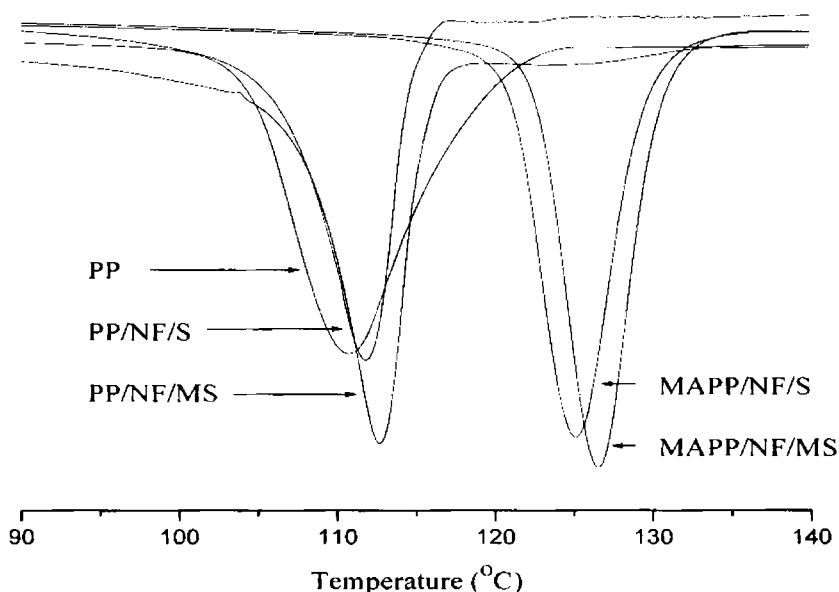


**Figure 5b.20:** DSC cooling scans (10 °C/min from 180 °C melt) of PP and PP composites

Smaller the degree of supercooling ( $\Delta T = T_m - T_c$ ), higher will be the crystallizability. The  $\Delta T$  values of the PP/nylon fibre or PP hybrid composites given in table 5b.3 are smaller by ~ 4 to 14 °C than that of pure PP. This reveals that the crystallizability of the nanocomposites is greater than that of pure PP.

**Table 5b.3:**  $\Delta T$  values of PP and PP composites

Sample	$\Delta T$ ( $^{\circ}\text{C}$ )	% of crystallization
PP	51.32	39.63
PP/NF	50.93	44.81
MAPP/NF	41.95	40.56
PP/NF/S	52.22	41.84
PP/NF/MS	50.06	38.66
MAPP/NF/S	38.34	40.6
MAPP/NF/MS	34.45	40.37

### 5b.3.5.2 Isothermal crystallization

Figure 5b.21 shows the typical isothermal crystallization curves of pure PP and PP composites at five temperatures (110, 115, 120, 125 and 130  $^{\circ}\text{C}$ ). The time corresponding to the maximum in the heat flow rate (exotherm) is taken as peak time of crystallization ( $t_{\text{peak}}$ ). For the case of pure PP, no peak is seen at the highest temperature of 130  $^{\circ}\text{C}$  because crystallization is very slow and would require longer time than the 4 minutes employed in the DSC program. On the other hand, for the nanocomposite samples with 1wt% silica, the rate of crystallization is so fast near the lowest temperatures that most of the crystallization occurs already during the cooling scan (60 $^{\circ}\text{C}/\text{min}$ ) employed to reach the temperatures (110 or 115  $^{\circ}\text{C}$ ). This results in absence of exothermic peaks in the heat flow curves at those temperatures.



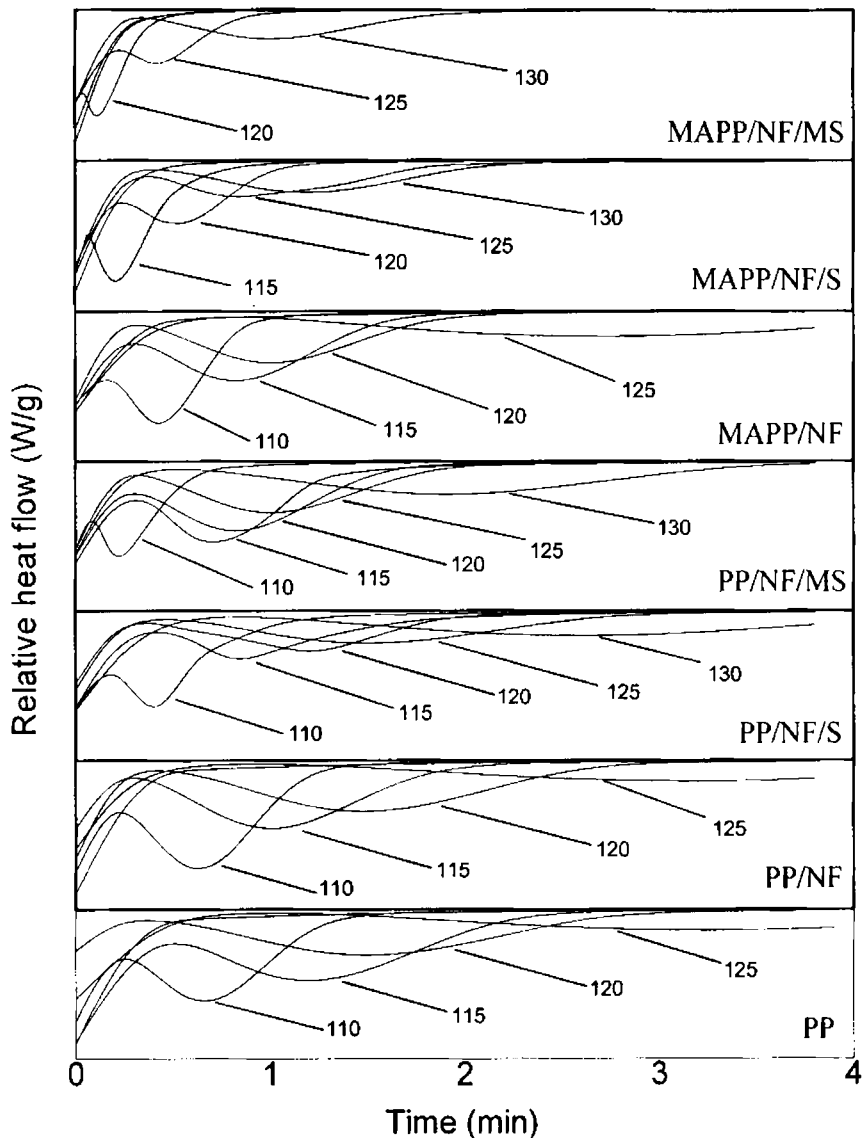


**Figure 5b.21:** Heat flow during isothermal crystallization of PP composites

The peak times of crystallization at each of the temperatures for all the PP-silica nanocomposite samples are plotted against the isothermal crystallization temperature (Figure 5b.22). It is noticeable that the  $t_{\text{peak}}$  values of the composite samples reduced to less than 40% as compared to pure PP due to the presence nano-micro filler. With the

modified silica and matrix grafting there is increase in the crystallization rate (as indicated by the decrease in  $t_{peak}$ ), demonstrating the role of modification on the surface of silica and polymer backbone for enhancing the matrix-filler interaction and thus enhancing the rate of crystallization.

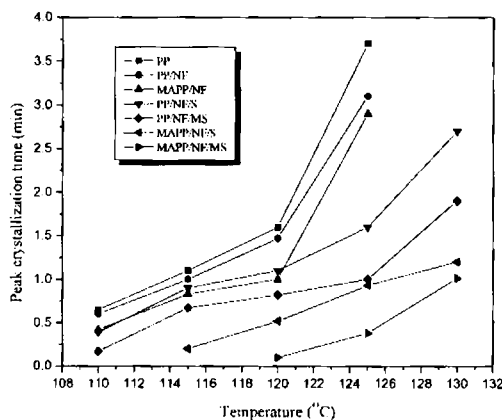


**Figure 5b.22:** Effect of hybrid filler and matrix grafting on the peak crystallization time of the composites at different isothermal crystallization temperatures

### 5a.3.6 Thermogravimetric analysis

The thermal degradation pattern of PP, PP composites and grafted PP composites in nitrogen atmosphere are shown at a programmed temperature range of 50-600 °C are shown in figures 5b.23 and 5b.24. The temperature of onset of degradation ( $T_i$ ), temperature at which maximum degradation occurs ( $T_{max}$ ) and the residue obtained at 600 °C are given in table 5b.4.

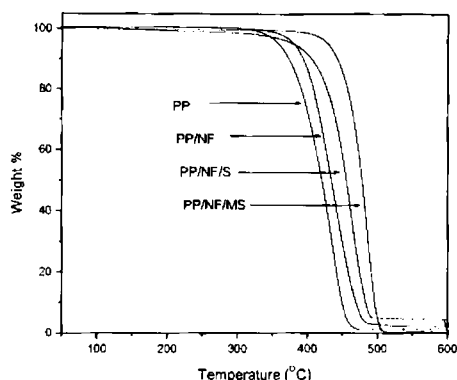


Figure 5b.23: Thermogravimetric traces of PP and PP hybrid composite

In the case of PP, degradation is observed in a single step. Up to 387 °C the sample is stable and thereafter sharp weight loss occurs. Degradation is completed at 480 °C and during this stage the weight loss observed is 99%. For nylon fibre the degradation take place between 400 to 500 °C in a single stage. Both the matrix and fibre follows single step degradation and also having comparable  $T_{max}$ . Hence the hybrid composite samples also show similar degradation pattern. The presence of nano-micro hybrid filler increased the thermal stability of PP from 387 to 457 °C. This improvement in thermal stability of the composites may result from the better interaction or good dispersion of fillers in the matrix. Gilman suggested that the improved thermal stability of polymers in presence of fillers is due to the hindered thermal motion of polymer molecular chains.<sup>25</sup>

Table 5b.4: Degradation characteristics of PP and hybrid composites

Sample	Onset temp. (°C)	Peak max	Residue at 600 °C
PP	387	436	0.6
PP/NF	396.7	435.9	0.9
PP/NF/S	427.6	462.5	2.9
PP/NF/MS	457.4	485.1	1.4
MAPP/NF	449.2	477.6	1.2
MAPP/NF/S	453.9	480.4	3.2
MAPP/NF/MS	451.9	478.8	2.6

MA grafted PP hybrid composite also shows higher thermal stability. This shows that the presence of inorganic filler improve the thermal stability of the polymer.

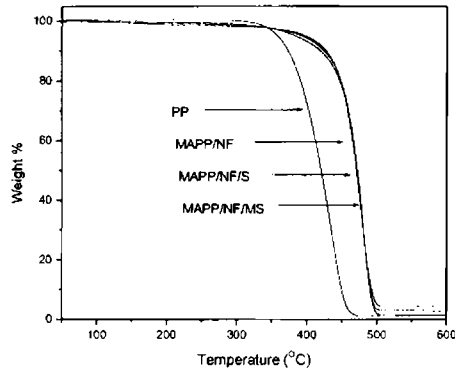


Figure 5b.24: Thermogravimetric traces of PP and MA-g-PP hybrid composite

## 5b.4 CONCLUSIONS

The study shows that PP-nylon fibre composites can be effectively reinforced with nanosilica and modified nanosilica by melt-mixing and the conclusions are

- The incorporation of nanosilica and modified nanosilica enhance the mechanical properties of PP-nylon fibre composites
- Storage modulus ( $E'$ ) improved for PP/NF composites with modified silica at all temperatures. But maleic anhydride grafted composite show high modulus even with unmodified nanosilica.
- The crystallization temperature of PP enhances with the presence of modified nanosilica
- Thermogravimetric studies show that the thermal stability of composites is slightly enhanced by the addition of nanosilica/ modified nanosilica with nylon fibre
- The modification of PP with nanosilica and nylon fibre hybrid filler is effective

## REFERENCES

1. (a) C.Pavithran, P.S.Mukherjee, M.Brahamakumar; *J.Reinforc.Plast. Compos.* **1991**, 10, 91.  
(b) A.Maurizio, C.Luca, D.Ramiro, F.Bonventura, M.Ezio, M.Annamaria, *J.Appl.Polym.Sci.* **1998**, 68, 1077.  
(c) M.WU, C.B.Lee; *J.Appl.Polym.Sci.* **1999**, 73, 2169.  
(d) A.K.Rana, B.C.Mitra, A.N.Banerjee; *J.Appl.Polym.Sci.* **1999**, 71, 531.
2. (a) P.R.Hornsby, C.L.Watson; *J.Mater.Sci.* **1995**, 30, 5347.  
(b) S.N.Maiti, K.K/Sahrma; *J.Mater.Sci.* **1992**, 27, 4605.  
(c) K.H.Rao, K.S.E.Forsberg, W.Forsling; *Physico.Chem.Engng.Aspects.* **1998**, 58, 747.  
(d) L.Domka; *Colloid.Polym.Sci.* **1994**, 272, 1190.  
(e) W.Y.Chiang, W.D.Yang; *J.Appl.Polym.Sci.* **1988**, 35, 807.  
(f) P.Mareri, S.Bastide, N.Binda, A.Crespy; *Compos.Sci.Technol.* **1998**, 58, 747.  
(g) M.Y.Faud, J.Mustafah, M.S.Mansor, Z.A.Ishak, A.K.M.Omar; *Polym.Int.* **1995**, 38, 33.
3. N.A.Thomas, K.E.George; *Progress in Rubber Plastics and Recycling Technology*, **2005**, 21 (1), 73.
4. N.A.Thomas, K.E.George; *Polymer-Plastics Technology and Engineering*, **2007**, 46, 321.
5. I.Miles, S.Rostami; *Multicomponent Polymer Systems*, Longman Scientific and Technical, Essex, UK, **1992**.
6. O.Carneiro, J.Maia; *Polym. Compos.* **2000**, 21, 961.

7. I.Miles, S.Rostami; *Multicomponent Polymer Systems*, Longman Scientific and Technical, Essex, UK, **1992**.
8. J.Kubat, A.Szalanczi; *Polym.Eng.Sci.* **1974**, 14, 873.
9. F.Folgar, C.Tucker; *J. Reinf. Plast. Compos.* **1984**, 3, 98.
10. R.Hegler, G.Menning; *Polym.Eng.Sci.*, **1985**, 25, 395.
11. (a) M.Weber,M.Kamal; *Polym.Compos.* **1997**, 18(6), 726.  
(b) A.Dani, A.Ogale; *Comp. Sci. Technol.* **1996**, 56, 911.  
(c) T.Ezquerria, R.Bayer, F.Balta; *J. Mater. Sci.*, **1998**, 23, 4121.  
(d) F.Lux ; *J.Mater.Sci.* **1993**, 28, 285.
12. M.L.Clingerman; *Synergistic Effects of Carbon Fillers in Electrically Conductive Nylon 6,6 and Polycarbonate Based Resins*, Ph.D.Thesis, Michigan Technological University, Houghton, **2001**.
13. M.Weber, M.Kamal; *Polym. Compos.*, **1997**, 18(6), 726.
14. M.Drubetski, A.Siegmann, M.Narkis; *Polym.Compos.* **2005**, 454.
15. F.C.Balta, R.Bayer,T.Ezquerria; *J. Mater. Sci.*, 1988, 23, 1411.
16. Y.C.Lam, X.Chena, K.W.Tan, J.C.Chai, S.C.M.Yu; *Compos. Sci. Technol.* **2004**, **64**, 1001.
17. S.Limand, J. White; *Int. Polym. Proc.*, 1993, **8**, 81.
18. N.A.Thomas, K.E.George, T.Peijjis; *Progress in Rubber, Plastics, and Recycling Technology*, **2005**, 21, 1.
19. S.H.Aziz, M.P.Ansell, *Comp.Sci.Technol.* **2004**, **64**, 1219.
20. D.Ray, B.K.Sarkar, S.Das, A.K.Rana; *Comp.Sci.Technol.* **2002**, 62, 911.

21. P.V.Joseph, G.Mathew, K.Joseph, G.Groeninckx, S.Thomas; *Comp. Part A* **2003**, 34, 275.
22. J.George, S.S.Bhagavan, S.Thomas; *J. Thermoplastic Comp. Mat.* **1999**, 12, 443.
23. D.Ray, B.K.Sarkar, S.Das, A.K.Rana; *Comp.Sci.Technol.* **2002**, 62, 911.
24. A.K.Saha, S.Das, D.Bhatta, B.C.Mitra; *J.Appl.Polym.Sci.* **1999**, 71, 1505.
25. J.W.Gilman; *Appl.Clay.Sci.* **1999**, 15, 31.

# Chapter 6

## Modification of HDPE-short fibre composite with nanosilica/modified nanosilica

Part – a

### High density polyethylene-glass fibre-silica hybrid nanocomposites

#### 6a.1 INTRODUCTION

In the plastic industry it is a common practice to compound polymers with fillers and fibres to reduce cost and attain desired properties. Desirable properties can be obtained from such composites by the proper combinations of fillers. Fibre-reinforced thermoplastics have the typical advantages of polymer matrix composites such as high weight savings, high strength, high stiffness, corrosion resistance, parts integration, and energy absorption. In addition, they have an indefinite shelf life, are recyclable, and are feasible for automated, high volume processing with a potential for rapid and low-cost fabrication. However, usage of thermoplastic is only to a limited extent nowadays for engineering applications, because of lack of dimensional stability and low heat distortion temperatures. In automotive industry the most used thermoplastics are glass filled thermoplastics developed for a variety of applications from intake manifolds to engine covers, and to a lesser extent for body panels. It has been estimated that significant use of glass-reinforced polymers as structural components could yield a 20-35% reduction in vehicle weight.<sup>1</sup> The 1995 Nissan Sentra served as the first use of thermoplastic (DuPont's Minlon mineral-reinforced nylon) for valve covers in North America. High density polyethylene (HDPE) is one of the most widely using thermoplastic for making composites to suit a wide variety of end use applications. The main attractiveness of thermoplastic composites is that their ease of processability and recyclability. But for getting desirable properties higher fibrous or filler materials required, this decrease the processability of the composite. Newly developed polymer nanocomposites are



advantageous due to the use of very low amount of fillers.<sup>2</sup> The synergetic effect of nano and fibrous fillers may give superior properties to the composites. Canova *et al.*<sup>3</sup> reported that exfoliated nano particles could improve the dimensional stability of glass fibre reinforced polypropylene composites. The use of nanoclay in wood/natural fibre polymer composites to improve the properties also reported.<sup>4,5</sup> So far, little work has been done on the properties of glass fibre reinforced plastic composites with nanosilica particles in combination with coupling agents.

Novel classes of polymer nano-micro hybrid composites are proposed to be developed in this study by reinforcing HDPE with glass fibre and nanosilica. The salient features of the study are given below.

## **6a.2 EXPERIMENTAL**

The short glass fibre reinforced high density polyethylene composites were prepared in a Torque Rheometer (Thermo Haake Rheocord 600). The matrix was modified with maleic anhydride according to US patent, 4,753,997. The modification of HDPE-glass fibre (PE/GF) composite with silica/modified silica was also done in Torque Rheometer. 1 and 2wt.% of silica/modified silica were added during the preparation of HDPE-glass fibre composite to get the nano-micro hybrid composite. The mixing time of 8 minutes was used at a rotor speed of 50 rpm. The tensile properties, flexural properties, impact strength, dynamic mechanical analysis, thermal properties and crystallization properties are analyzed according to various standards as described in chapter 2.

## **6a.3 RESULTS AND DISCUSSION**

### **6a.3.1 High density polyethylene-glass fibre composite**

#### **6a.3.1.1 Torque studies**

The variation of mixing torque with time of mixing at different fibre loading is shown in figure 6a.1. It shows that 8 minutes mixing time was sufficient for the proper mixing of the ingredients. The temperature of the mixing chamber was fixed as 150 °C since the matrix properly melted and homogenized at this temperature under the shear employed. The torque-time behaviour of HDPE/glass fibre composite is similar to that of PP/glass fibre composite as expected. Here also there is no reduction in torque on continued

mixing up to 8 min. This implies that there is no appreciable degradation taking place during this time.

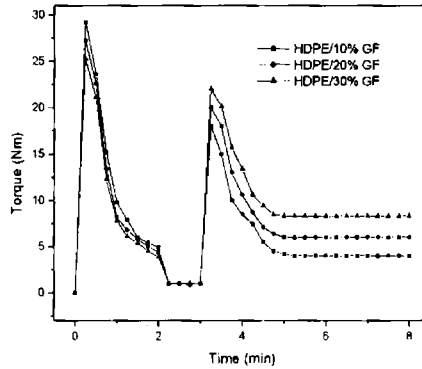


*Figure 6a.1: Torque – Time curves of HDPE composites*

### 6a.3.1.2 Tensile properties

#### a) Effect of fibre length

To study the effect of fibre length on tensile strength of the present system 10% fibre filled composites were prepared with different average fibre length of 2, 4, 6, 8 and 10 mm and the tensile strength of the composites were compared. The variation of tensile strength of the composites with fibre length is shown in figure 6a.2. Higher strength is observed for the composites prepared with a fibre length of 6 - 8 mm as in the case of glass fibre/PP composite. Hence 6 mm length was select for further studies

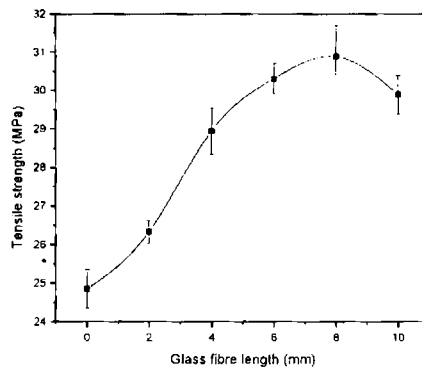


*Figure 6a.2 Variation of tensile strength with fibre length*

**b) Effect of fibre loading**

Figure 6a.3 shows the effect of variation of tensile strength and tensile modulus of HDPE/glass fibre composites with fibre loading. In this case the tensile strength increases with fibre loading up to 30% and decreases thereafter.

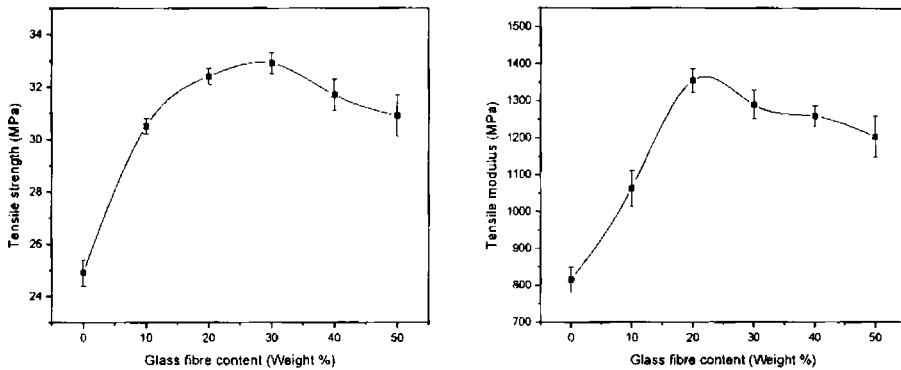


Figure 6a.3 Variation of tensile strength and modulus with fibre loading

**6a.3.1.3 Flexural properties**

**a) Effect of fibre length**

The effect of fibre length on the flexural strength is given in figure 6a.4. Flexural strength increases with increase in fibre length up to 6 mm. higher flexural strength is observed for the composites with fibre length 6-8 mm and then decreases. This result is in uniformity with the result obtained for PP/glass fibre composites.

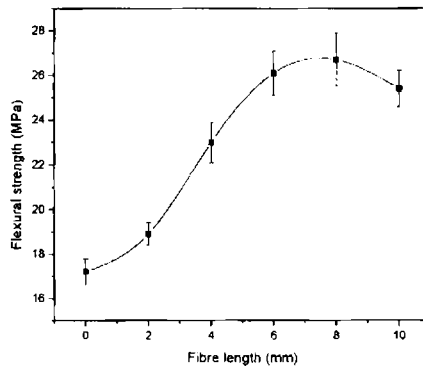


Figure 6a.4: Variation of flexural strength with fibre length

**b) Effect of fibre loading**

The effect of fibre loading on the flexural strength and flexural modulus of HDPE/glass fibre composites is shown in figures 6a.5. From the figures it is clear that both flexural strength and modulus increases with fibre content. The maximum modulus is observed at 30% fibre loading.

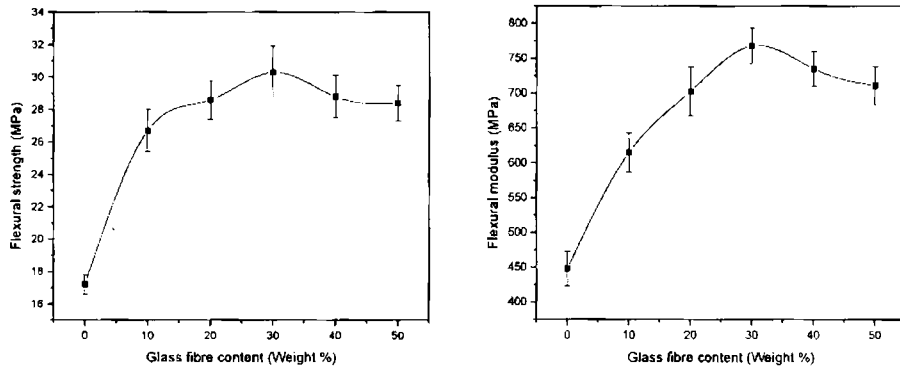


Figure 6a.5: Variation of flexural strength and modulus with fibre loading

**6a.3.2 Modification of HDPE-glass fibre composite with silica/modified silica**

**6a.3.2.1 Torque studies**

Figure 6a.6 shows the variation of torque with time of mixing of different filler loading. The temperature of the mixing chamber was kept at 150 °C. The torque values turn into steady during the 8 minutes of mixing time. The nano fillers added along with the matrix initially.

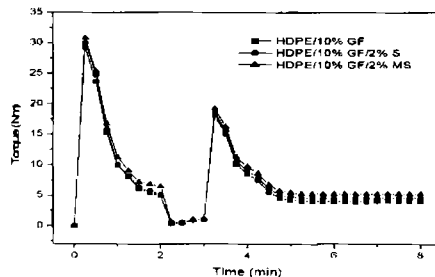


Figure 6a.6: Torque – Time curves of HDPE composites

From section 4b we conclude that the presence of 2wt.% nanosilica and modified nanosilica gives better performance for HDPE nano composites. Hence the properties of the 2wt.% nanosilica/ modified nanosilica reinforced composites are discussed in detail in this chapter. When the nano filler disperse well with the aid of fibres the stress will be transferred effectively from the matrix to the nano filler and fibre by a shear transfer mechanism. The maximum tensile strength of the composites (Figure 6a.2) is at 10 mm length of the fibre. Hence 10 mm length was taken as optimum fibre length for the hybrid composite fabrication.

### 6a.3.2.2 Tensile properties

Figure 6a.7 shows the effect of variation of tensile strength and tensile modulus of HDPE/glass fibre composites with fibre and silica/modified silica loading. The tensile strength increases with fibre loading up to 20% and decreases thereafter.

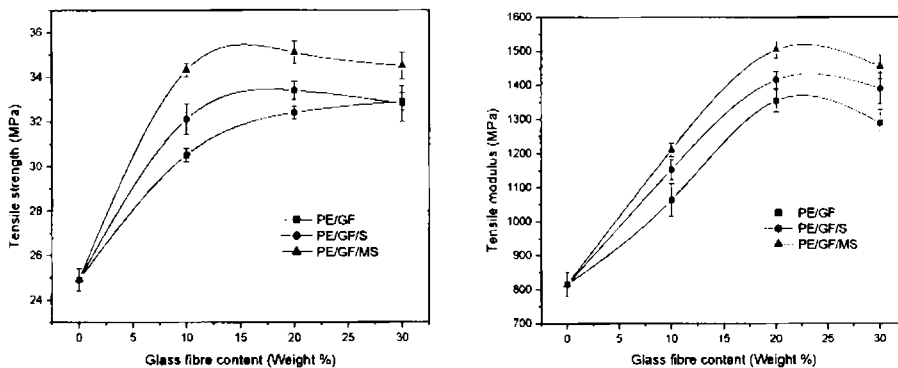


Figure 6a.7: Variation of tensile strength and modulus with fibre loading and silica content

### 6a.3.2.3 Flexural properties

Figures 6a.8 show the effect of nanofiller loading on the flexural strength and flexural modulus of HDPE/glass fibre composites. From the figures it is clear that both flexural strength and modulus increases with fibre as well as nanosilica content. The modulus is found to be higher at 30% fibre loading along with nano filler. The increase of modulus by the addition of nanosilica and modified nanosilica with 10 wt.% fibre loading is more prominent when compared to other combinations.

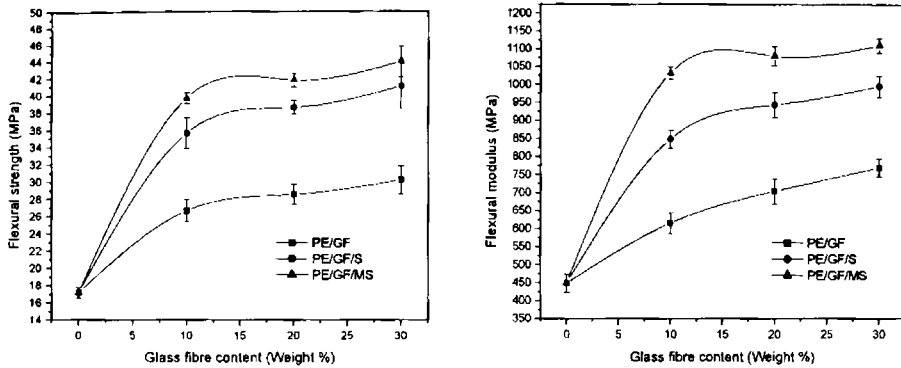


Figure 6a.8: Variation of flexural strength and flexural modulus with fibre loading and silica content

#### 6a.3.2.4 Impact strength

The effect of nanofiller loading on the impact strength of the glass fibre-HDPE composites are shown in figure 6a.9. The impact strength of HDPE/glass fibre composites improved by the presence of silica or modified silica. Significant improvement was observed for 10% glass fibre loaded hybrid composites and the higher fibre loaded composites show inferior properties. This is probably due to decrease in fibre-matrix-nanofiller interactions at higher fibre loadings by the crowding of fibres as discussed earlier.

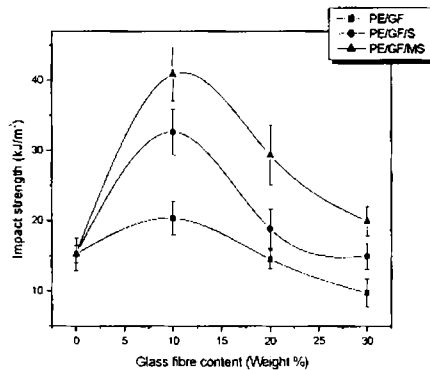


Figure 6a.9: Variation of impact strength with fibre loading and silica content

### 6a.3.3 Effect of matrix modification on hybrid composites of HDPE

The nonpolar HDPE matrix was grafted with polar monomer (maleic anhydride) to make it polar.<sup>6,7,8</sup> The polar nature of matrix may increase the interaction of matrix with polar filler.

#### 6a.3.3.1 Torque studies

A mixing time of 8 minutes was used for making modified hybrid composites since the torque values stabilized during this time. The variation of mixing torque with time of mixing at different stages of composite preparation is shown in figure 6a.10. The temperature of the mixing chamber was fixed as 150 °C as earlier.

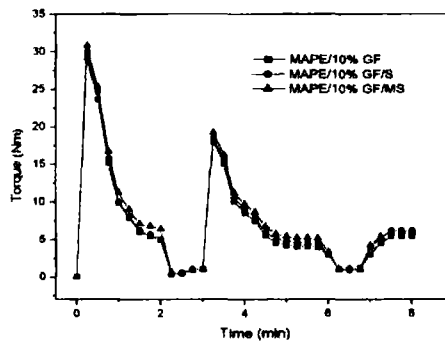


Figure 6a.10: Variation of mixing torque with time

#### 6a.3.3.2 Tensile properties

Figure 6a.11 shows the effect of variation of tensile strength and tensile modulus of glass fibre/HDPE composites with fibre and silica/modified silica loading. The tensile strength and modulus increases with fibre loading up to 20% thereafter level off or decreases. The decrease in strength at higher fibre loading may be due to the agglomeration of nanofiller by the crowding of fibres as expected. The improvement of properties is higher for MA grafted HDPE hybrid composites compared to the composites prepared from unmodified HDPE as in the case of PP/glass fibre composite. The improvement in the tensile strength and modulus of MA grafted HDPE hybrid composite at 10% fibre content and 2% modified silica is about 58% and 54% respectively when compared to neat HDPE.

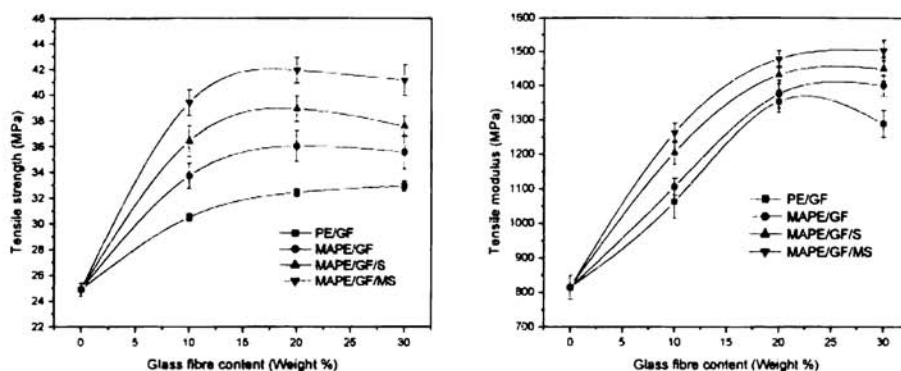


Figure 6a.11: Variation of tensile strength and modulus with fibre loading and silica content

The improvement of adhesion between the filler and MA treated matrix can be seen from the scanning electron micrographs (SEM) of the fractured surface of HDPE/glass fibre/silica hybrid nanocomposite and that of MA-g-HDPE/glass fibre/modified silica hybrid nanocomposites (Figures 6a.12 and 6a.13). The fractured surface of unmodified matrix shows holes and the fibre surface retain low amount of matrix indicating poor adhesion between the fibre and matrix while in the case of modified matrix, the fractured surface shows evidence for fibre breakage rather than pullout, and the fibre surface fully covered with matrix indicating better interfacial adhesion.

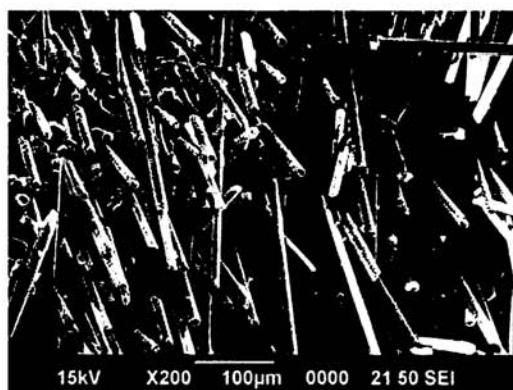


Figure 6a.12: SEM picture of the fracture surface of HDPE hybrid nanocomposite



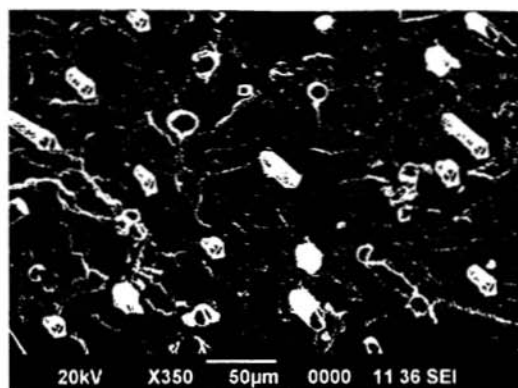


Figure 6a.13: SEM picture of the fracture surface of MA-g-HDPE hybrid nanocomposite

### 6a.3.3.3 Flexural properties

The flexural properties of the MA grafted HDPE hybrid composites are compared with those of HDPE/fibre composites in figure 6a.14. From the figures it is clear that both flexural strength and modulus increases with fibre as well as nanosilica content. There is a significant improvement in the flexural strength and modulus with 10% fibre loading and level off at higher fibre loading. About 129% improvement in flexural modulus is obtained for MAPE/GF/MS.

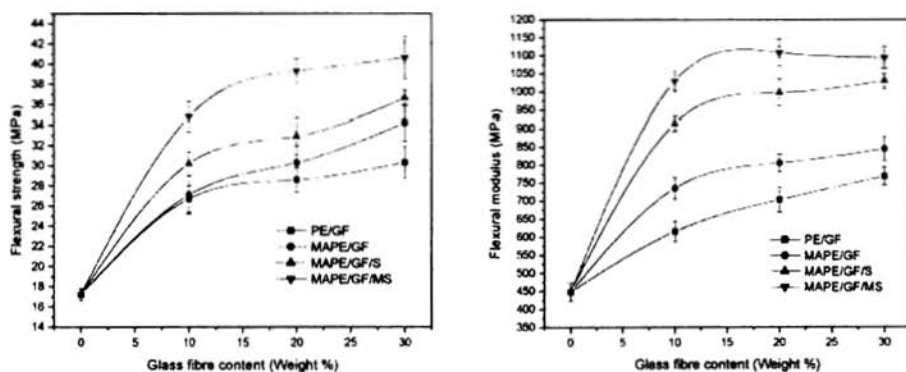


Figure 6a.14: Variation of flexural strength and modulus with fibre loading and silica content

### 6a.3.3.4 Impact strength

The impact strength of the HDPE/glass fibre composite is compared with MA-g-PE hybrid composites in figure 6a.15. Maleic anhydride grafting causes a significant improvement in impact strength at lower fibre content and at same loading (2%) of nano fillers. The polar nature of the matrix may increase the interaction with nano and micro fillers. At higher fibre loadings, the fibre crowding may limit the interaction of fibre with matrix and uniform dispersion of nano filler in the matrix, thus cause a decline in impact strength.

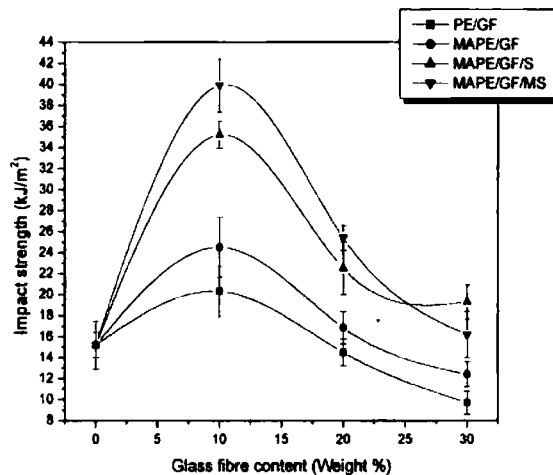


Figure 6a.15: Variation of impact strength with fibre loading and silica content

### 6a.3.4 Dynamic mechanical analysis

Figure 6a.16 illustrates the variation of storage modulus ( $E'$ ) of HDPE-glass fibre (10wt.%) - silica hybrid composites as a function of temperature. It is found that the storage modulus of the composites increased with the presence of nanosilica and modified nanosilica and it is more pronounced at low temperatures. The modified silica loading gives higher  $E'$  values for the hybrid composite at all temperatures

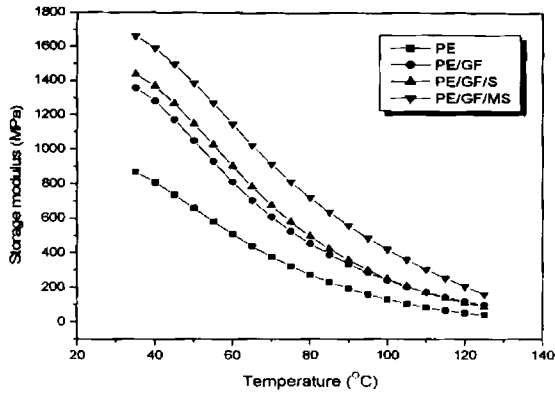


Figure 6a.16: Variation of storage modulus of HDPE/glass fibre-silica hybrid composites with temperature

Figure 6a.17 illustrates the variation of  $E'$  by the presence of silica or modified silica on MA-g-HDPE/10wt.% glass fibre as a function of temperature. Here also it is found that the storage modulus of the composites increased with the presence of nanosilica/modified silica. When compared with nanosilica filled composite, the composite containing modified nanosilica showed low  $E'$  values at lower temperatures and similar  $E'$  values at higher temperatures. The decrease in modulus at higher temperature is associated with the chain mobility of the matrix<sup>9</sup> and the thermal expansion occurring in the matrix resulting in reduced intermolecular forces.<sup>10</sup>

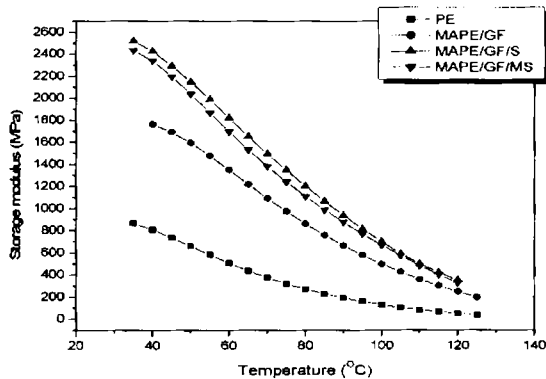


Figure 6a.17: Variation of storage modulus of MA-g-HDPE-Glass fibre-silica hybrid composites with temperature

Table 6a.1 shows the storage modulus and relative (normalized) storage modulus ( $E'_c/E'_m$  where  $E'_c$  and  $E'_m$  are the storage moduli of composite and matrix respectively) values of nano-micro hybrid composites at temperatures 40, 80 and 120 °C.

**Table 6a.1:** Variation of storage modulus and normalized storage modulus of HDPE/glass short fibre composites with nanosilica/modified nanosilica at 40, 80 and 120 °C

Sample	Storage modulus (MPa)			Normalized storage modulus		
	40 °C	80 °C	120 °C	40 °C	80 °C	120 °C
PE	781.2	286.3	63.49	1	1	1
PE/GF	1281	453.3	119.3	1.62	1.58	1.88
PE/GF/S	1367	496.5	110.9	1.75	1.73	1.75
PE/GF/MS	1590	719.9	205.8	2.04	2.51	3.25
MAPE/GF	1694	762.8	249.3	2.17	2.66	3.93
MAPE/GF/S	2426	1206	352.7	3.11	4.21	5.56
MAPE/GF/MS	2340	1113	328.8	2.99	3.89	5.18

The storage modulus and the normalized storage modulus of the composites increased with the presence of silica/modified nanosilica at all temperatures. The normalized modulus values at 40 °C and 80 °C do not show considerable variation, but at 120 °C high normalized modulus values are obtained by maleic anhydride grafting, compared to the pure polymer.

The variation of  $\tan \delta$  of HDPE/glass fibre and MA-g-HDPE-Glass fibre composites with nano filler loading, as a function of temperatures is shown in figure 6a.18 and 6a.19 respectively. Incorporation of stiff fibres and nanofiller reduces the  $\tan \delta$  peak of the composite by restricting the movement of polymer molecules and also due to the reduction in the viscoelastic lag between the stress and the strain.<sup>11,12</sup> The  $\tan \delta$  values were lowered in the composites compared to the pure polymer may also because of the less matrix by volume to dissipate the vibrational energy. The figures indicate that the relatively high viscoelastic damping character ( $\tan \delta$  value) for the pure polymer becomes lowered on reinforcement with nano-micro hybrid. The height of  $\tan \delta$  peaks of the

composites is also lowered with maleic anhydride grafting. The lowering of the  $\tan \delta$  peak height is a measure of enhanced interfacial bond strength and adhesion between the fillers and the matrix.

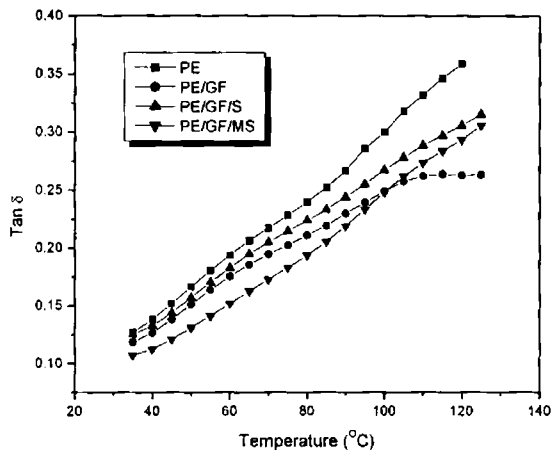


Figure 6a.18: Temperature dependence of  $\tan \delta$  values of HDPE/glass short fibre composites with nanosilica/modified nanosilica

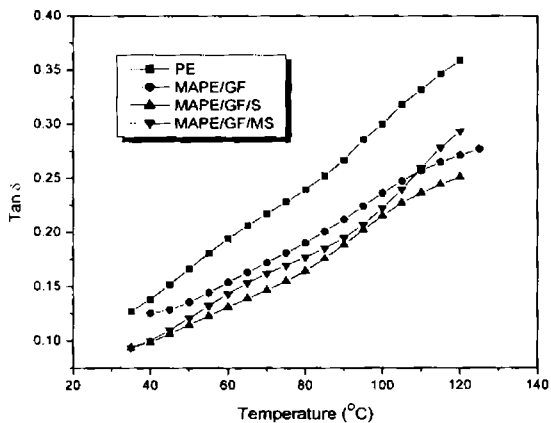


Figure 6a.19: Temperature dependence of  $\tan \delta$  values of MA-g-HDPE/glass short fibre composites with nanosilica/modified nanosilica

### 6a.3.5 Crystallization characteristics

The presence of fillers usually affects the crystallization behaviour of a polymer. Differential Scanning Calorimetry (DSC) is the widely accepted technique to study the crystallization and thermal behaviour of polymer.

#### 6a.3.5.1 Non-isothermal Crystallization

The effect of glass fibre and glass fibre-nano hybrid fillers on the crystallization characteristics of melt compounded HDPE composite samples was analyzed first with non-isothermal DSC experiments. The crystallization temperatures ( $T_c$ ), the apparent melting temperatures ( $T_m$ ) and the corresponding enthalpies ( $\Delta H_c$  and  $\Delta H_m$ ) for all the samples are reported in table 6a.2.

*Table 6a.2 Thermal characteristics of nano-micro hybrid composites*

Sample	$T_c$ (°C)	$\Delta H_c$ (J/g)	$T_m$ (°C)	$\Delta H_m$ (J/g)
PE	115	193.3	131.9	172.7
PE/GF	115.9	186.3	133.9	171
PE/GF/S	116	185.8	132.1	170.2
PE/GF/MS	118	188.9	128.5	171.5
MAPE/GF/S	118.3	186.8	130.5	170
MAPE/GF/MS	117.8	187.2	129.4	170.4

Figure 6a.20 shows the DSC cooling scans of HDPE and Glass fibre/silica/modified silica composite samples with HDPE and MA-g-HDPE. During cooling from the melt, the hybrid composite samples show crystallization exotherms little earlier than pure HDPE, as seen from the corresponding  $T_c$  values indicated in table 6a.2.

The  $T_c$  values show a small increment with silica and modified silica addition in HDPE-glass fibre composites. MA grafting does not show a noticeable increment for the  $T_c$  value. It is found that the hybrid nanocomposite sample prepared with MA grafted HDPE crystallizes about 3 °C earlier than pure HDPE. This indicates that grafting increases the interaction of matrix with filler and thus the hybrid filler can act as nucleating agent for HDPE crystallization.

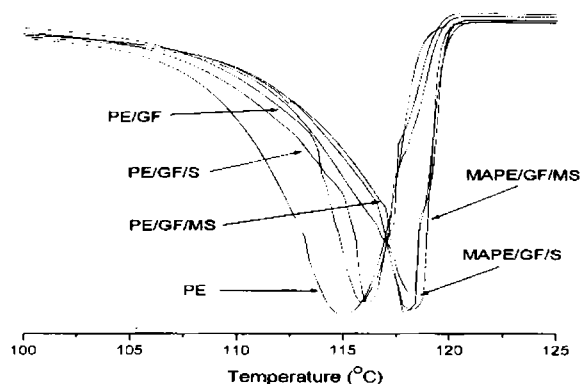


Figure 6a.20: DSC cooling scans ( $10\text{ }^{\circ}\text{C}/\text{min}$  from  $180\text{ }^{\circ}\text{C}$  melt) of hybrid composites

Smaller the degree of supercooling ( $\Delta T = T_m - T_c$ ), higher will be the crystallizability. The  $\Delta T$  values of hybrid nanocomposites given in table 6a.3 are smaller by  $\sim 0.8$  to  $7\text{ }^{\circ}\text{C}$  than that of pure HDPE. This reveals that the crystallizability of the nanocomposites is little better than that of pure HDPE.

Table 6a.3:  $\Delta T$  values of HDPE and HDPE composites

Sample	$\Delta T$ ( $^{\circ}\text{C}$ )
PE	16.9
PE/GF	18
PE/GF/S	16.1
PE/GF/MS	10.5
MAPE/GF/S	12.2
MAPE/GF/MS	11.6

### 6a.3.5.2 Isothermal crystallization

Figure 6a.21 shows the typical isothermal crystallization curves of pure HDPE and HDPE composites at five temperatures ( $110$ ,  $115$ ,  $120$  and  $122\text{ }^{\circ}\text{C}$ ). The time corresponding to the maximum in the heat flow rate (exotherm) is taken as peak time of crystallization ( $t_{\text{peak}}$ ). In the case of pure HDPE, no peak is seen at highest temperature of  $122\text{ }^{\circ}\text{C}$  because crystallization is very slow and would require longer time than the 4

minutes employed in the DSC program. On the other hand, for the hybrid composite samples, the rate of crystallization is so fast near the lowest temperatures that most of the crystallization occurs already during the cooling scan (60 °C/min) employed to reach the temperatures (110 or 115 °C). This results in absence of exothermic peaks in the heat flow curves at those temperatures.

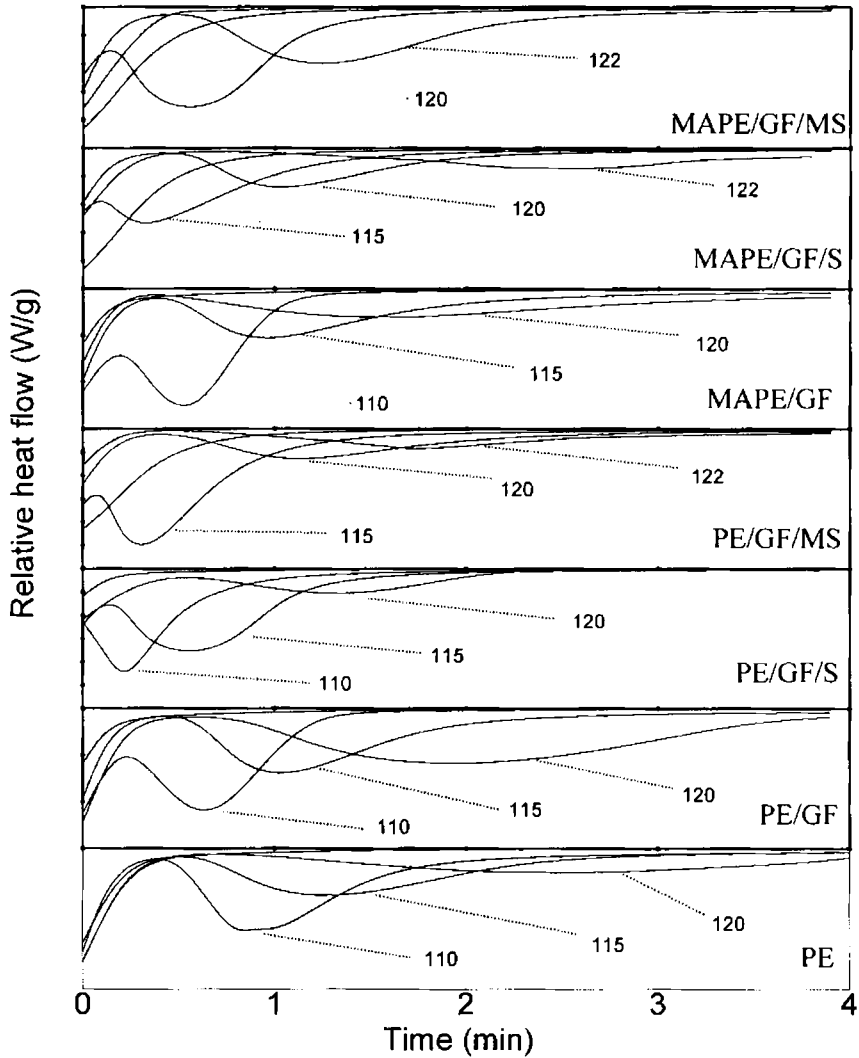
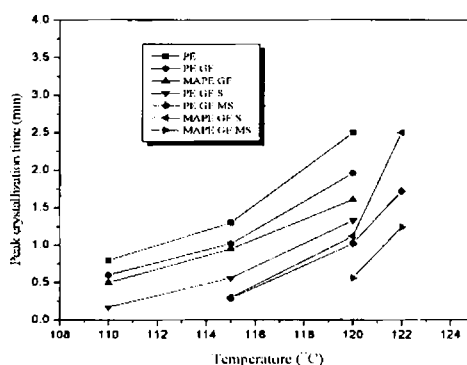


Figure 6a.21: Heat flow during isothermal crystallization of HDPE composites



The peak time of crystallization at each of the temperatures for all hybrid nanocomposite samples are plotted against the isothermal crystallization temperature (Figure 6a.22). It is noticeable that the  $t_{\text{peak}}$  values of the composite samples reduced to less than 40% as compared to pure HDPE due to the presence nano-micro hybrid fillers. With the modified silica and MA grafting there is increase in the crystallization rate (as indicated by the decrease in  $t_{\text{peak}}$ ), demonstrating the role of modification on the surface of silica and polymer backbone for enhancing the matrix-filler interaction and thus enhancing the rate of crystallization.



*Figure 6a.22: Effect of hybrid filler and matrix grafting on the peak crystallization time of the composites at different isothermal crystallization temperature*

### 6a.3.6 Thermogravimetric analysis

The thermal degradation pattern of HDPE and its composites in nitrogen atmosphere are shown in figures 6a.23 and 6a.24. The temperature of onset of degradation ( $T_i$ ), temperature at which maximum degradation occur ( $T_{\text{max}}$ ) and the residue obtained at 600 °C are given in table 6a.4.

HDPE shows degradation in a single step. It is stable up to 365 °C thereafter sharp weight loss occurs till 520 °C. Glass fibre and silica are thermally stable above 1000 °C. So the hybrid composite samples show single stage degradation pattern. The presence of nano-micro hybrid filler amplified the thermal stability of HDPE. The  $T_{\text{max}}$  of HDPE improved from 476 °C to 491 °C for HDPE hybrid composite. This improvement in thermal stability of the composites may result from the presence of thermally stable inorganic fillers and their good dispersion in the matrix. Improved thermal stability of

polymers in presence of fillers is due to the hindered thermal motion of polymer molecular chains.<sup>13</sup>

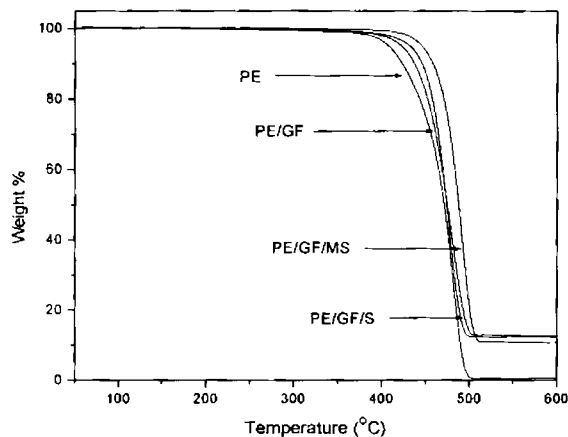


Figure 6a.23: Thermogravimetric traces of HDPE and HDPE hybrid composite

Table 6a.4: Degradation characteristics of HDPE and hybrid composites

Sample	Onset temp. (°C)	Peak max ( $T_{max}$ )	Residue at 600°C
PE	362.6	476	0.51
PE/GF	452.3	476.91	10.85
PE/GF/S	447.47	478.25	12.63
PE/GF/MS	468.32	491.78	12.15
MAPE/GF	468.37	489.36	11.02
MAPE /GF/S	469.7	491.79	13.07
MAPE /GF/MS	467.38	490.87	12.03

$T_{max}$  does not show much variation for the MA grafted hybrid nanocomposites. The MA grafting is not affect the thermal stability of the hybrid composites.

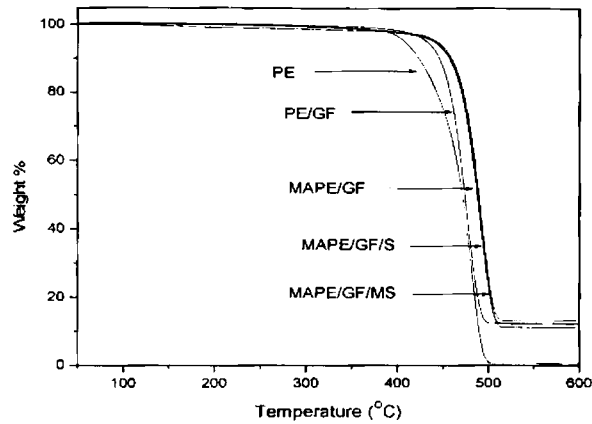


Figure 6a.24: Thermogravimetric traces of HDPE and MA-g-HDPE hybrid composite

## 6a.4 CONCLUSIONS

The study shows that nanosilica and modified nanosilica can upgrade HDPE-glass fibre composites and the following conclusions can be drawn.

- Nanofiller additions at low concentrations can improve the performance of HDPE short fibre composites.
- Nanofillers with 10% fibre show good mechanical properties for the HDPE hybrid composites.
- Storage modulus increases with the presence of hybrid fillers and maleic anhydride grafting.
- The hybrid fillers have not much effect on crystallization temperature of HDPE.
- Thermal stability of composites is enhanced by the addition of hybrid fillers.

## REFERENCES

1. D.Sujit; *The cost of automotive polymer composites: a review and assessment of doe's lightweight materials composites research*, ORNL/TM-2000/283.
2. (a) K.Yano, A.Usuki, A.Okada, T.Kurauchi, O.Kamigaito; *J.Polym.Sci.Part A:Polym.Chem.*, **1993**, 31(10), 2493.  
(b) J.Li, C.X.Zhou, G.Wang, W.Yu, Y.Tao; *Polym.Compos.* **2003**, 24(3), 323.  
(c) Y.Wang, F.B.Chen, K.C.Wu; *Compos.Interfaces.* **2005**, 12(3), 341.  
(d) T.P.Mohan, M.R.Kumar, R.Velmurugan; *J.Mater.Sci.*, **2006**, 41, 5915.  
(e) Q.Y.Kong, H.L.Hu, Z.Chen, W.Fan; *J.Mater.Sci.* **2005**, 40(17), 4505.
3. L.A.Canova, L.W.Ferguson, L.M.Parrinello, R.Subramanian, H.F.Giles; *Effect of combinations of fibre glass and mica on the physical properties and dimensional stability of injection molded polypropylene composites*, **1997**, The 55th annual technical conference of Society of Plastics Engineers (SPE), Toronto, Canada, 2112.
4. Y.Lei, Q.Wu, C.Clemons, F.Yao, Y.Xu; *J.Appl.Polym.Sci.* **2007**, 103, 3056.
5. G.Han, Y.Lei, Q.Wu, Y.Kojima, S.Suzuki; *J.Polym.EnvIRON.* **2008**, 94, 7.
6. W.Y.Chiang, W.D.Yang; *J.Appl.Polym.Sci.* **1988**, 35, 807.
7. K.H.Rao, K.S.E.Forsberg, W.Forsling; *Physico.Chem. Engng.Aspects.* **1998**, 58, 747.
8. S.N.Maiti, K.K.Sahrma; *J.Mater.Sci.* **1992**, 27, 4605.
9. P.V.Joseph, G.Mathew, K.Joseph, G.Groeninckx, S.Thomas; *Comp. Part A* **2003**, 34, 275.
10. J.George, S.S.Bhagavan, S.Thomas; *J. Thermoplastic Comp. Mat.* **1999**, 12, 443.
11. D.Ray, B.K.Sarkar, S.Das, A.K.Rana; *Comp.Sci.Technol.* **2002**, 62, 911.

12. A.K.Saha, S.Das, D.Bhatta, B.C.Mitra; *J.Appl.Polym.Sci.* **1999**, 71, 1505.
13. J.W.Gilman; *Appl.Clay.Sci.* **1999**, 15, 31.

## **High density polyethylene-nylon fibre-silica hybrid nanocomposites**

### **6b.1 INTRODUCTION**

Fibre reinforced polymer composite materials have been widely used in many structural applications such as aerospace, automotive, civil and marine structures due to their excellent strength-to-weight ratio, chemical and weather resistances, tailor-able mechanical, thermal and electrical properties. The conventional micro-fibre reinforced polymer composite usually consists of polymer as the matrix system and micro-fibres with diameter of 5-30 $\mu$ m as the reinforcement system. The reinforcement of polymers using nano fillers such as silica, clay, carbon nanotube etc. is also widely practised these days. The dispersion of nanoparticles is a critical factor in the development of such nanocomposites. High-density polyethylene (HDPE) due to its lightness, mechanical properties, cheapness and availability is used for making various products.<sup>1</sup> All polymer composites like nylon reinforced HDPE has the additional advantage of recyclability.<sup>2</sup> In most of the cases fibre reinforced composites require fairly high fibre loading to get the desired property.<sup>3,4</sup> A composite with improved properties at low filler loading is always the optimum choice. Hence hybrid composites based on particulate fillers, fibre and plastic matrices are yet to be investigated in detail.

Development of polyethylene based composites for improving the mechanical properties is the topic of this study. The reinforcing effects of nanosilica and modified nanosilica on HDPE-nylon fibre composite is also proposed to be studied at different loading levels of nylon fibre and nanosilica/modified nanosilica powder.

### **6b.2 EXPERIMENTAL**

The short nylon fibre reinforced high density polyethylene composites were prepared in a Torque Rheometer (Thermo Haake Rheocord 600). The modification of HDPE-nylon fibre composite with silica/modified silica was also done by melt mixing in

Torque Rheometer. 1 and 2wt.% of silica/modified silica were added during the preparation of HDPE-nylon fibre composite to get the nano-micro hybrid composite. The modification of hybrid nanocomposite was done by maleic anhydride (MA) grafting. The mixing time of 8 minutes was used at a rotor speed of 50 rpm. The mixing chamber was kept at 150 °C. In all cases the torque stabilized to a constant torque in this time. The tensile properties, flexural properties, impact strength, dynamic mechanical analysis, thermal properties and crystallization properties were analyzed according to various standards as described in chapter 2.

## 6b.3 RESULTS AND DISCUSSION

### 6b.3.1 High density polyethylene-nylon fibre composites

#### 6b.3.1.1 Torque studies

The variation of mixing torque with time of mixing at different fibre loading is shown in figure 6b.1. A mixing time of 8 minutes was fixed as earlier since the torque stabilized to a constant value during this time. The temperature of the mixing chamber was fixed as 150 °C since the matrix properly melted and homogenized at this temperature under the shear employed. The torque-time behaviour of HDPE/nylon fibre composites is similar to that of PP/nylon fibre composites. Here also there is no reduction in torque on continued mixing up to 8 min. This suggests that there is no appreciable degradation taking place during this time.

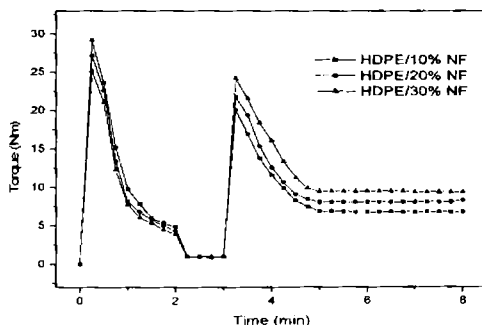
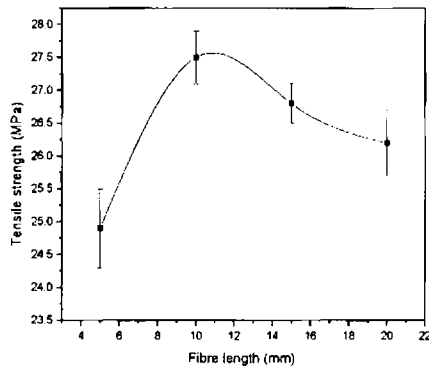


Figure 6b.1 Torque - Time curves of HDPE composites

### **6b.3.1.2 Tensile properties**

#### **a) Effect of fibre length**

To study the effect of fibre length on the tensile strength of the system, 10% fibre filled composites were prepared with different average fibre length of 5, 10, 15 and 20mm and the tensile strength of the composites were compared. The variation of tensile strength of the composites with fibre length is shown in figure 6b.2. The maximum strength is observed for the composites prepared with a fibre length of 10 mm as in the case of PP/nylon fibre composite.



*Figure 6b.2 Variation of tensile strength with fibre length*

#### **b) Effect of fibre loading**

Figure 6b.3 shows the variation of tensile strength and tensile modulus of HDPE/nylon fibre composites with fibre loading. The tensile strength increases with fibre loading up to 30% and decreases thereafter.



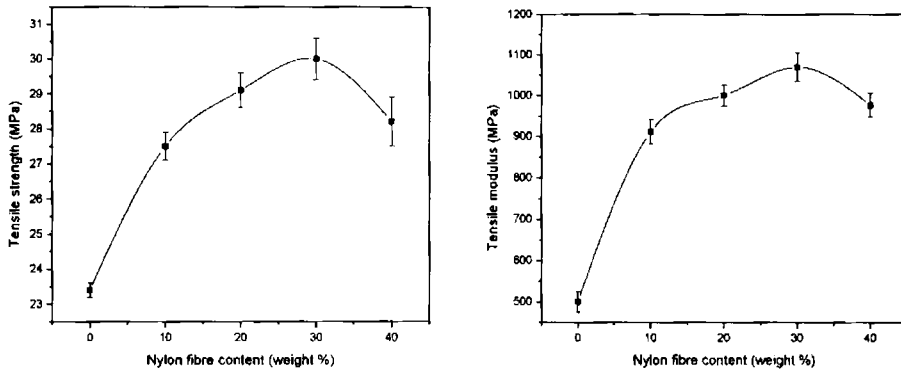


Figure 6b.3 Variation of tensile strength and modulus with fibre loading

### 6b.3.1.3 Flexural properties

#### a) Effect of fibre length

The effect of fibre length on the flexural strength is given in figure 6b.4. Flexural strength increases with increase in fibre length up to 10 mm and thereafter decreases.

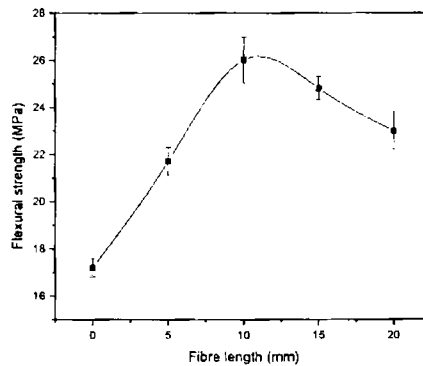


Figure 6b.4: Variation of flexural strength with fibre length

### b) Effect of fibre loading

Figure 6b.5 shows the effect of fibre loading on the flexural strength and flexural modulus of HDPE/nylon fibre composites. From the figure it is clear that both flexural strength and modulus increases with fibre content. The maximum modulus is observed at 30% fibre loading.

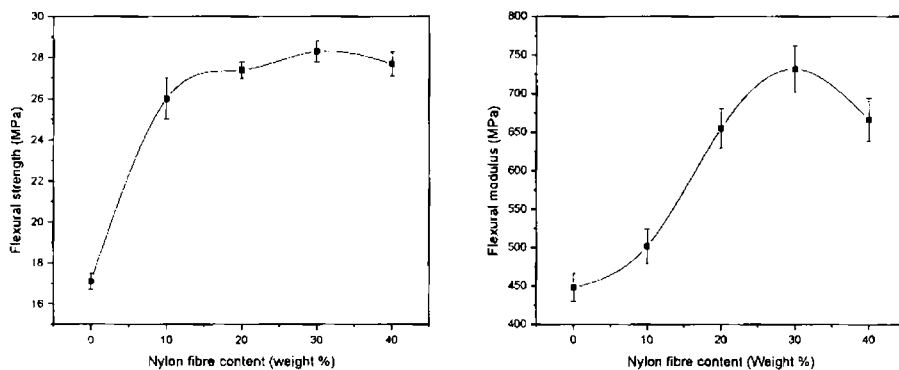


Figure 6b.5: Variation of flexural strength and modulus with fibre loading

### 6b.3.2 Modification of HDPE-nylon fibre composite with silica/modified silica

Good tensile and flexural properties for HDPE-nylon fibre composites were observed at 10 mm length of the fibre. Hence 10 $\times$ 2 mm length was taken as fibre length to make hybrid composites.

#### 6b.3.2.1 Torque studies

The variation of mixing torque with time of mixing at different filler loading is shown in figure 6b.6. The mixing time of 8 minutes was fixed since the torque stabilized to a steady value. The temperature of the mixing chamber was kept at 150 °C. The nano filler additions have not much effect the initial and final torque values.

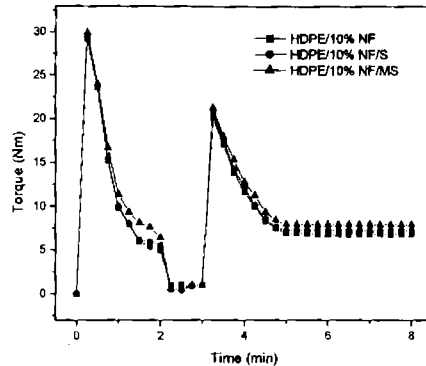


Figure 6b.6: Torque – Time curves of HDPE composites

To study the effect of nanosilica/modified nanosilica on the properties of HDPE/nylon fibre composites, 1 and 2 wt.% of nanofillers filled HDPE/nylon fibre composites were prepared. The composites with 2 wt.% nanosilica and modified nanosilica showed better performance. Hence the properties of 2 wt.% nanosilica/modified nanosilica reinforced hybrid nanocomposites are discussed in detail.

### 6b.3.2.2 Tensile properties

Figure 6b.7 shows the variation of tensile strength and tensile modulus of HDPE/nylon fibre composites with fibre and silica/modified silica loading. The presence of silica/modified silica increases the tensile strength of the hybrid composites. This shows that the presence of nanofiller inside the composite positively interact with the micro filler and matrix.

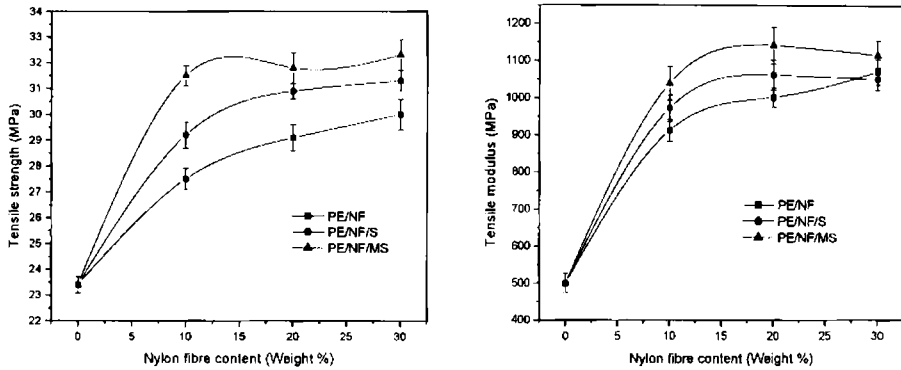


Figure 6b.7: Variation of tensile strength with fibre loading and silica content

### 6b.3.2.3 Flexural properties

Figure 6b.8 shows the effect of nanofiller loading on the flexural strength and flexural modulus of HDPE/nylon fibre composites. From the figure it is clear that both flexural strength and modulus increases with fibre as well as nanosilica content. Here also the presence of nano filler shows constructive result. The improvement in properties is more pronounced at 10% fibre content.

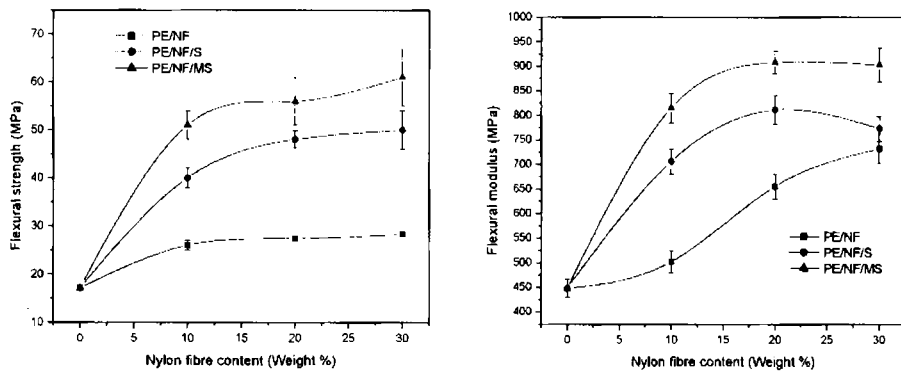


Figure 6b.8: Variation of flexural strength with fibre loading and silica content

### 6b.3.2.4 Impact strength

Figure 6b.9 shows the effect of nanofiller loading on the impact strength of HDPE/nylon fibre composites. The figure shows that the impact strength improves at 10% fibre loading and thereafter it decreases with fibre loading. The nano filler addition also follows the same trend but it improves the strength at all fibre loadings.

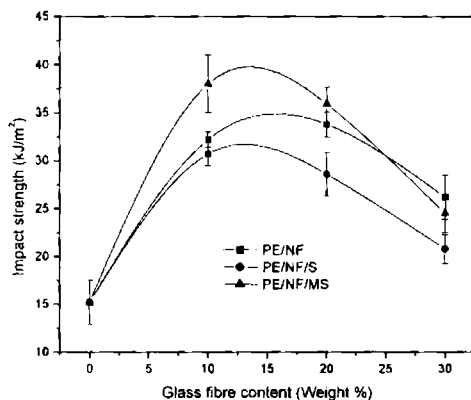


Figure 6b.9: Variation of impact strength with fibre loading and silica content

### 6b.3.3 Effect of matrix modification on nano-micro hybrid composites of HDPE

The nonpolar HDPE matrix was grafted with polar monomer (maleic anhydride) to make it polar. During the grafting nano and micro reinforcements added with the matrix to get hybrid composite as in section 6a. The nanofiller additions kept constant as 2%.

#### 6b.3.3.1 Torque studies

The variation of mixing torque with time of mixing at different fibre loading is shown in figure 6b.10. The mixing time of 8 minutes set as earlier since the torque stabilized to constant value during this time. The temperature of the mixing chamber was fixed as 150°C.

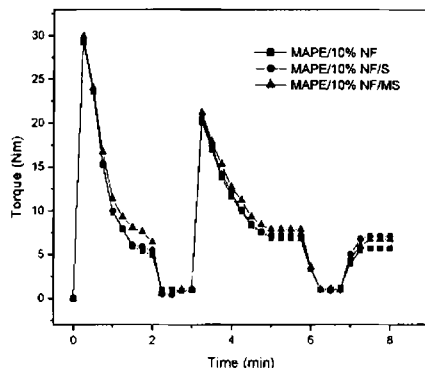


Figure 6b.10: Variation of mixing torque with time

### 6b.3.3.2 Tensile properties

The effect of chemical treatment on the tensile properties of HDPE/nylon fibre composite is described in the reference.<sup>2</sup> Figure 6b.11 shows the effect of chemical treatment on HDPE/nylon fibre/silica hybrid composites. It is observed that there is a significant improvement in tensile modulus for MA grafted HDPE hybrid nanocomposites compared to the composites prepared from pure HDPE.

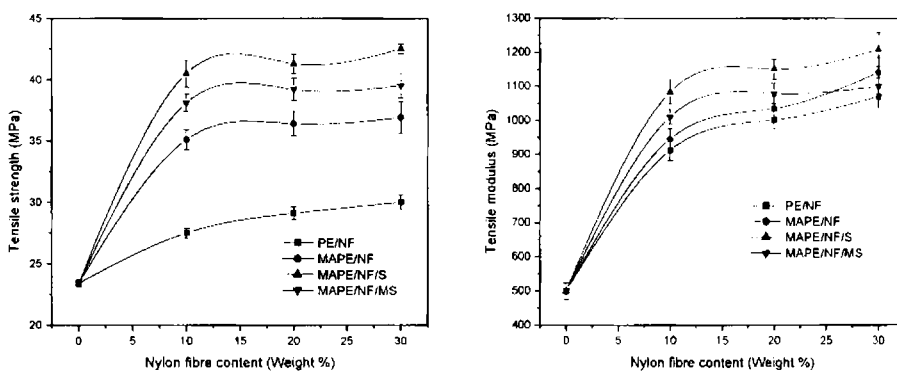


Figure 6b.11: Variation of tensile strength and modulus with fibre loading and silica content

### 6b.3.3.3 Flexural properties

The flexural properties of the HDPE hybrid composites are compared with those of chemical treated HDPE hybrid composites in figure 6b.12. A noticeable improvement in flexural properties is observed for the composites with 10% fibre loading. From the figure it is clear that both flexural strength and modulus increases with fibre as well as nanosilica content.

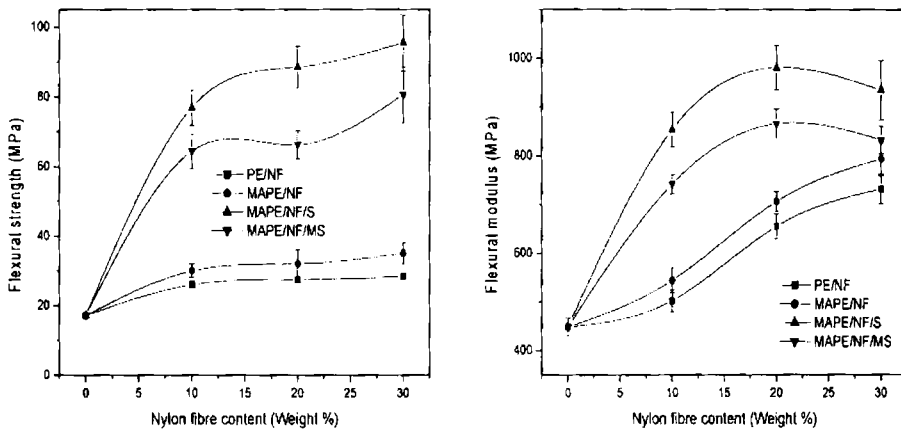


Figure 6b.12: Variation of flexural strength and modulus with fibre loading and silica content

### 6b.3.3.4 Impact strength

The impact strength of the nano-micro hybrid composites of HDPE are compared with MA treated HDPE hybrid composites in figure 6b.13. The figure shows that the impact strength is improved at 10% fibre loading and thereafter decreases with fibre loading. The hybrid composite also shows the same trend, but the impact strength is improved than the fibre composites.

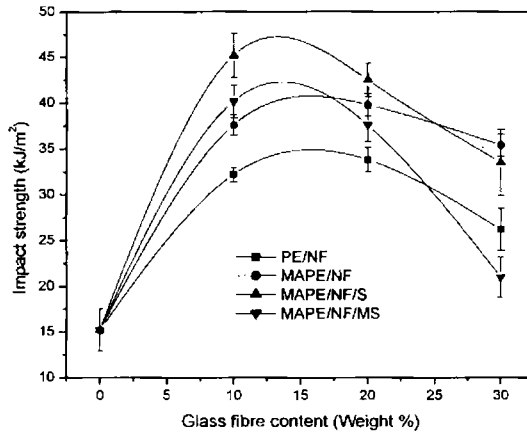


Figure 6b.13: Variation of impact strength with fibre loading and silica content

### 6b.3.4 Dynamic mechanical analysis

Figure 6b.14 illustrates the variation of storage modulus ( $E'$ ) with the addition of 2wt.% silica and modified silica on HDPE/nylon fibre (10wt.%) as a function of temperature. It is found that the storage modulus of the composites is increased with the presence of nanosilica and modified nanosilica and it is more pronounced at low temperatures.

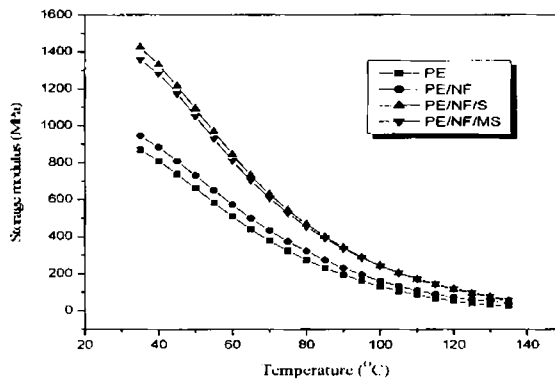


Figure 6b.14: Variation of storage modulus of HDPE/nylon fibre-silica hybrid composites with temperature



Figure 6b.15 illustrates the variation of  $E'$  with the addition of 2wt.% silica or modified silica on MA-g-HDPE/nylon fibre (10wt.%) as a function of temperature. Here also it is found that the storage modulus of the composites is increased with the presence of nanosilica/modified. When compared with nanosilica filled composite, the composite containing modified nanosilica showed low  $E'$  values at lower temperatures and high  $E'$  values at higher temperatures. This indicates that the grafted samples show higher interaction only at higher temperatures. The decrease in modulus at higher temperature is associated with the chain mobility of the matrix<sup>5</sup> and the thermal expansion occurring in the matrix resulting in reduced intermolecular forces.<sup>6</sup>

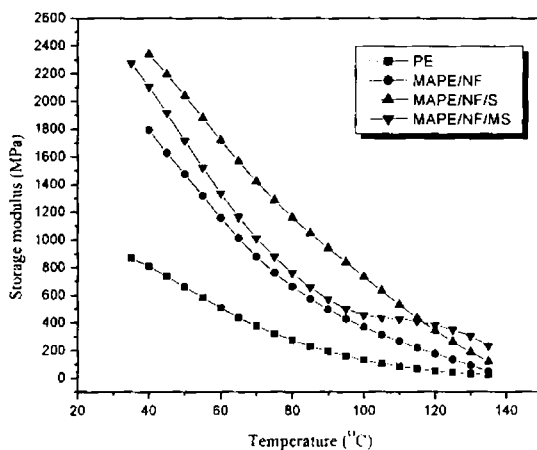


Figure 6b.15: Variation of storage modulus of MA-g-HDPE/nylon fibre-silica hybrid composites with temperature

Table 6b.1 shows the storage modulus and relative (normalized) storage modulus ( $E'_c/E'_m$  where  $E'_c$  and  $E'_m$  are the storage moduli of composite and matrix respectively) values of nano-micro hybrid composites at temperatures 40, 80 and 120 °C.

**Table 6b.1.** Variation of storage modulus and normalized storage modulus of HDPE and HDPE hybrid nanocomposites at 40, 80 and 120 °C

Sample	Storage modulus (MPa)			Normalized storage modulus		
	40 °C	80 °C	120 °C	40 °C	80 °C	120 °C
PE	781.2	286.3	63.49	1	1	1
PE/NF	882.2	320.2	72	1.13	1.12	1.13
PE/NF/S	1328	467.6	114.7	1.69	1.632	1.81
PE/NF/MS	1281	453.3	119.3	1.64	1.58	1.88
MAPE/NF	1792	661.4	176.2	2.29	2.31	2.78
MAPE/NF/S	2339	1161	343.3	2.99	4.06	5.41
MAPE/NF/MS	2107	760.7	385	2.69	2.66	6.06

The storage modulus and the normalized storage modulus of the hybrid composites increased with the presence of silica/modified nanosilica at all temperatures. MA-g-HDPE hybrid composite containing modified silica showed higher modulus only at higher temperature. The normalized modulus values at 40 °C and 80 °C do not showed considerable variation, but at 120 °C high normalized modulus values are obtained by maleic anhydride grafting, compared to the pure polymer.

The variation of  $\tan \delta$  of HDPE/nylon fibre and MA-g-HDPE/nylon fibre composites with nano filler loading, as a function of temperatures is shown in figure 6b.16 and 6b.17 respectively. Incorporation of stiff fibres and nanofiller reduces the  $\tan \delta$  value of the composite by restricting the movement of polymer molecules and also due to the reduction of viscoelastic lag between the stress and strain.<sup>7,8</sup> The  $\tan \delta$  values were lowered in the composites compared to the pure polymer may also because of the less matrix by volume to dissipate the vibrational energy. The figures indicate that the relatively high viscoelastic damping character ( $\tan \delta$  value) for the pure polymer becomes lowered on reinforcement with nano-micro hybrid. The lowering of the  $\tan \delta$  value is a measure of enhanced interfacial bond strength and adhesion between the fillers and matrix.

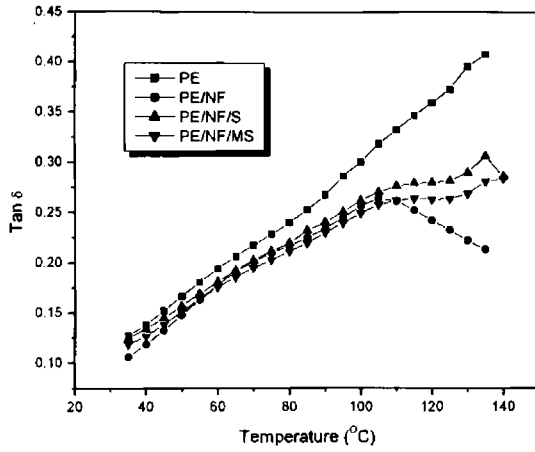


Figure 6b.16: Temperature dependence of  $\tan \delta$  values of HDPE/nylon short fibre composites with nanosilica/modified nanosilica

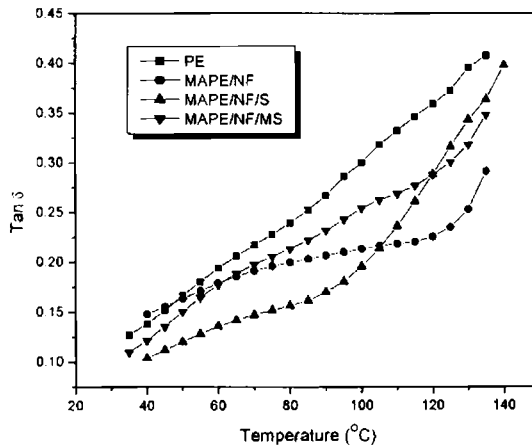


Figure 6b.17: Temperature dependence of  $\tan \delta$  values of MA-g-HDPE/nylon short fibre composites with nanosilica/modified nanosilica

### 6b.3.5 Crystallization characteristics

The presence of fillers usually affects the crystallization behaviour of a polymer. The crystallization may have major influence on the structure of composites and thereby on the mechanical properties. Hence it is very important to study the crystallization kinetics of composites which determines the final properties of a polymeric product. Differential Scanning Calorimetry (DSC) is the widely accepted technique to study the crystallization and thermal behaviour of polymer.

#### 6b.3.5.1 Non-isothermal Crystallization

The effect of hybrid fillers on the crystallization characteristics of melt compounded HDPE/nylon fibre-silica/modified silica nanocomposite samples were analyzed first with non-isothermal DSC experiments. The crystallization temperatures ( $T_c$ ), the apparent melting temperatures ( $T_m$ ) and the corresponding enthalpies ( $\Delta H_c$  and  $\Delta H_m$ ) for all the samples are reported in table 6b.2.

*Table 6b.2 Thermal characteristics of nano-micro hybrid composites*

Sample	$T_c$ (°C)	$\Delta H_c$ (J/g)	$T_m$ (°C)	$\Delta H_m$ (J/g)
PE	115	193.3	131.9	172.7
PE/NF	115.3	193.1	132.1	183.1
PE/NF/S	114.9	188.2	129.1	171.1
PE/NF/MS	115.6	187.2	128.9	171.8
MAPE/NF	115.7	186.5	128.1	168.1
MAPE/NF/S	118.1	189.1	129.3	170.5
MAPE/NF/MS	117.5	188.3	128.6	168.1

Figure 6b.18 shows the DSC cooling scans of HDPE, HDPE hybrid nanocomposites and MA-g-HDPE hybrid nanocomposites. During cooling from the melt,

the hybrid composite samples show crystallization exotherms earlier than pure HDPE, as also seen from the corresponding  $T_c$  values indicated in table 6b.2.

The  $T_c$  values show small increment with silica or modified silica addition in HDPE-nylon fibre composites. The hybrid sample prepared with MA grafted HDPE crystallizes about 3 °C earlier than pure HDPE. This indicates that grafting increases the interaction of matrix with filler and thus the hybrid filler can act as nucleating agent for HDPE crystallization.

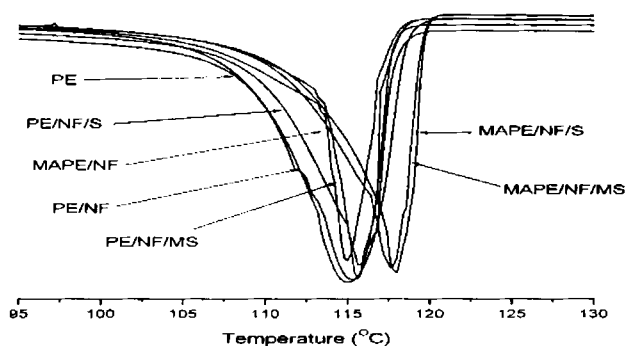


Figure 6b.18: DSC cooling scans (10 °C/min from 180 °C melt) of hybrid composites

Smaller the degree of supercooling ( $\Delta T = T_m - T_c$ ), higher will be the crystallizability. The  $\Delta T$  values of the HDPE/nylon fibre and HDPE hybrid composites given in table 6b.3 are also not show much variation. The  $\Delta T$  values vary by ~ 2 to 6 °C than that of pure HDPE. This reveals that the crystallizability of the hybrid nanocomposites is better than that of pure HDPE.

Table 6b.3:  $\Delta T$  values of HDPE and HDPE composites

Sample	$\Delta T$ (°C)
PE	16.9
PE/NF	16.8
PE/NF/S	14.2
PE/NF/MS	13.3
MAPE/NF	12.4
MAPE/NF/S	11.2
MAPE/NF/MS	11.1

### 6b.3.5.2 Isothermal crystallization

Figure 6b.20 shows the isothermal crystallization curves of pure HDPE and HDPE composites at four temperatures (110, 115, 120 and 122 °C). The time corresponding to the maximum in the heat flow rate (exotherm) is taken as peak time of crystallization ( $t_{peak}$ ). In the case of pure HDPE, no peak is seen at the highest temperature of 122 °C because crystallization is very slow and would require longer time than the 4 minutes employed in the DSC program. On the other hand, for the MA treated hybrid nanocomposite samples with 2wt.% silica, the rate of crystallization is so fast near the lowest temperatures that most of the crystallization occurs already during the cooling scan (60 °C/min) employed to reach the temperatures (110 or 115 °C). This results in absence of exothermic peaks in the heat flow curves at those temperatures.

The peak times of crystallization at each of the temperatures for all the hybrid nanocomposite samples are plotted against the isothermal crystallization temperature (Figure 6b.19). It is noticeable that the  $t_{peak}$  values of the composite samples reduce to less than 40% as compared to pure HDPE due to the presence nano-micro filler. With the modified silica and grafting the crystallization rate is increased (as indicated by the decrease in  $t_{peak}$ ), demonstrating the role of modification on the surface of silica and polymer backbone for enhancing the matrix-filler interaction and thus enhancing the rate of crystallization.

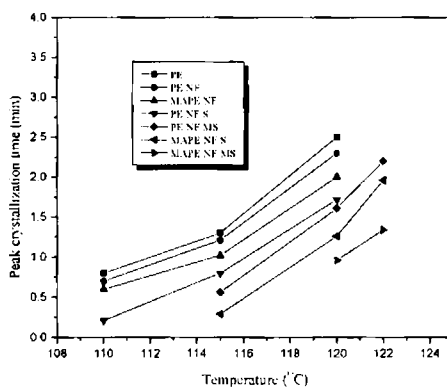


Figure 6b.19: Effect of hybrid filler and matrix grafting on the peak crystallization time of the composites at different isothermal crystallization temperature

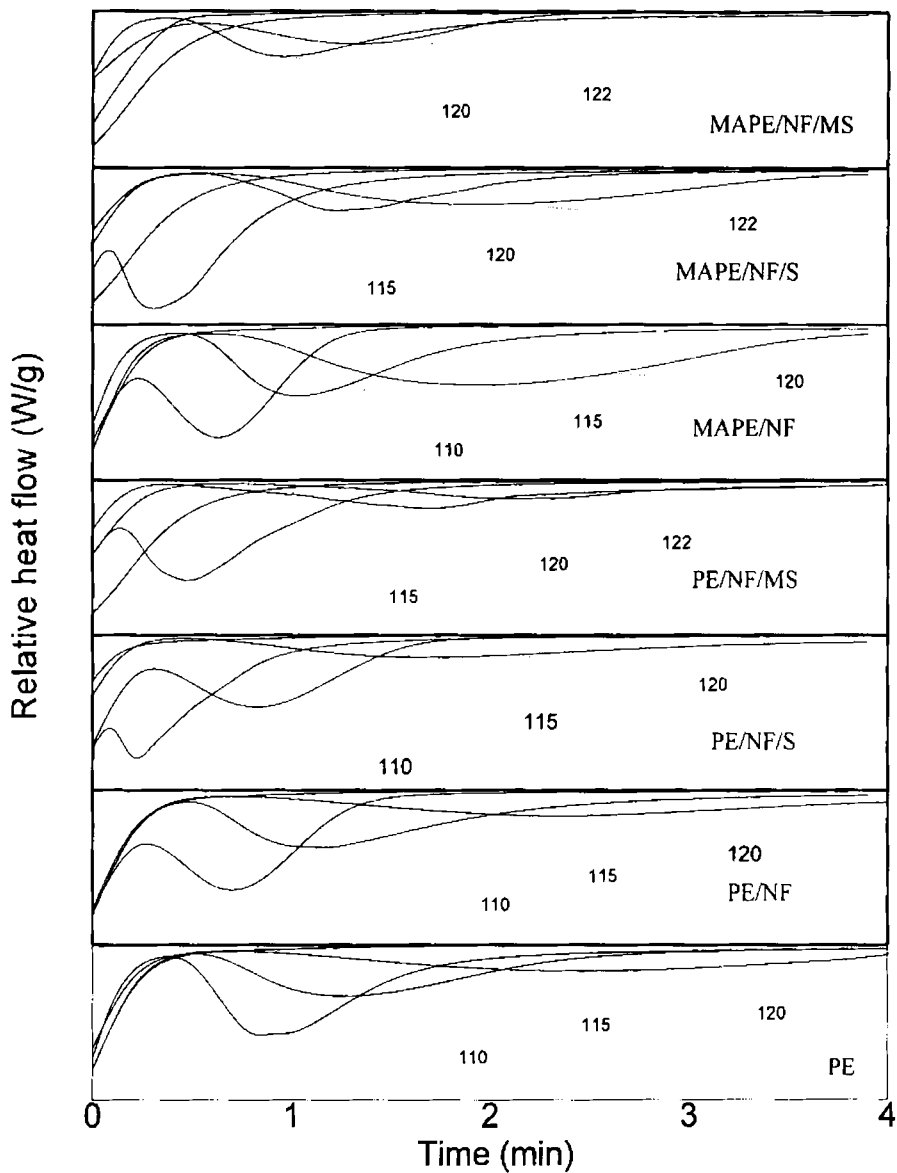


Figure 6b.20: Heat flow during isothermal crystallization of HDPE composites

### 6b.3.6 Thermogravimetric analysis

The thermal degradation pattern of HDPE and its composites in nitrogen atmosphere at a programmed temperature range of 50-600 °C are shown in figures 6b.21 and 6b.22. The temperature of onset of degradation ( $T_i$ ), temperature at which maximum degradation occur ( $T_{max}$ ) and the residue obtained at 600 °C are given in table 6b.4.

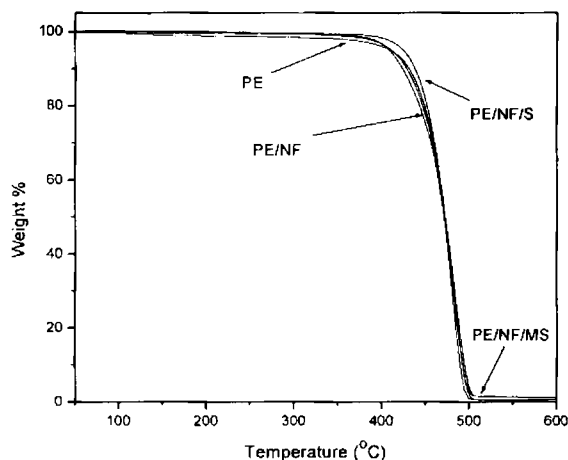


Figure 6b.21: Thermogravimetric traces of HDPE and HDPE hybrid composite

In the case of HDPE, degradation is observed in a single step and up to 365 °C the sample is stable thereafter sharp weight loss occurs till 520 °C. For nylon fibre the degradation take place between 400 to 500 °C in a single stage. Both the matrix and fibre follows single step degradation and also having comparable  $T_{max}$ . Hence the hybrid composite samples also showed similar degradation pattern. But the presence of nano-micro hybrid filler is increased the thermal stability of HDPE. The  $T_{max}$  of HDPE improved from 476 °C to 483 °C for HDPE hybrid composite. This improvement in thermal stability of the composites may result from the presence of thermally stable inorganic filler and its good dispersion in the matrix. Gilman suggested that the improved thermal stability of polymers in presence of fillers is due to the hindered thermal motion of polymer molecular chains.<sup>9</sup>



Table 6b.4: Degradation characteristics of HDPE and hybrid composites

Sample	Onset temp. (°C)	Peak max (T <sub>max</sub> )	Residue at 600 °C
PE	362.6	476	0.51
PE/NF	443.15	484.9	0.56
PE/NF/S	445.3	481.9	1.19
PE/NF/MS	450.8	483.2	1.14
MAPE/NF	419.4	456.9	2.3
MAPE/NF/S	448.7	484.58	4.4
MADPE/NF/MS	446.2	483.9	4.2

MA grafted hybrid composite with nanosilica showed higher T<sub>max</sub> (484 °C). This shows that the interaction of polar filler with matrix can be improved by making it polar.

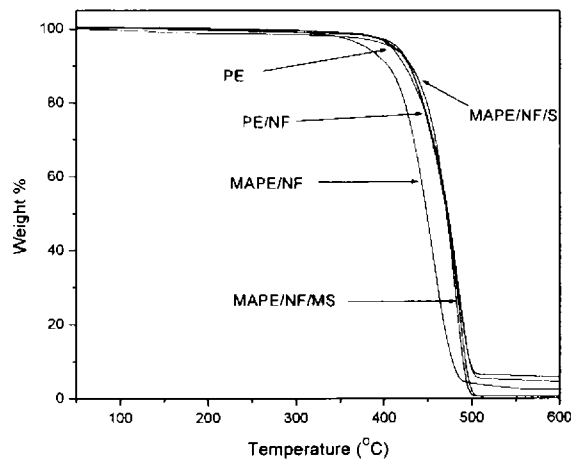


Figure 6b.22: Thermo gravimetric traces of HDPE and MA-g-HDPE hybrid composite

#### **6b.4 CONCLUSIONS**

The study shows that HDPE/nylon fibre composites can be upgraded with nanosilica/modified nanosilica and the following conclusions can be drawn.

- The incorporation of nanosilica and modified nanosilica improves the mechanical properties of HDPE-nylon fibre composites.
- Storage modulus increases with the presence of hybrid fillers and maleic anhydride treatment.
- The hybrid fillers not have much effect on crystallization temperature of HDPE.
- Thermal stability of composites is enhanced by the addition of hybrid fillers.
- HDPE can be successfully reinforced with nylon fibre-silica hybrid fillers.

## REFERENCES

1. C.H.White, R.H.Gough, J.U.McGregor, V.V.Vickroy; *J.Dairy Sci.*, **1991**, 74, 96.
2. T.N.Abraham; *Recyclable short fibre reinforced plastics*, Ph.D. thesis, August **2005**.
3. R.Varatharajan, S.K.Malhothra, L.Vijayaraghavan, M.Krishnamurthy; *Materials Science and Engineering:B*, **2006**, 132, 134.
4. M.Z.Rong, M.Q.Zhang, Y.X.Zheng, H.M.Zeng, K.Friedrich; *Polymer* **2001**, 42, 3301.
5. P.V.Joseph, G.Mathew, K.Joseph, G.Groeninckx, S.Thomas; *Comp. Part A*, **2003**, 34, 275.
6. J.George, S.S.Bhagavan, S.Thomas; *J. Thermoplastic Comp. Mat.* **1999**, 12, 443.
7. D.Ray, B.K.Sarkar, S.Das, A.K.Rana, *Comp. Sci. Technol.* **2002**, 62, 911.
8. A.K.Saha, S.Das, D.Bhatta, B.C.Mitra; *J.Appl.Polym.Sci.* **1999**, 71, 1505.
9. J.W.Gilman; *Appl.Clay.Sci.* **1999**, 15, 31.

# Chapter 7

## Summary and conclusions

Upgrading two widely used standard plastics, polypropylene (PP) and high density polyethylene (HDPE) has been the main objective of this study. Upgradation was effected by using nanomodifiers and/or fibrous modifiers. PP and HDPE were selected for modification due to their attractive inherent properties and wide spectrum of use.

Nanosilica was synthesized from sodium silicate and hydrochloric acid by a matrix assisted precipitation process under controlled conditions. It is a cost effective method for the preparation of nanoparticles. Here chitosan was used as matrix to condense the silica particles and thus to produce low sized uniform particles. This synthesized silica was characterized by using X-ray diffraction (XRD), Scanning Electron Microscopy (SEM), Transmission Electron Microscopy (TEM), BET Adsorption and Infrared Spectroscopy (IR). The prepared nanosilica had an average particle size of 18 nm. To reduce the polarity of the silica particles by reducing the number of surface hydroxyl groups, it was modified using vinyl triethoxy silane (VTES) by hydrolysis followed by condensation. This modification also reduced the agglomeration tendency of nanosilica.

PP-silica and HDPE-silica nanocomposites were prepared by melt mixing in a torque rheometer. The mechanical properties of the polymers improved marginally on addition of modified nanosilica. The maleic anhydride grafting of the polymers enhanced the properties further indicating that the interaction of nanofiller with the polymers increases by the chemical treatment. From dynamic mechanical analysis it was observed that the nanosilica/modified nanosilica improved the storage modulus of the nanocomposites at all temperatures at low concentrations. The material becomes more stiff and elastic by the presence of nano fillers. Thermogravimetric studies proved that the thermal stability of the polymers can be improved by the incorporation of nanosilica. Differential scanning calorimetry studies revealed that nanosilica/modified nanosilica acts as effective nucleating agents for PP melt crystallization. Nanosilica at a concentration as low as 1% enhance the crystallization temperature of PP by 6°C. This

study also demonstrated the importance of the chemical treatment of the matrix polymer for the effective interaction with nanofillers because the presence of nanofiller in MA treated PP improved the crystallization temperature of PP by 16°C. However the effect of nano silica as a modifier of the crystallization temperature seems to be less significant in the case of HDPE since it enhances the crystallization temperature by 3°C only. But nanosilica reduces the melt's isothermal crystallization time by more than 40% in both PP and HDPE.

The effect of nanosilica/modified nanosilica on PP-short fibre and HDPE-short fibre composites was also investigated. The combined use of nano-micro hybrid filler improved the properties of polymers. The improvement depends on the concentration of nano & micro filler, type of the fillers & matrix, chemical treatment and mostly on the interaction of matrix, fibre and nanofiller. The mechanical properties of the nylon fibre composites and glass fibre composites improved by the presence of nanosilica/modified nanosilica. This improvement is marginal but the chemical treatment improves the mechanical performance of hybrid composites further. This shows that the introduction of polar nature into the polymer helps it to interact strongly with polar fillers. The impact strength of PP hybrid and HDPE hybrid nanocomposites is highest at 10% fibre loading. Dynamic mechanical properties also improve in the presence of hybrid filler and chemical treatment. Hybrid fillers also act as effective nucleating agents in PP melt crystallization. This effect is comparatively less in the case of HDPE. Glass fibre-silica hybrid filler enhance the crystallization temperature ( $T_c$ ) of PP by 14°C but the same combination enhances crystallization temperature only by 1°C for HDPE. Here also the MA grafting helped to improve  $T_c$  of the hybrid composites. The hybrid fillers reduce the melt's isothermal crystallization time by more than 50% in both PP and HDPE. Thermal stability of PP and HDPE improve by the presence of hybrid filler as expected.

A significant observation from this study is that the requirement of higher fibre loading for efficient reinforcement of polymers can be substantially reduced by the presence of nanofiller together with fibre in the composite. Higher loading of fibre will naturally make the melt more viscous and hence processing will become more difficult. However, hybrid fillers can alleviate this problem and maintain the easy processability of the polymer.

## Abbreviations and symbols

ASTM	American standards and testing methods manual
AFM	Atomic Force microscopy
BET	Brunauer, Emmett and Teller
b	Width of specimen tested
CMC	Carboxymethyl chitosan
CNTs	Carbon nanotubes
cm	centimetre
d	Depth of specimen
DMA	Dynamic mechanical analysis
DSC	Differential scanning calorimetry
DTA	Differential thermal analysis
DTG	Derivative thermogravimetry
E'	Storage modulus
E''	Loss modulus
EB	Elongation-at-break
FRC	Fibre reinforced composite
FRP	Fibre reinforced plastics
FTIR	Fourier Transform infrared
GP	General Purpose
GPa	Giga pascal
HDPE	High density polyethylene
hrs	Hours
Hz	Hertz
IR	Infra Red Spectroscopy
$l_c$	Critical fibre length
LDPE	Low density poly ethylene
L.R.	Laboratory reagent
m	metre
MA	Maleic anhydride
MA-g-HDPE	Maleic anhydride grafted high density polyethylene

MAPE	Maleic anhydride grafted high density polyethylene
MAPP	Maleic anhydride grafted PP
MA-g-PP	Maleic anhydride grafted PP
min	Minutes
mm	millimetre
mol	Mole
$\mu\text{m}$	Micrometer
MPa	Mega Pascal
MMC	Metal matrix composite
MS	Modified nanosilica
nm	Nanometre
Nm	Newton meter
PE	Polyethylene
PET	Polyethylene terephthalate
phr	Parts by hundred parts by weight of resin
PMC	Polymer matrix composite
PP	poly propylene
ppm	parts per million
rpm	Revolutions per minute
S	Nanosilica
SEM	Scanning electron microscopy
SiO <sub>2</sub>	Silica
tan $\delta$	Loss factor
T	Temperature
T <sub>g</sub>	Glass transition temperature
TGA	Thermo gravimetric analysis
UTM	Universal Testing Machine
V <sub>f</sub>	Volume fraction of fibre
V <sub>m</sub>	Volume fraction of matrix
VTES	Vinyl triethoxy silane
XRD	X- ray diffraction
ZnO	Zinc oxide

## Publications in International Journals

1. Modification of Polypropylene/Glass Fiber Composites with Nanosilica, *Sinto Jacob, Suma K.K., Jude Martin Mendez, Abhilash George, K.E.George, Macromolecular Symposia*, 2009, 277(1), 138.
2. Paint Formulation Using Water Based Binder and Property Studies, *Suma K.K., Sinto Jacob, Rani Joseph, Macromolecular Symposia* 2009, 277(1), 144.
3. Reactive compatibilization of nylon copolymer/EPDM blends: experimental aspects and their comparison with theory, *Cibi Komalan, Sinto Jacob, K.E George, S.Thomas, Polym. Adv. Technol.*, 2008, 19, 351.

## Publications in International Conferences

1. Micro/Nano Hybrid Fillers For Polypropylene Modification, *Sinto Jacob, Suma K.K., Jude Martin Mendez, K.E.George, MACRO 2009, Chennai, India, 2009.*
2. HDPE/SiO<sub>2</sub> nanocomposites with improved mechanical properties, *Sinto Jacob, Suma K.K., Jude Martin Mendez, K.E.George, Plastindia 2009, Delhi. [Best poster award]*
3. Effect of nanosilica on the mechanical properties of HDPE-Nylon fibre composite, *Sinto Jacob, Suma K.K., Jude Martin Mendez, K.E.George, APT, Kochi 2008.*
4. Polypropylene/SiO<sub>2</sub> nanocomposites with improved mechanical properties, *Sinto Jacob, K.E.George, International Conference on Materials Science Research and Nanotechnology (ICMSRN), Kodaikanal 2008.*
5. Reinforcing effect of nanosilica on HDPE-Nylon fiber composite, *Sinto Jacob, Suma K.K., Jude Martin Mendez, K.E.George, International conference on polymer blends, composites (ICBC), Kottayam, 2008. [Best poster award]*



6. Modification of Polypropylene/Glass Fiber Composites with Nanosilica, *Sinto Jacob, Suma K.K., Jude Martin Mendez, Abhilash George, K.E.George*, POLYCHAR-16, Luknow, 2008.
7. Reinforcing Effect of Nanosilica on Polypropylene-Nylon Fibre Composite, *Sinto Jacob, Suma K.K., Jude Martin Mendez, K.E.George*, SAMPADA 2008, Pune, India

T34

